GEOLOGY, TECTONIC SETTING AND GENESIS OF TALC AROUND WONU, IBADAN-APOMU AREA, SOUTHWESTERN NIGERIA

BY

Morenike Abimbola ADELEYE
(Matric. No.:130975)
B.Sc. (Hons.) Geology (UNAD); M.Sc. Mineral Exploration (Economic & Mining Geology) (Ibadan)

A Thesis in the Department of Geology

Submitted to the Faculty of Science

In partialfulfilment of the requirementsfor the Degree of

DOCTOR OF PHILOSOPHY

of the

UNIVERSITY OF IBADAN

APRIL, 2021

CERTIFICATION

I certify that this work was carried out by Mrs. Morenike Abimbola ADELEYE in the Department of Geology, University of Ibadan, Ibadan, Nigeria, under my supervision.

……

Supervisor

Anthony Temidayo Bolarinwa
B.Sc. Hons. (Ilorin), M.Sc., Ph.D., PGDTHE (Ibadan)
Reader, Department of Geology
University of Ibadan, Ibadan

DEDICATION

This research work is dedicated to the KING OF KINGS, the ROCK OF AGES and GOD ALMIGHTY for his guidance and to my dear husband, Prince Adedamola Adegbenga Adeleye, for his love, support, encouragement and understanding at all times.

ACKNOWLEDGEMENTS

I would like to communicate my heartfelt and most profound gratitude to my supervisor and mentor,Dr A.T. Bolarinwa for his initiative and thorough supervision of this work. I want to thank him for his thoughtfulness, suggestions, guidance and encouragement throughout the work. I appreciate the support of his wife, Dr. Mrs. A.O. Bolarinwa for her concern and regular prayers, which were very helpful in the course of this work.

I acknowledge the academic support of theVice-Chancellor, Prof. A.I. Olayinka, the Head of Geology Department, Prof. O.A. Okunlola, the immediate past Head of Geology Department, Prof. O.A. Ehinola and other Professors in the Department, including G.O. Adeyemi, M.N. Tijani, and M.E. Nton. I also acknowledge the encouragement of late Professors A.A. Elueze, A.F. Abimbola and Dr I.M. Akaegbobi. May their soul rest in perfect peace.

My profound appreciation goes to Drs O.A. Boboye, M.A. Oladunjoye, A.S. Olatunji, A.I. Oyediran, O.C Adeigbe, O.O. Osinowo, A.M .Adeleye, F.F. Ajayi and especially, Dr. O.K. Aromolaran for their very useful suggestions in the course of this research work.

I am very grateful to Prof. Thomas Axel Hofmann for facilitating my trip to the Department of Geology, University of Johannesburg, South Africa and for the technical assistance provided during the petrographic, Scanning Electron Microscope (SEM) and Electron Probe Micro Analysis (EMPA). I equally appreciate all members of staff at the University, most especially Dr Christian Reinke, the Senior Instrument Scientist (EMPA and XRD), Mr. Siyasanga Mpelane (SEM), Misses Dora Paprika, Gabrielle Ficq, Juliet Akoh and Mrs Diana Faseka.

The technical assistance provided by Mr. J.A. Mafoluku, Mr. M.A. Uwaje and Mr. S.O. Akhihiero-Ata are equally appreciated. The moral support of Mrs. R.O. Fakunle, Mr. Wale Oyekunle and Mr. R.K. Adelakun of the Department of Geology, University of Ibadan, is highly appreciated. I am grateful to Mr. J.M. Olumoyegun of the Department of Geography, University of Ibadan.

My profound thanks goes to Mrs. S.O. Bamidele and Mrs. M.A. Bademosi for their prayers, moral support and encouragement. My special thanks goes to Dr.

Franck Wilfried, Dr.Maryam Abdus-Salam, Miss Oghenerume Oroh and Mrs. Yemi Ademola for being of immense assistance.

I remember with love my late mother, Mrs. J.O. Adedayo who longed to attend my convocation but for death in 2019 and my late father, Engr. N.A. Adedayo, who had always wanted me to further my academic career. I also appreciate my late father-in-law the Elekole of Ikole-Ekiti Oba Adetunla Adeleye and my late mother-in-law Olori Ayodele Adeleye for their good wishes. I acknowledge my father and mother in the lord, Bishop T.V Adelakun and Pastor (Mrs) Dolapo Adelakun, and my spiritual mentor, Dr D.K. Olukoya and also Pastors Feyisayo Makinde, Omisore, Olarewaju Olorode and Chiazor for their prayers and encouragement.

I am grateful to my siblings, Mr. Dokun Adedayo, Mrs. Mojisade Adeyeye and Mr. Babatunde Adedayo for their moral support. A special thanks to you my wonderful sister-in-law Mrs. Janet Adedayo. I am most grateful to my uncle, Mr. Adebayo Talabi and his wife, Mrs. Olufunmilayo Talabi. My appreciation goes to Engr S.A. Laoye and my sister Mrs Adenike Laoye. I am grateful to my sisters, Miss Abiodun Adewale, Dr. Roseline Aromolaran, Mrs Bolanle Babalola and my aunties, Dr. Ngozi Efosa-Uroghide, Mrs E.T. Oni and Dr. Yemisi Ladi-Badmus, for their encouragement and unflinching support.

My most immense gratitude goes to my darling husband, my crown, Prince Adedamola Adegbenga Adeleye, for being the architect of my postgraduate studies. Darling Dgov, I appreciate your love, sleepless nights, understanding, encouragement, financial and emotional support from the beginning, to the concluding part of this research work.

I say big thank you to my darling daughter and her husband, Adeyinka and Babafemi Awe, to my wonderful sons, Samuel, David, Solomon and Joseph Adeleye for their understanding, patience and love. May God Almighty bless you and empower you all to excel in life in Jesus Name, Amen.

Above all, I give thanks to the Almighty God, who is my Rock of ages for His faithfulness to me and for His grace made available to me to complete this research work. Indeed I can say, “MY GOD IS THE PROMISE KEEPER”.

ABSTRACT

Talc is formed from diverse geological processes including hydrothermal alteration and contact or regional metamorphism of mafic, ultramafic rocks and dolomitic carbonates. Previous studies on the genesis of talc deposits in Nigeria have been speculative due to inadequate compositional data leading to misclassification of the talc genesis. Therefore, this study was aimed at investigating the geology, tectonic setting and composition of rocks around Wonu, Ibadan-Apomu area, southwestern Nigeria.

Geological mapping on a scale of 1:25,000 was carried out around Wonu, Ibadan-Apomu area. Representative samples (105) of the rocks were collected from outcrops and subjected to petrographic analysis. Polished sections were prepared from the rocks and were subjected to electron probe micro-analysis to determine the mineral chemistry. Scanning electron microscope-energy dispersive spectrometry was used to determine the morphology and fluid components. Additional mineralogical study was carried out using X-ray diffraction. Major, trace and rare-earth elements of the rocks were obtained using X-ray fluorescence, and inductively coupled plasma-mass spectroscopy. Geochemical discrimination diagrams were used to interprete the data obtained.

The lithologic units mapped were migmatites, talc schist, granites, amphibolites and lherzolites. These have been intruded variably by the pegmatites. The migmatites and the granitic intrusive are composed of quartz, oligoclase, albite, K-feldspar, ferro-hornblende, and biotite. The amphibolite is fine-grained, composed of enstatite, augite, anthophyllite, actinolite, magnesio-hornblende, magnesio-anthophyllite, titanium-K-alumino-anthophyllite, potassium-gedrite, potassium-alumino-anthophyllite, cummingtonite, tremolite, actinolite, biotite, bytownite, oligoclase, andesine, albite, K-feldspar, perthites, ilmenite, magnetite and garnet. The lherzolite and talc are composed of forsterite and fayalite, orthopyroxenes, clinopyroxenes, magnesio-hornblende, tchermakitic-hornblende, magnesio-gedrite, anthophyllite and bytownite. Alteration minerals include serpentine, amesite, talc, Cr-bearing clinochlore, ferritchromite, graphite and carbonate. Ilmenite, garnet, spinel, chromite, pyrite and magnetite are the opaque minerals present. Olivine-spinel geothermometry of 700-750ºC is consistent with

medium to high amphibolite regional metamorphism prior to talc formation. Alteration of olivines, pyroxenes and amphiboles to talc, chlinochlore; and spinel to ferritchchromite, depicted on the Cr/(Cr+Al) vs Fe^{2+}/(Fe+Mg) and Al_2O_3 vs Cr_2O_3 diagrams showed retrograde amphibolites-greenschist facies metasomatism at 500-550ºC. This led to the formation of asbestiform amesite, anthophyllite, actinolite and tremolite. The Al_2O_3-Fe_2O_3+TiO_2-MgO discrimination diagram suggests tholeiitic protolith for the amphibolite and komatitic protolith for the lherzolite. The lherzolites have flat rare-earth element patterns typical of komatiites and dunites. The MgO+FeO+CaO vs SiO_2+Al_2O_3 diagram indicated ultramafic-hosted talc with variable purity.

The talc deposits around Wonu, Ibadan-Apomu area is derived from metasomatic alteration of the amphibolites and the lherzolites. The tectonic setting is an island arc basaltic material deposited near supra-subduction-zone.

Keywords: Amphibolites, Lherzolites, Talc schist, Ferritchromite, Metasomatism, Komatiite

Word count: 474

TABLE OF CONTENTS

LIST OF TABLES

LIST OF FIGURES

LIST OF ABBREVIATIONS

EDS	-	Energy Dispersive Spectrometer
EMPA	-	Electron Microprobe Analyser
GPS	-	Global Positioning System
HFSEs	-	High Field Strength Elements
HREEs	-	Heavy Rare-Earth Elements
ICDD	-	International Centre for Diffraction Data
ICP-ES	-	Inductively Coupled Plasma-Electron Spectrometry
ICP-MS	-	Inductively Coupled Plasma-Mass Spectrometry
LCD	-	Liquid Crystal Display
LILEs	-	Large Ion Lithophile Elements
LOI	-	Loss on Ignition
LREEs	-	Light Rare-Earth Elements
PGE	-	Platinum Group Elements
PGM	-	Platinum Group Minerals
REE	-	Rare-Earth Elements
SPSS	-	Statistical Package for Social Sciences
TIMS	-	Thermal Ionization Mass Spectrometry
WDS	-	Wavelength Dispersive Spectrometer
XRD	-	X –Ray Diffraction
XRF	-	X- Ray Fluorescence Spectrometry

CHAPTER ONE

INTRODUCTION

1.1 Background to the Study

The Precambrian Basement Complex of Nigeria is within the Pan African mobile belt, which occupies the region between the Archean to early Proterozoic West African Craton and Congo-Gabon Cratons (Kennedy, 1966), and South of the Tuareg Shield (Black, 1980).

The Nigerian Basement Complex (Fig. 1.1) can be comprehensively divided into migmatite-gneiss-quartzite complex, the N-S trending schist belts, and the Pan-African intrusives (Elueze 1988, Adekoya*et al*, 2003). All these are subsequently cross-cut by minor felsic and mafic intrusives. Within the rejuvenated basement complex are occurrences of the schist belts, mainly characterized by pelitic and semipelitic rocks, psammitic units with subordinate intercalations of mafic-ultramafic assemblages, marbles and calc-silicate gneisses (McCurry, 1976; Elueze and Emofurieta, 1995).

The metaultramafic-mafic units comprises of amphibolites, amphibole schist, talc schist, serpentinite and komatitic rocks that have undergone low temperature regional metamorphism of upper greenschist to amphibolites facies (Ige and Asubiojo, 1991; Kehinde-Phillips and Tiez, 1995). Talc bearing rocks are constrained to the western half of Nigeria. In northwestern Nigeria, the metaultramafic-mafic rocks including serpentinite are reported to occur in Mallam Tanko, Sado, Maikwonaga and Ribah in the Zuru and Anka schist belts (Wright and Ogezi 1977). Other occurrences in northern Nigeria include those ofZungeru-Birnin Gwari, Kushaka, Maru, Wonaka, and Karaukarau schist belts (Ogezi, 1977; Elueze, 1980; 1982; 1985; Egbuniwe, 1982; Ajibade and Fitches, 1988; Okonkwo andWinchester,1996;OlobaniyiandMûcke,2011)(Fig.1.2).

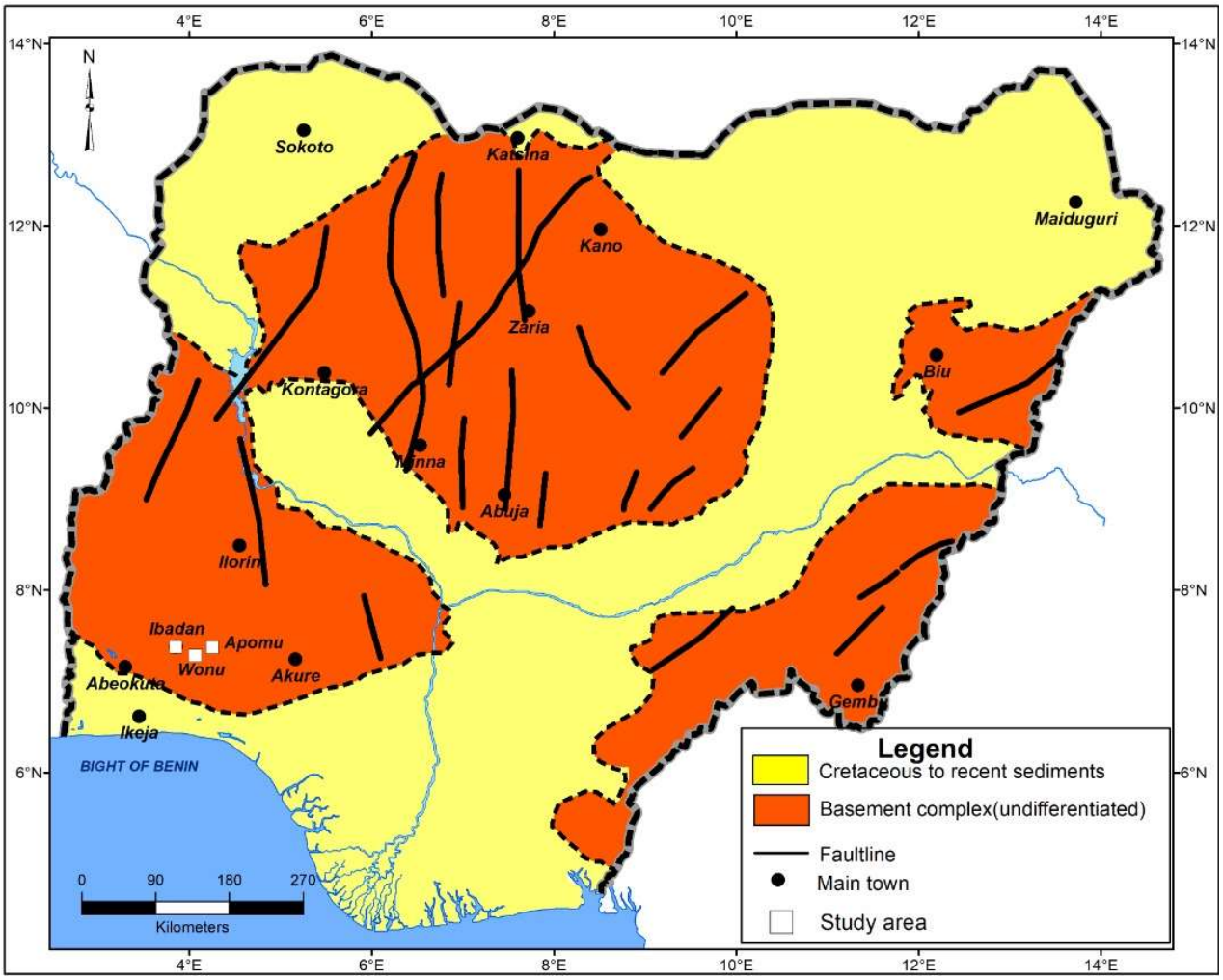

Fig. 1.1: The Geological distribution of major rocks in Nigeria indicating the location of Wonu, Ibadan-Apomu area (modified after Malomo, 2004).

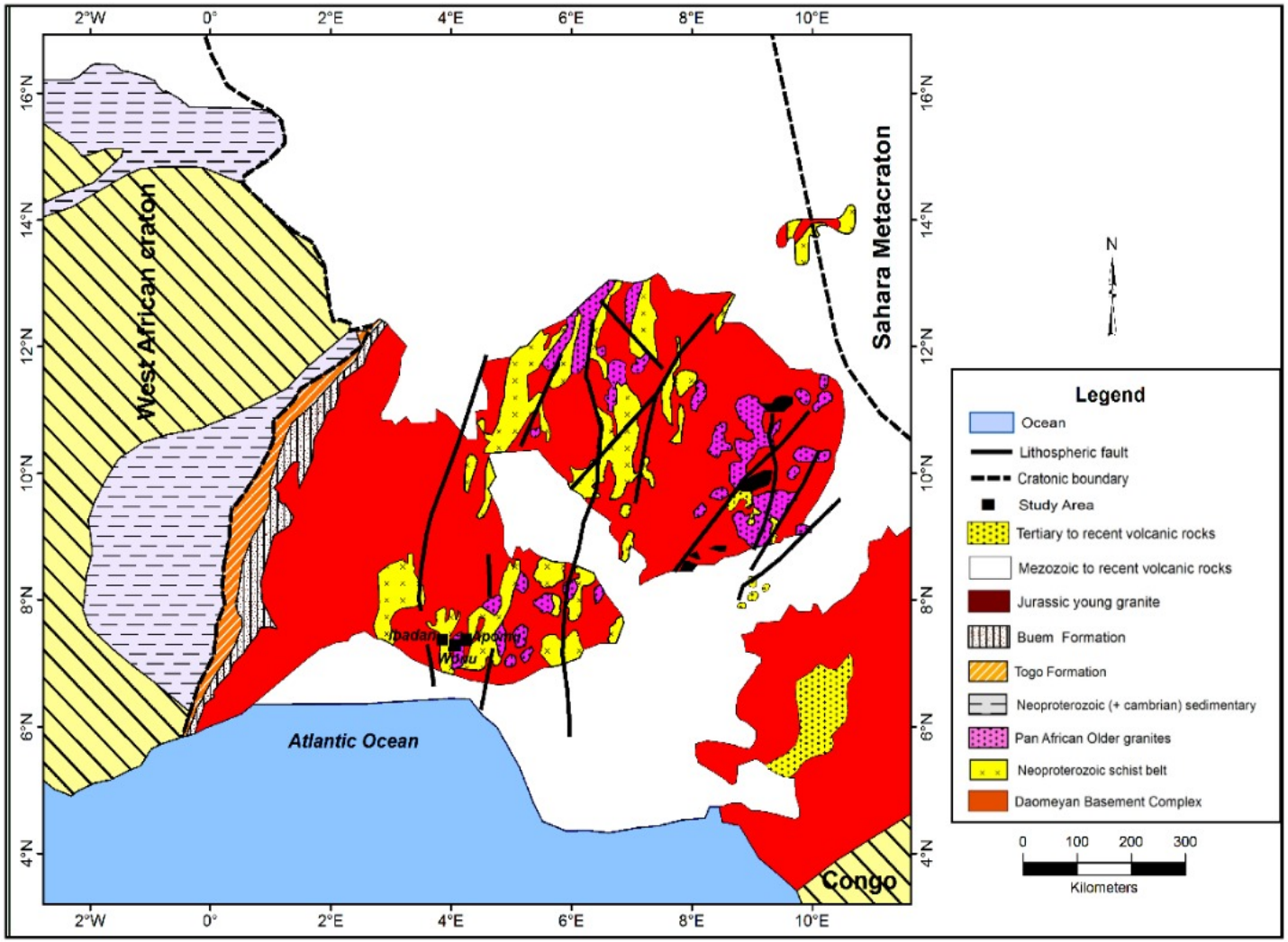

Fig. 1.2:Map showing location of the schist belts in the southwestern part of Nigeria, (modified after Turner,1983).

Various research works have been conducted on talcose rocks and their affliiated ultramafic rocks involving essentially works on the petrochemistry of the amphibolites as probable source of the associated gold mineralization, particularly in Egbe-Isanlu and Ife-Ilesha areas. Elueze (1980) described the rock units in the Ilesha schist belt as massive, schistose, banded, and gneissic amphibolites, tremolite-actinolite-chlorite schist, anthophyllite schist and epidote schist. Based on the chemical characteristics, it was revealed that the amphibolites, anthophyllite and talc-tremolite schists were derived from tholeiitic basalts, associated with ultramafic sills and lavas. It was also observed that the talc-tremolite schists occur in close association with the amphibolites. Ajayi (1980) also revealed that these rocks were altered derivatives of the ultramafic bands associated with the basic volcanics from which the amphibolites were derived. Subsequent studies by (Adeleye, 2009) on the Apomu and Ilesha talc-schists revealed the presence of chromium-bearing chlorite (clinochlore), as essential mineral constituents inthe talc-schist.

In southwestern Nigeria it was revealed that the chlorite had a composition of clinochlore, initially contained in the ultramafic rocks (peridotite) on the basis of the mineral chemistry of the Isanlu amphibolites (Olobaniyi and Mûcke (2011). Hence, it is therefore imperative to study the transition phases between the amphibolites and talcose rocks of the Wonu, Ibadan-Apomu area.

A number of research works on compositional and petrogenetic studies of the amphibolites and talc- schist belts relied solely on geochemical analysis (Olade and Elueze, 1979; Ajayi 1980; Kehinde-Phillips and Tietz 1995). The current research however has the principal objective of investigating the geology, tectonic processes and genesis of the talc schists, amphibolites and other associated rocks of Wonu, Ibadan-Apomu area through the study of field relationships, petrography, mineral chemistry of various transitional phases in the rock units and the whole rock geochemistry. The data obtained is expected to reveal more on the petrogenesis and tectonic processes of the rocks of Wonu, Ibadan-Apomu in affliation to talc genesis.

1.2 Justification for the Research

Talc is an hydrated magnesium layered-silicates having a chemical formula of $Mg_3(Si_2O_5)$ or $Mg_3Si_4O_{10}(OH)$ and belonging to the phyllosilicate group (Deer*et al.,* 1962). Talcose rocks also results from alteration of serpentinised rocks.The serpentinization process was probably brought about by the reaction of carbondioxide and water with olivine (Kehinde-Phillips, 1991, Kehinde-Phillips and Tietz, 1995).

$$Mg_2SiO_4 + CO_2 + 2H_2O \longrightarrow Mg_3Si_2O_5(OH)_4 + 2MgCO_3$$
(Forsterite) (Serpentine) (Magnesite)

$$2Mg_2Si_2O_5(OH)_4 + 3CO_2 \longrightarrow Mg_3Si_4O_{10}(OH)_2 + 3MgCO_3 + 3H_2O$$
(Serpentine) (Talc) (Magnesite)

As mentioned earlier, studies on the composition and petrogenesis of the amphibolites and talc-schist relied mainly on geochemical data. Ige(1988), Ige and Asubiojo (1991), and Bolarinwa and Adepoju (2017) utilized geochemical data to tointerprete the petrotectonic settingsof the mafic units.

In this research, detailed mineral chemistry of the essential and accessory minerals in the metaultramafic and mafic rocks of Wonu, Ibadan-Apomu area are used to determine chemical alteration phases in the rocks.Since the protoliths and genesis of talc impact their mineralogical, chemical composition and crystal chemistry, which ultimately impact their industrial usability, there is the need to investigate the amphibolite to talc schists transitionphases, their tectonic environments, as well as the source and effects of the hydrothermal fluids responsible for their transformation. In order to obtain a deeper insight to the Pan-African orogeny and metamorphism in Nigeria and also give a better insight into the discussion of the affliation between the rocks of the basement complex of southwestern Nigeria with regard to the genesis and geodynamic evolution of these mafic-ultramafic rocks.

1.3 Aim and Objectives of the Research

The purpose of this study is to determine the geology, tectonic setting and genesis of talc around Wonu, Ibadan-Apomu area, southwestern Nigeria (Fig. 1.1).

The major objectives of the research are to:

(i) Distinguish the metaultramafic-mafic and other rock types in Wonu-Ibadan-Apomu area and their field relationships.

(ii) Determine the petrography and morphology of the minerals in the rocks.

(iii) Determine mineral chemical composition, of primary and secondary mineral phases, in the rocks, so as to unravel the magma chemical evolution and subsequent hydrothermal alterations.

(iv) Determine the nomenclature, petrogenesis and discriminate the tectonic setting, so as to evaluate the stages involved during the evolution of the rocks, using the geochemical analysis.

(v) Use the mineral chemical data to calculate the pressure-temperature and chemical fluid (*P-T-X*) prevalent at the crystallization and evolution of the metaultramafic-mafic rocks protoliths.

1.4 Scope of the Investigation

Geological mapping of Wonu, Ibadan-Apomu area, southwestern Nigeria was carried out between October 2013 and February 2015. Field characteristics and relationship of rock units were observed. Outcrops, sampling sites and geological features were recorded with a geographical positioning system (GPS). Geological map of the study area was prepared from the field information obtained. Talcose rock samples and other rock samples were collected from accessible outcrops.

The rock samples collected were cut into thin sectionsin the Department of Geology, University of Ibadan, Nigeria and polished thin sections in the Department of Geology, University of Johannesburg for petrographic and ore microscopic studies, respectively. Scanning Electron Microscope-Energy Dispersive Spectrometry (SEM-EDS) and Electron Microprobe Analyses (EMPA) were also carried out.

1.5 Location and Accessibility

Wonu is located between Ibadan city and Apomu town in the southwestern part of Nigeria (Fig. 1.1). The area is located to the southeast of Ibadan and southwest of Apomutowns (Fig. 1.3). The area lies between latitudes $7^{o}15'$ and $7^{o}30'$ N and longitude $4^{o}00'$ and $4^{o}15'$ E. Some of the villages around the amphibolite and talc schists are Wonu, Gbada-Efon, Adetonwa, Pagbo, Adigun, Gbangba, Laduntan, Elepo, and Ojewunmi. Others are Idiodun, Ekerin, Matako, Elewe, Arinokuta, Onikeke and Aroaran (Fig. 1.3).

The study area can be accessed by road from Ibadan through Akanran in the Egbeda Local Government Area. The roads leading to the study area is barely motorable during the rainy season because they are not paved. However, there is good access during the dry season. Trasverseswere made during the field mapping and sample collection was carried out using the untarred roads and the numerous foot paths in the area as access to the rock outcrops and talc mines (Fig. 1.3).

1.6 Topography and Drainage

The Wonu village, in Ibadan-Apomu area forms part of the southwesternBasement Complex of Nigeria and occurs in the southern side of the Iseyin-Oyan schist belt and on the west of the Ilesha schist belt (Bolarinwa and Adeleye, 2015a; Bolarinwa and Adepoju. 2017). It is characterized by a suite of medium to low grade gneissic metasedimentary, metavolcanics and granitic rocks (Fig. 1.2) namely; the migmatite-gnesis complex, amphibolite, talc and talc schist, Older Granites and pegmatites. The studyarea is characterized by relatively simple topographic features which appear to have been essentially influenced by the differential weathering of the underlying lithologies. The area to the south generally lower in elevation between 400m and 500m above the sea level. The topography of the area rises gradually towards the northern parts, where few hills ofgneisses, porphyritic granite and quartzite outcrops occur. The inselbergs and residual hills are dissected by rejuvenated rivers in the lowland areas. The inselbergs are few and isolated, and they exhibit joints and exfoliation.

The OsunRiver, near Asejire in Ibadan is the main tributary in the study area. It occupies the central part of the region (Fig. 1.4). Most of the other minor streams are tributaries that flow from a central ridge, which serves as watershed in the area. Many of the streams are seasonal. Wonu, Ibadan-Apomu area is

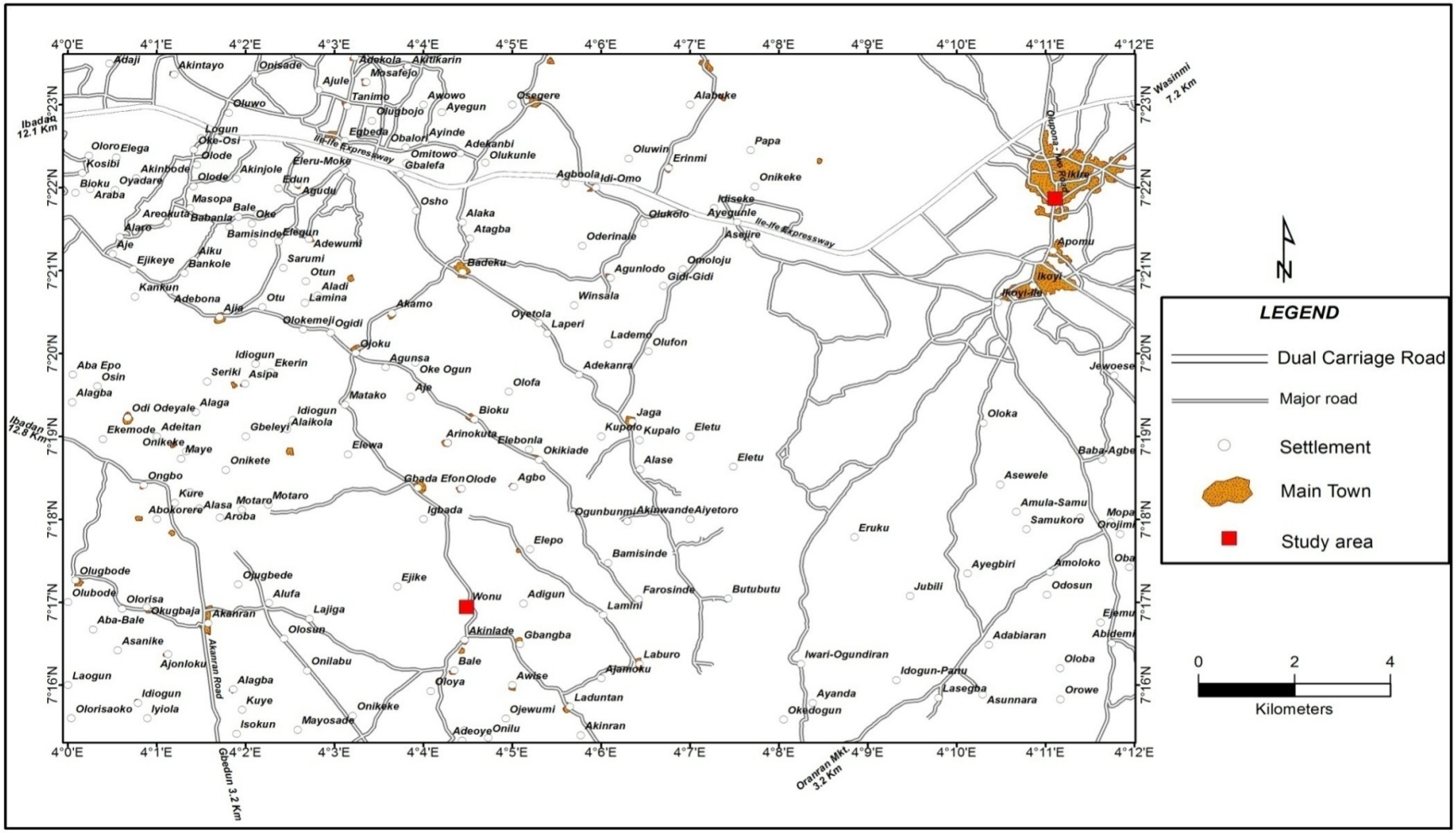

Fig. 1.3: Major Road network in Wonu-Ibadan-Aponu area and its environs

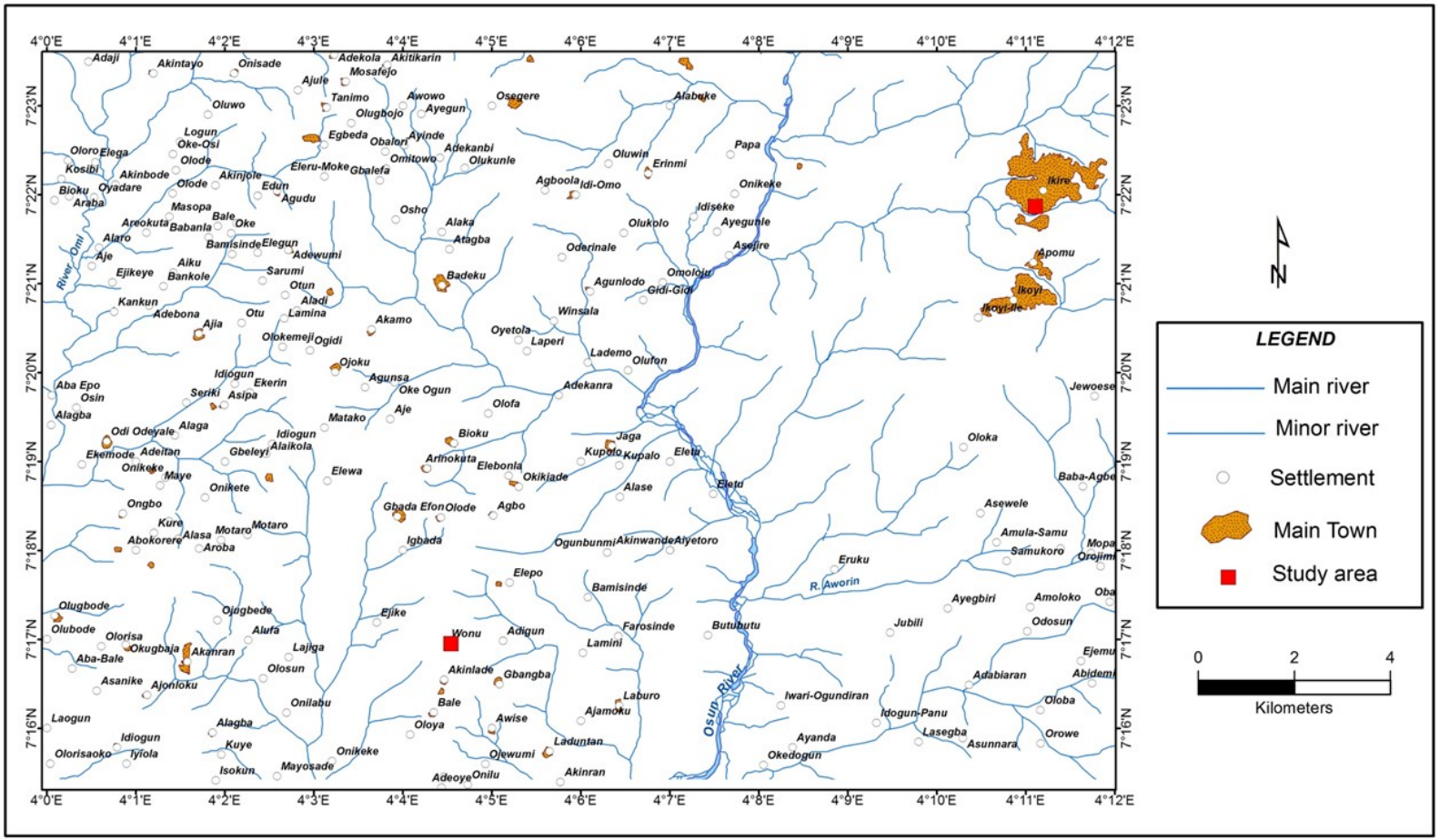

Fig. 1.4: Drainage pattern of Wonu, Ibadan-Apomu area southwestern Nigeria.

characterized by trellis drainage pattern, indicative of the influence of the structures of the underlying rocks and the general relief of the area. The other minor rivers and streams flow into River Osun from there, flows directly southwards (Fig. 1.4). The Osun River forms the eastern boundary of the talc bodies in the south central part (Fig. 1.4). The river appear to be flowing through a lithological contact between the mafic-ultramafic rocks and the higher terrain composed of dominantly felsic rocks, notably porphyritic granite, porphyroblastic gneiss, fine-grained granite and pegmatised schist of Apomu-Ikire area. It is also possible that the river is flowing through a major N-S trending tectonic lineament.

1.7 Climate and Vegetation

The region of investigation has sub-equitorial climate with heavy rainfall from March and November and a arid season from December and February. The average annual rainfall is ranges from 1800 to 2100mm, while the mean annual temperature range from 29to 32^{o}C with maximum values during the months of February to March.

Vegetation cover in the study area is typified by deciduous forest, which is duly exemplified by dense vegetation with perennial trees, shrubs, climbers and bushy undergrowth. However, human activities including provision of settlement, subsistence farming and bush burning have transformed the vegetation of the area to a derived savannah (Fig. 1.5). Plantations of cash crops, such as, cocoa, kolanut, citrus and subsistence crops notably plantain, cassava, yam, maize and banana occupy acres of land in many of the localities, thus resulting in secondary forest.

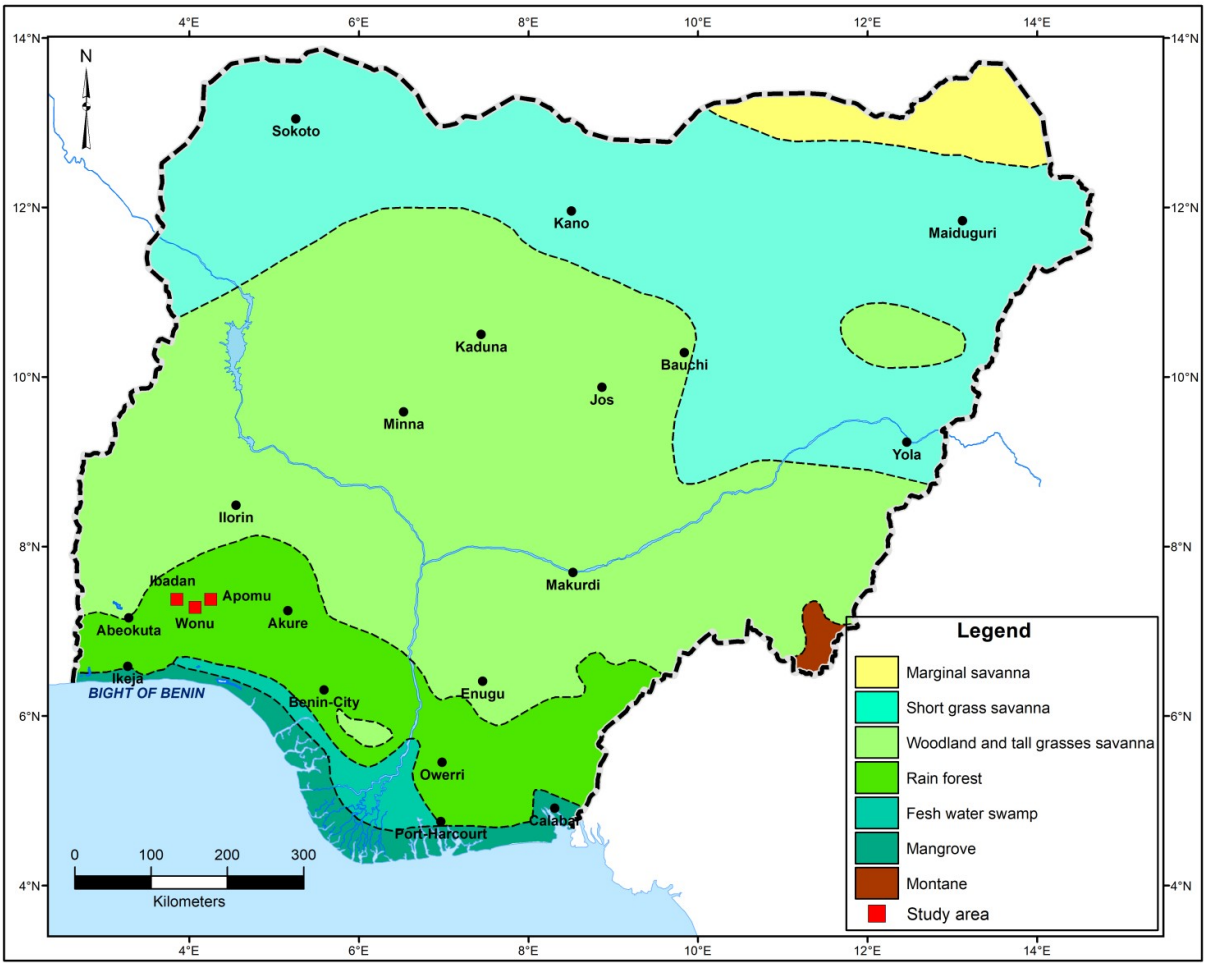

Fig. 1.5: Map of Nigeria showing the vegetation of Wonu, Ibadan-Apomu area (Iloeje, 1981).

CHAPTER TWO

LITERATURE REVIEW

2.1 Review of Regional Geology

The Nigerian Precambrian Basement complex occurs within the Pan-African Mobile belts,located eastwards of the West-African Craton and West of the Congo Craton (Fig. 2.1). The Pan-African province east of West African Craton is known as the Trans-Sahara Fold Belt (Caby, 1989) and includes the Nigerian sector and the adjoining Dahomeyan Belt, which reaches out from the Hoggar (Algeria) to the Dahomeyides (Ghana, Togo, Benin, Nigeria and Cameroon Republics) along Air, Adrar, de Iforas and Gourma. It is associated with the Borborema province of Brazil (Caby, 1989) (Fig. 2.2). The Dahomeyan Fold Belts represent the southern portion of the Trans-Saharan Fold Belt (Caby, 1989). The Buem Formation and the Atacora units of the Dahomeyan Belt separate the Pan-African mobile belt from the West African Craton. Nigeria lies within the heart of the mobile zone between the West African and Congo Cratons.In the northern segment of the Trans-SaharanFold Belt, three major structural provinces, separated by north-south shear zone, have been distinguished: the Pharusian in the West, the Central Hoggar and the Easthen Hoggar (Betrand and Caby 1978). The Pharusian Belt is composed essentially of the late Pan-African calc-alkaline volcanic, while the Central and Eastern Hoggar zones are largely supracrustals.

The basement complex of Nigeria (Fig 2.2)is intruded by the Mesozoic peralkaline ring complexes (Younger Granites) of the Jos Plateau and is unconformably overlain by the Cretaceous and younger sediments of the sedimentary basins. The Nigerian basement complex rocks (Fig. 2.3) are believed to be the consequence of three significant orogenic cycles of deformative translation, metamorphism and remobilization. The earlier three cycles were identified by intense deformation and isoclinal folding, accompanied by regional metamorphism which was closely followed by extensive migmatisation.

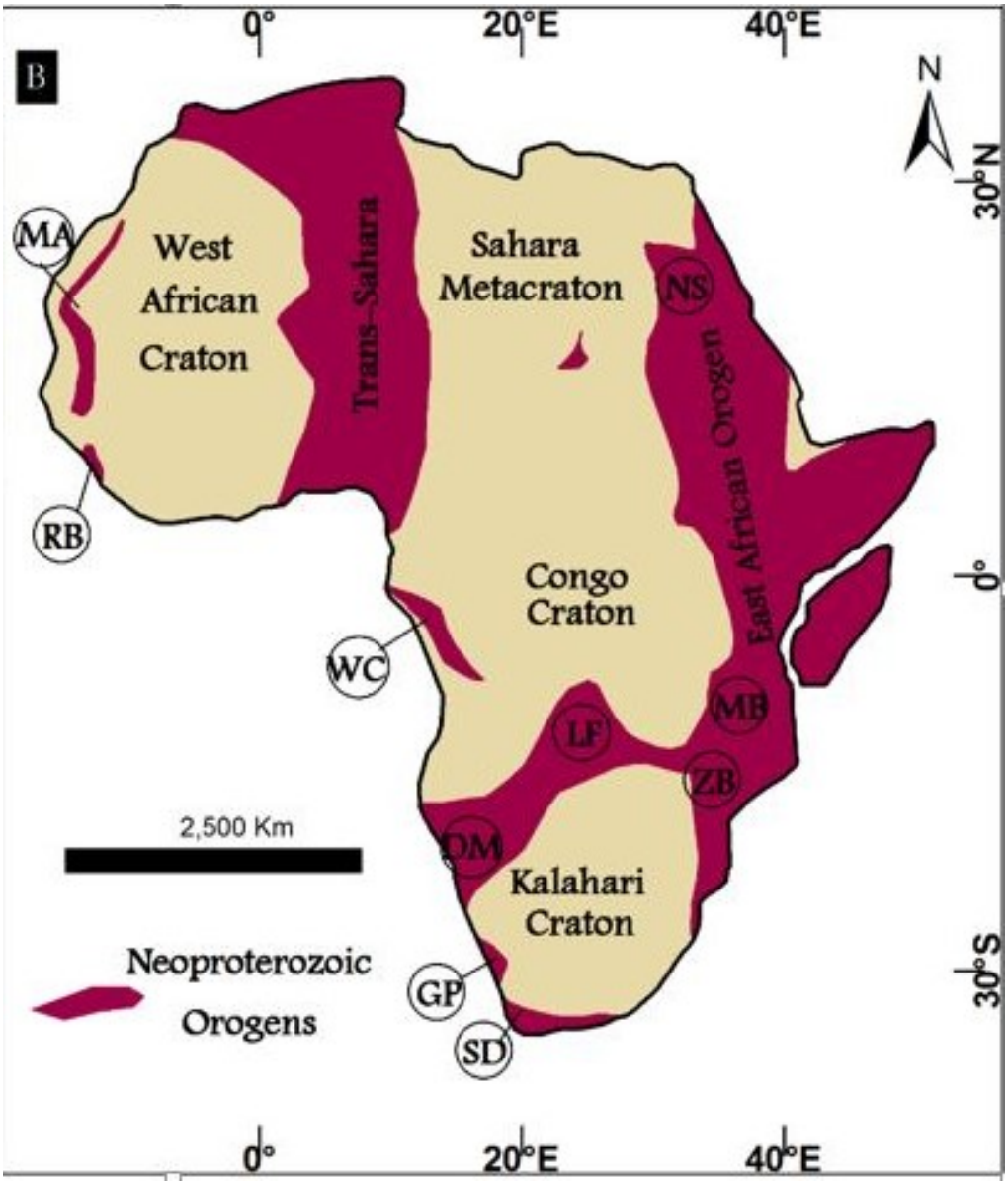

Fig. 2.1.Map of Africa showing the cratons and areas of Pan African Orogeny(Modified after Unrug, 1998).DM – Damara, GP – Gariep, LF – Lufillian fold belt, MA – Mauritanides, NS – Nubian shield, MB – Mozambique belt, RB – Rockelides belt, SD – Saldania, WC – West Congo belt, ZB – Zambezi belt.

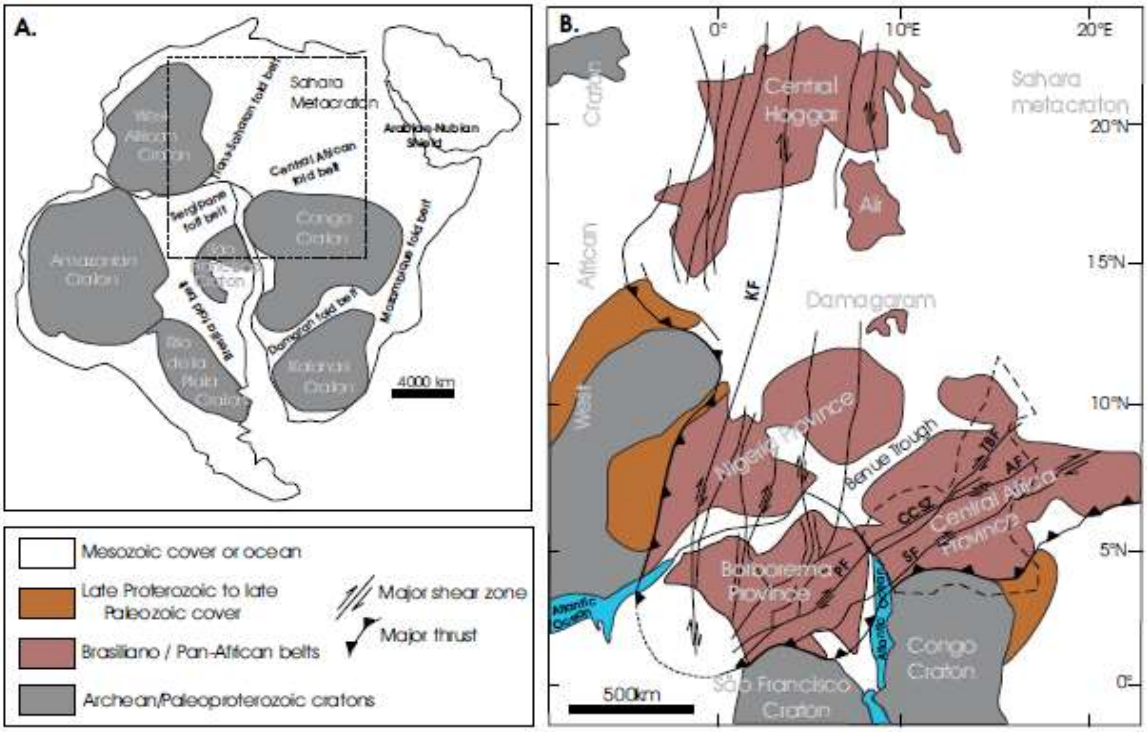

Fig. 2.2: **(a) diagram showing the Pan-African/Brasiliano cratons and major orogenic belts within Western Gondwana adapted from Trompette (2000) and Abdelsalam et al. (2002). (b) Geological sketch map of west-central Africa and northern Brazil showing the cratonic masses and the Pan-African/Brasiliano provinces in a Gondwana (pre-drift) reconstruction (modified from Castaing et al., 1994). TBF: Tcholliré-Banyo Fault, AF: Adamaoua Fault, CCSZ: Central Cameroon Shear Zone, PF: Pernambuco Fault, SF: Sanaga Fault, KF: Kandi Fault.**

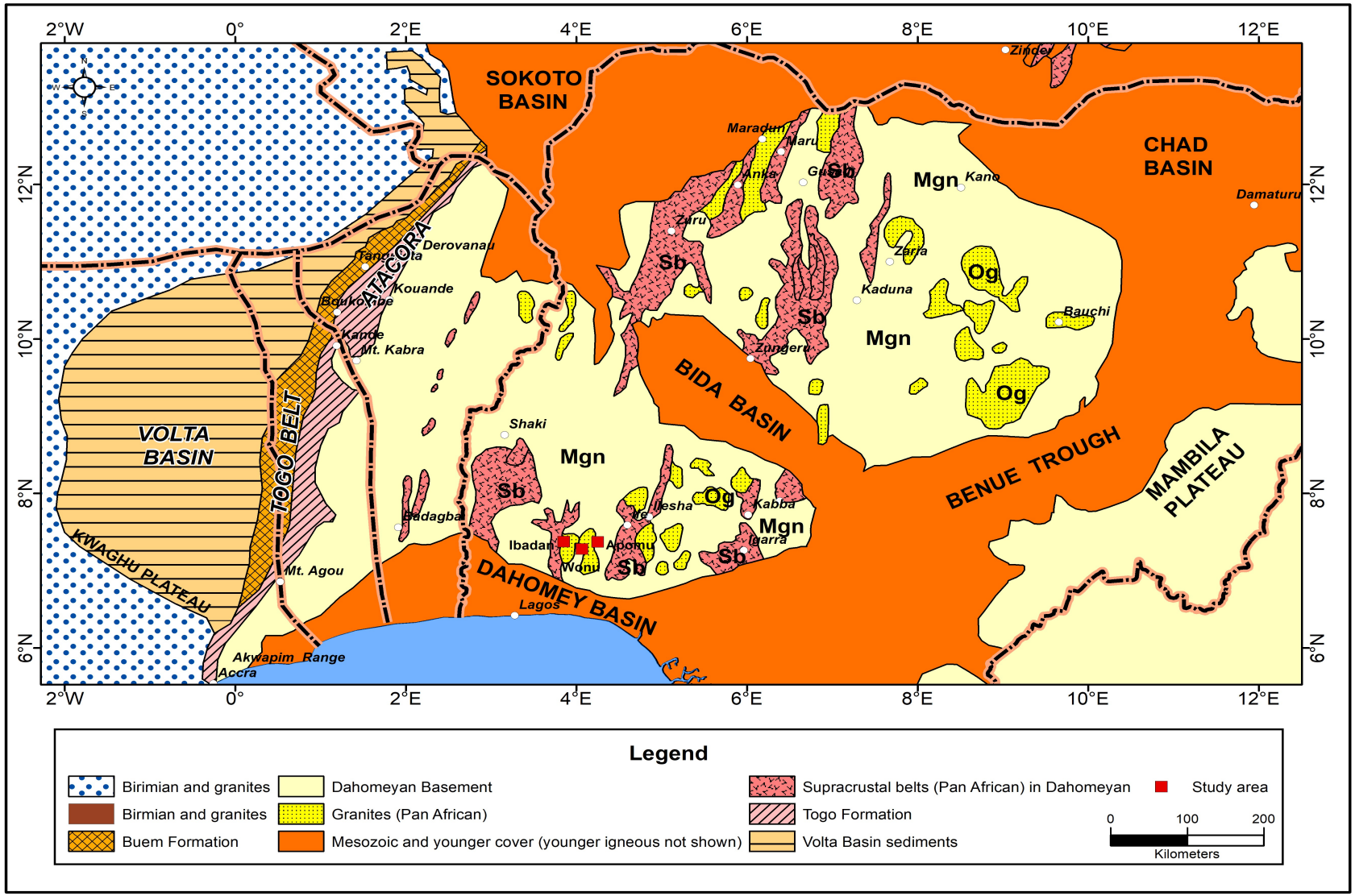

Fig. 2.3: Geological map of Nigeria indicating the location of Ibadan within major rock units (after Wright, 1985).

The last cycle, the Pan-African orogeny (tectonism), was followed by a regional metamorphism, migmatization and extensive granitization and gneissification which brought forth syntectonic granites and homogeneous gneisses (Abaa, 1983). Late tectonic emplacement of granites and granodiorites and associated contact metamorphism accompanied the latestages of the last deformation. The final events of the tectonism included faulting and fracturing. Each of these orogenic cycles were associated with some major rock types (Ajibade *et al*, 1987; Kehinde Phillips, 1991). For example, the imprints of the Liberian orogeny were recorded mainly by banded gneiss in Nigeria.

Many lithostratigraphic divisions of the basement have been proposed by different workers (Elueze 1980; Odeyemi, 1981). Six main groups of rocks have been submitted by Rahaman, (1976). Adekoya *et al* (2003) later subdivided the rocks of the Basement Complex of Nigeria into four main petro-lithological units. These are the migmatite-gneiss-quartzite complex, the schist belts (metasedimentary and metavolcanic rocks), the Older Granite (Pan-African intrusive series) and the minor of felsic and mafic intrusives

2.1.1 The Migmatite-Gneiss Complex

The migmatite-gneiss complex has the most widespread occurrence in Nigeria. It is the most ancient rock unit that evolved through at least three to four polycyclic orogenies. Apart from the Early to Mid Archaean ages (> 3000 Ma) obtained by Ekwueme and Kroner (1993), which was interpreted to reflect initiation of crustal formation (sedimentation) in the Leonean, the Liberian (ca. 2700 ± 200 Ma, Rahaman, 1988; Dada *et al.,* 1993; Annor, 1995), the Eburnean (ca. 2000 ± 200 Ma, Rahaman, 1988; Ocan, 1990; Annor, 1995), the Kibaran (ca. 1100 ± 200 Ma, Ogezi, 1977; Ferre, *et al.,* 1996), and the Pan-African (ca. 600 ± 150 Ma, Ogezi, 1977; Ferre, *et al.,* 1996) ages reflected metamorphism during the subsequent orogenic events. According to Rahaman (1976) and Odeyemi (1981) the Migmatite-Gneiss Complex of southwestern Nigeria is composed of early gneiss, mafic-ultramafic gneiss and schist, and granitic components.

Early gneiss: It is either medium-grained or coarse-grained, light to dark grey, with thin leaf-likelayers of biotite, hornblende quartzo-feldspathic rocks of tonalitic to granodioritic composition. The foliation is distinguished by segregation

of light coloured minerals (quartz and feldspars) and dark colouredminerals (biotite and/or amphibole) into distinct bands 2-5mm wide, with preferred alignment of the long axes of the ferromagnesian minerals. More commonly, however, the quartzfeldspathic bodies take the form of impersistent streaks only a few mm or less thick, invariably aligned parallel to the foliation as defined by the mafics.

Mafic-ultramafic gneiss: The mafic component include bands, lenses and concordant sheets of amphibolites, amphibole shists, marble, calc-silicate rocks, biotite and biotite hornblende gneisses. The bands, lenses and sheets are foliated with the foliation being concordant with the foliation in the gneisses. Irregular quartzo-feldspathic veins sometimes form a continuous network cuttinglarge amphibolitic sheets into irregular blocks. It may be difficult to differentiate the mafic-ultramafic gneiss from similar occurrences in the schist belts, which are presumably younger in age (Pan-African).

Felsic (granitic) components: The felsic component is of granitic composition and varies from fine-grained to pegmatitic texture. It is usually present as concordant to discordant discrete bands, veins and dykes, which, in places, show pinch and swell structures and ptygmatitic folds or as swarms of augen-shaped porphyrobalsts of white or pink microcline. These are usually aligned following the pre-existing foliation in the host rocks. A prominent member of the felsic component is granite gneiss, which can occur as mappable units within the migmatite. Some of the felsic components are augen gneisses which occur locally. Interaction between the felsic components and augen components and the early gneiss produces different types of migmatites. The most common lithology developed from such interaction is the banded gneiss. It is composed of parallel, alternating dark and light layers. The banding is usually parallel to the foliation (Rahaman, 1976, and Odeyemi, 1981).

2.1.2 The SchistBelts

The schist belts of Nigeria are composed of low grade metasediment dominated belts trending N-S (Figs. 1.2 and 2.3). They are more prevalent in the western half of Nigeria. (Turner, 1983). Some schist belts have been reported in the eastern area of Nigeria. (Ekwueme and Kroner, 1997). The rock typesof the schist belts include psammites, quartzitesand quartz schists, biotite schists,

muscovite schists, graphitic schists, banded iron formations and carbonate rocks (marbles or dolomitic marbles). Other minor rocks include amphibolites, amphibole schists, talc-bearing schists, serpentinites and pyroxenites, metaconglomerates and calc-silicate rocks (Elueze 1985; Odeyemi, 1988; Ige and Asubiojo, 1991; Elueze and Akin-Ojo, 1993; Adekoya, 1988; 1995; 1996; Olobaniyi *et al.,* 2001; Elueze and Okunlola, 2003; Olobaniyi and Annor, 2003; Danbatta and Garba, 2007; Olobaniyi and Mucke, 2011, Bolarinwa and Adepoju, 2017). They are distinguishable from the older ancient metasediments of the migmatite-gneiss complex in terms of age and contact relationship, which may be sharp due to shearing, faulting and thrusting or gradational at intrusive contacts. Some workers including Bolarinwa and Adeleye (2015) have suggested tectonic evolution characterized by faulting and rifting of back arc basins and island arcs for the formation of the schist belts. The variations observed in the lithologies of the schist belts from the west to the east may reflect the depths of deposition of the sediments.

The petrogenesis of the amphibolites in the schist belts have been very controversial. Klemm *et al* (1984) suggested that the Ilesha Schist Belt may be an Archean greenstone belt. Ogezi (1977), affirmed continental crust processes in the petrogenesis of the schist belts. Some other workers affirmed that some of the rocks have ensimatic tholelitic materials. They all agreed that metamorphic grades ranged from greenschist to lower amphibolite facies.

2.1.3 The Pan African Granitoids

They are also called Older Granites. They are syntectonic to late tectonic granitoids which intruded both the migmatite complex and the schist belts. The Older Granites are Precambrian suites of plutonic gneissose granites, coarse porphyritic granites, fine grained granites, adamellites, granodiorites and quartzdiorites, which occur as conspicious batholithic masses in many places within the Basement Complex. They are generally typified by a thick piling of euhedral to subhedral feldspar phenocrysts. Granodiorite and quartz-diorites are wide-reaching though they are limited in extent. They consists of biotite, feldspar and quartz which weather into clays depending on the amount of biotite present. (Odeyemi, 1981).

The Older Granites are Pan-African (ca. 600 ± 150 Ma) in age, and hence older than the tin-bearing Jurassic (ca. 180 Ma), anorogenic Younger Granites of Jos Plateau (Falconer, 1911; Adetunji, *et al.,* 2015, 2018). They vary in size from minor circular intrusives to bottomless, extended plutons covering several kilometres. They intrude both the migmatite gneiss and the schists with which the commonly have diffused, sheared or migmatised contacts and sharp intrusive contacts, respectively.

2.1.4 Minor Felsic and Mafic Intrusives

The minor felsic and mafic intrusives cut across the migmatite-gneiss-complex, the schist belts and the Older Granites suites. These include felsic intrusives that are related with the late to post tectonic Pan-African granitoids(Dada 2006). The mafic intrusives are more often regarded as the youngest rocks in the Nigerian Basement Complex, which comprises syenitesdykes, gabbro, pyroxenites, serpentinites and lamprophytic dykes. Radiometric dating gave an age of about 580 to 478 ± 19 Ma.(Grant, 1970).

2.2 Review of Previous Works on Mafic and Metaultramafic Rocks

Several research works have been conducted by different researchers on the mafic and metaultramafic rocks occurring in the southwestern part of the Nigerian Basement Complex. The emphases of these investigations have been essentially centred on petrochemistry of the protolith basaltic rocks, in order to unravel its petrogenesis and possible provenance of associated gold mineralization.

The schist belts of southwestern Nigeria have been mapped by many workers including Ige (1988) and Kehinde-Phillips (1991). Thereis a general consensus in the division of the petrologic units of southwestern Nigeria into migmatite gneiss-quartzite complex, quartzite and quartz-schist complex, mafic andultramafic complex and the Older Granite complex (Hubbard, 1975; Elueze, 1977; Klemm *et al*, 1978). The mafic-ultramafic complex attracted more attention possibly because of the general belief that it is a possible source rock for the gold mineralization in the area.

Mineralogical studies of the amphibolites by Olade and Elueze (1979), indicated the presence of massive, gneissic, schistose and banded textural varieties of amphibolites around Ilesha area.(Fig. 2.3). Elueze (1982) also identified ore minerals, notably pyrite, chalcopyrite, covellite, pentladite, ilmenite, marcasite,

rutile and arsenopyrite in the amphibolites of Ilesha area. Olarewaju and Ajayi (1993) classified the amphibolites into foliated leucocratic amphibolites (FLA) and massive melanocratic amphibolites (MMA).

Petrochemical and petrogenetic studies using, major, trace and REEs have invariably revealed tholelitic basalts as the ancestral rock for the amphibolites of Ilesha area (Ajayi, 1980). Some workers supported an ensialic tectonic environment while Ajayi (1980) and Rahaman (1988) suggested an ensimatic one for the emplacements of the basalts. Similarly, Olobaniyi (2006) revealed from the mineral chemistry of Isanlu amphibolites a basaltic rock precursor, but showed that the precursor rock materials have been subjected to an earliermetamorphism indicative of amphibolite facies metamorphism.

Mineralogical discrimination of the talc schists revealed talc-tremolite, talc-chlorite, talc-actinolite and talc-anthophyllite schist within the Ife-Ilesha schist belts (Ige, 1988; Ige and Asubiojo, 1991; Kehinde-Phillips, 1991; Akin-Ojo, 1992; Elueze and Akin-Ojo, 1993; Elueze and Kehinde -Phillips, 1992; Kehinde-Phillips and Tietz 1995).

The compositional attributes of the weathered rock mass above ultramfic-mafic rocks have been investigated (Elueze and Kehinde-Phillips, 1992; Ige *et al* 2005); while the industrial suitability of the talc bodies of Ife-Ilesha schist belts have been lucidly highlighted (Elueze and Ogunniyi, 1984; Ige, 1988; Elueze and Akin-Ojo, 1993; Bolarinwa, 2001, Bolarinwa and Adeleye, 2015).

Alteration of ultramafic rocks due to the effects of metasomatic and mineralizing fluids have been documented in literatures. It has been deduced that fluid evolution studies may provide important constraint on the pressure (P), temperature (T) and fluid activity during the metamorphic history of the rock (Harley, 1989).

The talcose rocks and amphibolites occurring within the Ilesha schist belt of Nigeria were studied by Adeleye (2009), who reported the presence of aluminium-bearing pyrophyllite and chromium-bearing clinochlore in the talc schists. Bolarinwa and Adeleye (2015) investigated the petrogenesis of the amphibolites of Wonu, Ibadan-Apomu and Ilesha areas in southwestern Nigeria. They indicated from the chemical data that the amphibolites had tholeiitic basaltic precursor and that the amphibolites were comparable to amphibolites occurring in other areas in Nigeria.

Ersoy *et al*.(2013) worked on the mineral chemistry and physiochemical characteristicsof talc from in Turkey and recognized four mineral groups. Bolarinwa and Adeleye(2015b) showed that the geochemical analysis of the talc bearing rocks of Wonu, Ibadan-Apomu and Ilesha areas reflects close petrogenetic affliation to the amphibolites. They further indicated that the talc bodies possess requisite composition and industrial characterizations to be utilized in several manufacturing industries (Bolarinwa and Adeleye, 2015b).

The distinct components characteristic of talc relies on their parent melt. Prochaska (1989), subdivided talc occurrences into ultramafic affliated talc deposits, talc deposits occurring in dolomites, metamorphism induced talc deposit, talc deposits within banded iron formations and secondary talcose ores. McCarthy *et al.,* 2006 and Gunter *et al.,* 2018 divided talc deposit based on the primary minerals and the conditions prevalent during their alteration; from low-temperature altered peridotite, from low-temperature altered gabbro, from low-grade metamorphosed dolomite and from high grade metamorphosed dolomite.

Linder *et al.* (1992) reported a talc deposit from ultrabasic rocks within aluminosilicate-rich rocks. Talc deposits has variously been reported as products of alteration of serpentinite (Anderson, 1985 and Bafor, 1986), metamorphism of submarine hydrothermal rocks associated with massive sulphide deposits (Nesbitt and Muehlenbachs, 1994;Bjerkgard and Bjorlykhe, 1996), and as products of prograde metamorphism of magnesium-rich silicates (Sandrone, 1993).

Majority of the research works on the mineralogy and geochemistry of talcose rocks have not invariably resolved the controversy on the genesis. Talc deposits in South Korea from magnesium carbonate origin are reported to be of purer and greater economic value than those related to ultramafic-mafic rocks (Park *et al*, 1997).

Shin and Lee (2002, 2003) worked on the contact aureolesof carbonate around granite intrusion and observed that the carbonate contact aureole has been subjected to fluid-rock interactions. The characteristics of the elements in talc deposits were used to constrain the physio-chemical parameters of the talc mineralization. Inadequate data regarding the composition of the mineralizing fluids makes it difficult to understand the affliation between the granitic rocks, contact aureole and talc formation.

2.3 Review of Harmful Effects of Mining of Talc Deposits

Talc could be formed from two major geological processes, namely, hydrothermal alteration of pre-existing mafic rocks and silica-rich dolomitic rocks. The process could be described as serpentinization and steatitization, respectively. These processes give rise to large quantities of asbestos minerals. The metamorphism of siliceous dolomites comsequently results in the formation of the asbestos mineral tremolite.

Economic talc usually comprises of natural mixtures of different minerals. Talc is a soft mineral and can be handled with little effort. Hence, several other materials have been used as replacement for talc. These materials have quantities of asbestos fibre, which can be harmful to health depending on the industrial use. Consequently the purity of economic talc is related to both the petrogenesis of the parental talc deposit and the degree of the talc beneficiation.

Undue exposure to talc dust from talc mining sites or industries utilizing the talc, could be linked to a diffuse interstitial lung scarring, which have been referred to as talcosis. With the aid of electron microscopy, amphibole and chrysotile asbestos fibres has been observed in lung tissues of some workers in the talc industry. Hence, utilizing talc products as lubricants and drying agents in food and foods packaging products should be scrutinized so as not to pose a health hazard in the gastrointestine system if ingested.

Research works have been carried out on the harmful effects of talc mining on the health of human beings. For instance, Balliranoet (2008) worked on the amphibole fibers environmental problem related to the proposed drilling of the Susa valley railway tunnel with a view to give advice on how to minimize human exposure to the potentially harmful materials. Lemen(2015), Ilgren *et al.*(2015), Ilgren and Hoskins(2018 a,b,c, 2019), McNamee and Gunter(2014) also worked on the role of anthophyllite abestos and the attendant mesothelioma risk when human beings are exposed to the talc dust.

The biological activity of the talc fibers has been attributed to numerous factors, which include chemical composition and harmful materials (Mastrantonio *et al.* 2002). Bignon *et al.* 1996, suggested that due consideration ought to be given to the impacts of asbestos on the ascent of plueral mesothelioma. Inspite of this, the system through which asbestos fiber leads to cancer is not yet totally apparent.

The problem of human exposure to the airborne mineral dusts in daily life has recently become very relevant. Apart from epidemiological investigation related to environmental exposure to fibers, there is a need for a prediction of excavation effects on the amount of fiber released into the environment. Tremolite has been proved to be very useful in the activation of biological reactivity (Turci *et al*. 2007).

Gazzano *et al*. (2007) discovered that tremolite-cell interaction relies on fiber morpho-structural, optical features and chemical components. Ballirano *et al*.(2008), used chemical, structural and spectroscopic characterization utilizing a combination electron microprobe analysis and other mineralogical analyses on the tremolite to give comprehensive crystal-chemical insights to evaluate relationships involving mineralogical patterns and human activities.

CHAPTER THREE

METHODOLOGY

3.1 Geological Field Sampling

Field studies including geological mapping of Wonu, Ibadan-Apomu area were conducted between 2013and 2018. Traverses were made through major and minor roads as well as footpaths in the study area. The good network of roads and footpaths provided unrestricted access to outcrops and profiles along road cuts. Outcrop locations and other relevant features were noted and writtenin the field notebook. Specific and important geographical information on the field were collected with the aid of radio direction finder. Such information include, location of outcrops and elevation. Digital camera was used to obtain photographs of various geological features observed on the field.Strike and dip of foliations, trends of lineations and joints were carried out using a compass clinometer. Fresh migmatite, amphibolite and granite samples were chipped from outcrops using a sledge hammer. Talc schist samples were also collected in other to determine their alteration phases. The rock samples were chiselled from the exposed rock units which were scattered in the area. The samples collected were numbered according to their locations, prepared and transported in sample bags to laboratory for analysis.

3.2 Sampling and Sample Preparation

Fresh representative samples of migmatites, amphibolites, talcschists and granites and pegmatites were chiselled from the outrops inthe study area. A total of one hundred and five (105) samples were collected. Thin sections were made from the rock samples in the petrographic laboratory of the Department of Geology, University of Ibadan, where detailed study of the various rock types were also observed. Polished thin sections were also prepared at the thin section laboratory of the Department of Geology, University of Johannesburg, South Africa. Selected

representative samples were ground, and pulverized in an agate mortar,to fusible-finess for geochemical analysis.

3.3 Petrographic Analysis

Thin sections were cut from small chips from rock pieces. The chips were grounded on a glass plate to produce a smooth glassy surface, which was then put on a heating surface to dry. A gum was used to glue the dried rock chip to the glass surface and was kept for twenty four hours. The chips were later subjected to grinding with silicon carbide to give a very thin layer. Fifteen samples each from the six rock samples were prepared in this way.

The minerals in each thin section were identified using their optical characteristics under plane and crossed polarized lights of the petrological microscope, such as, texture, colour, cleavage, twining, extinction and pleochroism. The modal compositions of the rocks in each of the thin sections were visually estimated.

3.4 X-Ray Diffraction Analysis

X-ray diffraction analysis is utilized for the qualitative cum quantitative study of geologic materials. Finely ground non-oriented samples of the talcschist were scanned at the Department of Geology, University of Johannesburg, South Africa using an X-ray diffraction spectrometer. Fifteen representative samples of the talc schist were analysed. The pulverized samples were pressed into an aluminium sample holder and passed through a PanalyticalX'pert pro diffractometer fitted with Cu X-ray source. Other instrumental conditions include:

Voltage:	40kV
Current:	50mA
Range:	3.88º 2θ
Stepsize**:**	0.22º2θ
Time for a step:	2 seconds
Divergence split:	Fixed
Receiving slit:	0.1mm
Sample rotation:	1 rev/sec.

The constituent minerals in the samples were indented and estimated using the peak intensities of the each mineral. The intensities were normalized from PDF database with values of K=1/1cor. The value of K measured and published by different researchers were gathered and depicted in the powder Diffraction database. The use of K factor enables semi-qualitative evaluation of the sample composition.Diffraction peaks obtained were converted from degree 2θ to the d spacing (Å). These parameters were corrected for with Joint Committee on Powder Diffraction Standards (JCPDS, 1974) tables of X-rays powder diffraction traces. The main rock-forming minerals and alteration phases in the talc schist were identified using this method.

3.5 Scanning Electron Microscope (SEM) Analysis

Scanning Electron Microscope (SEM) analysis was carried out on minerals including olivine, pyroxenes, amphiboles, biotite, plagioclase, talc, chlorite, actinolite, tremolite, chromite, spinel, magnetite and ilmenite, using a JEOL 840 SEM with an Oxford Instruments energy dispersive X-ray spectrometer (EDs) link (AN10000 system) housed in the Department of Geology, University of Johannesburg, South Africa (Fig. 3.1). Data were reduced using the ZAF4FLS and link analytical system software.

A focused beam of high-energy electrons were utilized by scanning electron microscope in order to produce a variety of signals on sample surfaces. The signals from electron-sample interactions show sample characteristics such as morphological characteristics (texture), surface analysis, as well as elemental composition, crystalline structure, and sample material orientation. The data were obtained over a targeted area of the sample surface, and a 2D image that reveals spatial variations in these properties was generated.

In the scanning mode, SEM facility can scan areas wideness between 1 cm and 5 microns. The design and function of a SEM is quite analogous to the electron-probe micro-analyzer (EPMA), and there is fairly significant overlap in capabilities between the two analytical instruments. Significant amount of kinetic energy can be produced by the accelerated electrons in a SEM machine, the energy generated, can be dissipated as signals due to electron-sample interactions.

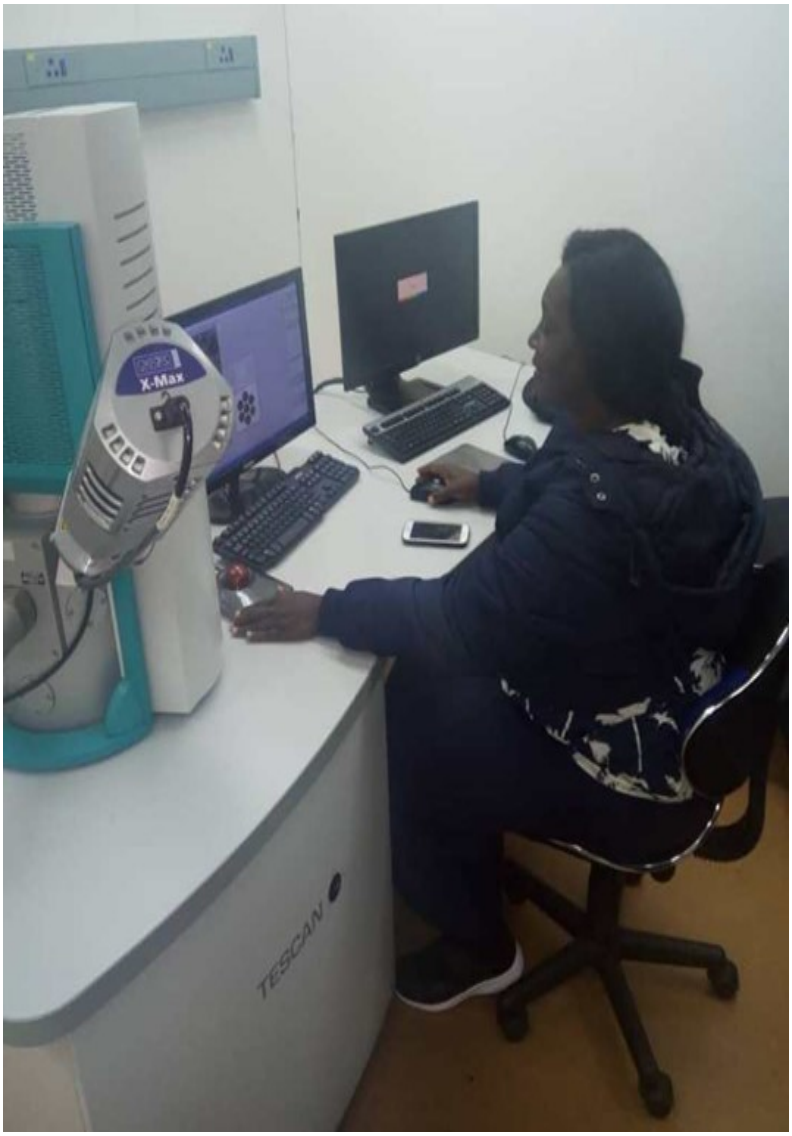

Fig. 3.1: Photograph showing the research student working on the SEM-EDS equipment at the University of Johannesburg, Johannesburg, South Africa.

3.6 Electron Probe Micro Analysis (EPMA)

EPMA is a micro-beam analytical technique utilized essentially for the non-destructive *insitu* chemical analysis of minute rock or soil specimen. It is essentially the same as an SEM (Scanning Electron Microprobe) but has the added function of chemical analysis. The EPMA has the proficiency for accurate, quantitative elemental analyses at very minute "spot" sizes specifically with a wavelength-dispersive spectrometer (WDS).*Insitu*analysis of geological materials and resolution of complex variations within single phases of glasses and minerals in geology are achievable due to the unique standard of caliberation integrated with enhancement to produce intricate pictures of the sample. A far higher resolution images can be acquired using the electron optics of EPMA or SEM compared to visible-light microscope.

In this study, BSE imaging, energy-dispersive spectroscopy (EDS) and wavelength-dispersive spectroscopy (WDS) were utilized to acquire compositional knowledge.Mineral chemistry analysis using EPMA requires preparation of flat, polished thick sections. Samples were prepareds standard rectangular sections of 27 x 46mm. Chips were mounted in epoxy discs, after which they were polished halfway to show a transection of the rock sample. Samples were given a fine polish before the analysis. The polishing produced a flat, uniformly smooth surface.

Since most silicate minerals are electric insulators, targeting an electron beam at the geologic sample can result in sample becoming electrically charged, which must be dissipated. They were thereafter smeared with a thin coating of a carbon that is a conducting substance by means of evaporative deposition, before the analytical procedure started. When the samples were placed in a tray, the surface of the coated sample was put in electrical contact with the tray that was made with a conductive film.

Samples were mounted via a vacuum interlock unto the sample chamber placed on a sample stage (Figs. 3.2a and b). The sample chamber was pumped to create a high vacuum. Condusive operation parameters, inclusive of accelerating voltage and electron beam current, were chosen to start a microprobe session and the electron beam must be focused properly. If quantitative investigations are intended, the machine first needs to be standardized for the desired elements.

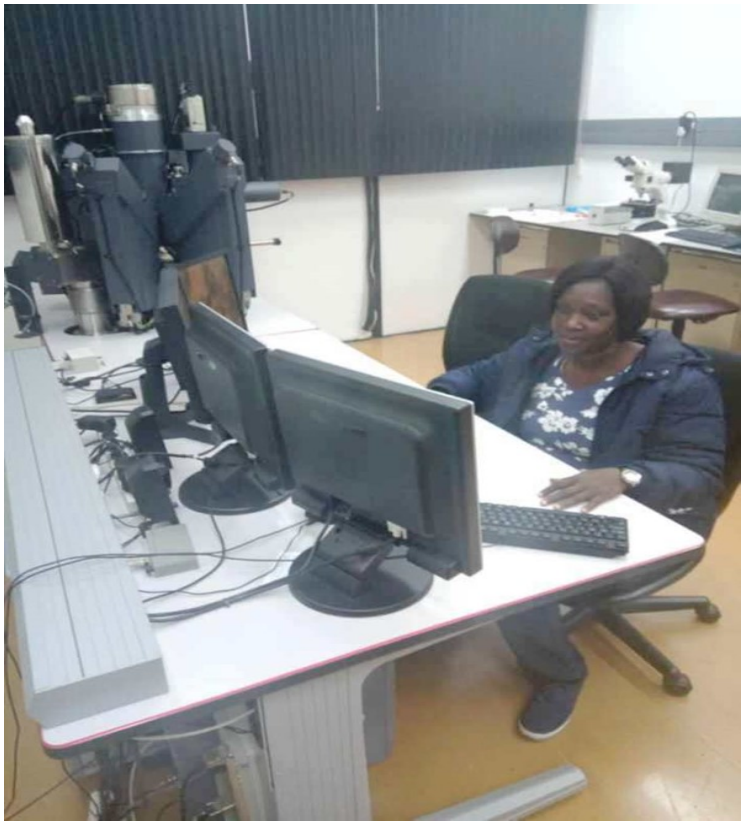

Fig. 3.2: Photograph of EMPA equipment showing research student working on (a) the sample loading section and (b) the computer screen to select mineral probe points at the University of Johannesburg, South Africa.

3.7 Geochemical Analysis

Major, minor and rare earth components in the migmatites, amphibolite, talc schist, granite and pegmatites were analysed at the Department of Geology, University of Johannesburg, South Africa using X-ray fluorescence (XRF) spectrometer and Inductively Coupled Plasma-Mass Spectrometry (ICP-MS). The major oxides were measured in weight percent (wt. %), while the minor and rare-earth components are given as parts per million (ppm).

Twelve samples of the talc and amphibolite in the area of investigation were also analyzed for both major and minor components at Activation Laboratory in Ontario Canada using ICP-MS analyses. The samples of talc and amphibolite were fed into chip monk jaw crusher. The crushed samples were then pulverized to give well ground powder of about 20 mesh size. During the crushing cum pulverizing, adequate attention was paid to avoid contamination by making sure both the crusher and pulverizer were both cleaned with methylated spirit after each sample was crushed and pulverized. The pulverized samples were packed and labelled appropriately and then sent to the laboratory in Canada.

3.7.1 X-ray Fluorescence (XRF) Spectrometry

Major components were calculated on fusion disks, on a PanalyticalMagiX PRO X-ray fluorescence spectrometer (SPECTRUM analytical facility) of the Department of Geology, University of Johannesburg, South Africa. Prior to fusion, Loss on Ignition (LOI) was calculated by the weight difference after ignition of powdered rock samples to 950° C in a furnace for 30 minutes. Fusion discs were made ready by mixing 0.7 g of ignited sample with a 6.1 g combination of lanthanum-bearing lithium borate flux and $LiNO_3$. The mixture was fused in Pt crucibles and poured into Pt molds for casting. Thirty-two USGS and GSJ standard reference samples were utilized for standardization of the XRF spectrometer.

3.7.2 Inductively Coupled Plasma – Mass Spectrometry (ICP-MS)

Trace elements of selected rock samples were determined at the School of Geosciences, University of the Witwatersrand, using a Perkin Elmer Sciex ELAN DRC-e against primary standard solutions and correlated against certified standard rock materials. 50 mg of powdered sample were liquified in a mixture of 3:2 HF and HNO_3 in a high pressure Teflon vessel in a CEM Mars Express Microwave

digester with 40 minute digestion times. Contents were heated until it was dried, in Teflon beakers during several steps of HNO_3 addition and evaporation until the HNO_3 analytical procedure was completed. The resultant solution was made up to 50 ml for analysis. Internal standards (Rh, In, Re and Bi) and calibration solutions were prepared from certified single and multi-element standard solutions. The quality of data was monitored using the international standards BCR-2, and BHVO-2.

3.7.3 Statistical Analyses

Analytical data obtained in this study were subjected to statistical analyses, using office software, such as, Microsoft Excel 2010, Power point and Microsoft office picture manager. Bivariate and ternary plots of the geochemical data were prepared using GCDKIT version 2.3, Petrograph version 2.0 and Grapher 9. Other computer aided software used are Surfer 11 and Adobe illustrator CS. Processing software include Global Mapper 11, Winrock and Winzard.

The bulk geochemical data obtained from the rocks were subjected to Person product-moment coefficient of linear correlation, using the Statistical Package for Social Sciences (SPSS 10 for Window ®). The significance of correlation coefficient was drawn at 0.05 level, which indicates 5 % or less (Hill et al. 2000).The derived correlation coefficients for major, minor and trace elements are presented as correlation matrices, which provide useful statistical information employed to identify and isolate consistent and highly correlative element pairs that can be used to derive suitable geochemical ratios and in plotting relevant discrimination diagrams to determine the protoliths of the rocks.

CHAPTER FOUR

RESULTS AND DISCUSSION

4.1 Geologyof Wonu, Ibadan-Apomu area

The major lithological units within the area of investigation are; migmatites, amphibolites, talc schist, quartzite, quartz schist, granites and pegmatite (Fig 4.1). The petrography of the rocks, the mineral chemistry of the main minerals and geochemical data from these rocks were used to determine the rock types and their petrogenesis.

4.2 The Granitic Rocks

4.2.1 Migmatites

4.2.1.1Petrography of the Migmatites

Migmatite outcrops occur in the western part of the study area. Some migmatites occur as low-lying ridges around Elewa, Ogunniran and Akanran in the western and southeastern part (Fig. 4.1). The N-S structure corresponding to the major lineament in Nigeria is prominent on the google photograph of the study area shown in Figs. 4.2 and 4.3. These features are depicted mainly by the quartzites, quartz veins and shear controlled pegmatite intrusions. The migmatites are trending northwest-southeast and are commonly banded and folded.(Fig. 4.4). In most of the outcrops the mafic and leucoratic components are intimately intermingled. The felsic quartzofeldspathic bands alternate with mafic bands of biotite and hornblende. The migmatites in the study area have different grain size. A few porphyroblasts were additionally seen on some of the outcrops.(Fig. 4.4).

Apart from the main N-S structural lineaments observed, several N-S trending joints, fractures and rock boundaries were recorded on the migmatite (Figs. 4.1-4.4).Also, there were NW-SE, NNE-SSW and W-E trending cross-cutting joints,fractures, pegmatiteand quartz veins showing evidence of displacement.

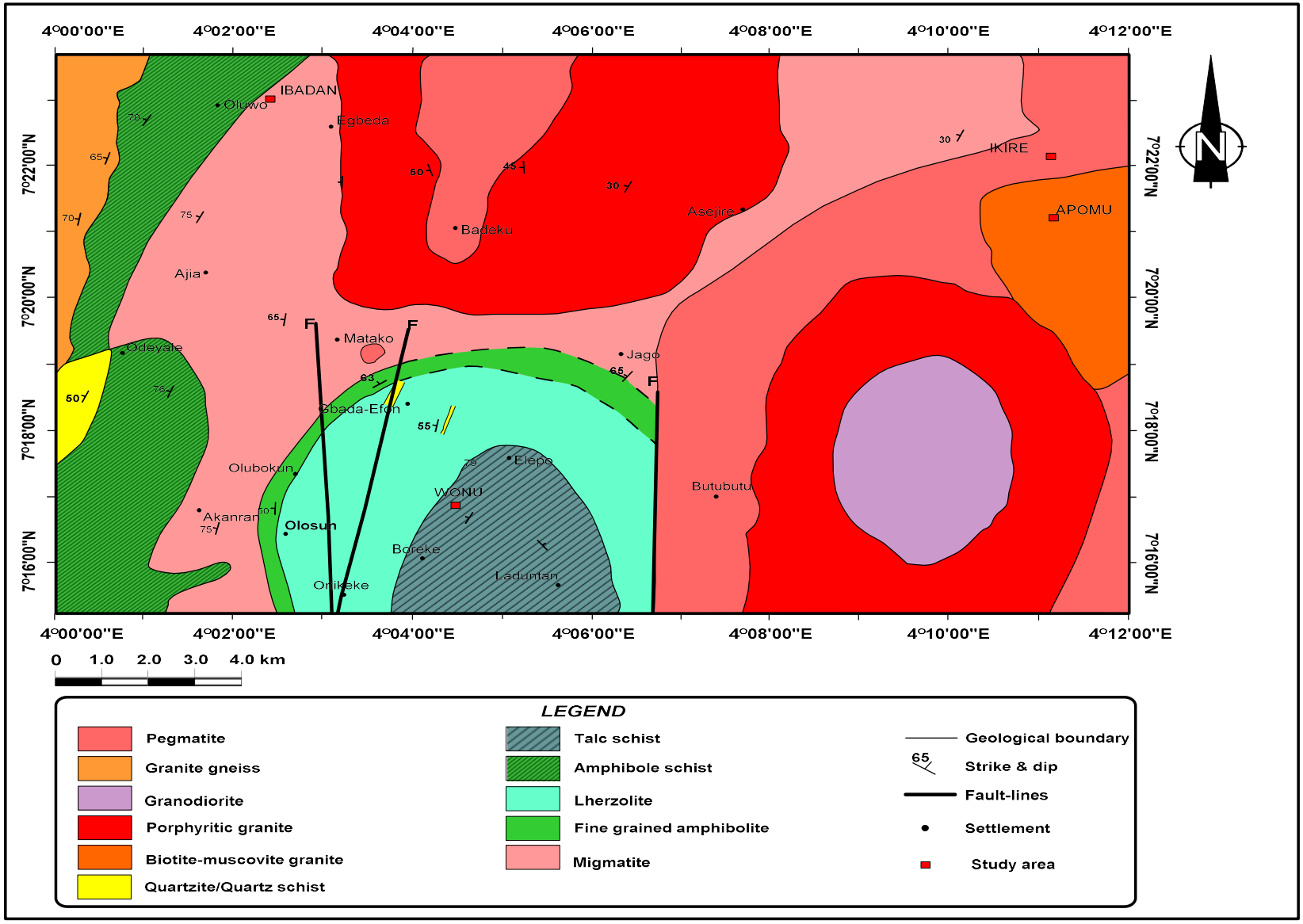

Fig. 4.1: Geological map of Wonu, Ibadan-Apomu and environs indicating talc schist locations.

Fig. 4.2: Aerial photograph of Wonu, Ibadan-Apomu area showing (a) settlements, major roads, vegetation and basement rocks (b) outcrop locations and major NE-SW flowing river.

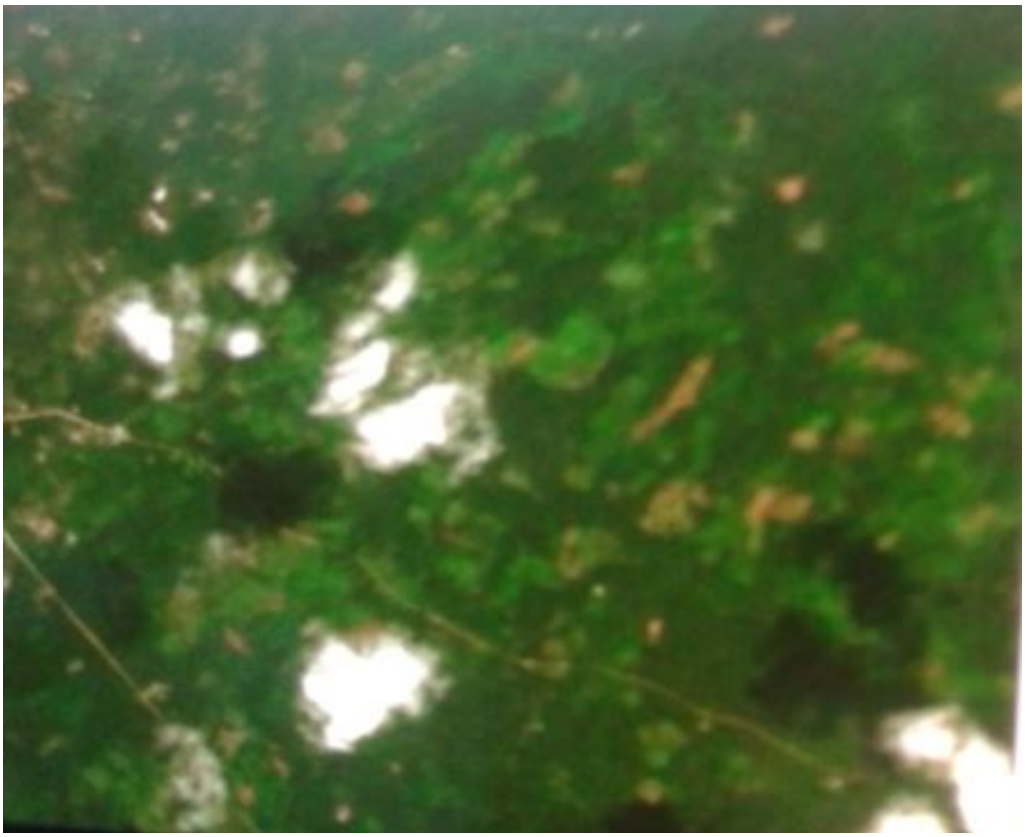

Fig. 4.3: Aerial photograph of Wonu, Ibadan-Apomu area showing felsic (white and brown) and ultramafic-mafic(dark) rock locations.

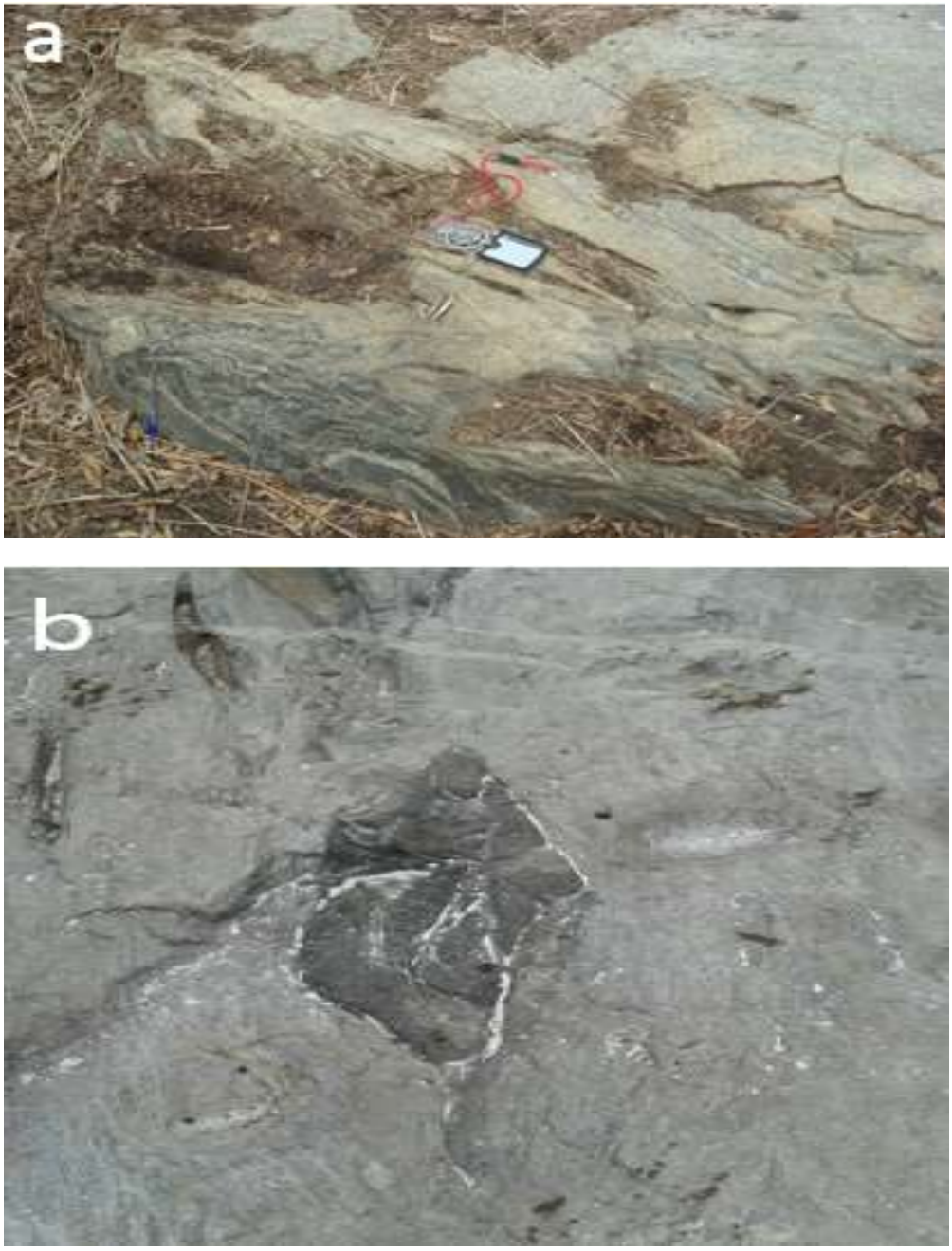

Fig. 4.4: Outcrops of migmatite in Wonu, Ibadan-Apomu area (a) showing kink folds and (b) mafic cumulates.

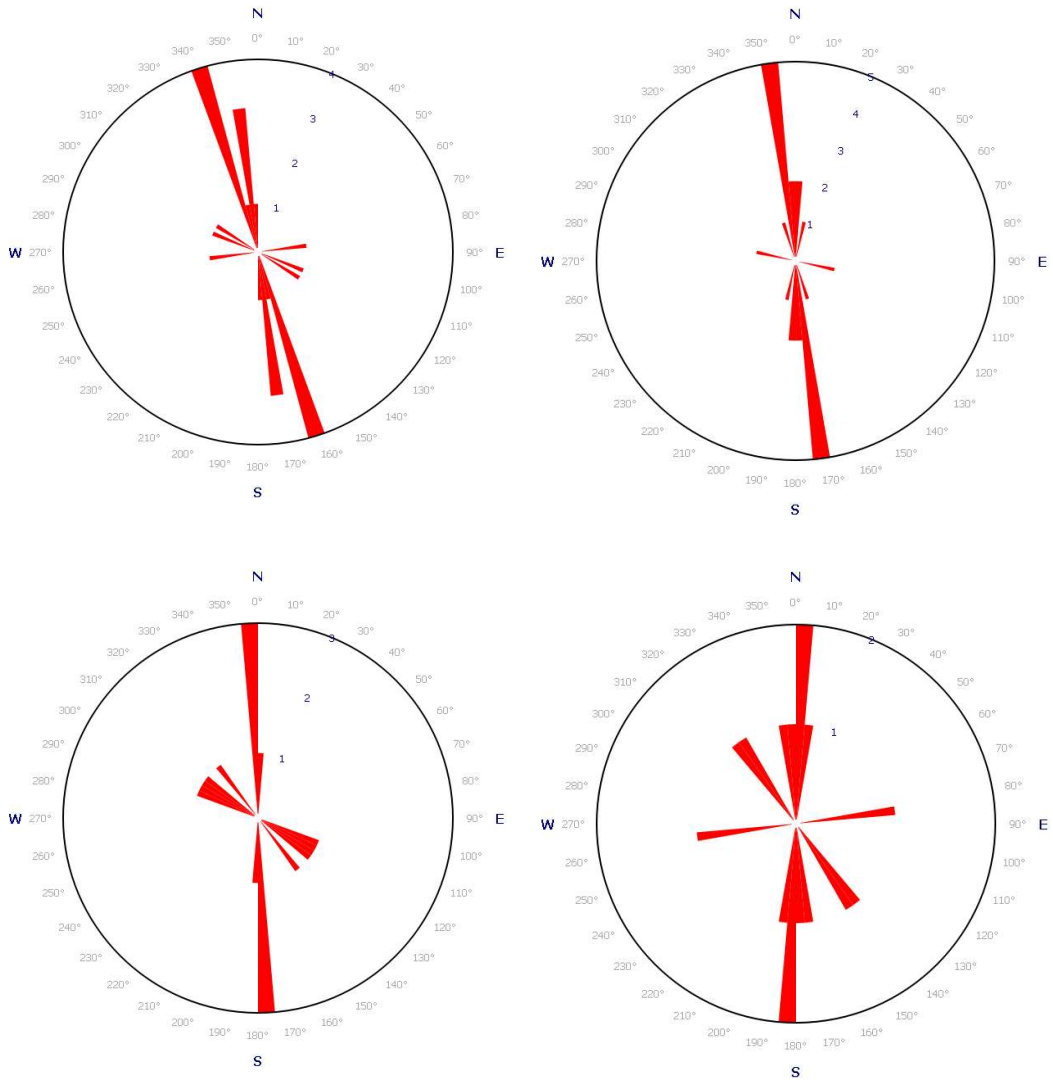

Fig. 4.5: Rose diagram for orientation of strike (Foliation) in (a) the migmatites, (b) talc schists, (c) amphibolites and (d) quartz/pegmatite veins of Wonu, Ibadan-Apomu area.

In thin section quartz (27-30 %), plagioclasefeldspar (28-33 %), microcline (6-10 %), biotite (10-15 %) and hornblende (8-12 %) are essential minerals in the migmatite (Table 4.1). Muscovite is generally ≤ 5 % (Table 4.1). Plagioclase feldspar is colourless with low relief and exhibits multiple twining under cross polar (Fig. 4.6), while microcline exhibit cross-hatched twinning. Accessory minerals present include zircon, rutile, titanite (sphene), ilmenite and magnetite. The felsic band is composed of quartz, feldspar and muscovite while the mafic band is composed of biotite and hornblende.

Plates of biotite with preferred orientation occurs in the rock. It is commonlysurrounded by quartz having a preferred orientation. Smaller crystals of quartz also occur as matrix around biotite. The biotite is identified by its opaque nature, having one directional cleavage, plank like and with mottled appearance under plane polarised light. Under cross polar, it occurs as olive brown to dark brown mineral. The biotite crystal are commonly sheared or granulated indicatingtheir occurrence in a shear zone (Fig. 4.6). Some of the biotite crystals are partially altered to chlorite.

Plagioclase feldspar is colourless and with low relief under plane polarized light and under cross polar. It shows multiple twinning. Inclusions of rutile and pyroxene occur within the plagioclase. Microcline is identified under cross polar as striated alternating light and dark coloured crystals and non-striated white crystal displaying cross-hatched polysynthetic twinning.Quartz is colourless in thin section with its characteristic wavy extinction which may probably be due to metasomatic alteration (Fig. 4.6). In summary, the mineralogy of the migmatite is composed of quartz + plagioclase + biotite +hornblende ± K-feldspar ± muscovite. This mineral assemblage was further confirmed bythe SEM-EDS results of the minerals in the migmatite.

4.2.1.2 SEM-EDS Backscattered Electron Images of Migmatites

The SEM-EDS backscattered electron images of the minerals in the migmatites from Wonu, Ibadan-Apomu area showed the presence of accessory zircon (Spectrum 10) in biotite (Spectrum 8) and oligoclase (Spectrum 9) (Figs. 4.7 and 8). Lath-shaped accessory crystals of ilmenite (Spectrum 5) occur as inclusions in biotite (Spectrum 6) and oligoclase (Spectrum 7) (Fig. 4.9).

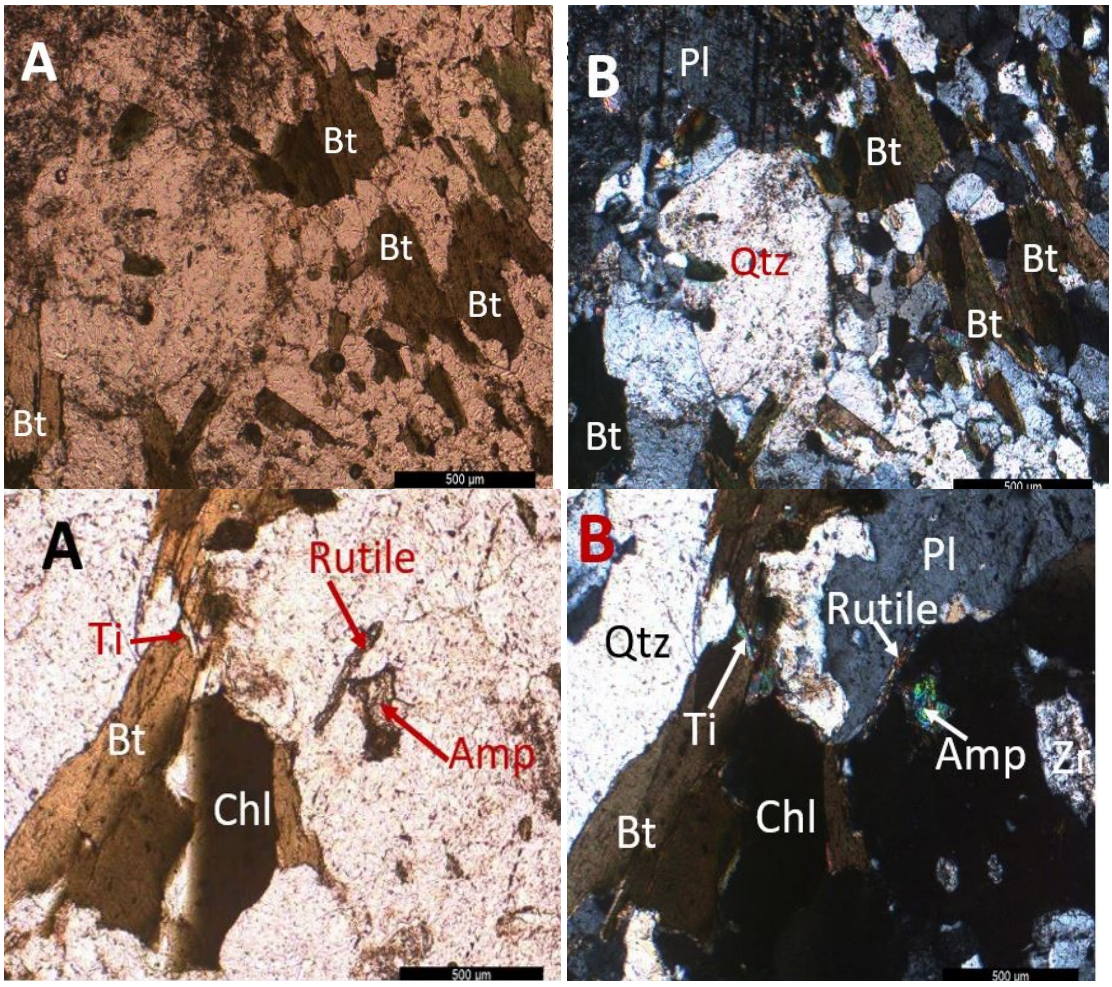

Fig.4.6: Photomicrographs of migmatite from Wonu, Ibadan-Apomu area (a) in plane-plarized light (b) in cross-polarised light. Quartz (Q), Plagioclase (P) (Oligoclase), Microcline (M), Biotite (B), Hornblende (H), Titanite (T).

Table 4.1:Average modal composition of the migmatite of Wonu, Ibadan-Apomu area

	1	2	3	4	5	6	7	8	9
Quartz	27	28	30	29	30	30	29	28	28
Plagioclase	30	28	29	28	31	32	33	30	31
Microcline	9	10	9	7	8	10	10	10	6
Biotite	12	10	11	15	11	12	12	15	12
Hornblende	10	10	9	10	9	8	10	12	12
Muscovite	4	5	3	2	1	3	4	1	2
Zircon	2	3	2	3	2	2	2	2	3
Rutile	1	1	1	1	1	1	1	1	1
Sphene	1	1	1	1	1	-	1	1	1
Ilmenite	3	2	3	2	3	1	2	3	2
Magnetite	1	2	2	2	3	1	1	2	2
Total	**100**	**100**	**100**	**100**	**100**	**100**	**100**	**100**	**100**

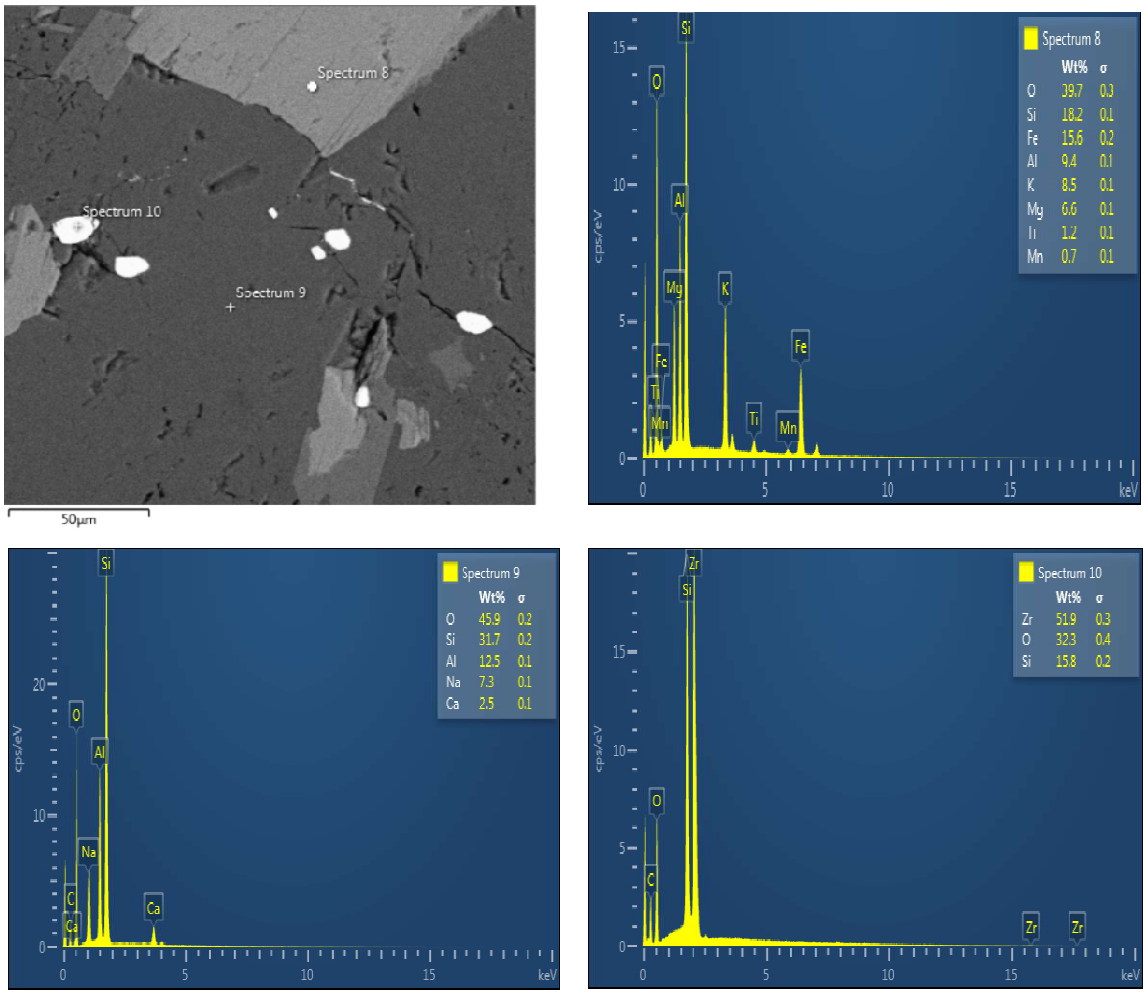

Fig. 4.7: SEM-EDS of migmatite from Ibadan-Apomu area showing biotite (Spectrum 8), oligoclase (Spectrum 9) and zircon (Spectrum 10).

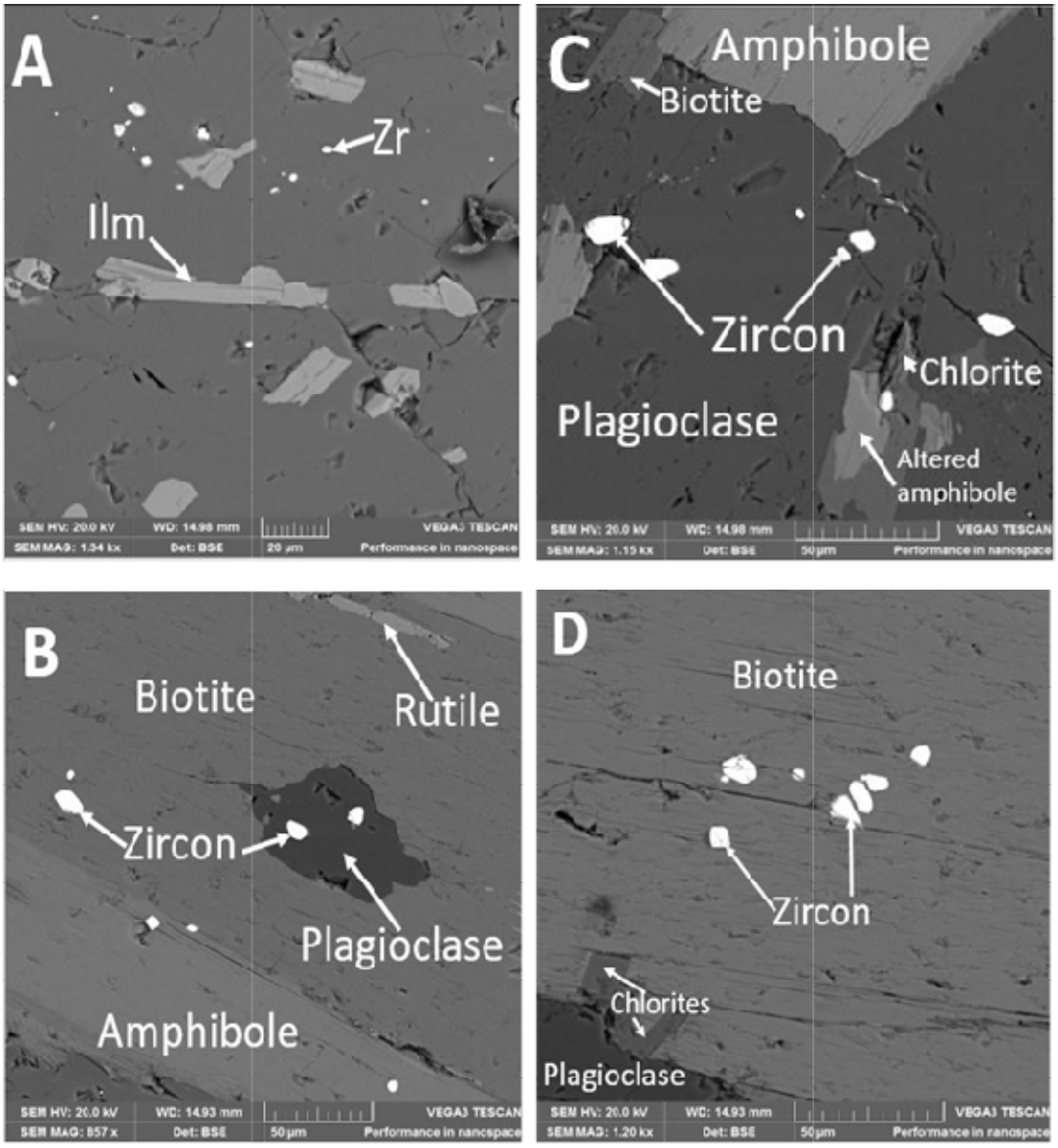

Fig. 4.8: SEM-EDS of migmatite from Ibadan-Apomu area showing amphibole, oligoclase (dark), biotite (grey) and zircon (white dots).

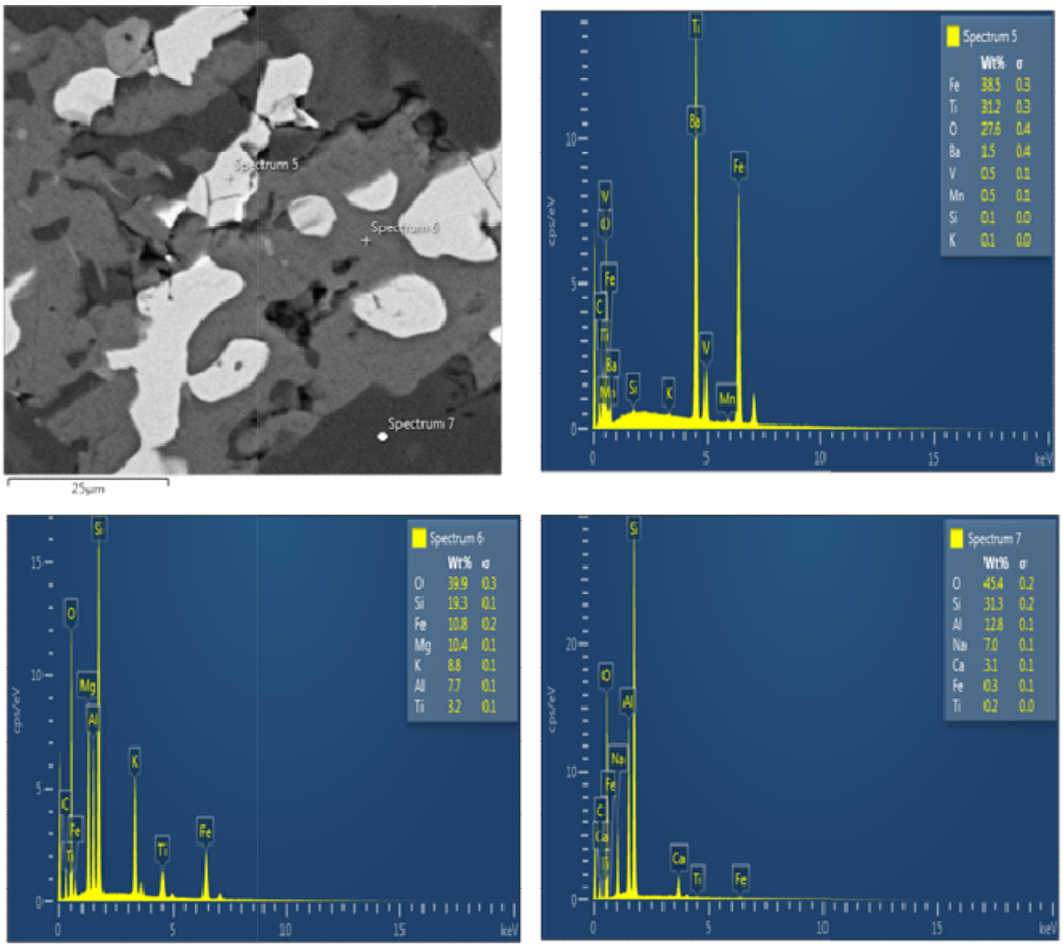

Fig. 4.9: SEM-EDS of migmatite from Ibadan-Apomu area showing ilmenite (Spectrum 5), biotite (Spectrum 6) and oligoclase (Spectrum 7).

4.2.1.3 Mineral Chemistry of the Migmatite

The mineral chemistry of discrete phases in the migmatite of Wonu, Ibadan-Apomu area revealed, quartz, plagioclase feldspar, minor microcline, biotite and hornblende. Minor minerals include zircon, rutile, ilmenite and magnetite.

Biotite in the migmatite

Biotite (k(Mg,Fe)3AlSiO3O10(F,OH)2 is the dominant ferromagnesian mineral in the granitic rocks. The mineral chemistry of the biotite in rocks is used to discriminate magma types and the tectonic setting of the rock sequence.

Representative chemical analyses of the biotite minerals are represented in Table 4.2. Biotite is low in TiO_2,which ranged from 0.65 to 2.29 wt% and high in $Al_2O_3$16.06 to 18.54 wt% and high FeO 15.16 to 23.23 wt%. Based on this composition, the biotite in the migmatite from Wonu, Ibadan-Apomu area could be said to belong to the ilmenite series.

Nachit *et al.* (1985), relate mica composition in granitic rocks to the magma types in which the biotite crystallized. For example the $Al_{(tot)}$ versus Mg classification diagram of the Wonu, Ibadan-Apomu biotite (Fig. 4.10)indicated that they belong to the peraluminous group. A peraluminous chemistry is one in which the mole percent alumina is greater than the combined mole percent of lime, soda and potash (Al_2O_3>$CaO+Na_2O+K_2O$). The peraluminous nature of the rock was reinforced on the Abel-Rahman(1994) Al_2O_3 vs. MgO diagram (Fig. 4.11). This diagram also indicatedimput from S-type sources as shown in Fig. 4.10. The binary plot of total Al^{iv} (apfu) vs. Fe/(Fe+Mg) showed that the biotites inthe migmatite are intermediate between annite to siderophyllite.

Table 4.2: Mineral chemistry of biotite minerals in migmatite

	MN1	MN2	MN9	MN16	MN18	MN19	MN23	MN24	MN29
SiO_2	36.56	36.69	36.84	36.82	35.15	36.52	36.18	32.52	34.76
TiO_2	2.09	2.1	2.22	2.12	1.79	2.29	2.07	0.92	1.4
Al_2O_3	16.5	16.4	16.23	16.34	16.06	16.51	16.06	16.67	15.89
FeO	19.79	19.89	19.45	19.85	20.87	19.83	19.98	23.21	19.71
MnO	0.87	0.81	0.88	0.88	0.89	0.88	0.87	1.06	0.89
MgO	10.15	10.13	10.22	9.98	10.55	9.95	10.07	11.82	9.19
CaO	0.04	0	0.01	0.01	0.04	0	0.03	0.14	0.07
Na_2O	0.08	0.07	0.05	0.05	0.05	0.07	0.05	0.04	0.04
K_2O	9.54	9.66	9.7	9.47	7.95	9.65	9.65	3.66	9.54
Cr_2O_3	0.01	0.01	0	0.01	0.01	0	0.01	0.01	0.01
NiO	0	0.01	0.01	0	0	0	0.03	0.01	0
H_2O*	3.93	3.93	3.93	3.93	3.83	3.93	3.89	3.72	3.73
Total	99.56	99.70	99.54	99.46	97.19	99.63	98.89	93.78	95.23
Structural formulae									
Si	5.583	5.597	5.620	5.623	5.504	5.577	5.582	5.246	5.587
Al iv	2.417	2.403	2.380	2.377	2.496	2.423	2.418	2.754	2.413
Al vi	0.553	0.547	0.538	0.565	0.468	0.549	0.502	0.416	0.598
Ti	0.240	0.241	0.255	0.243	0.211	0.263	0.240	0.112	0.169
Cr	0.001	0.001	0.000	0.001	0.001	0.000	0.001	0.001	0.001
Fe	2.527	2.538	2.481	2.535	2.733	2.533	2.578	3.132	2.650
Mn	0.113	0.105	0.114	0.114	0.118	0.114	0.114	0.145	0.121
Mg	2.310	2.304	2.324	2.272	2.463	2.265	2.316	2.843	2.202
Ca	0.007	0.000	0.002	0.002	0.007	0.000	0.005	0.024	0.012
Na	0.024	0.021	0.015	0.015	0.015	0.021	0.015	0.013	0.012
K	1.858	1.880	1.887	1.845	1.588	1.880	1.899	0.753	1.956
OH*	4.000	4.000	4.000	4.000	4.000	4.000	4.000	4.000	4.000
TOTAL	19.633	19.637	19.617	19.592	19.604	19.624	19.674	19.439	19.722
Y total	5.744	5.736	5.713	5.731	5.994	5.724	5.755	6.649	5.741
X total	1.888	1.900	1.904	1.861	1.610	1.900	1.919	0.790	1.980
Al total	2.970	2.949	2.918	2.941	2.964	2.972	2.921	3.170	3.011
Fe/Fe+Mg	0.522	0.524	0.516	0.527	0.526	0.528	0.527	0.524	0.546

Table 4.2(contd): Mineral chemistry of biotite minerals in migmatites

	MN17	MN10	MN11	MN41	MN40	MN35	MN37	MN43
SiO_2	41.87	46.53	46.19	46.36	50.75	36.37	37.8	36.95
TiO_2	0.37	0.87	0.47	0.88	0.32	1.35	0.65	1.64
Al_2O_3	19.35	29.27	29.97	29.53	29.31	17.06	18.54	16.89
FeO	14.55	5.43	6.11	0.51	5.02	19.66	15.16	19.58
MnO	0.53	0.08	0.09	0.06	0.05	0.87	0.44	0.85
MgO	7.13	1.66	1.49	1.66	1.74	9.97	4.83	9.82
CaO	0.11	0.00	0.01	0.00	0.01	0.01	13.35	0.01
Na_2O	0.01	0.15	0.19	0.13	0.24	0.08	0.03	0.07
K_2O	6.47	10.42	10.25	10.53	10.46	9.79	3.16	9.85
Cr_2O_3	0.00	0	0.01	0	0	0	0.01	0.01
NiO	0.01	0	0	0.01	0	0.03	0	0
H2O*	3.98	4.36	4.37	4.25	4.57	3.91	3.98	3.93
Total	94.38	98.77	99.15	93.92	102.47	99.10	97.95	99.60
			Structural formulae					
Si	6.308	6.398	6.342	6.536	6.664	5.582	5.697	5.632
Al iv	1.692	1.602	1.658	1.464	1.336	2.418	2.303	2.368
Al vi	1.745	3.142	3.193	3.443	3.200	0.669	0.991	0.666
Ti	0.042	0.090	0.049	0.093	0.032	0.156	0.074	0.188
Cr	0.000	0.000	0.001	0.000	0.000	0.000	0.001	0.001
Fe	1.833	0.624	0.702	0.060	0.551	2.524	1.911	2.496
Mn	0.068	0.009	0.010	0.007	0.006	0.113	0.056	0.110
Mg	1.601	0.340	0.305	0.349	0.341	2.281	1.085	2.231
Ca	0.018	0.000	0.001	0.000	0.001	0.002	2.156	0.002
Na	0.003	0.040	0.051	0.036	0.061	0.024	0.009	0.021
K	1.243	1.828	1.795	1.893	1.752	1.917	0.607	1.915
OH*	4.000	4.000	4.000	4.000	4.000	4.000	4.000	4.000
TOTAL	18.555	18.074	18.106	17.882	17.943	19.689	18.890	19.630
Y total	5.290	4.206	4.259	3.953	4.129	5.747	4.118	5.693
X total	1.264	1.868	1.847	1.929	1.814	1.942	2.772	1.937
Al total	3.436	4.744	4.850	4.907	4.536	3.086	3.294	3.034
Fe/Fe+Mg	0.534	0.647	0.697	0.147	0.618	0.525	0.638	0.528

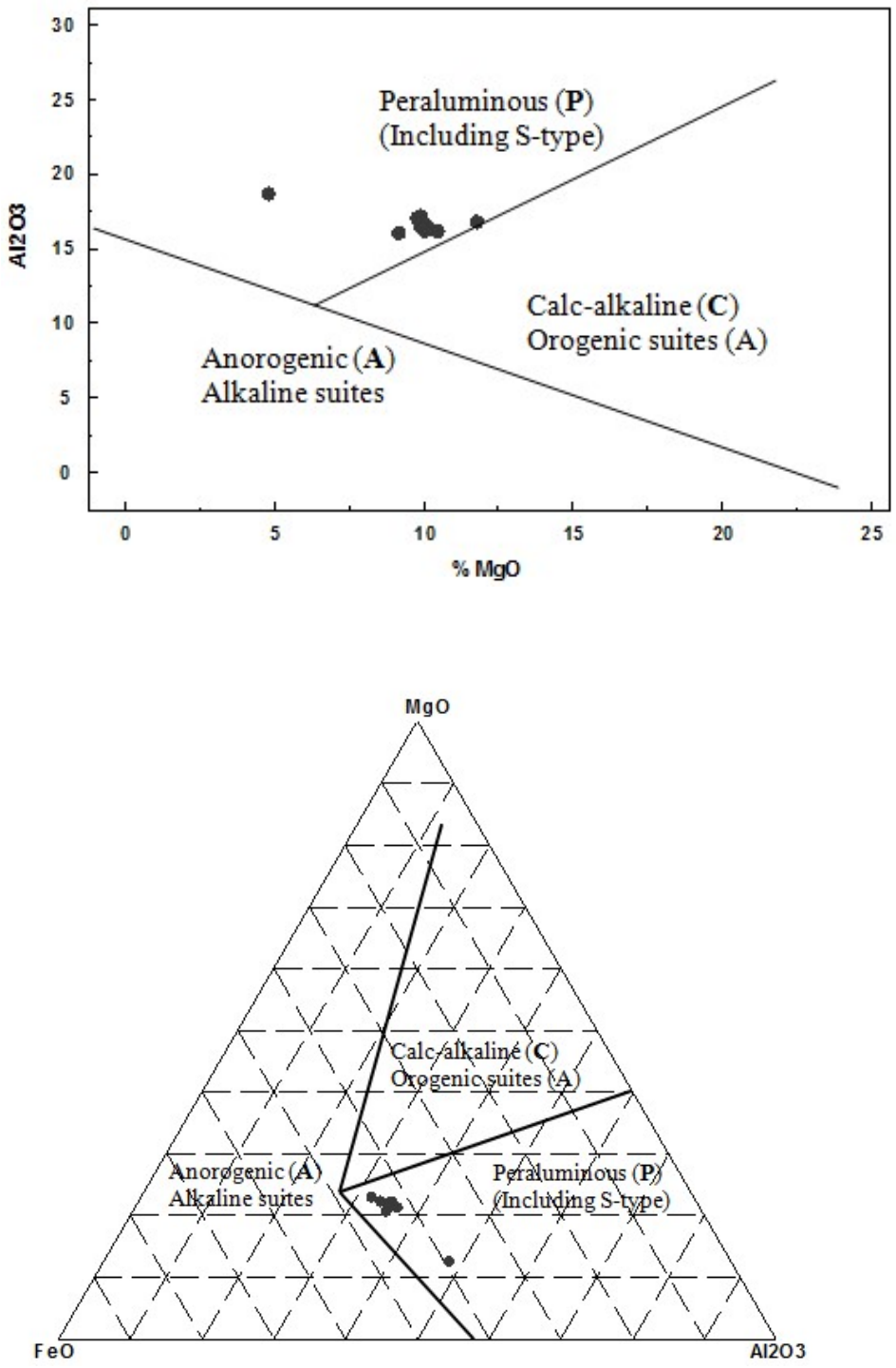

Fig. 4.10: The peraluminous character of the biotite in the migmatite of Wonu, Ibadan-Apomu areas are depicted on the (a) Al_2O_3 versus MgO and (b) MgO–$FeO_{(tot)}$–Al_2O_3 tectonomagmatic biotite discrimination diagram(Abdel-Rahman, 1994).

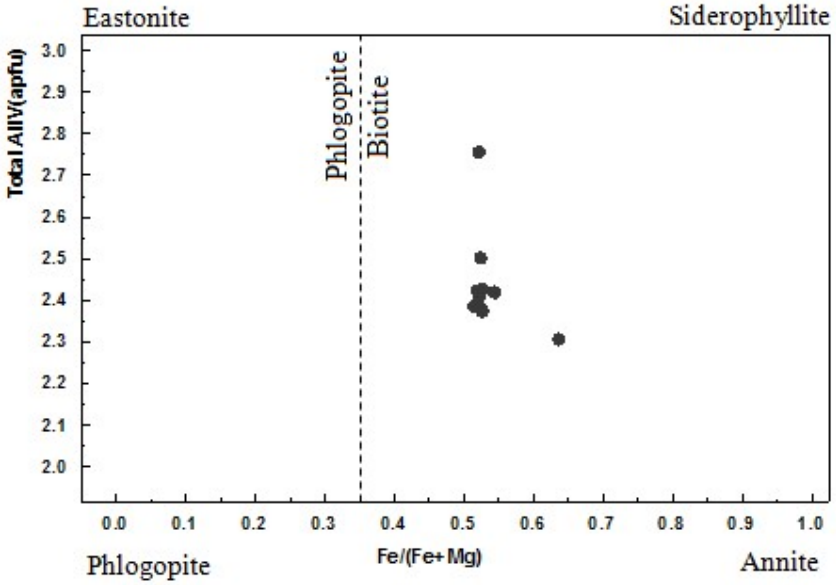

Fig. 4.11: Classification of biotite in migmatite of Wonu, Ibadan-Apomu area (after Deer, 1992).

Amphibole in the migmatite

Representative chemical analyses of amphiboles in the migmatites in Wonu, Ibadan-Apomu area are presented in Table 4.3. The amphiboles vary from green to dark brown. The structural formulae of the amphiboles in the migmatites were calculated on an anhydrous basis assuming 23oxygen atoms.The general formula of amphibole is $AX_2Z_5(Si,Al,Ti)_8O_{22}(OH,F, Cl,O)_2$, where: A could be Na^+, K^+Ca or Pb^{2+}in the A site, X could be Li, Na, Mg, $Fe^{2+}Mn^{2+}$ Ca. Z could be Li, Na, Mg, Fe^{2+}, Mn^{2+}, Zn, Co, Ni, Al^{3+}, Fe^{3+}, Cr^{3+}, Mn^{3+}, V^{3+}, Ti^{4+}, Zr.

Si contents of the amphiboles ranged from 6.59 to 8.22 apfu. The Ca is low and ranged from 0.001 to 0.46 apfu. The Na content ranged from 0.003 to 1.83 apfu. Amphiboles have lower Al^{iv} and higher Al^{vi}. On the basis of the classification of Giret *et al*, (1980),shown on the plot of Na(B) versus (Ca+Na)(B) (Fig. 4.12a), the amphiboles in the migmatite are not calcic but are rather the Fe-Mg-Mn type. Using the International Mineralogical Association (IMA) nomenclaturein Leake *et al.*(1997), on a plot of Xmg versus Si (apfu) diagram (Fig. 4.12b), the amphibole vary in composition from dominantly ferro-hornblende to minor magnesio-hornblende and ferro-actinolite (Fig. 4.12b).

Feldspars in the migmatites

The feldspars (K, Na, Ca (AlSi3O3))in the migmatite of Wonu, Ibadan-Apomu area are zoned and occur as euhedral to equigranular grains. Representative chemical analyses of the feldspars are shown in Table 4.4. Anorthite contents ranged from 10.26 to 16.86, the albite content ranged from 80.84 to 89.04, while the orthoclasecontent ranged from 0.29 to 2.03 (Table 4.4).The chemical data of the plagioclase feldspar plotted on the Ab (albite) - An (Anorthite) - Or (Orthoclase) Deer *et al*.(1963) ternary diagram showed that they are dominantly oligoclase with very few albitecrystals (Fig. 4.13).

K-feldspars are minor constituents in the migmatite. The only spot analysed under EPMA has the composition An 0.00, Ab 5.04 and Or 94.96. The cross-hatch polysynthetic twinning of the K-felspars in thin section clearly showed that they are microcline and not orthoclase feldspars. Thus, the mineral chemistry of the feldspars confirmed that the migmatite are plagioclase-rich and K-feldspar-poor.

Table 4.3: Mineral chemistry of amphibole minerals in migmatites

	MN6	MN17	MN10	MN11	MN41	MN40
SiO_2	58.19	41.87	46.53	46.19	46.36	50.75
TiO_2	0.00	0.37	0.87	0.47	0.88	0.32
Al_2O_3	20.65	19.35	29.27	29.97	29.53	29.31
Cr_2O_3	0.00	0.00	0.00	0.01	0.00	0.00
Fe_2O_3	0.00	0.00	0.00	0.00	0.00	0.00
FeO	0.03	14.55	5.43	6.11	0.51	5.02
MnO	0.00	0.53	0.08	0.09	0.06	0.05
MgO	0.00	7.13	1.66	1.49	1.66	1.74
NiO	0.01	0.01	0.00	0.00	0.01	0.00
CaO	3.06	0.11	0.00	0.01	0.00	0.01
Na_2O	6.67	0.01	0.15	0.19	0.13	0.24
K_2O	0.10	6.47	10.42	10.25	10.53	10.46
H_2O*	2.12	1.90	2.09	2.09	2.03	2.18
Total	90.83	92.30	96.50	96.87	91.70	100.08
			Structural formulae based on 23 oxygens			
Si	8.225	6.595	6.689	6.631	6.833	6.967
Al iv	0.000	1.405	1.311	1.369	1.167	1.033
Al vi	3.440	2.188	3.648	3.701	3.962	3.709
Ti	0.000	0.044	0.094	0.051	0.098	0.033
Cr	0.000	0.000	0.000	0.001	0.000	0.000
Fe^{3+}	0.000	0.000	0.000	0.000	0.000	0.000
Fe^{2+}	0.004	1.917	0.653	0.734	0.063	0.576
Mn	0.000	0.071	0.010	0.011	0.007	0.006
Mg	0.000	1.674	0.356	0.319	0.365	0.356
Ni	0.001	0.001	0.000	0.000	0.001	0.000
Ca	0.463	0.019	0.000	0.002	0.000	0.001
Na	1.828	0.003	0.042	0.053	0.037	0.064
K	0.018	1.300	1.911	1.877	1.980	1.832
OH*	2.000	2.000	2.000	2.000	2.000	2.000
Total	15.978	17.216	16.714	16.748	16.513	16.577
Amphibole group	Alkali	Fe-Mg-Mn	Fe-Mg-Mn	Fe-Mg-Mn	Fe-Mg-Mn	Fe-Mg-Mn
(Ca+Na) (B)	2.000	0.022	0.042	0.054	0.037	0.065
Na (B)	1.537	0.003	0.042	0.053	0.037	0.064
(Na+K) (A)	0.309	1.300	1.911	1.877	1.980	1.832
Mg/(Mg+Fe2)	0.000	0.466	0.353	0.303	0.853	0.382
Fe3/(Fe3+Alvi)	0.000	0.000	0.000	0.000	0.000	0.000
Sum of S2	11.669	13.894	12.761	12.816	12.496	12.680

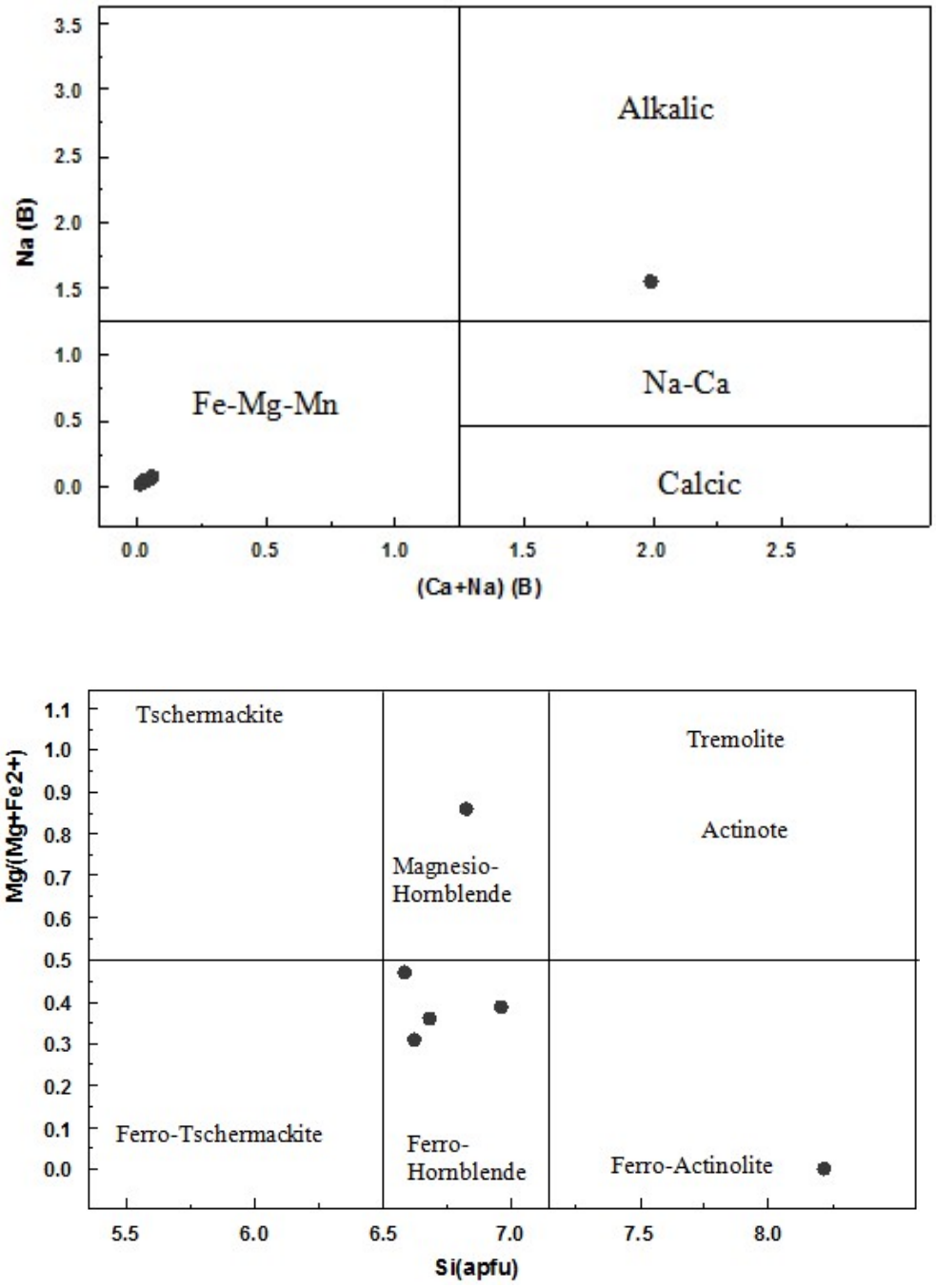

Fig. 4.12: Classification of the amphiboles in the migmatite of Wonu, Ibadan-Apomu area (a)on the *B (Na)* vs *B (Ca+Na)* diagramof Giret *et al.* (1980) and (b) on the X_{Mg} vs Si (apfu) diagram of Leake *et al.* (1997).

Table 4.4: Mineral chemistry of feldspar minerals in migmatites

	86 MN3	88 MN5	90 MN7	93 MN8	106 MN21	107 MN22	128 MN42	133 MN46	112 MN26	87 MN4	110 MN25
SiO_2	64.55	64.65	64.78	64.72	64.37	61.44	63.92	66.3	65.25	67.01	67.26
TiO_2	0.00	0.00	0.02	0.00	0.02	0.00	0.00	0	0.00	0.02	0.00
Al_2O_3	22.26	22.13	22.22	22.31	22.14	20.37	22.54	20.97	22.49	21.69	20.10
Cr_2O_3	0.01	0.00	0.01	0.01	0.00	0.00	0.00	0.01	0.00	0	0.00
Fe_2O_3	0.00	0.04	0.00	0.00	0.13	0.00	0.18	0	0.00	0	0.00
FeO	0.05	0.00	0.01	0.04	0.00	0.13	0.00	0	0.05	0	0.01
MnO	0.00	0.00	0.00	0.00	0.00	0.00	0.00	0	0.00	0	0.00
MgO	0.00	0.00	0.00	0.00	0.00	0.05	0.00	0	0.00	0	0.00
CaO	3.43	3.25	3.39	3.34	3.55	2.11	3.89	1.92	3.55	1.87	0.69
BaO	0.00	0.00	0.00	0.00	0.00	0.00	0.00	0	0.00	0	0.00
Na_2O	9.75	9.91	9.76	9.79	9.87	8.36	9.57	9.21	9.60	10.29	10.97
K_2O	0.08	0.10	0.19	0.10	0.10	0.30	0.18	0.11	0.11	0.08	0.05
Total	100.13	100.08	100.38	100.31	100.18	92.76	100.28	98.52	101.05	100.96	99.08
Structural formula units recalculated based on 8 oxygens											
Si	2.843	2.846	2.846	2.845	2.832	2.940	2.814	2.984	2.853	2.923	2.975
Ti	0.000	0.000	0.001	0.000	0.001	0.000	0.000	0.000	0.000	0.001	0.000
Al	1.156	1.148	1.151	1.156	1.148	1.149	1.169	1.113	1.159	1.115	1.048
Cr	0.000	0.000	0.000	0.000	0.000	0.000	0.000	0.000	0.000	0.000	0.000
Fe^{3+}	0.000	0.001	0.000	0.000	0.004	0.000	0.006	0.000	0.000	0.000	0.000
Fe^{2+}	0.002	0.000	0.000	0.001	0.000	0.005	0.000	0.000	0.002	0.000	0.000
Mn	0.000	0.000	0.000	0.000	0.000	0.000	0.000	0.000	0.000	0.000	0.000
Mg	0.000	0.000	0.000	0.000	0.000	0.004	0.000	0.000	0.000	0.000	0.000
Ca	0.162	0.153	0.160	0.157	0.167	0.108	0.183	0.093	0.166	0.087	0.033
Ba	0.000	0.000	0.000	0.000	0.000	0.000	0.000	0.000	0.000	0.000	0.000
Na	0.833	0.846	0.831	0.834	0.842	0.776	0.817	0.804	0.814	0.870	0.941
K	0.004	0.006	0.011	0.006	0.006	0.018	0.010	0.006	0.006	0.004	0.003
Tot. cat.	5.000	5.000	5.000	5.000	5.000	5.000	5.000	5.000	5.000	5.000	5.000
Tot. oxy.	8.003	7.995	8.001	8.003	7.985	8.118	7.988	8.136	8.022	8.043	8.027
An	16.20	15.26	15.93	15.77	16.49	11.99	18.16	10.26	16.86	9.08	3.35
Ab	83.35	84.18	83.01	83.67	82.96	85.98	80.84	89.04	82.52	90.45	96.36
Or	0.45	0.56	1.06	0.56	0.55	2.03	1.00	0.70	0.62	0.47	0.29
Name	**Oligo**	**Oligo**	**Oligo**	**Oligo**	**Oligo**	**Oligo**	**Oligo**	**Oligo**	**Oligo**	**Albite**	**Albite**

Table 4.4 contd.: Mineral chemistry of feldspar minerals in migmatites

	113 MN27	116 MN30	117 MN31	118 MN32	119 MN33	120 MN34	122 MN36	125 MN39	131 MN44	132 MN45	124 MN38
SiO_2	65.83	62.92	64.46	64.29	64.61	64.12	65.53	64.61	64.14	64.01	63.84
TiO_2	0.00	0.00	0.00	0.02	0.00	0.00	0.00	0.02	0.00	0.00	0.00
Al_2O_3	22.52	23.45	22.62	22.50	22.56	22.50	22.67	22.47	22.45	22.47	18.25
Cr_2O_3	0.00	0.00	0.01	0.00	0.00	0.00	0.00	0.00	0.01	0.00	0.00
Fe_2O_3	0.00	0.11	0.00	0.00	0.00	0.00	0.00	0.00	0.09	0.14	0.00
FeO	0.04	0.00	0.10	0.10	0.12	0.09	0.06	0.05	0.00	0.00	0.00
MnO	0.01	0.01	0.00	0.00	0.01	0.00	0.05	0.00	0.00	0.00	0.00
MgO	0.00	0.00	0.00	0.00	0.00	0.00	0.00	0.00	0.00	0.00	0.00
CaO	3.51	4.88	3.79	3.86	3.71	3.88	3.34	3.50	3.62	3.72	0.00
BaO	0.00	0.00	0.00	0.00	0.00	0.00	0.00	0.00	0.00	0.00	0.00
Na_2O	6.32	9.02	9.38	9.46	9.42	9.46	9.58	9.61	9.68	9.64	0.55
K_2O	0.08	0.12	0.16	0.17	0.24	0.18	0.06	0.13	0.08	0.08	15.76
Total	98.31	100.51	100.52	100.40	100.67	100.23	101.29	100.39	100.07	100.06	98.40
Structural formula units recalculated based on 8 oxygens											
Si	3.033	2.771	2.836	2.830	2.837	2.826	2.860	2.841	2.827	2.823	2.997
Ti	0.000	0.000	0.000	0.001	0.000	0.000	0.000	0.001	0.000	0.000	0.000
Al	1.223	1.217	1.173	1.167	1.168	1.169	1.166	1.165	1.166	1.168	1.010
Cr	0.000	0.000	0.000	0.000	0.000	0.000	0.000	0.000	0.000	0.000	0.000
Fe^{3+}	0.000	0.004	0.000	0.000	0.000	0.000	0.000	0.000	0.003	0.005	0.000
Fe^{2+}	0.002	0.000	0.004	0.004	0.004	0.003	0.002	0.002	0.000	0.000	0.000
Mn	0.000	0.000	0.000	0.000	0.000	0.000	0.002	0.000	0.000	0.000	0.000
Mg	0.000	0.000	0.000	0.000	0.000	0.000	0.000	0.000	0.000	0.000	0.000
Ca	0.173	0.230	0.179	0.182	0.175	0.183	0.156	0.165	0.171	0.176	0.000
Ba	0.000	0.000	0.000	0.000	0.000	0.000	0.000	0.000	0.000	0.000	0.000
Na	0.565	0.770	0.800	0.807	0.802	0.808	0.811	0.819	0.827	0.824	0.050
K	0.005	0.007	0.009	0.010	0.013	0.010	0.003	0.007	0.004	0.005	0.944
Tot. cat.	5.000	5.000	5.000	5.000	5.000	5.000	5.000	5.000	5.000	5.000	5.000
Tot. oxy.	8.360	7.993	8.018	8.005	8.014	8.001	8.036	8.011	7.996	7.995	8.005
An	23.33	22.86	18.09	18.22	17.63	18.29	16.10	16.63	17.05	17.50	0.00
Ab	76.03	76.47	81.00	80.82	81.01	80.70	83.56	82.63	82.50	82.05	5.04
Or	0.64	0.67	0.91	0.96	1.36	1.01	0.34	0.74	0.45	0.45	94.96
Name	**Oligo**	**Oligo**	**Oligo**	**Oligo**	**Oligo**	**Oligo**	**Oligo**	**Oligo**	**Oligo**	**Oligo**	**K-feldsp**

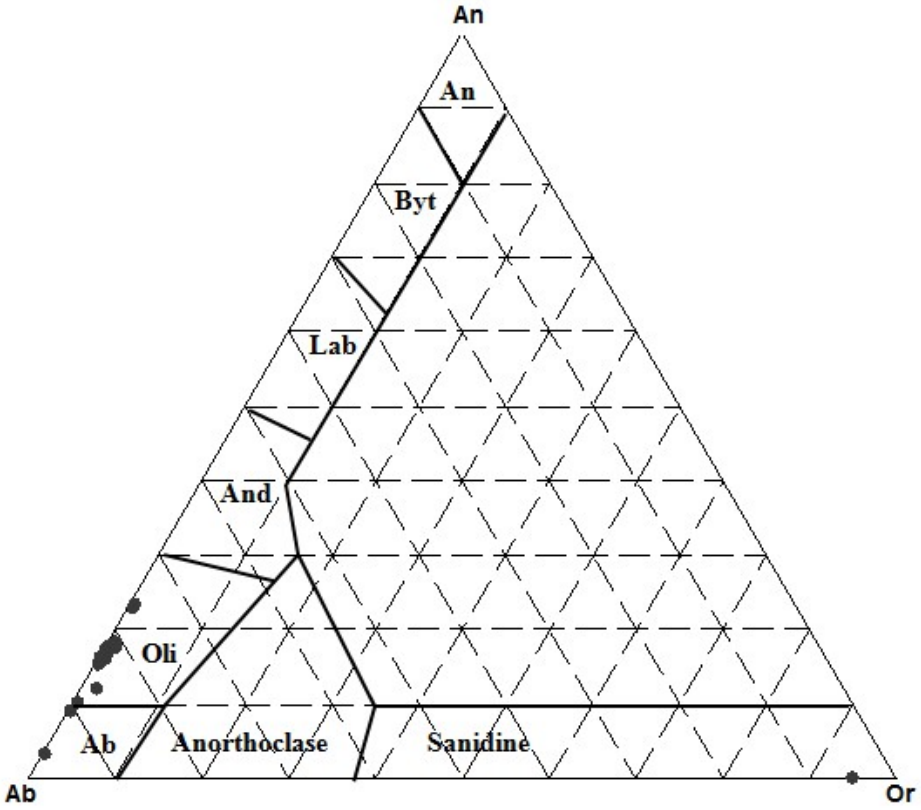

Fig. 4.13: Feldspar varieties in migmatite from the study area (Deer *et al.*, 1963).

4.2.1.4 Interpretation of the tectonic environment based on geochemical analysis of the Migmatite

Major oxides and traceelements in the migmatite in Wonu, Ibadan-Apomu area are given in Table 4.5. The average SiO_2contents is 68.87%. The Al_2O_3ranged between 14.15 – 16.95% while the Fe_2O_3 contents ranged from 2.72 – 4.03%. Also, the MgO values are between 0.04 – 0.91%. The MnO ranged between 0.04 – 0.85% while TiO_2contents are between 0.32 – 0.58%. The values of CaO ranged between 2.02 – 3.01%. These values are comparable to those of the granites in the investigated area. The K_2O values, which ranged between 3.77 – 5.54% and Na_2O from 2.40 to 3.96% suggesting contributions from K-feldspars biotite and muscovite. The LOI values of 0.56 – 1.25% (Table 4.5) showed that the magmatite have been slightly altered.

Harker diagrams (Fig. 4.14) of most of the oxides and trace elements of the migmatite showed negative correlation with SiO_2 with the exceptions of K_2O, which is clearly positive. Also, MgO, Ni, Ba and Nb exhibited indefinite scatter with SiO_2, though with some negative tendencies for MgO and Ni; and positive for Ba and Nb. Data clusters of these major and trace elements indicated low geochemical mobility during the metamorphism of the protoliths.

The plot of the Na_2O/Al_2O_3 versus K_2O/Al_2O_3 data of the migmatite on the Garrels and McKenzie (1971) diagram (Fig. 4.15) showed that the protoliths of the migmatite are both sedimentary and igneous.

An attempt at chemical classification of the protolith using the sum alkalinity plot (Na_2O+K_2O)versus SiO_2diagram adapted afterMiddlemost (1994) for plutonic rocks showed that the migmatite has subalkaline granite affinity(Fig. 4.16). The calc-alkaline nature of the magmatic protolith was further reinforced by the (Na_2O+K_2O) - Fe_2O_3– MgO (AFM) ternary diagram (Fig. 4.17). The migmatite is peraluminous as shown by the chemical composition of the rock and the mineral constituents, originated from calc-alkaline magmatic suite in contact with oceanic crustal material in a syn-collisional (syn-COLG), (Pearce *et al*. 1984), tectonic setting (Fig. 4.18).

Table 4.5: Major oxides (%), trace components and rareearth (ppm) components composition in migmatite

	1	2	3	4	5	6	7	8	9	10	Average	Range	
SiO_2	70.29	69.73	68.06	69.25	67.48	67.88	69.75	68.87	67.75	69.64	68.87	70.29	67.48
TiO_2	0.35	0.52	0.55	0.53	0.56	0.53	0.32	0.53	0.45	0.58	0.49	0.58	0.32
Al_2O_3	14.15	14.69	15.09	14.73	16.95	14.93	15.01	15.95	14.98	15.86	15.23	16.95	14.15
Fe_2O_3	2.91	2.72	3.55	3.01	3.44	3.82	3.03	2.85	4.03	3.54	3.29	4.03	2.72
MnO	0.05	0.05	0.04	0.06	0.06	0.05	0.85	0.06	0.07	0.05	0.13	0.85	0.04
MgO	0.91	0.30	0.51	0.82	0.60	0.45	0.04	0.71	0.09	0.13	0.45	0.91	0.04
CaO	2.05	2.73	3.01	2.91	2.31	2.77	2.53	2.44	2.89	2.02	2.57	3.01	2.02
Na_2O	2.40	2.71	2.53	3.70	3.00	3.96	2.55	3.90	3.31	3.28	3.13	3.96	2.40
K_2O	5.23	4.86	4.57	4.63	4.49	4.65	5.54	4.56	4.45	3.77	4.67	5.54	3.77
P_2O_5	0.15	0.21	0.16	0.18	0.15	0.13	0.14	0.12	0.16	0.14	0.15	0.21	0.12
LOI	1.00	1.25	1.00	0.73	0.85	0.62	0.56	0.74	1.01	0.66	0.84	1.25	0.56
Total	99.49	99.77	99.07	100.55	99.89	99.79	100.24	100.73	99.19	99.67			
Trace elements (ppm)													
Ba	705	949	722	856	727	1069	1127	1009	907	662	873.3	1127	662
Nb	5.3	4.8	9	9	11	16	12	17	14	20	11.81	20	4.8
Rb	68.2	66.2	112	130	122	141	113	194	122	150	121.8	194	66.2
Sr	596.6	610.5	551	626	323	420	370	338	472	421	472.8	626	323
Y	7.8	8.9	6.9	8.2	9.1	10	26	22	11	25	13.5	26	6.9
Zr	226.7	285.1	385	430	311	355	450	375	368	412	359.8	450	226.7
Co	10.3	10.1	12	15	9	18	16	13	12	12	12.74	18	9
Ni	2.5	3.0	5.4	2.4	2.5	3.7	3.0	3.1	4.3	4.6	3.45	5.4	2.4
Cu	5.0	8.1	6.6	4.3	5.4	3.8	4.1	2.3	1.7	6.2	4.75	8.1	1.7
Pb	1.4	1.7	1.5	2.1	3.5	2.3	2.2	1.4	2.0	3.1	2.12	3.5	1.4
Zn	20	22	25	19	18	26	32	21	20	10	21.3	32	10
Cs	0.8	0.9	1.7	3.2	1.5	1.8	1.5	3.0	2.5	3.1	2	3.2	0.8
Ga	23.7	22.6	18	16	18	21	17	26	22	25	20.9	26	16
Sc	5	4	9	8	5	4	9	10	12	6	7.2	12	4
Hf	5.6	7.3	10	12	8	6	10	12	9	7	8.69	12	5.6
Th	4.8	3.1	18	8	9	16	20	15	10	13	11.7	20	3.1
U	0.4	0.8	1.3	1.2	1.4	0.9	1.5	1.3	1.1	0.6	1.05	1.5	0.4
V	45	49	26	32	31	55	26	42	33	82	42.1	82	26
Rare-Earth elements (ppm)													
La	23.80	18.71	16.32	15.61	18.23	16.55	17.91	22.53	14.32	10.96	17.494	23.8	10.96
Ce	45.10	34.09	35.27	33.85	36.14	33.73	31.56	37.15	12.94	32.02	33.185	45.1	12.94
Pr	4.79	3.84	4.44	4.34	4.20	3.94	4.22	4.88	5.69	3.08	4.342	5.69	3.08
Nd	17.70	14.22	19.01	17.45	14.76	15.13	15.41	14.88	15.11	14.40	15.807	19.01	14.22
Sm	2.82	2.56	3.94	3.95	2.93	2.90	2.85	2.56	2.98	3.44	3.093	3.95	2.56
Eu	0.94	0.97	1.47	1.41	0.93	0.96	0.75	0.72	0.96	0.87	0.998	1.47	0.72
Gd	2.27	2.34	4.13	3.97	2.41	2.78	1.79	2.62	4.54	4.19	3.104	4.54	1.79
Tb	0.31	0.31	0.71	0.69	0.46	0.51	0.93	0.46	0.44	0.33	0.515	0.93	0.31
Dy	1.71	1.74	3.78	3.71	2.38	2.99	2.39	4.88	4.86	4.16	3.26	4.88	1.71
Ho	0.28	0.36	0.67	0.56	0.51	0.45	0.38	0.31	0.43	0.50	0.445	0.67	0.28
Er	0.78	0.86	0.55	1.79	1.33	1.61	0.99	0.86	0.62	1.70	1.109	1.79	0.55
Tm	0.11	0.12	0.20	0.24	0.26	0.31	0.22	0.27	0.26	0.13	0.212	0.31	0.11
Yb	0.68	0.67	0.51	0.45	0.85	0.50	0.88	0.84	0.67	0.54	0.659	0.88	0.45
Lu	0.09	0.10	0.21	0.26	0.27	0.25	0.22	0.19	0.33	0.21	0.213	0.33	0.09
Rare-Earth Elements ratios													
Eu/Eu*	1.13	1.21	1.11	1.09	1.07	1.03	1.01	0.85	0.80	0.70	1.00	0.70	1.21
LaN/YbN	23.82	19.00	21.78	23.61	14.60	22.53	13.85	18.25	14.55	13.81	18.58	13.81	23.82
LaN/SmN	5.29	4.58	2.60	2.48	3.90	3.58	3.94	5.51	3.01	2.00	3.69	2.00	5.51
CeN/YbN	17.46	13.40	18.21	19.80	11.19	17.76	9.44	11.64	5.08	15.61	13.96	5.08	19.80
CeN/SmN	3.88	3.23	2.17	2.08	2.99	2.82	2.68	3.52	1.05	2.26	2.67	1.05	3.88
EuN/YbN	3.96	4.15	8.25	8.97	3.13	5.50	2.44	2.45	4.10	4.61	4.76	2.44	8.97
Sum_REE	101.4	80.89	91.21	88.28	85.66	82.61	80.50	93.15	64.15	76.53	84.44	64.15	101.4

A.S.I. is Alumina Saturation Index = Al_2O_3/ ($CaO+Na_2O+K_2O$), (After Zen, 1986).

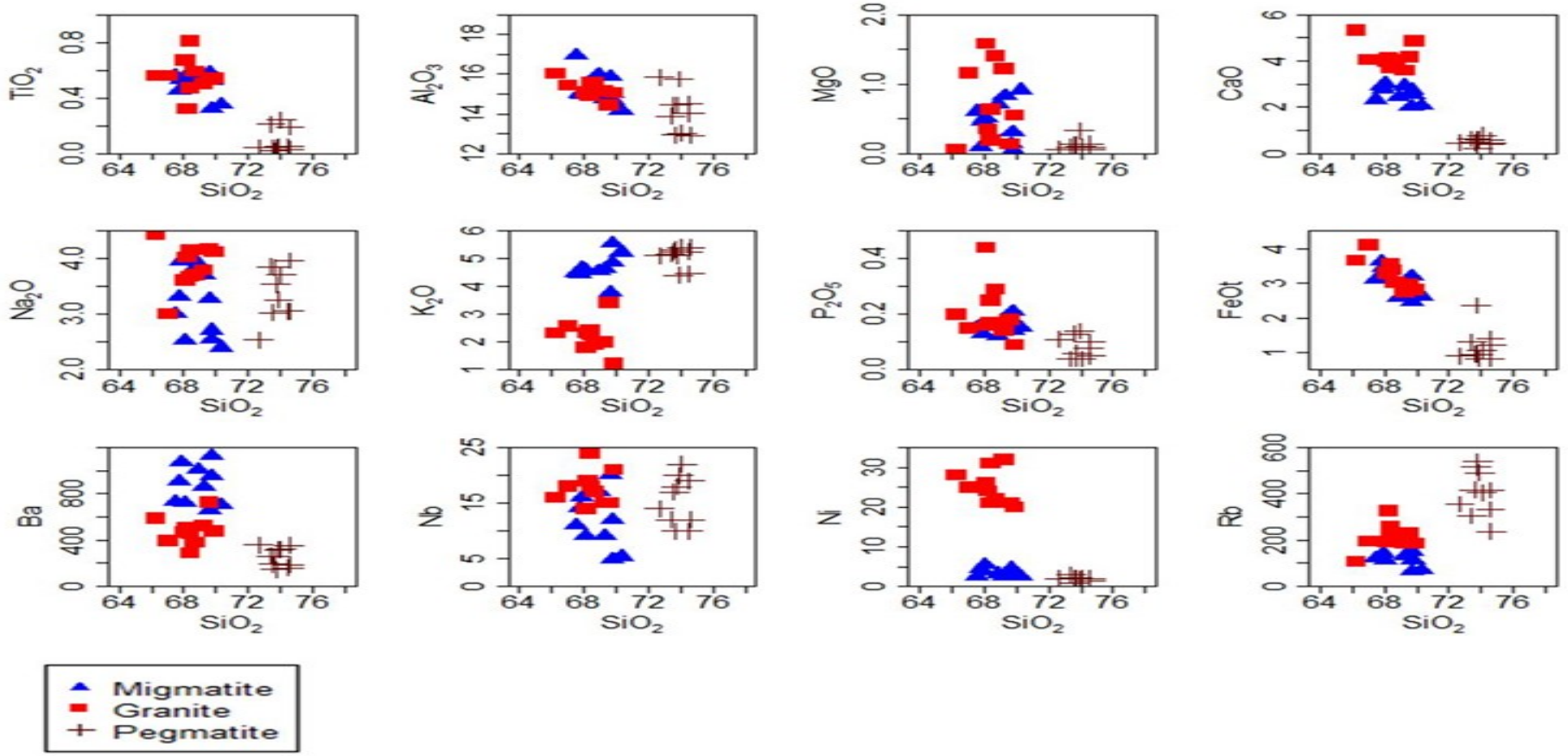

Fig. 4.14: The Harker diagrams of the Wonu, Ibadan-Apomu area migmatite and granitic rocks.

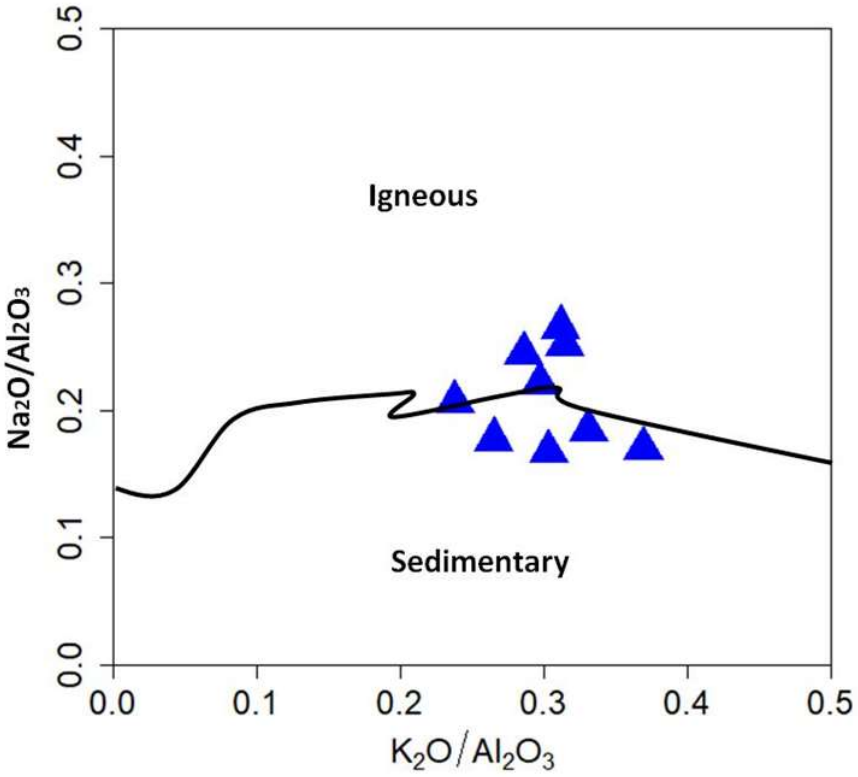

Fig. 4.15:The (a) Na_2O/Al_2O_3 versus K_2O/Al_2O_3 diagram in migmatite (after Garels and McKenzie, 1971) showing both sedimentary and igneous protolith for the migmatite.

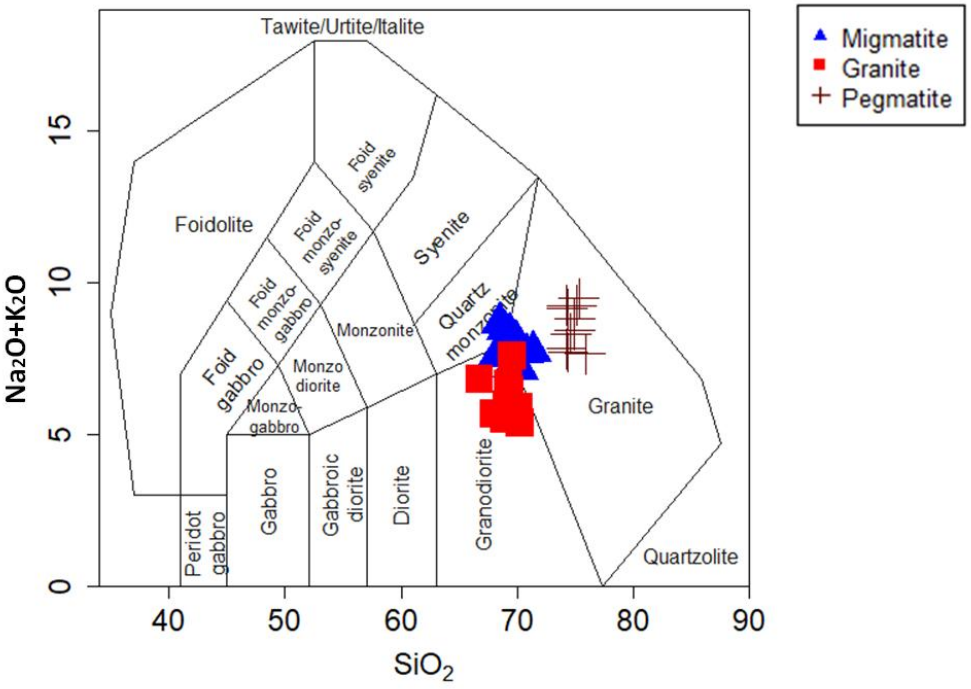

Fig. 4.16:Sum Alkalinity plot (Na_2O+K_2O)versus SiO_2diagram showing compositional ranges of the migmatite and granitic rocks from Wonu, Ibadan-Apomu area (after Middlemost 1994). Note that the migmatite has a compositional range similar to the granitoids in the area.

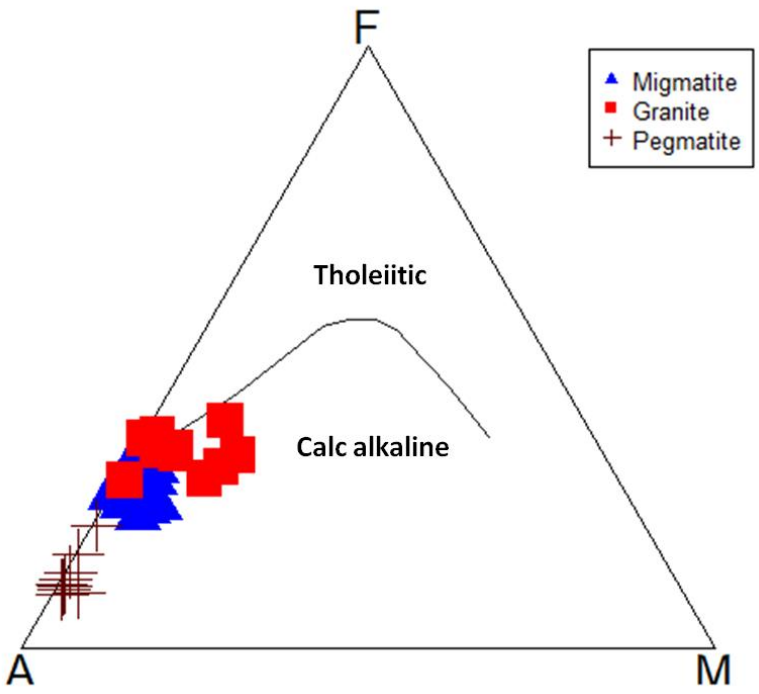

Fig. 4.17:The calc-alkaline nature of the magmatic protolith as revealed on the (Na_2O+K_2O) - Fe_2O_3– MgO (AFM) ternary diagram (after Irvine and Baragar 1971).

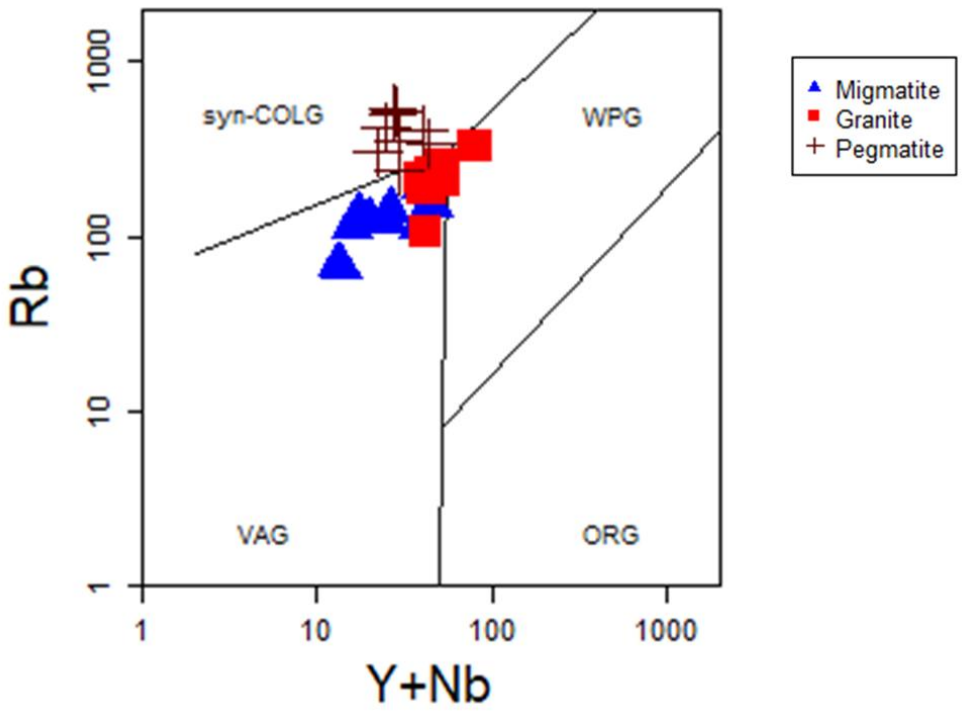

Fig. 4.18:The granitic rocks of Wonu, Ibadan-Apomu area drawn on the Rb-(Y+Nb) discrimination plot of Pearce *et al*. (1984). Syn-COLG - syn-collisional granites. WPG - within plate granites, ORG - ocean ridge granites, VAG volcanic arc granites.

Rare-earth element(REE) compositions of the migmatite of Wonu, Ibadan-Apomu Area are presented in Table 4.5. The chondrite-systemized REE patterns for the migmatites in Figs. 4.19 a &b showed higher enrichment of light rare-earth elements (LREEs) than the middle rare-earth elements (MREEs) and heavy rare-earth elements (HREEs). Ce yielded the highest LREE, having values ranging from 12.94-45.10 ppm, while Gd, the highest MREE, ranged from 1.79-4.54 ppm.The highest HREE was Er, with a range of 0.55-1.79 ppm,Lu was 0.09 – 0.33 and Eu 0.72-1.47 ppm. The migmatites showed LREE of moderately enriched patterns, with no distinctive Eu anomaly, indicating dual or more protoliths. The La_N/Yb_Nratios ranged from 3.04-6.14; while La_N/Sm_Nrange from 0.96-3.04 and Ce_N/Yb_Nranged from 1.84-4.23. The Eu/Eu* ranged from 0.22 -1.30, indicating positive, no anomaly and negative Eu anomalies (Fig. 4.19b).

According to Rudnick (1992), dehydrationmelting reactions and fluid movement inthe lower continental crust is the main mechanism responsible for the genesis of granite gneiss in the Proterozoic and that melting of an undifferentiated mantle-derived basaltic protoliths would produce a granite gneiss upper crust having a negative Eu anomaly and a mafic restitic lower crust with a positive Eu anomaly. In this study it was observed that many Proterozoic granulite facies terranes have bulk granitic compositions. In this research work, when such mafic granulites forms granite with a negative Eu anomaly, a significant fraction of the melt fraction left after with the residue (restitic) granulites will have either no Eu anomaly or a negative anomaly and moderately large ion lithophile elements (LILE) ratios, because of the predominance of the incompatible element-rich melt. Mafic granulite xenoliths with positive anomalies are commonly referred to as melts or cumulates derived from lower plate basaltic magmas rather than restites.

Condie *et al*. (1985) and Rudnick (1992)opined that the magma derived from the differentiation of basalt in the lower crust could eventually be melted in a post tectonic event and cross-cut the upper continental crust to yield the negative, no anomaly and positive anomaly in this migmatite.

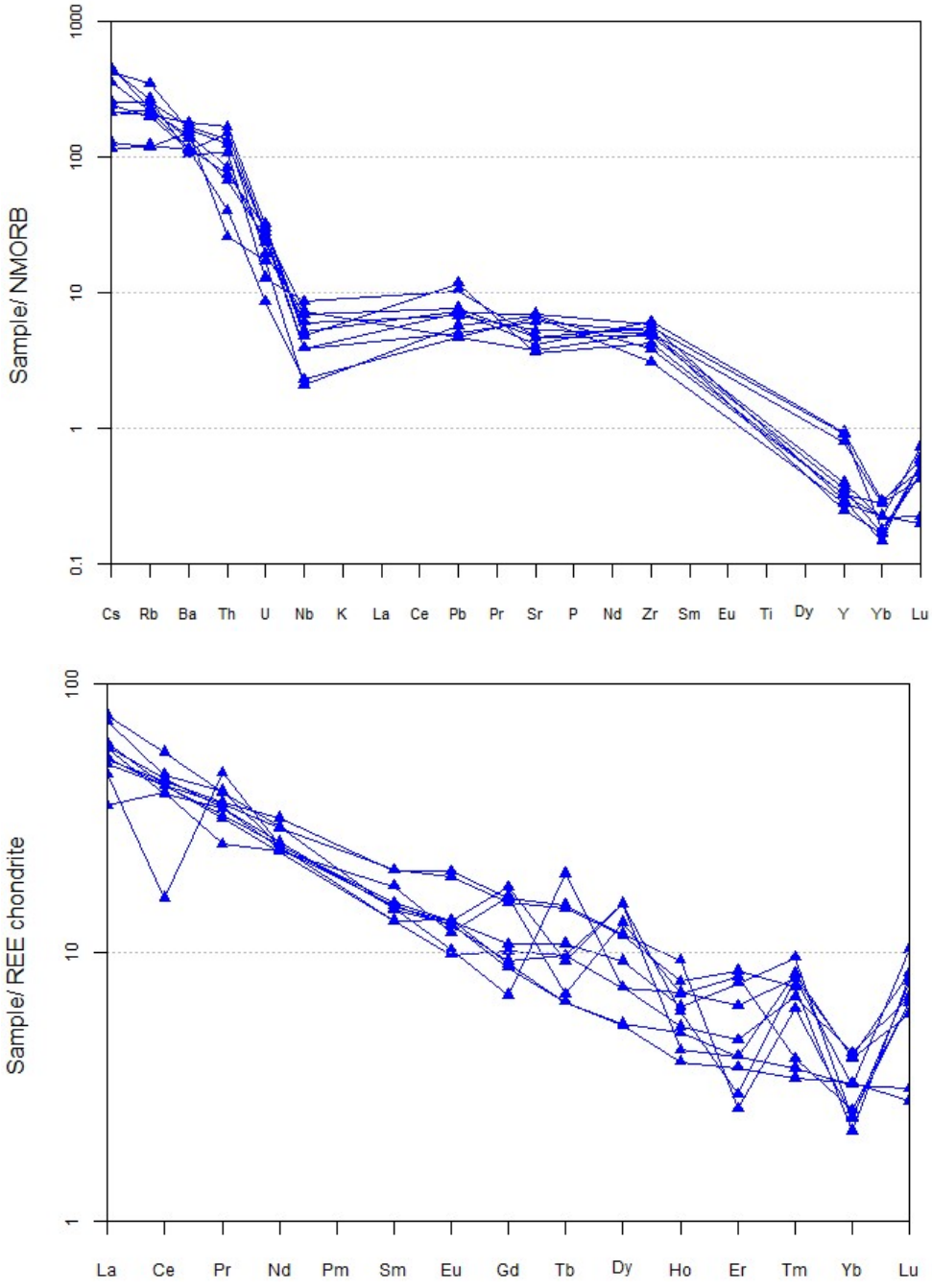

Fig. 4.19:Chondrite normalized (a) trace elements and rare earth (b) rare earth elements diagram of the migmatites of Wonu, Ibadan-Apomu area (after Mc Donough and Sun, 1995).

Several workers on the basement complex of Nigeria affirmed that migmatites are metasedimentary in origin but associated with igneous rocks (Rahaman, 1988). Some, including McCurry (1976), suggested that they are lateral equivalents of the Birrimian ancient metasediments of the West African Craton. Bolarinwa (2001) and Elueze and Bolarinwa (2004) noted that the granitic gneisses and migmatites of Ibadan and Abeokuta areas are dominantly granitic without prejudice to the metasedimentary input. In this study, evidence of granitisation and migmatisation of Liberian sediments by Eburnean granitoids (Proterozoic rocks) are obvious (Figs.4.15-4.17).

The trace elements data (Table 4.5) inferred the migmatites to be moderately rich in lithophile trace elements. The harker diagrams (Fig. 4.14)confirmed close association of the migmatite with the granitoids around the area. The calc-alkaline nature in the parent magma and in differentiation trend of the rock suites are shown in (Fig. 4.20). Evidence of fractional crystallization of the protolith are better depicted on the V versus Rb diagram of Cocherie (1986) (Fig. 4.21a) than the Ni versus Ba diagrams of de-Souza *et al*.(2007) (Fig. 4.21b). The log of compatible element versus log of incompatible element plots (Ni vs Rb, Ni vs Ba, Co vs Rb, V vs Rb, and Co vs Rb) are commonly used to determine the main mechanism of differentiation, whether it is through partial melting (PM) or crystal fractionation (CF). From this study, despite the disorientatation of the incompatible elements, the patterns displayed by the migmatite and the granite are vertical, indicating that the major procedure of differentiation is fractional crystal fractionation. However, within each of the rock units, that is,the migmatite and the granite as separate entities, partial melting is significant as depicted by the horizontal spread of the samples (Figs. 4.21a and b). The higher Ba composition of the migmatite with a range of 662 to 1127 and average of 873 ppm are characteristic of high grade granulite facies terrain.

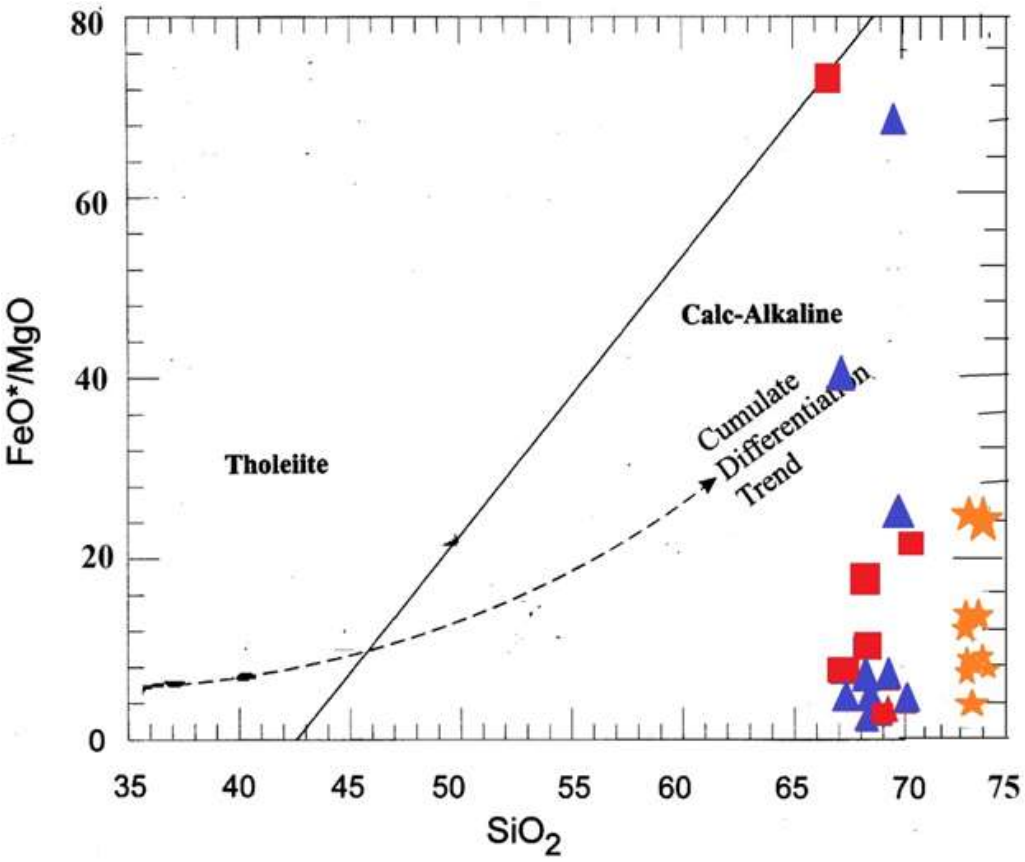

Fig. 4.20: TheFeO*/MgO vs. SiO_2diagram showing the differentiation trend of themigmatite and granitic rock suites from the Wonu, Ibadan-Apomu area.Note the calc-alkaline nature of the magmatic source.

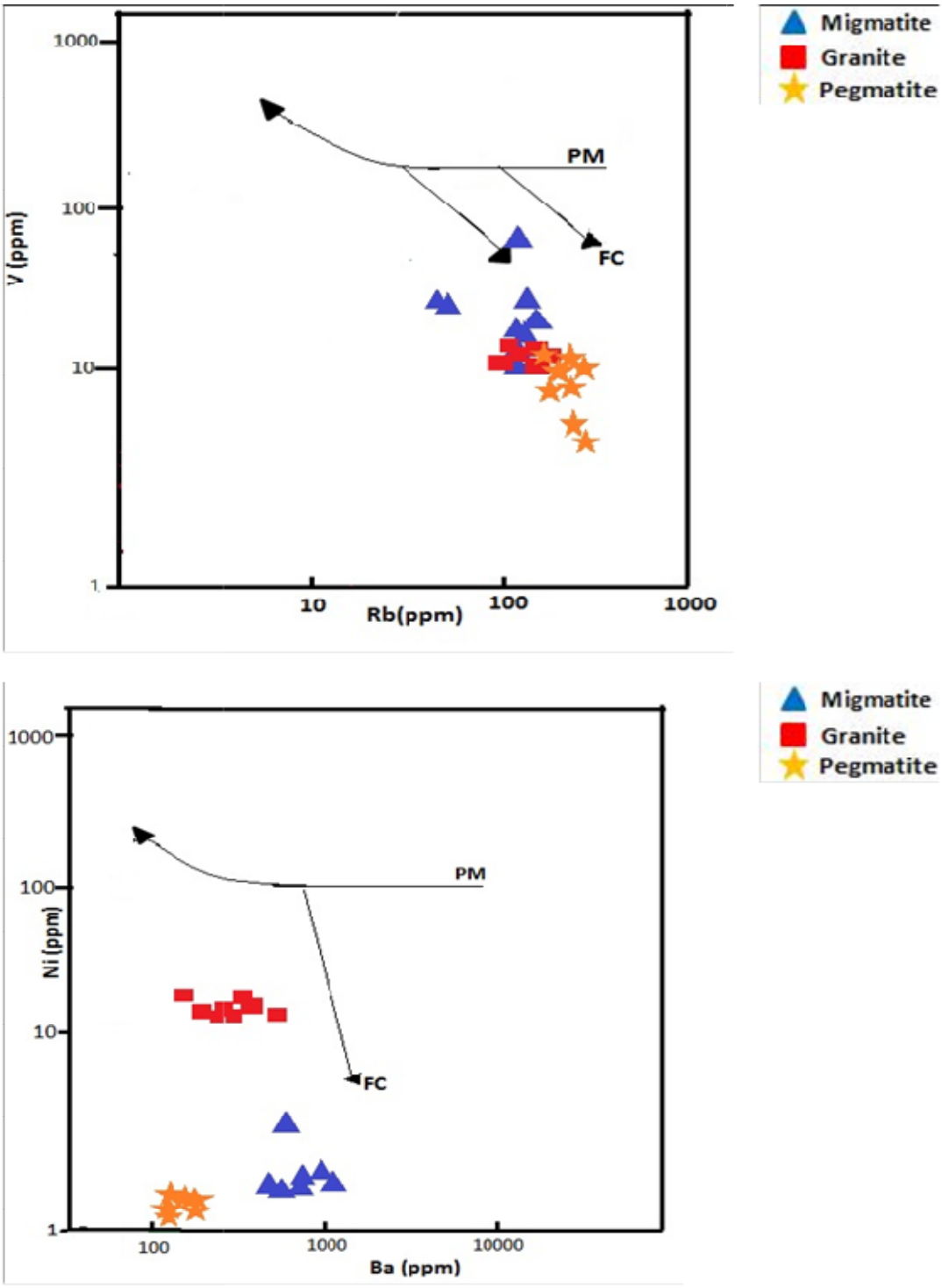

Fig. 4.21: The (a) V vs Rb and (b) Ni vs Ba diagrams indicating evolution of the granitic rocks through fractional crystallization (after Cocherie, 1986; De-Souza *et al*, 2007).

4.2.2 Granites

4.2.2.1 Geology and Petrography of the Granites

Outcrops of granitesin the Wonu, Ibadan-Apomu area showed medium grained granites, coarse grained granites and porphyritic granites(Fig. 4.22). The porphyritic granties are the most widespread in thearea (Figs.4.1-4.3). They are predominant in the southwestern part of the area. They form discrete large, circular to elliptical bodies(Fig. 4.22)and occur in association with the migmatites, quartz-schist and the amphibolites. Most of the granite outcrops are weathered and covered by soil, however, fresh outcrops are still available. They range in size from medium to coarse grained. They are partly tectonised as indicated by the eye-like (augen) structure in some samples around the migmatite outcrop in the area. The porphyritic variety also have large feldspar and quartz crystals, feldspar, biotite with muscovite.

Under the microscope, microcline constitutes between 15 and 25 % in the average composition with other main minerals inclusive of quartz (25-32 %), plagioclase (25-39 %), biotite (5-12 %), hornblende (4-8 %) and muscovite (2-3 %)(Table 4.6, Fig. 4.23). Minor minerals include zircon, sphene, tourmaline, apatite and opaque. Microcline was recognized by cross-hatch polysynthetic twining. The quartz crystals are clear of inclusions and vary from white to first order yellow in thin section. Plagioclase is either untwinned or showing fine multiple twinning charactestic of albite to oligoclase composition. Perthitic intergrowth of microcline and albite are observed in the thin sections. Myrmekite occurs as an interstitial component between plagioclase and microcline. The biotite crystals are lath-shaped and pleochroic from brown to green and partly oriented in some thin sections. Some biotite grains are altered from brown to green chlorite(Fig. 4.23).Sericitisation of muscovite and feldspars were observed in some samples. Hornblende crystals are green to brown with the characteristic acute/obtuse cleavage for crystals cut across the traverse section and parallel for those cut along the longitudinal section.Muscovite grains are deep yellow under crossed polarized light and showed parallel cleavage. Their crystals are in most cases wider than those of biotite. Few crystals of zoned augite were observed in one of the thin sections. The zone augite demonstrated parallel extinction characteristic of such mineral (Fig. 4.23). The opaque minerals are ilmenite and magnetite.

Fig. 4.22: Field photograph of porphyritic granite at Wonu, Ibadan-Apomu area.

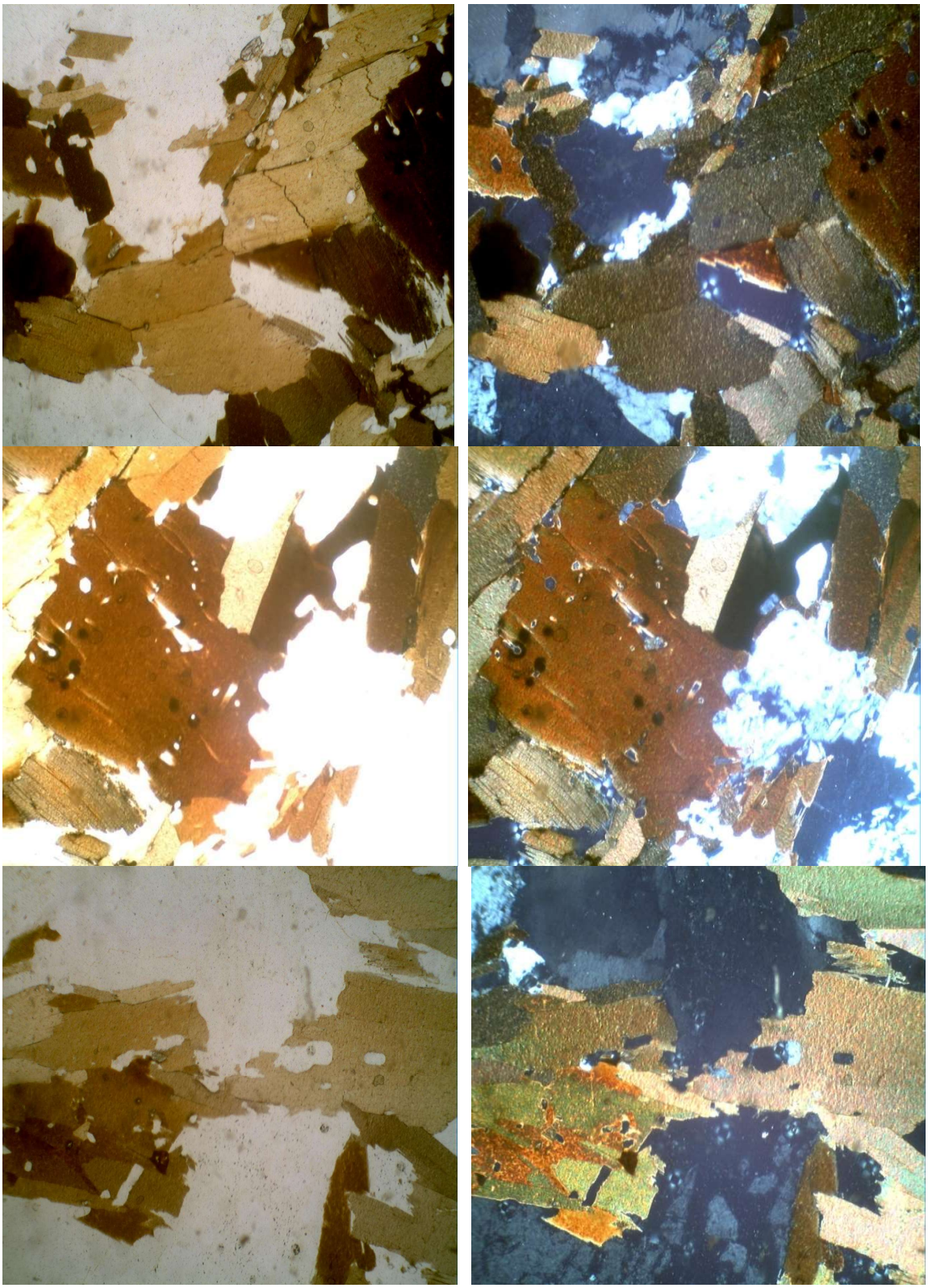

Fig. 4.23:Photomicrograph of granite of Wonu, Ibadan-Apomu area showing quartz, plagioclase feldspar, microcline, biotite, muscovite, hornblende and augite.

Table 4.6:Average modal composition of the granites in Wonu, Ibadan-Apomu area

Minerals	1	2	3	4	5	6	7	8	9	10
Quartz	28	27	25	26	32	28	25	26	25	27
Plagioclase	31	30	39	34	30	30	35	25	30	35
K feldspar	25	23	24	20	12	21	16	23	20	15
Biotite	5	8	6	8	10	8	10	10	10	12
Hornblende	4	5	4	5	8	5	7	8	7	3
Muscovite	2	2	3	2	2	2	2	2	2	2
Sphene	2	2	1	2	2	2	1	1	2	2
Apatite	1	1	2	1	1	2	1	2	2	1
Opaque	1	1	2	1	2	1	2	2	1	2
Zircon	1	1	1	1	1	1	1	1	1	1
Total	100	100	100	100	100	100	100	100	100	100

4.2.2.2 Geochemistry of the Granites of Wonu, Ibadan-Apomu area

The major oxides and trace elements in the granites are presented in Table 4.7. Silica content values were from 66.27 – 69.88%. The average value of the Al_2O_3 is 15.23 % and uniformly ranged from 14.44 – 16.02%. The Fe_2O_3 with an average value of 3.64% and range of 3.05 – 4.55% are normal. The average values of MgO ranged from 0.05-1.58 while the average value is 0.73. The CaO 4.15, Na_2O 3.87 and K_2O 2.23% are normal. The average value of the TiO_2 is 0.56% and ranged from 0.32 – 0.81 %.The average value of the $P_2O_5$is 0.21%. The LOI value revealed average contents of is 0.70%.

The Harker diagrams (Fig. 4.14) of most of the oxides and trace elements of the granites showed negative correlation with SiO_2 with the exceptions of Na_2O, Nb and Rb which are clearly positive. Others exhibited indefinite scatter with SiO_2. These major and trace elements distribution are characteristic of low geochemical mobility during crystallization and metamorphism of the area.

The Na_2O/Al_2O_3 versus K_2O/Al_2O_3 (Garrels and McKenzie, 1971) diagram (Fig. 4.26) classified the rock as igneous while the total alkalis (TAS) (Na_2O+K_2O)versus SiO_2diagram of Cox *et al.* (1979) adapted by Middlemost (1994) showed that they are granodioritic in composition(Fig. 4.16). The (Na_2O+K_2O) - Fe_2O_3– MgO (AFM) ternary diagram of Irvine and Baragar (1971) (Fig. 4.17) showed that the granite is peraluminous and calc-alkaline in nature.Furthermore, the Na_2O+K_2O versus SiO_2 and Na_2O versus K_2O plot for the granitic rocks of Wonu, Ibadan-Apomu area indicate that they are subalkaline (Fig. 4.24). The granite that is erupted in a syn-collisional tectonic setting (Figs. 4.18).

Trace element data showed that Rb (210ppm), Sr (294ppm), Y (31ppm), Zr (388 ppm) and Ba (481 ppm) are high.The Th (27ppm) and U (4ppm) are particularly higher inthe granitesthan in the migmatite (Table 4.7). The bulk chemical data indicated that the granites are enriched in lithophile elements. Compared to the migmatites the Rb and Y are higher while the Sr and the Ba (481ppm) are lower in the granite than the (Ba 873 ppm) in the migmatites. The Zr (360ppm)in both the migmatite and (388ppm) inthe granites are similar. Both U (3-5 ppm) and Th (21-36 ppm) are enriched in the granite.

Table 4.7: Major oxides (%), trace elements and rare earth (ppm) elements ofgranite

	1	2	3	4	5	6	7	8	9	10	Average	Range	
SiO_2	66.27	68.42	69.6	68.14	69.25	68.70	67.05	69.88	68.40	68.25	68.40	69.88	66.27
TiO_2	0.56	0.81	0.53	0.67	0.50	0.59	0.56	0.54	0.47	0.32	0.56	0.81	0.32
Al_2O_3	16.02	15.56	14.44	15.05	15.12	15.59	15.42	15.06	14.88	15.11	15.23	16.02	14.44
Fe_2O_3	4.05	3.75	3.31	3.66	3.05	3.36	4.55	3.12	3.96	3.62	3.64	4.55	3.05
MnO	0.07	0.05	0.06	0.08	0.06	0.07	0.05	0.04	0.06	0.05	0.06	0.08	0.04
MgO	0.05	0.19	0.13	1.58	1.22	1.40	1.16	0.55	0.63	0.35	0.73	1.58	0.05
CaO	5.32	4.04	4.16	3.95	3.58	3.77	4.04	4.85	3.67	4.12	4.15	5.32	3.58
Na_2O	4.44	3.68	4.17	3.61	3.80	3.71	3.01	4.12	4.15	4.03	3.87	4.44	3.01
K_2O	2.32	2.25	3.42	1.81	2.00	1.91	2.58	1.22	2.43	2.33	2.23	3.42	1.22
P_2O_5	0.20	0.25	0.18	0.44	0.14	0.29	0.15	0.09	0.17	0.16	0.21	0.44	0.09
LOI	0.60	0.70	0.60	0.80	0.65	0.73	0.60	0.70	0.85	0.75	0.70	0.85	0.6
Total	99.9	99.7	100.6	99.79	99.37	100.12	99.17	100.17	99.67	99.09			
Trace elements (ppm)													
Ba	586	288	727	469	521	380	395	478	455	506	480.5	727	288
Nb	16	18	15	14	15	17	18	21	24	19	17.7	24	14
Rb	106	211	230	193	185	213	194	186	256	326	210	326	106
Sr	425	470	338	400	450	251	266	133	139	72	294.4	470	72
Y	26	35	30	28	30	23	24	20	27	62	30.5	62	20
Zr	517	398	429	466	486	426	242	554	211	148	387.7	554	148
Co	11	10	12	12	18	15	13	9	12	10	12.2	18	9
Ni	28	31	21	26	32	22	25	20	21	24	25	32	20
Cu	21	28	15	18	20	35	27	16	10	31	22.1	35	10
Pb	25	16	18	12	15	24	15	13	20	22	18	25	12
Zn	66	97	62	56	60	44	55	64	47	54	60.5	97	44
Ga	13	21	17	16	19	16	15	22	19	21	17.9	22	13
Sc	9	8	9	10	12	9	7	5	3	4	7.6	12	3
Hf	4	9	5	5	9	6	6	5	5	6	6	9	4
Th	29	24	23	21	21	33	28	36	25	28	26.8	36	21
U	4	3	5	4	5	3	4	5	5	3	4.1	5	3
V	18	24	12	23	17	15	20	10	25	13	17.7	25	10
Rare-Earth elements (ppm)													
La	58.06	60.34	48.11	37.27	229.4	228.4	72.00	145.3	79.41	88.12	104.64	229.4	37.27
Ce	50.23	79.22	44.27	54.09	122.1	123.2	58.41	65.27	43.36	55.34	69.549	123.2	43.36
Pr	5.26	4.19	6.55	3.42	13.40	14.34	6.06	7.15	4.24	5.07	6.968	14.34	3.42
Nd	42.14	34.26	67.20	60.08	47.25	47.09	47.22	20.07	25.01	28.26	41.858	67.2	20.07
Sm	28.06	7.19	29.42	30.16	15.06	21.16	10.18	12.10	15.27	14.11	18.271	30.16	7.19
Eu	0.59	0.44	0.64	0.52	0.75	0.72	0.36	0.58	0.28	0.55	0.543	0.75	0.28
Gd	7.08	5.49	6.98	6.14	6.17	5.85	3.04	6.73	6.87	6.74	6.109	7.08	3.04
Tb	1.12	0.89	0.71	0.69	1.00	0.93	0.99	0.51	0.87	0.71	0.842	1.12	0.51
Dy	3.78	3.71	6.56	5.00	4.86	4.88	5.42	3.58	3.63	4.55	4.597	6.56	3.58
Ho	0.66	0.62	0.54	0.61	0.86	0.89	0.77	0.76	0.68	0.62	0.701	0.89	0.54
Er	3.02	1.99	2.55	3.03	2.47	2.32	2.20	2.09	2.92	1.99	2.458	3.03	1.99
Tm	0.56	0.47	0.44	0.36	0.31	0.29	0.52	0.27	0.54	0.30	0.406	0.56	0.27
Yb	1.85	1.82	1.66	2.16	1.78	1.76	1.88	1.59	1.39	1.50	1.739	2.16	1.39
Lu	0.29	0.28	0.26	0.30	0.27	0.28	0.25	0.29	0.23	0.26	0.271	0.3	0.23
Rare-Earth Elements ratios													
Eu/Eu*	0.13	0.21	0.14	0.12	0.24	0.20	0.20	0.20	0.08	0.17	0.17	0.08	0.24
LaN/YbN	21.36	22.56	19.72	11.74	87.71	88.32	26.06	62.19	38.88	39.98	41.85	11.74	88.32
LaN/SmN	1.30	5.26	1.02	0.77	9.54	6.76	4.43	7.52	3.26	3.91	4.38	0.77	9.54
CeN/YbN	7.15	11.46	7.02	6.59	18.06	18.43	8.18	10.81	8.21	9.71	10.56	6.59	18.43
CeN/SmN	0.43	2.67	0.36	0.43	1.97	1.41	1.39	1.31	0.69	0.95	1.16	0.36	2.67
EuN/YbN	0.91	0.69	1.10	0.69	1.21	1.17	0.55	1.04	0.58	1.05	0.90	0.55	1.21
Sum_REE	202.7	200.9	215.9	203.8	445.68	452.11	209.3	266.29	184.7	208.1	258.95	184.7	452.11

A.S.I. is Alumina Saturation Index = Al_2O_3/ ($CaO+Na_2O+K_2O$), (After Zen, 1986).

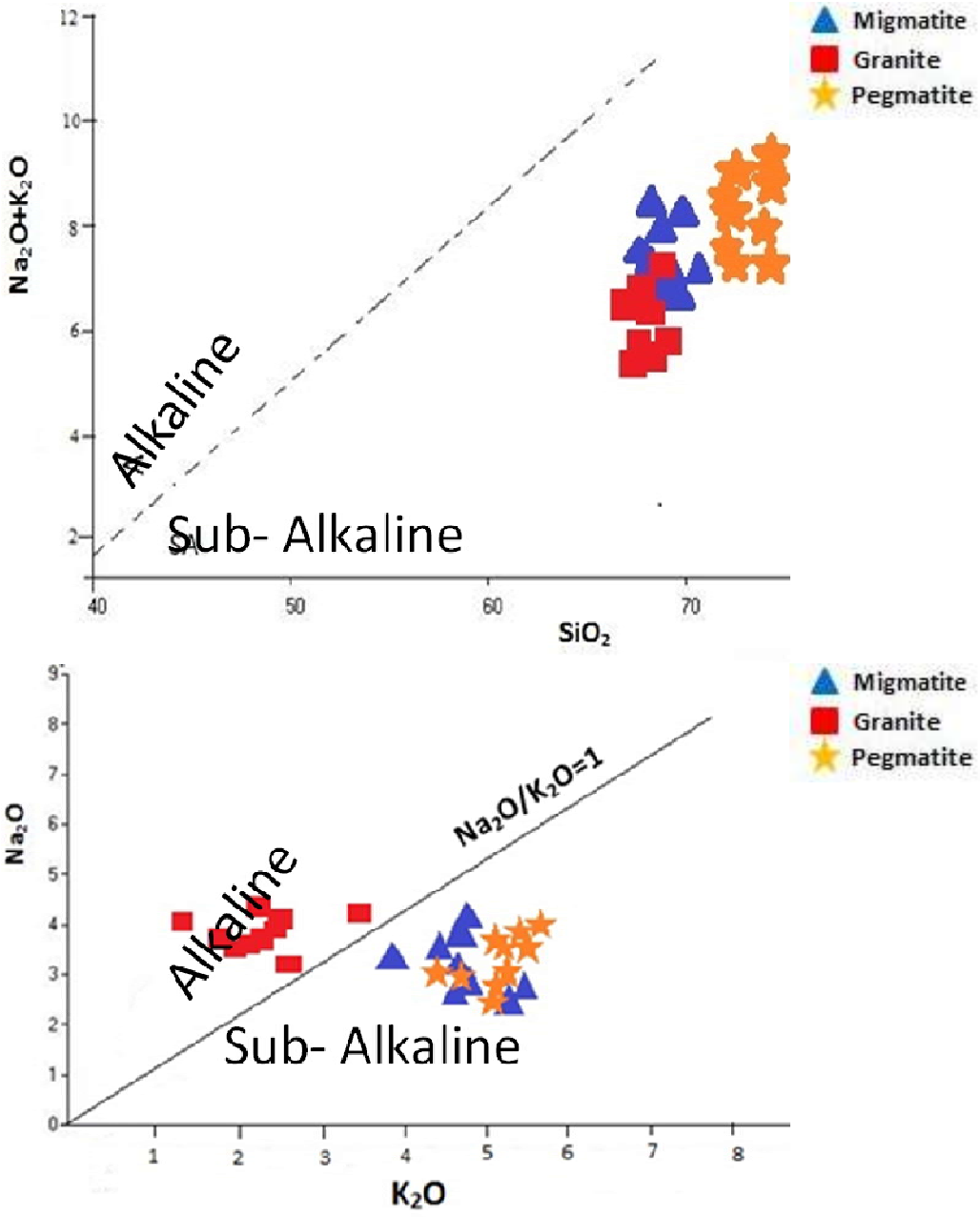

Fig. 4.24:The (a) (Na_2O+K_2O)versus SiO, and (b) Na_2O versus K_2O plot for the granitic rocks of Wonu, Ibadan-Apomu area.

The rare-earth element compositions of the granite in Wonu, Ibadan Apomu area are shown in Table 4.7.The chondrite-normalized REE patterns for granites (Figs. 4.25 a & b) showed enrichment in light rare-earth elements (LREE), which is higher than those of the middle rare-earth element (MREE). The heavy rare - earth elements (HREE) are however depleted. The La concentrations are highest among the LREE with values varying from 48.11 - 229.4 followed by Ce, with 43.36- 123.2. Peak of Gd is highest for the middle rare-earth element (MREE), with values varying from 3.04-7.08, while Er had the highest values of heavy rare-earth element (HREE) with values of 1.99- 3.03. Eu concentrations are low(0.28-0.75). The concentration of Lu (0.23- 0.29)are lowest in the whole array of the rare earth elements (Table 4.7).

The granites from the study area showed the typical LREE enriched granite patterns with a distinct negative Eu anomalies (Figs. 4.25b). The La_N/Yb_N ratios ranged from 11.74-88.32; while La_N/Sm_Nrange from 0.77- 9.54 and ratios of Ce_N/Yb_N range from 6.59-18.06. The high REE fractionation factor of La_N/Sm_N ranged from 11.74-88.32. The prominent negative europium (Eu/Eu*) anomaly, which ranged from 0.08-0.24 (Table 4.7) is lower than the Eu/Eu* of the upper continental crust value of 0.72. These values suggested derivation of the granite from partial melting of hornblende and plagioclase-rich crustal sources with the occurrence of accessory minerals which appear to control the REE contents. The parent magma from which the granite was fractionated could be sourced from underplated basaltic magma related to the lower crust.

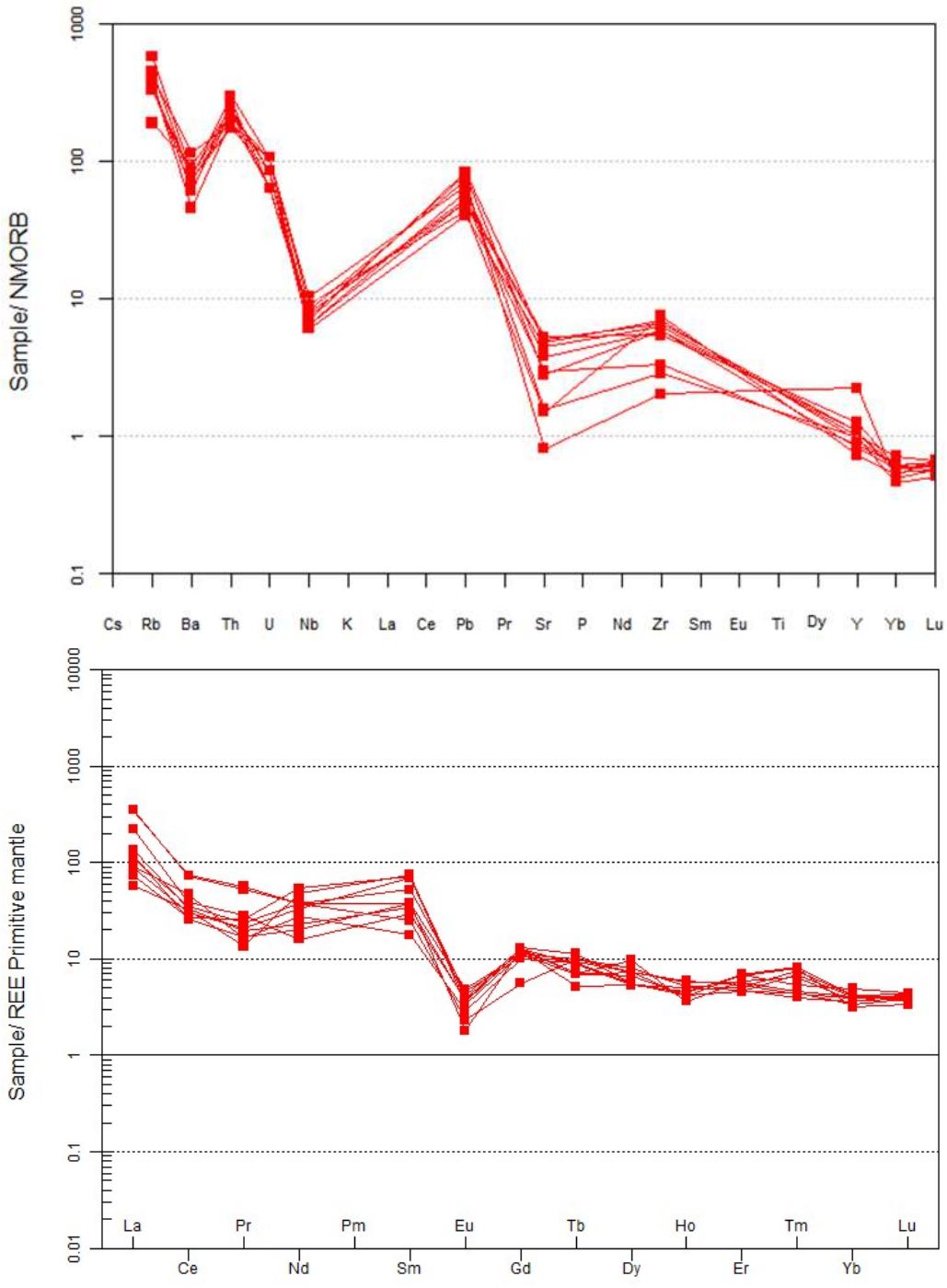

Fig. 4.25: Chondrite normalized (a) trace and rare-earth (b) rare earth elements diagram of granites in Wonu, Ibadan-Apomu area (after Mc Donough and Sun, 1995).

4.2.3 Pegmatite

4.2.3.1 Geology and Petrography of the Pegmatites

The pegmatite in the Wonu, Ibadan-Apomu area occursas minor intrusions in the Older Granites and the migmatites. They occur as near vertical dykes and striking mainly in the NNW-SSE direction. The pegmatite occurs as coarse unequal granular veins, whitish in colour. Weathered pegmatite veins with relics of quartz rubbles were seen across the road.

In thin section, the pegmatites comprises; microcline, quartz and minor amounts of plagioclase, mainly albite, biotite, tourmaline with trace amounts of opaques (Fig.4.26a and b).Quartz exhibits euhedral shape with wavy extinction. The plagioclase feldspar shows polysynthetic twining and is observed intergrown with quartz. Biotite occurs as deep platy brown in colour. The photomicrographs of altered pegmatite in (Fig. 4.26) (under cross polar), showedlarge quartz crystals, microcline and perthite, sericitised plagioclase and muscovite.

The microcline feldspars are large and showed cross-hatch polysynthetic twinning. Plagioclase feldspar showed parallel multiple twinning of albite composition. Perthitic intergrowth of microcline are recorded in the pegmatite. Plagioclase crystals occur as irregular veins randomly distributed in the microcline. The occurrence of these perthites indicated replacement and exolution.

Quartz crystals are large, euhedral, xenomorphic with characteristic first order yellow and undulose extinction indicating primary igneous source. They are mostly transparent or milky quartz with some smoky tint where tourmaline is present. Muscovite is predominant while biotite is subordinate. Both muscovite and biotite are flacky and possess perfect basal cleavage.Muscovite is transparent white while the biotite is shining black. Large blocks of muscovite occur in some outcrops while biotite crystals are small. Accessory minerals include apatite, tourmaline and opaques (Table 4.8).

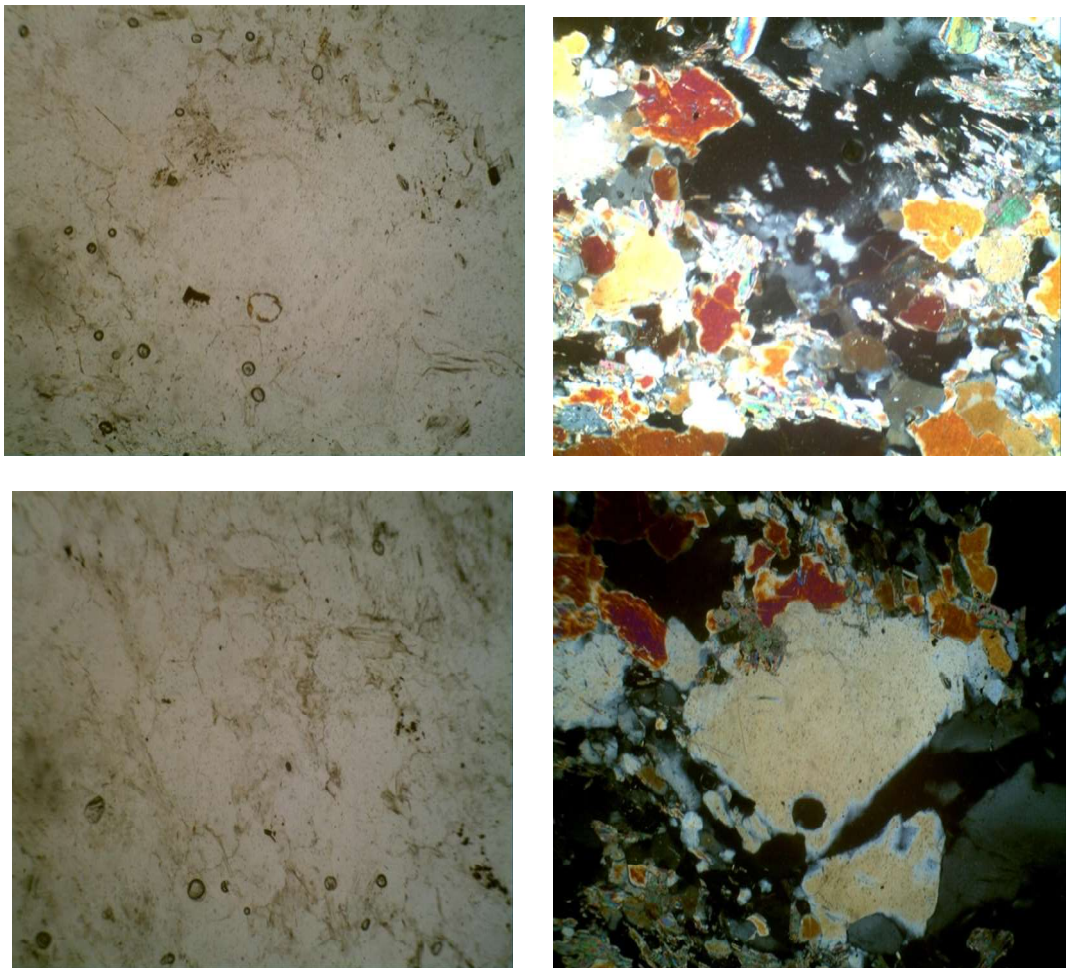

Fig. 4.26:Photomicrographs of altered pegmatite of Wonu, Ibadan-Apomu area (under cross polar), showing large quartz crystals, microcline and perthite, sericitised plagioclase and muscovite.

Table 4.8: Average modal composition (vol. %) of the Wonu, Ibadan-Apomu pegmatite

	1	2	3	4	5	6	7	8	9	10
Quartz	32	34	36	27	28	31	28	30	28	26
Microcline	27	30	31	30	30	30	34	30	32	28
Plagioclase	21	20	21	20	21	27	20	22	25	25
Muscovite	10	8	7	16	11	7	10	10	7	14
Biotite	7	5	3	4	8	2	5	6	5	5
Tourmaline	2	1	1	1	1	1	0	1	2	1
Opaques	1	2	1	2	1	2	3	1	1	1
Total	100	100	100	100	100	100	100	100	100	100

4.2.3.2 Geochemistry of the Pegmatite

Major and trace element compositionsof pegmatites in Wonu, Ibadan-Apomu are presented in Table 4.9. Pegmatites arehigh in silica, which ranged 72.66 – 74.58%. The Al_2O_3ranged between 21.91 – 15.85% while the Fe_2O_3 contents are 0.91- 2.62%. The Fe_2O_3 contents are very low with an average concentration of 1.31%. The average MnO and MgO is 0.12 while CaO is 0.52%. The Na_2O and K_2O on the other hand are 3.39% and 5.0% respectively. With an average alumina saturation index (ASI =Fe_2O_3/(CaO +Na_2O + K_2O) of 1.57, the pegmatite is peraluminous. The average LOI is 0.86% while TiO_2 contents are generally below 0.24%.

The average Rb (401),Ba (256) are high, Sr (41), Zr (30), Y (14) are moderate whileTh (5) and U (3) ppm are low.The Nb and V are 15 and 11ppm respectively. Other trace elements are less than 5 ppm. Both the U and Th content of the pegmatite are low (Table 4.9), which is characteristic of simple pegmatite.

The rare-earth elements (REEs) compositions of pegmatitesare shown in Table 4.9 while the chondrite-normalized REE patterns are shown in Fig. 4.27a & b. The REE chondrite-normalized values showed high enrichment of the light rare-earth elements (LREE),moderate middle rare-earth element (MREE) enrichment and high depletion in heavy rare-earth element (HREE). The Ce concentration for the LREEranged from 3.71-8.92, while Gd of theMREEranged from 0.71-2.23. Er had the highest concentration of HREE, with values that ranged from 0.29-0.95. Eu concentration vary from 0.09-0.72 while Lu had the lowest concentration values of 0.05-0.09.

The La_N/Yb_N ratios of the pegmatite ranged from 3.04-6.14; La_N/Sm_N 0.96-3.04 and Ce_N/Yb_N 1.84-4.23. The pegmatitesshowed negative Ceand Eu anomalies (Figs 4.26b). The Eu/Eu* ranged from 0.22-1.30. This composition suggests that the pegmatite was probably fractionated from the granites in the area (Figs. 4.20-4.21a), in the courseof the Pan-African orogeny or younger period.

Comparative studies of the granitic rocks showed that the granite is richer in REEs than the migmatites and the pegmatite (Figs. 4.28a and b). The simple mineralogy of the pegmatite was probably responsible for the low REEs.

Table 4.9: Major oxides (%),trace elements and rare earth (ppm) elements composition of pegmatite

	1	2	3	4	5	6	7	8	9	10	Average	Range	
SiO_2	74.5	73.74	73.67	74.55	73.39	74.04	74.58	73.56	72.66	73.88	73.86	74.58	72.66
TiO_2	0.05	0.04	0.02	0.03	0.21	0.24	0.19	0.04	0.04	0.05	0.09	0.24	0.02
Al_2O_3	14.5	14.45	12.93	14.01	13.87	13.01	12.91	14.45	15.85	15.75	14.17	15.85	12.91
Fe_2O_3	0.92	1.06	2.62	1.55	1.46	1.19	1.35	1.06	1.00	0.91	1.31	2.62	0.91
MnO	0.78	0.05	0.04	0.06	0.04	0.05	0.03	0.05	0.07	0.05	0.12	0.78	0.03
MgO	0.14	0.13	0.09	0.05	0.09	0.1	0.08	0.13	0.06	0.33	0.12	0.33	0.05
CaO	0.58	0.20	0.62	0.39	0.63	0.79	0.45	0.48	0.45	0.59	0.52	0.79	0.2
Na_2O	3.06	3.54	3.85	3.06	3.86	3.71	3.97	3.03	2.54	3.26	3.39	3.97	2.54
K_2O	5.25	5.12	5.33	4.46	5.17	5.42	5.42	5.25	5.12	4.41	5.10	5.42	4.41
P_2O_5	0.08	0.06	0.04	0.10	0.04	0.04	0.05	0.13	0.11	0.14	0.08	0.14	0.04
LOI	0.65	0.96	0.72	1.11	0.7	0.70	0.72	1.03	1.15	0.85	0.86	1.15	0.65
Total	100.5	99.35	99.93	99.37	99.46	99.29	99.75	99.21	99.05	100.22			
Trace elements (ppm)													
Ba	161	146	256	356	261	321	185	194	359	319	255.8	359	146
Nb	10	18	10	19	12	22	12	17	14	20	15.4	22	10
Rb	416	539	516	333	305	405	237	417	356	491	401.5	539	237
Sr	45	53	36	44	36	45	28	42	51	29	40.9	53	28
Y	15	9	18	25	10	18	17	8	15	7	14.2	25	7
Zr	19	24	16	15	18	38	16	82	54	17	29.9	82	15
Co	2.4	1.5	1	1.3	1	2	1	1.2	1.0	0.8	1.32	2.4	0.8
Ni	1.9	2.1	0.8	1.5	3.0	2.0	2.0	2.2	2.0	1.8	1.93	3	0.8
Cu	0.8	1.2	1.3	1.7	5.0	3.0	3.0	0.8	2.4	1.5	2.07	5	0.8
Pb	3	3	5	5	4	7	4	2.7	2.5	2.8	3.9	7	2.5
Zn	22	26	13	25	14	16	11	20	31	25	20.3	31	11
Ga	43	46	43	31	42	44	43	43	46	27	41	46	27
Sc	5	3	4	3	5	6	3	4	4	3	4	6	3
Hf	0.7	1.1	3	5	3	2	4	4.2	2.3	3.2	2.85	5	0.7
Th	2.9	0.8	1.7	4.3	1.0	1.5	18.1	4.3	8.1	5	4.77	18.1	0.8
U	4.4	2.7	2.5	2.8	2.4	2.7	4.0	2.0	2.4	3	2.89	4.4	2
V	10	5	11	8	18	12	15	8	13	6	10.6	18	5
Rare-Earth elements (ppm)													
La	4.22	2.55	3.69	4.38	2.81	2.43	2.90	3.37	3.01	4.06	3.342	4.38	2.43
Ce	6.91	4.03	5.91	8.92	4.70	3.71	6.33	6.74	6.53	5.50	5.928	8.92	3.71
Pr	1.53	1.34	1.53	1.64	1.24	1.73	2.02	2.23	1.82	2.14	1.722	2.23	1.24
Nd	4.01	2.38	3.11	3.69	2.11	2.02	4.05	3.59	3.54	3.81	3.231	4.05	2.02
Sm	1.96	0.87	1.12	1.48	0.58	0.71	1.95	1.37	1.97	1.09	1.31	1.97	0.58
Eu	0.15	0.09	0.15	0.23	0.22	0.12	0.16	0.26	0.72	0.15	0.225	0.72	0.09
Gd	2.23	1.17	1.17	1.08	0.71	1.02	1.77	1.01	1.46	1.52	1.314	2.23	0.71
Tb	0.47	0.25	0.19	0.21	0.12	0.17	0.86	0.18	0.17	0.20	0.282	0.86	0.12
Dy	0.74	1.35	1.10	1.08	0.69	1.17	1.05	1.14	0.81	0.85	0.998	1.35	0.69
Ho	0.45	0.22	0.22	0.14	0.13	0.18	0.32	0.15	0.19	0.33	0.233	0.45	0.13
Er	0.95	0.46	0.64	0.55	0.32	0.44	0.46	0.58	0.29	0.44	0.513	0.95	0.29
Tm	0.10	0.18	0.11	0.10	0.08	0.06	0.07	0.09	0.07	0.06	0.092	0.18	0.06
Yb	0.69	0.42	0.56	0.55	0.63	0.53	0.43	0.42	0.56	0.45	0.524	0.69	0.42
Lu	0.09	0.06	0.05	0.07	0.09	0.07	0.06	0.05	0.07	0.08	0.069	0.09	0.05
Rare-Earth Elements ratios													
Eu/Eu*	0.22	0.27	0.40	0.56	1.05	0.43	0.26	0.67	1.30	0.36	0.55	0.22	1.30
LaN/YbN	4.16	4.13	4.48	5.42	3.04	3.12	4.59	5.46	3.66	6.14	4.42	3.04	6.14
LaN/SmN	1.35	1.84	2.06	1.85	3.04	2.14	0.93	1.54	0.96	2.33	1.80	0.93	3.04
CeN/YbN	2.64	2.53	2.78	4.27	1.96	1.84	3.88	4.23	3.07	3.22	3.04	1.84	4.27
CeN/SmN	0.85	1.12	1.28	1.46	1.96	1.27	0.79	1.19	0.80	1.22	1.20	0.79	1.96
EuN/YbN	0.62	0.61	0.77	1.20	1.00	0.65	1.07	1.77	3.68	0.95	1.23	0.61	3.68
Sum_REE	24.50	15.37	19.55	24.12	14.43	14.36	22.43	21.18	21.21	20.68	19.78	14.36	24.50

A.S.I. is Alumina Saturation Index = Al_2O_3/ ($CaO+Na_2O+K_2O$), (After Zen, 1986).

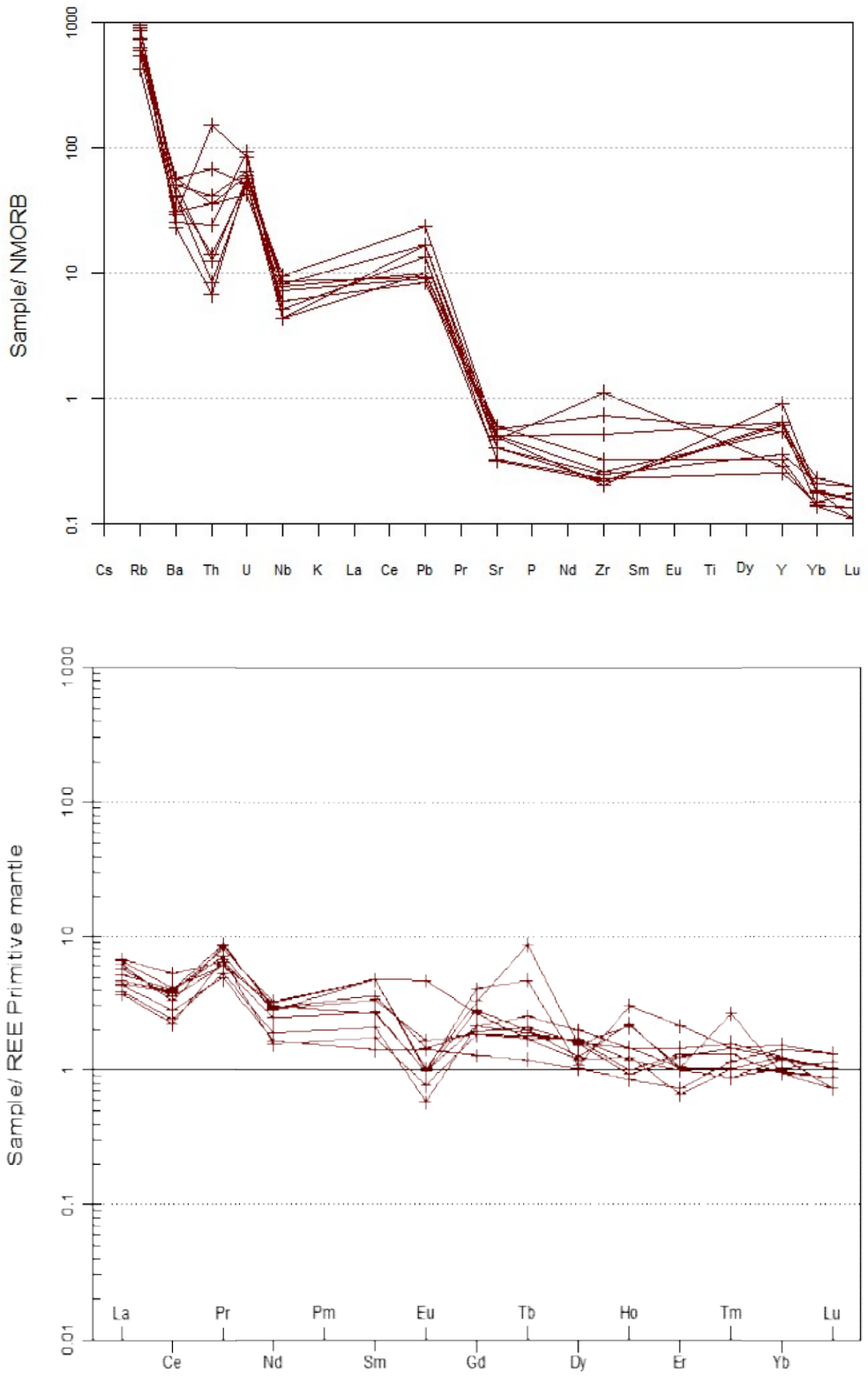

Fig. 4.27: Chondrite normalized (a) trace elements and rare earth (b) rare earth elements diagram of pegmatites of Wonu, Ibadan-Apomu area(after Mc Donough and Sun, 1995).

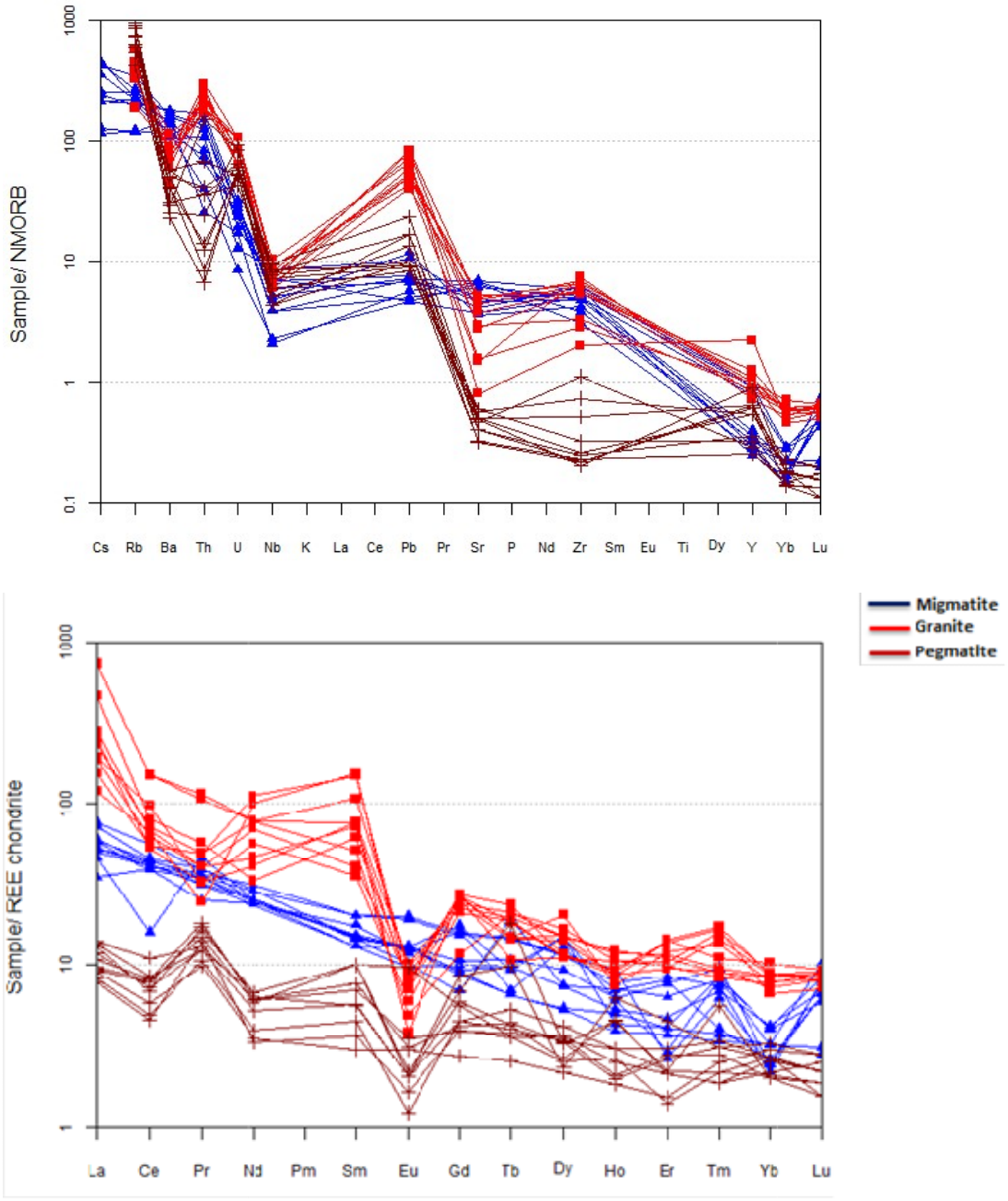

Fig. 4.28: (a) N-Type MORB-normalized multi-element diagram (b) chondrite normalized REE diagram for granitic rock suites from the Wonu, Ibadan-Apomu area (after Boynton, 1984).

4.3 The Mafic-Ultramafic Rocks

4.3.1 Fine-grained amphibolites

4.3.1.1 Petrographyof the Fine-grained Amphibolite

The outcrops of the fine-grained amphibolite are scattered and weathered. Outcrops of the fine-grained amphibolite are lowlying, dark grey to black in colour and have restricted extent. Most outcrops appear rounded, smooth, dense, very hard and difficult to break (Fig. 4.29). The hand specimen showed that they vary slightly in textural and mineralogical compositions. Some are uniformly fine-grained while others are porphyritic.Both varieties contain clusters of oriented amphibole prisms giving the rock a gneissic outlook. Foliation in the rock is defined by impersistent amphibole-rich and felsic bands. The porphyritic variety displays phenocrysts of augite and calcic plagioclase in fine-grained array of amphibole, plagioclase, pyroxene, biotite and quartz. Field occurrences indicated that the amphibolites in Wonu, Ibadan-Apomu area occur around the lherzolite and the major talc bodies

In thin section, amphiboles(42-55 %), pyroxenes (14-17 %), plagioclase (9-10 %), biotite (4-5 %),K-felfspar (4-7 %) and quartz (2-5 %) (Table 4.10). Accessory minerals include ilmenite magnetite, garnet and pyrite, which are generally less than 3%. Alteration minerals include talc, chlorite and ferritchromite. The amphiboles are mainly magnesio-hornblende and actinolite. Stout prisms of hornblende appear clustered together. The hornblende is pleochroic from dark grey to olive green. Amphibole commonly forms symplectite with plagioclase (Fig. 4.30). Olivine crystals are generaly altered to secondary pyroxenes, serpentine and talc(Fig. 4.30). Clinopyroxene is subhedral-anhedral augite. Opaque minerals are ilmenite, magnetite and ferrichromite.There are corona haloes around the augite(Figs.4.31 and 4.32). The augites and the hornblendes formed symplectite with plagioclase feldspar on which they nucleate, while others are largely replaced by hornblende. The plagioclase exhibits multiple twinning, characteristic ofandesine to labradorite in composition(Fig. 4.30). Biotite formed a brown rim around the opaque minerals, which suggests that the opaque minerals were formed first followed by the biotite. Biotite (deep brown) is altered to greenish chloriteat the edges and around cleavages.

Fig.4.29: Hand specimens of the fine-grained amphibolites from Wonu, Ibadan-Apomu area.

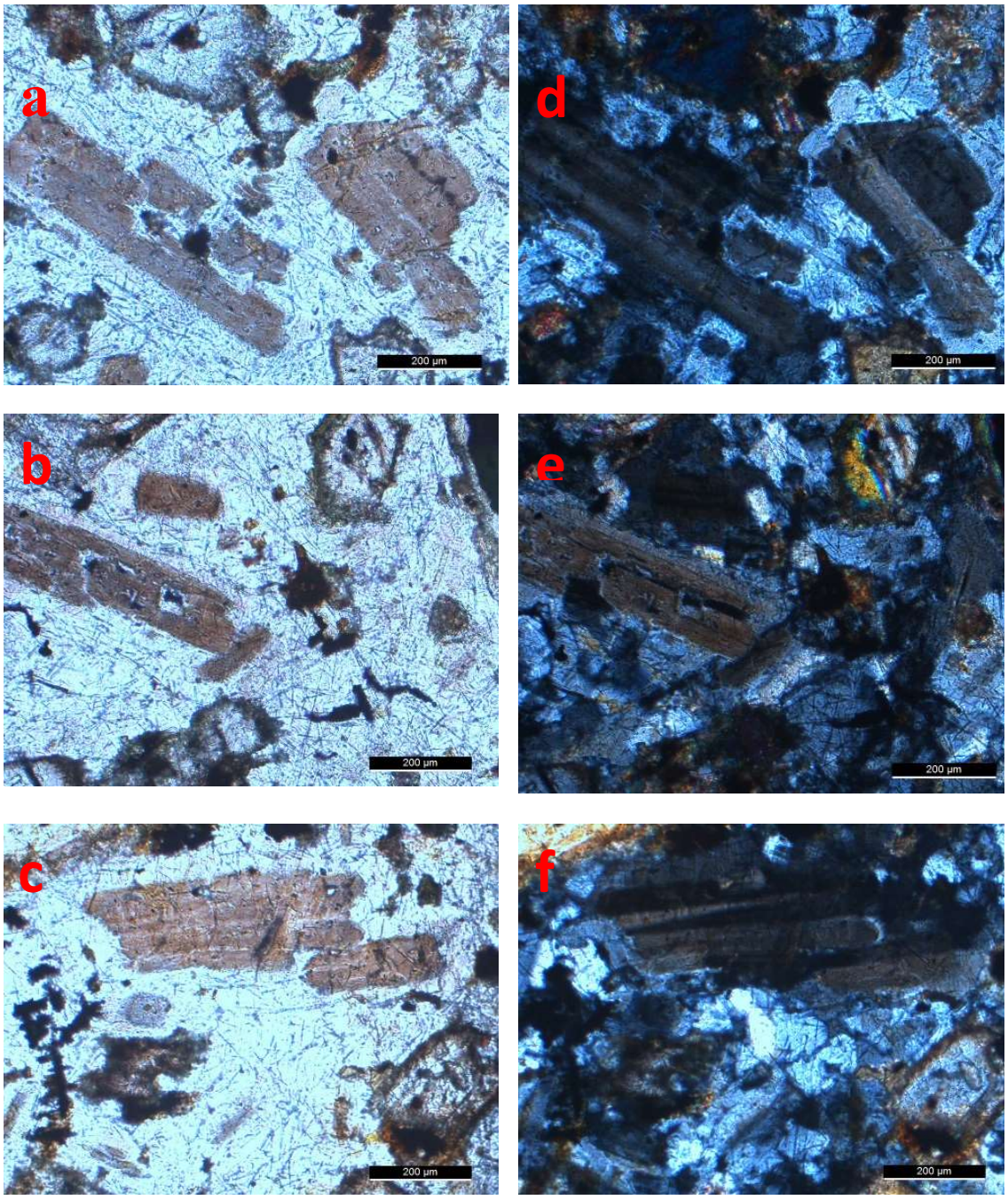

Fig.4.30: Photomicrograph of fine-grained amphibolite from Wonu, Ibadan-Apomu area showing hornblende-plagioclase intergrowth (a-c) under plane polarized light (d-f) under cross-polarised light. Hornblende (H), Plagioclase (P) laths, Pyroxene (Px) with corona haloes, talc and serpentine (Black).

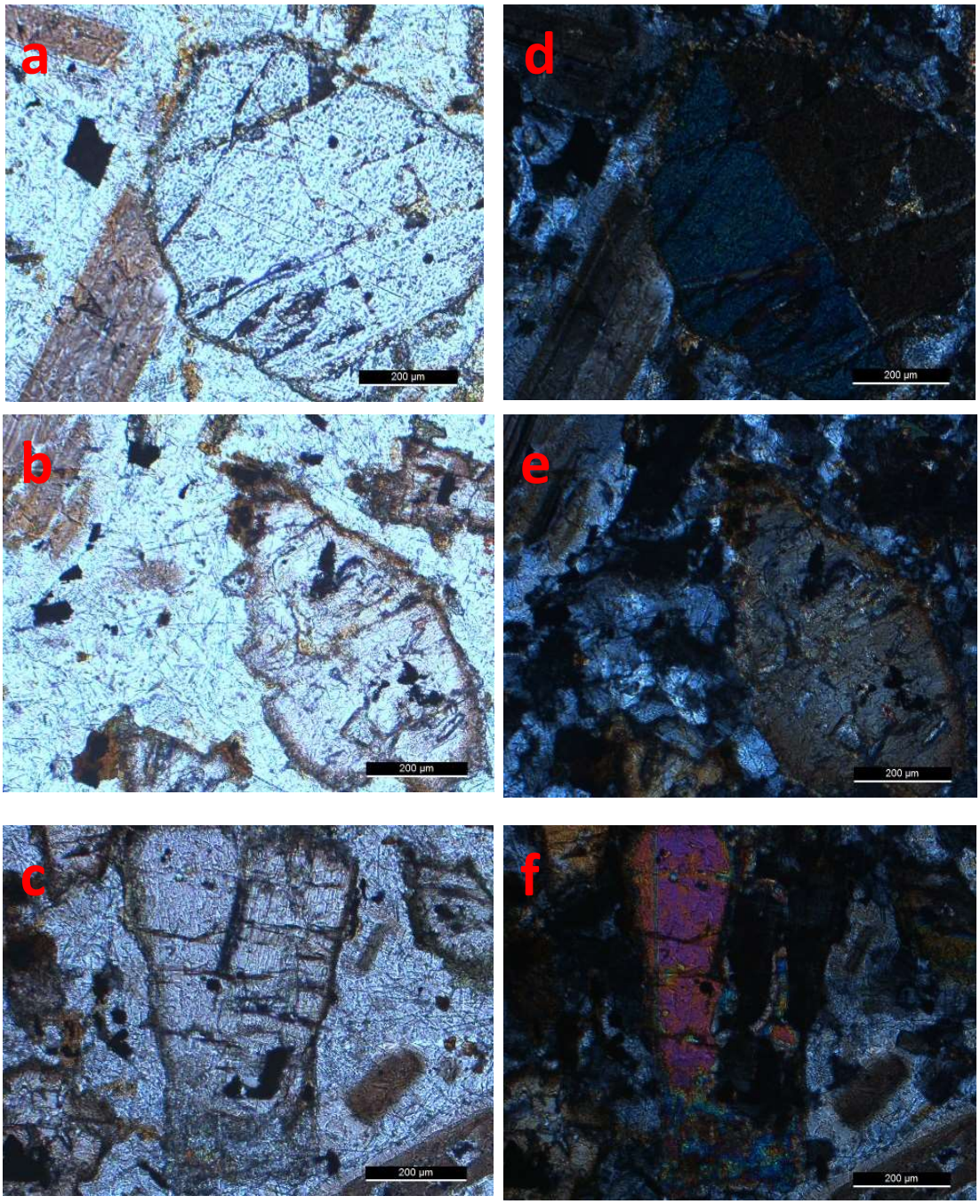

Fig.4.31: Photomicrograph showing fine-grained amphibolite from Wonu, Ibadan-Apomu area showing feathery pyroxene (Augite), hornblende (H), Opaques (O), Corona haloes around pyroxenes, (a-c) in plane-polarized light (d-f) in cross-polarized light.

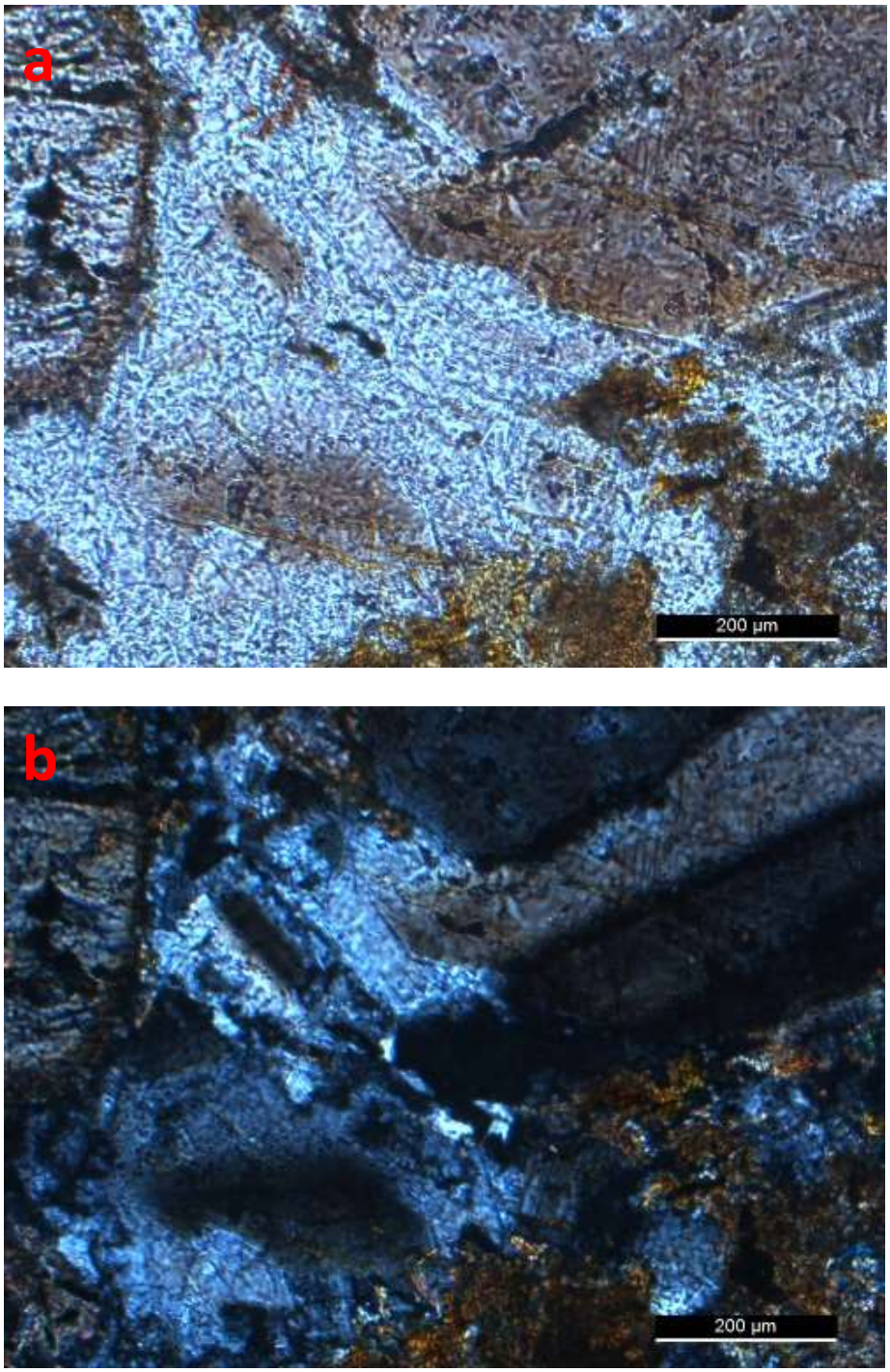

Fig.4.32: Photomicrograph showing fine-grained amphibolite from Wonu, Ibadan-Apomu area showing zoned augite, altered orthopyroxene, skeletal olivine phenocrysts altered to talc. Corona haloes around pyroxenes, (a) in plane-polarized light (b) in cross-polarized light.

Table 4.10:Modal composition of the fine-grained amphibolite in Wonu, Ibadan-Apomu area

	1	**2**	**3**	**4**	**5**	**6**	**7**	**8**	**9**	**10**
Actinolite	28	27	30	26	33	25	32	25	30	28
Hornblende	15	16	15	14	18	15	18	14	19	16
Tremolite	2	3	5	2	4	6	5	4	5	5
Orthopyroxene	12	12	12	12	10	11	10	11	10	12
Clinopyroxene	3	4	4	5	2	3	4	4	6	3
Plagioclase	10	9	10	10	10	9	9	10	10	9
K-Feldspar	7	5	5	6	5	4	5	5	4	6
Biotite/Phlogopite	5	4	4	4	5	5	5	4	4	5
Quartz	5	4	3	5	2	5	2	5	2	3
Ilmenite	2	2	2	1	2	1	2	2	1	2
Magnetite	1	2	2	2	1	2	1	2	2	1
Talc	2	3	3	5	3	4	2	4	2	2
Chlorite	3	5	2	4	2	5	2	5	2	4
Ferritchromite	1	1	1	1	1	1	1	1	1	1
Pyrite	3	2	1	2	1	3	1	3	1	2
Garnet	1	1	1	1	1	1	1	1	1	1
Total	100	100	100	100	100	100	100	100	100	100

4.3.1.2 SEM-EDS Images of the Fine-grained Amphibolites

The SEM-EDS backscattered image of the fine-grained amphibolite from Wonu, Ibadan-Apomu area confirmed the presence of the essential minerals identified in the thin sections. In addition, the amphibolite showed the presence of hornblende-plagioclase symplectite (Fig. 4.33),spinel alteration to ferritchromite (Spectrum 8), altered calcic amphibole (Spectrum 9), plagioclase (Spectrum 10) and altered spinel surrounded by chlorite (Spectrum 11)(Fig. 4.33).Disintegration of orthopyroxene to clinopyroxene-plagioclase symplectite was also observed.Inclusions of elongated ilmenite in altered calcic amphibole was also observed. Cr-spinel altered to ferritchromite withmagnetiterim are surrounded by chlorite. Similar mineralogy were depicted in Fig. 4.34.

Some of the samples of thefine-grained amphibolite from Wonu, Ibadan-Apomu area showed pyrite in graphite/carbonate matrix (Fig. 4.35).(Spectrum 1). Altered calcic amphibole and chloroapatite were seen in graphitic/carbonate groundmass of the amphibolite.Inclusions of olivine, chromite and apatite in Cr-spinel was surrounded by graphite/carbonate matrix (Spectrum 3).The graphite/carbonate groundmass also contain Cl^- as shown in Spectrum 4(Fig. 4.35). These are generally evidence of mantle plume greenstone erupted in shallow marine (carbonate) environmentof a back arc basin or subducted oceanic crust.

The SEM-EDS of the fine-grained amphibolite from Wonu, Ibadan-Apomu area further showed stratiform Cr-spinels of volcanic origin subjected to metamorphism as shown by mineral alignment with ample evidence of fluid invasion and alteration(Fig. 4.36). Fossilized cells and trace fossils, identical to thosereported by Furnes *et al*. (2008) was identified in some of the fine-grained amphibolite. The survival of such fossils is an indication of the presence of sea water that are H_2O and Cl^-bearing, which supports the growths of biogenic organisms in cracks of the basaltic rock. Pyrite and graphite bearing-dolomitic carbonate rock**(**Fig. 4.35) supports a reducing shallow marine environment. Invasion of the basaltic rock resulted in the deposition of allanite and monazite and alteration of olivine as observed in Fig. 4.35.

In conclusion, the SEM-EDS studies confirmed that the rock is a fine-grained olivine-pyroxene-bearing amphibolite with a mantle plume or oceanic pillow basalt protolith. The basaltic rock of volcanic origin was subjected tometamorphism and metasomatism as shown by mineral alignment.

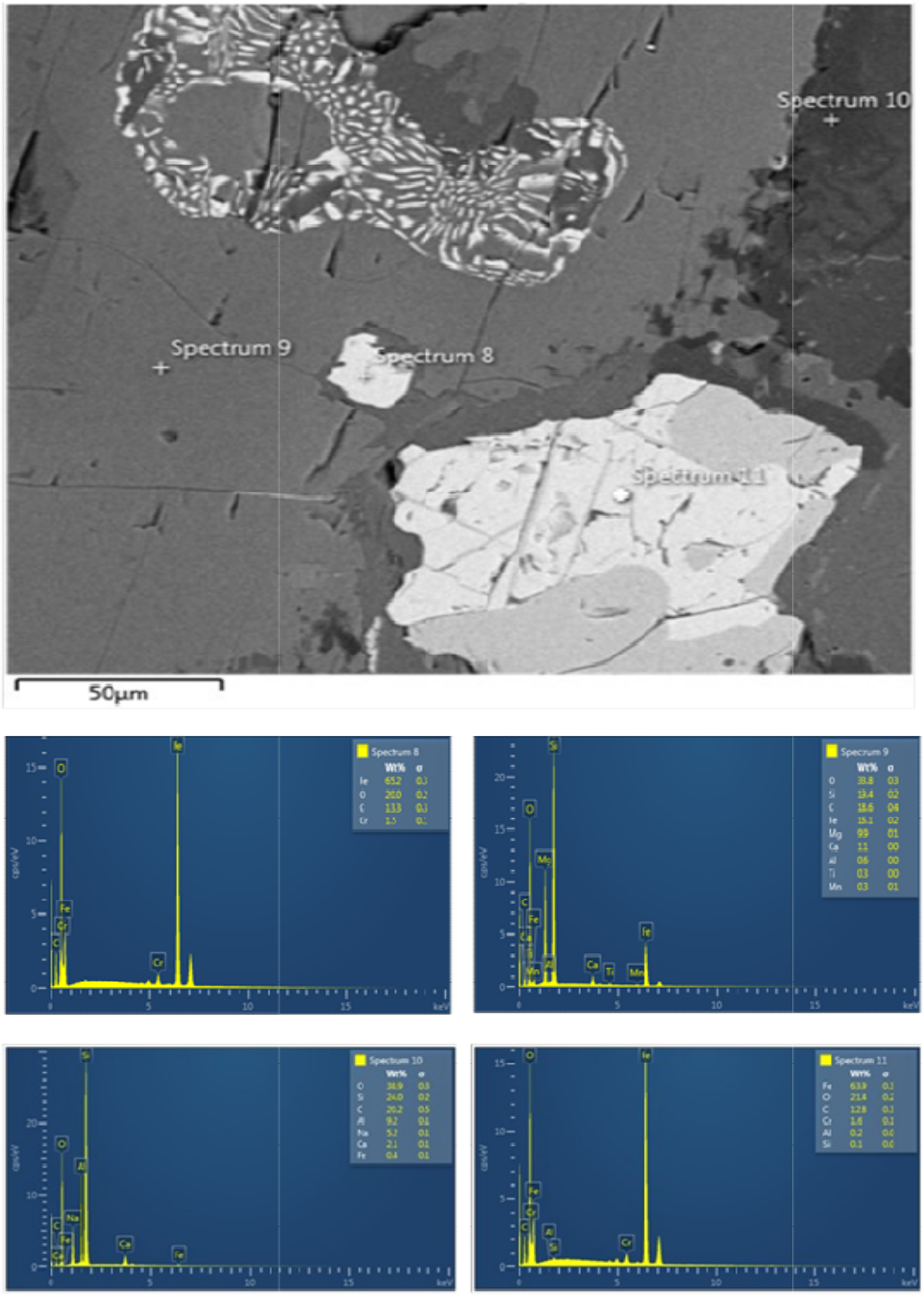

Fig. 4.33: SEM-EDS of fine-grained amphibolite from Wonu, Ibadan-Apomu area showing Cr-spinel alteration to ferritchromite (Spectrum 8), altered calcic amphibole (Spectrum 9), plagioclase (Spectrum 10) and altered spinel surrounded by chlorite (Spectrum 11).

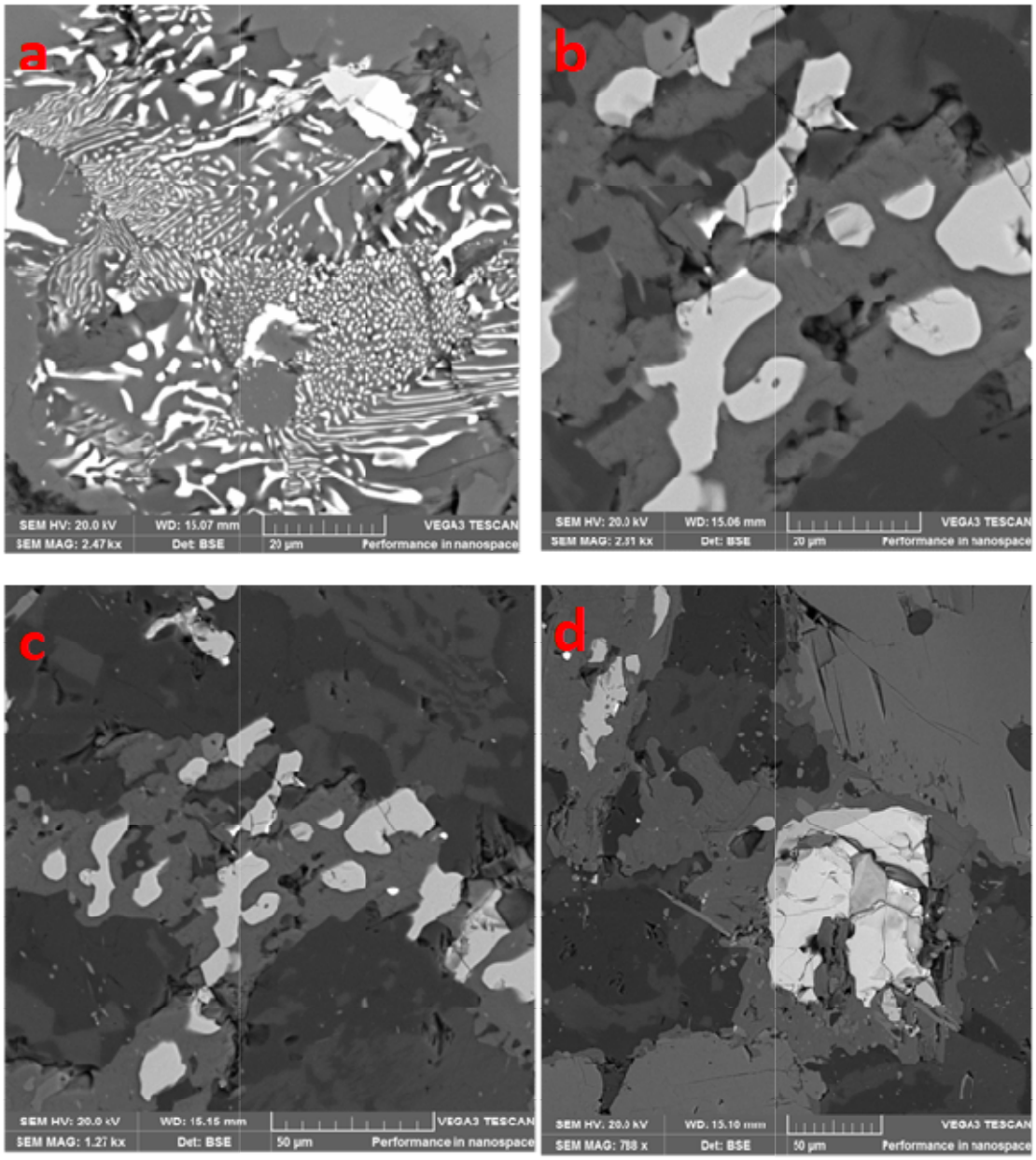

Fig. 4.34: SEM-EDS of fine-grained amphibolite from Ibadan-Apomu area showing (a) disintegration of orthopyroxene to clinopyroxene-garnet-plagioclase symplectites, (b& c) amphiboles with inclusions of elongated ilmenite in altered calcic amphibole and (d) Cr-spinel alteration into ferritchromite and magnetite surrounded by chlorite in altered amphibolite.

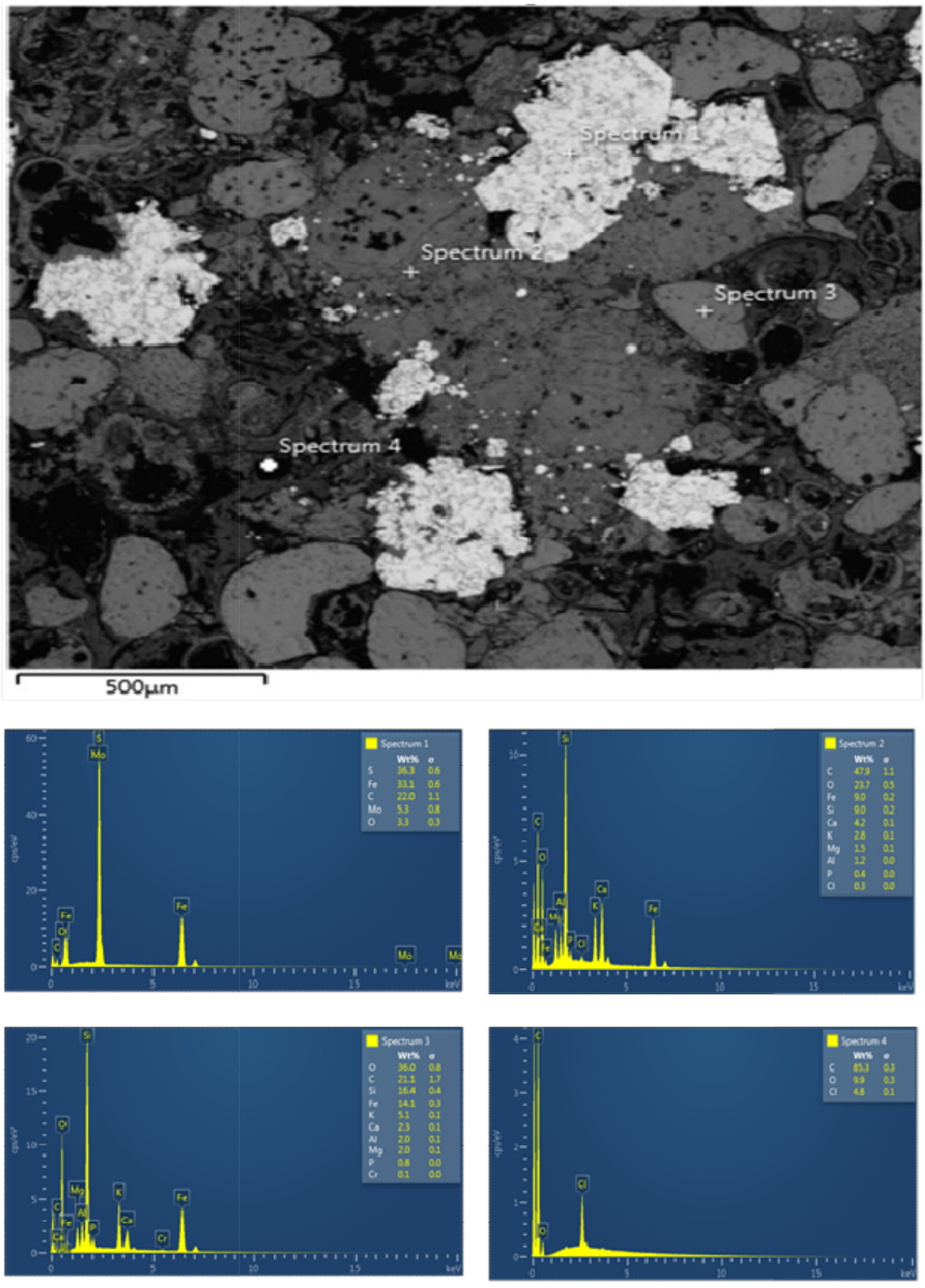

Fig. 4.35: SEM-EDS of fine-grained amphibolite from Wonu, Ibadan-Apomu area showing pyrite in graphite/carbonate matrix (Spectrum 1), altered calcic amphibole and chloroapatite in graphite/carbonate groundmass (Spectrum 2), inclusion of olivine, chromite and apatite in spinel surrounded by graphite/carbonate matrix (Spectrum 3) and the graphite/carbonate groundmass with Cl^- (Spectrum 4). Evidence of greenstone erupted in marine (carbonate) environment.

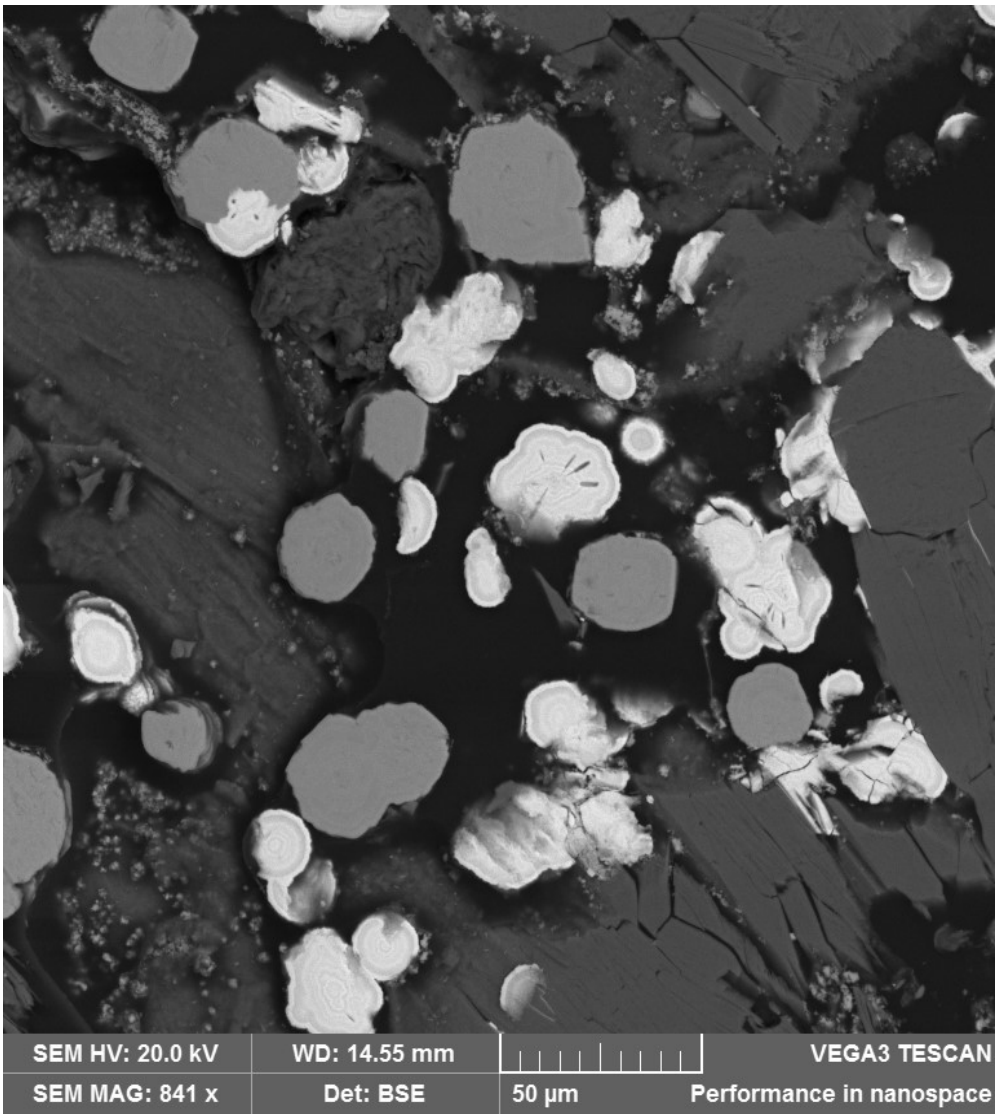

Fig. 4.36: SEM-EDS of fine-grained amphibolite from Wonu, Ibadan-Apomu area showing Cr-spinels of volcanic origin subjected to metamorphism as shown by mineral alignment with ample evidence of hydrothermal fluid invasion and alteration as shown by the presence of allanite, monazite and altered olivine (Forsterite).

4.3.1.3 Mineral Chemistry of the Fine-grained Amphibolites

The mineral chemistry of the fine-grained amphibolites revealed the presence of amphiboles, orthopyroxenes, clinopyroxenes. Biotite, chlorite, plagioclase and K-feldspars are 10% and below. Ilmenite, magnetite, altered olivine and Cr-spinel and quartz are less than 5%.

Olivines

Olivine crystals are altered to such an extent that the true chemical compositions are difficult to determine. The mineral chemistry (Table 4.11), showed that the MgO contents are low (17.21-32.08 %) while the FeO are high (26.55-47.08) indicating mainly intermediate olivine composition of between 40 to 67 % forsterite (Table 4.11). This composition is characteristic of Fe-tholeiites. Such olivines are common in differentiated magmatic basalts.

Pyroxenes

The mineral chemistry of pyroxene minerals revealed the presence of two-pyroxenes, namely orthopyroxene and clinopyroxene. The orthopyroxenes are more abundant than the clinopyroxenes. The representative mineral chemisty of the pyroxenes are shown in Tables4.12 and 4.13, respectively.

The Mg# = (Mg/Mg+Fe)composition in theorthopyroxene ranged from 0.55 to 0.68 (Table 4.11), while those of the clinopyroxene ranged from 0.75 to 0.95(Table 4.13).The orthopyroxene plotted mainly in the Mg-rich enstatite field, while the clinopyroxene plotted in the Mg-Ca-rich augite field, as shown in Fig. 4.40. The CaO content of the orthopyroxene ranged from 0.33 to 2.00 wt.%,while the CaO content of the clinopyroxene (18.04 to 20.17 wt.%), which may reflect submicroscopic orthopyroxene exsolution lamellae.

The clinopyroxenes are zoned with corona haloes at the rims (Figs.4.30 and 4.31), which showed a diopsidic composition (Morimoto,1988; Sushchevskaya *et al*. 2008) (Fig. 4.37).In Fig. 4.37 (after Sushchevskaya *et al*. 2008), Plot of Cr_2O_3 versus Al_2O_3, showed that the clinopyroxenes are Mg-augite, with low $Cr_2O_3$and Al_2O_3contents(Fig. 4.38). The high TiO_2 content of the clinopyroxenes (0.79-0.89 wt%) (Table 4.13) indicated low plagioclase-type cumulate magma generated from low degree of partial melting in the fine-grained amphibolite.

Table 4.11: Mineral chemistry of olivine in fine grained amphibolites

	1	2	3	4	5	6	7
SiO_2	35.86	37.00	38.86	39.92	40.33	38.05	40.46
TiO_2	0.08	0.05	0.02	0.04	0.02	0.02	0.02
Al_2O_3	0.03	0.02	0.01	0.02	0.03	0.02	0.02
Cr_2O_3	0.07	0.05	0.05	0.03	0.02	0.01	0.01
Fe_2O_3	0.00	0.00	0.00	0.00	0.00	0.00	0.00
FeO	47.08	34.61	37.69	26.55	32.08	41.66	40.66
MnO	0.16	0.15	0.23	0.12	0.22	0.14	0.14
MgO	17.21	27.37	23.44	32.08	27.54	18.97	18.97
CaO	0.20	0.22	0.05	0.17	0.21	0.29	0.29
Total	100.60	99.47	100.35	99.93	100.45	99.16	100.57
Formula units based on 4 oxygens							
Si	1.061	1.035	1.104	1.078	1.113	1.123	1.176
Ti	0.002	0.001	0.000	0.001	0.000	0.000	0.000
Al	0.001	0.001	0.000	0.001	0.001	0.001	0.001
Cr	0.002	0.001	0.001	0.001	0.000	0.000	0.000
Fe^{3+}	0.000	0.000	0.000	0.000	0.000	0.000	0.000
Fe^{2+}	1.165	0.810	0.895	0.622	0.740	1.028	0.988
Mn	0.004	0.004	0.006	0.003	0.005	0.003	0.003
Mg	0.759	1.142	0.992	1.291	1.133	0.835	0.822
Ca	0.006	0.007	0.002	0.005	0.006	0.009	0.009
Tot. cat.	3.000	3.000	3.000	3.000	3.000	3.000	3.000
Tot. oxy.	4.064	4.037	4.105	4.079	4.114	4.124	4.177
End member							
Fo	39.24	58.20	52.38	67.22	60.12	44.50	45.09
Fa	60.22	41.28	47.25	32.38	39.28	54.82	54.22

Table 4.12: Mineral chemistry of orthopyroxenes in fine grained amphibolite

	AM7/3	2/1 AM7/5	5/1 AM7/8	6/1 AM7/9	7/1 AM7/10	8/1 AM7/11	18/1 AM7/21	26/1 AM7/29	27/1 AM7/30	52/1 AM7/54
SiO_2	56.31	52.61	53.26	57.69	52.83	52.39	54.28	52.08	53.43	51.40
TiO_2	0.47	0.39	0.47	0.13	0.43	0.39	0.38	0.46	0.42	0.29
Al_2O_3	2.04	1.17	1.28	2.68	1.45	1.16	0.86	1.38	1.07	1.85
Cr_2O_3	0.10	0.07	0.11	0.01	0.08	0.08	0.07	0.11	0.08	0.10
Fe_2O_3	0.00	0.66	0.00	0.00	0.00	0.34	0.00	0.26	0.00	3.12
FeO	22.24	20.26	20.15	18.28	20.09	19.54	27.66	22.44	20.11	19.85
MnO	0.48	0.46	0.38	0.38	0.45	0.47	0.66	0.38	0.40	0.40
MgO	16.19	22.35	22.57	15.95	22.08	22.78	18.91	20.86	22.76	22.54
CaO	1.96	1.96	2.02	0.38	1.93	1.78	0.33	1.95	2.00	0.97
Na_2O	0.07	0.04	0.02	0.04	0.02	0.02	0.00	0.04	0.05	0.01
Total	99.86	99.97	100.26	95.54	99.36	98.95	103.15	99.96	100.32	100.53
Si	2.155	1.955	1.968	2.289	1.973	1.958	2.013	1.953	1.972	1.907
Ti	0.014	0.011	0.013	0.004	0.012	0.011	0.011	0.013	0.012	0.008
Al	0.092	0.051	0.056	0.125	0.064	0.051	0.038	0.061	0.047	0.081
Cr	0.003	0.002	0.003	0.000	0.002	0.002	0.002	0.003	0.002	0.003
Fe^{3+}	0.000	0.018	0.000	0.000	0.000	0.010	0.000	0.007	0.000	0.087
Fe^{2+}	0.712	0.629	0.623	0.606	0.627	0.611	0.858	0.703	0.621	0.616
Mn	0.016	0.014	0.012	0.013	0.014	0.015	0.021	0.012	0.013	0.013
Mg	0.924	1.238	1.244	0.943	1.229	1.269	1.045	1.166	1.252	1.247
Ca	0.080	0.078	0.080	0.016	0.077	0.071	0.013	0.078	0.079	0.039
Na	0.005	0.003	0.001	0.003	0.001	0.001	0.000	0.003	0.004	0.001
Tot. cat.	4.000	4.000	4.000	4.000	4.000	4.000	4.000	4.000	4.000	4.000
Tot. oxy.	6.213	6.000	6.010	6.354	6.017	6.000	6.043	6.000	6.006	6.000
XWo = $Ca/Ca+Mg+Fe_T$	4.68	3.97	4.11	1.03	3.99	3.63	0.68	4.01	4.05	1.94
XEn = $Mg/Ca+Mg+Fe_T$	53.83	63.04	63.89	60.24	63.56	64.73	54.55	59.64	64.15	62.70
XFs = $Fe_T/Ca+Mg+Fe_T$	41.48	32.99	32.00	38.73	32.44	31.64	44.76	36.36	31.80	35.36
Total	100.00	100.00	100.00	100.00	100.00	100.00	100.00	100.00	100.00	100.00
Fe_T/Fe_T+Mg	0.44	0.34	0.33	0.39	0.34	0.33	0.45	0.38	0.33	0.36
$Fe^{2+}/Fe^{2+}+Mg$	0.44	0.34	0.33	0.39	0.34	0.32	0.45	0.38	0.33	0.33

Table 4.12 contd.: Mineral chemistry of orthopyroxenes in fine grained amphibolites

	33/1 AM7/ 36	**34/1 AM7/3 7**	**45/1 AM7/ 47**	**48/1 AM7/ 50**	**49/1 AM7/ 51**	**51/1 AM7/ 53**	**16 AM9/ 17**	**17 AM9/ 18**	**18 AM9/ 19**	**19 AM9/ 20**
SiO_2	52.71	52.18	50.13	55.57	55.27	53.61	53.43	51.40	52.71	52.18
TiO_2	0.40	0.37	0.39	0.43	0.47	0.41	0.42	0.29	0.40	0.37
Al_2O_3	1.08	1.31	1.37	1.43	1.38	1.17	1.07	1.85	1.08	1.31
Cr_2O_3	0.10	0.12	0.10	0.14	0.14	0.10	0.08	0.10	0.10	0.12
Fe_2O_3	0.00	0.16	6.46	0.00	0.00	0.00	0.00	3.12	0.00	0.16
FeO	23.38	22.56	12.51	19.57	17.13	21.62	20.11	19.85	23.38	22.56
MnO	0.52	0.45	0.35	0.37	0.38	0.41	0.40	0.40	0.52	0.45
MgO	20.65	20.82	25.16	22.65	24.90	21.26	22.76	22.54	20.65	20.82
CaO	1.88	1.88	1.80	1.97	2.03	1.95	2.00	0.97	1.88	1.88
Na_2O	0.02	0.04	0.06	0.03	0.04	0.04	0.05	0.01	0.02	0.04
Total	100.74	99.90	98.33	102.16	101.74	100.57	100.32	100.53	100.74	99.90
Si	1.967	1.958	1.869	2.015	1.985	1.992	1.972	1.907	1.967	1.958
Ti	0.011	0.010	0.011	0.012	0.013	0.011	0.012	0.008	0.011	0.010
Al	0.047	0.058	0.060	0.061	0.058	0.051	0.047	0.081	0.047	0.058
Cr	0.003	0.004	0.003	0.004	0.004	0.003	0.002	0.003	0.003	0.004
Fe^{3+}	0.000	0.005	0.181	0.000	0.000	0.000	0.000	0.087	0.000	0.005
Fe^{2+}	0.730	0.708	0.390	0.593	0.514	0.672	0.621	0.616	0.730	0.708
Mn	0.016	0.014	0.011	0.011	0.012	0.013	0.013	0.013	0.016	0.014
Mg	1.149	1.165	1.398	1.224	1.333	1.177	1.252	1.247	1.149	1.165
Ca	0.075	0.076	0.072	0.077	0.078	0.078	0.079	0.039	0.075	0.076
Na	0.001	0.003	0.004	0.002	0.003	0.003	0.004	0.001	0.001	0.003
Tot. cat.	4.000	4.000	4.000	4.000	4.000	4.000	4.000	4.000	4.000	4.000
Tot. oxy.	6.003	6.000	6.000	6.058	6.027	6.029	6.006	6.000	6.003	6.000
XWo = $Ca/Ca+Mg+Fe_T$	3.85	3.87	3.52	4.04	4.06	4.03	4.05	1.94	3.85	3.87
XEn = $Mg/Ca+Mg+Fe_T$	58.80	59.64	68.50	64.63	69.23	61.11	64.15	62.70	58.80	59.64
XFs = $Fe_T/Ca+Mg+Fe_T$	37.35	36.49	27.98	31.33	26.72	34.86	31.80	35.36	37.35	36.49
Total	100.00	100.00	100.00	100.00	100.00	100.00	100.00	100.00	100.00	100.00
Fe_T/Fe_T+Mg	0.39	0.38	0.29	0.33	0.28	0.36	0.33	0.36	0.39	0.38
$Fe^{2+}/Fe^{2+}+Mg$	0.39	0.38	0.22	0.33	0.28	0.36	0.33	0.33	0.39	0.38

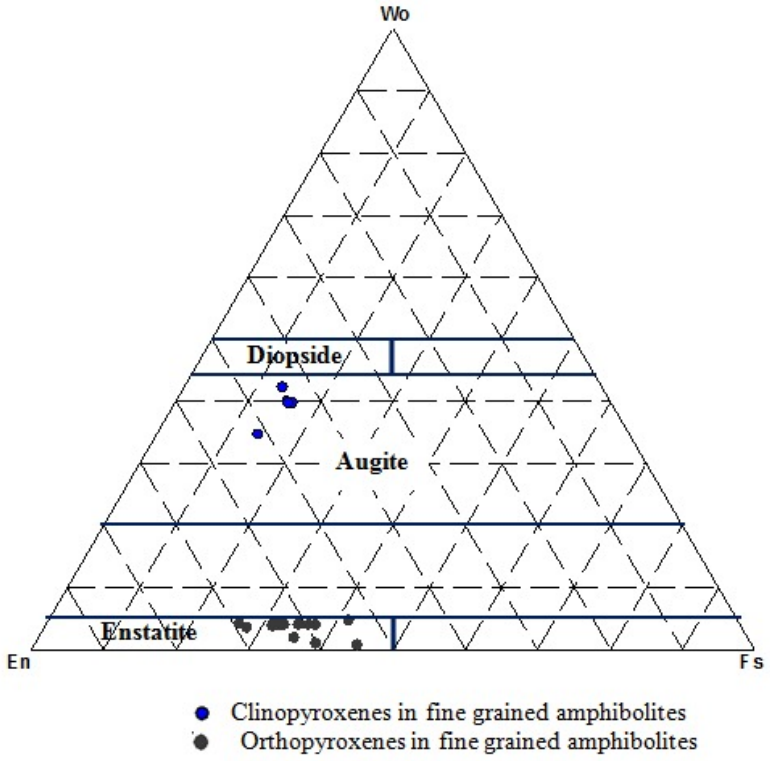

Fig. 4.37: Classification of pyroxenes in the fine-grained amphibolites of the Wonu, Ibadan-Apomu areas (after Sushevskaya *et al*, 2008).

Table 4.13: Mineral chemistry of clinopyroxenes in fine grained amphibolites

	AM7/56	AM7/59	AM7/60	AM7/61	AM7/62
SiO_2	52.89	50.91	51.82	51.58	52.29
TiO_2	0.89	0.79	0.79	0.83	0.88
Al_2O_3	2.72	1.84	2.16	2.32	2.27
Cr_2O_3	0.24	0.22	0.24	0.23	0.17
Fe_2O_3	0.00	8.65	1.05	1.15	0.53
FeO	8.34	1.67	8.57	9.01	9.23
MnO	0.23	0.24	0.28	0.27	0.25
MgO	15.20	19.16	15.53	15.17	15.44
CaO	20.17	18.04	19.24	19.07	19.16
Na_2O	0.27	0.52	0.32	0.36	0.38
Total	100.95	102.04	100.01	99.98	100.60
Si	1.942	1.837	1.924	1.919	1.930
Ti	0.025	0.021	0.022	0.023	0.024
Al	0.118	0.078	0.095	0.102	0.099
Cr	0.007	0.006	0.007	0.007	0.005
Fe^{3+}	0.000	0.235	0.029	0.032	0.015
Fe^{2+}	0.256	0.050	0.266	0.280	0.285
Mn	0.007	0.007	0.009	0.009	0.008
Mg	0.832	1.031	0.860	0.842	0.850
Ca	0.794	0.697	0.765	0.760	0.758
Na	0.019	0.036	0.023	0.026	0.027
Tot. cat.	4.000	4.000	4.000	4.000	4.000
Tot. oxy.	6.020	6.000	6.000	6.000	6.000
XWo = $Ca/Ca+Mg+Fe_T$	42.17	34.64	39.85	39.72	39.73
XEn = $Mg/Ca+Mg+Fe_T$	44.22	51.19	44.76	43.96	44.55
XFs = $Fe_T/Ca+Mg+Fe_T$	13.61	14.16	15.39	16.32	15.72
Total	100.00	100.00	100.00	100.00	100.00
Fe_T/Fe_T+Mg	0.24	0.22	0.26	0.27	0.26
$Fe^{2+}/Fe^{2+}+Mg$	0.24	0.05	0.24	0.25	0.25

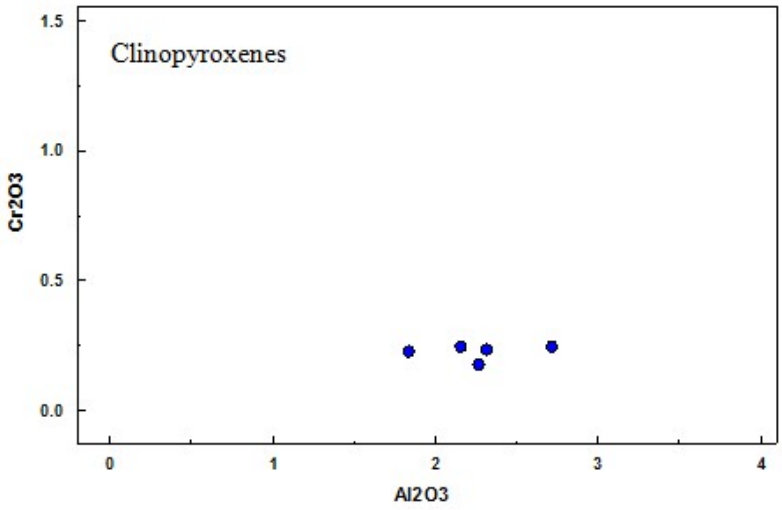

Fig. 4.38: The Cr_2O_3 vs. Al_2O_3 in clinopyroxenes of the fine grained amphibolite of Wonu, Ibadan-Apomu area.

Amphiboles

The mineral chemistry of the amphibole in the fine-grained amphibolite of Wonu, Ibadan-Apomu areaare presented in Table 4.14.The amphiboles vary from green to dark brown. The amphibole grains showed preferred orientation and are altered to chlorite along cleavage planes. They also have metacarbonate intercalations, garnet and are cut by quartzite veins.

The structural formulae of the amphiboles were calculated on an anhydrous basis, assuming 23 oxygen atoms per half unit cell.The amphiboles are mainly the Fe-Mg-Mn and calcic varieties as depicted on the Na(B) versus (Ca+Na) (B) diagram of Giret *et al*.(1980) (Fig. 4.39a). This indicates that the amphiboles are ferroan rich and calcic rich. The Si content ranged from 6.46 to 8.80 apfu, while the X_{Mg} contents ranged from 0.565 to 0.811apfu.The Ca content is very low, ranging from 0.006 to 0.300 apfu. In the calcic rich samples, the Si content ranged from 6.57 to 7.42 apfu, Ca content is very high in comparison with the Ca content of the ferroan rich samples, which ranged from 1.47 to 3.10 apfu. The Na content is very low in both the ferroan-rich and calcic-rich amphiboles ranging from 0.003 to 0.502 apfu(Table. 4.14).

Using the Xmg ($Mg(Mg+Fe^{2+})$) versus Si (apfu) diagram of the International Mineralogical Association (IMA) as recorded by Leake *et al*.(1997), the fine-grained amphibolite are mainly tremolite and magnesio-hornblende with subordinate tremolite (Fig. 4.39b).The amphiboles are weakly titaniferous and have most of their alumina in the tetrahedral site. The amphiboles showed evidence of retrogression from magensio-hornblende to actinolite. Small equant grains of actinolite surround large porphyroblasts or poikilitic hornblende. Some of the hornblende grains are altered to chlorite, while plagioclase are altered to sericite. These alteration phases are reflected in the myriads of mineral chemistry of the amphibolites.

The amphibolite does not have the required mineral assemblage that can be used for the aluminium hornblende geobaromometer (Schmidt, 1992) calculation due to alteration and retrograde metamorphism. Most of the primary minerals that could have been used for the hornblende-plagioclase geothermometer (Holland and Blundy, 1994), particularly along rim contact of the two minerals, have been altered to secondary minerals and as such no longer usable.

Table 4.14: Structural formulae of amphibole in fine-grained amphibolitesfromWonu, Ibadan-Apomu area

	AM7/3	AM7/5	AM7/8	AM7/9	AM7/10	AM7/11	AM7/21	AM7/29	AM7/30	AM7/36
SiO_2	56.31	52.61	53.26	57.69	52.83	52.39	54.28	52.08	53.43	52.71
TiO_2	0.47	0.39	0.47	0.13	0.43	0.39	0.38	0.46	0.42	0.40
Al_2O_3	2.04	1.17	1.28	2.68	1.45	1.16	0.86	1.38	1.07	1.08
Cr_2O_3	0.10	0.07	0.11	0.01	0.08	0.08	0.07	0.11	0.08	0.10
Fe_2O_3	0.00	9.86	8.70	0.00	8.11	9.63	6.41	9.36	8.78	9.15
FeO	22.24	11.97	12.32	18.28	12.80	11.18	21.89	14.25	12.21	15.15
MnO	0.48	0.46	0.38	0.38	0.45	0.47	0.66	0.38	0.40	0.52
MgO	16.19	22.35	22.57	15.95	22.08	22.78	18.91	20.86	22.76	20.65
CaO	1.96	1.96	2.02	0.38	1.93	1.78	0.33	1.95	2.00	1.88
Na_2O	0.07	0.04	0.02	0.04	0.02	0.02	0.00	0.04	0.05	0.02
K_2O	0.04	0.01	0.00	1.12	0.01	0.02	0.03	0.02	0.00	0.00
H_2O*	2.12	2.15	2.16	2.10	2.14	2.14	2.16	2.13	2.16	2.14
Total	102.02	103.05	103.29	98.76	102.32	102.04	105.98	103.02	103.36	103.80
Structural formulae based on 23 oxygens										
Si	7.976	7.335	7.384	8.248	7.400	7.346	7.548	7.328	7.400	7.379
Al^{iv}	0.024	0.192	0.209	0.000	0.239	0.192	0.141	0.229	0.175	0.178
Al^{vi}	0.316	0.000	0.000	0.452	0.000	0.000	0.000	0.000	0.000	0.000
Ti	0.050	0.041	0.049	0.014	0.045	0.041	0.040	0.049	0.044	0.042
Cr	0.011	0.008	0.012	0.001	0.009	0.009	0.008	0.012	0.009	0.011
Fe^{3+}	0.000	1.035	0.907	0.000	0.854	1.016	0.671	0.991	0.915	0.964
Fe^{2+}	2.634	1.396	1.429	2.186	1.499	1.311	2.546	1.676	1.414	1.773
Mn	0.058	0.054	0.045	0.046	0.053	0.056	0.078	0.045	0.047	0.062
Mg	3.418	4.646	4.665	3.400	4.610	4.762	3.920	4.376	4.699	4.309
Ca	0.297	0.293	0.300	0.058	0.290	0.267	0.049	0.294	0.297	0.282
Na	0.019	0.011	0.005	0.011	0.005	0.005	0.000	0.011	0.013	0.005
K	0.007	0.002	0.000	0.204	0.002	0.004	0.005	0.004	0.000	0.000
OH*	2.000	2.000	2.000	2.000	2.000	2.000	2.000	2.000	2.000	2.000
Total	16.812	17.013	17.005	16.619	17.007	17.009	17.005	17.015	17.013	17.005
Amphibole group	Fe-Mg-Mn	Fe-Mg-Mn	Fe-Mg-Mn	Fe-Mg-Mn	Fe-Mg-Mn	Fe-Mg-Mn	Fe-Mg-Mn	Fe-Mg-Mn	Fe-Mg-Mn	Fe-Mg-Mn
(Ca+Na) (B)	0.317	0.293	0.300	0.069	0.290	0.268	0.049	0.294	0.297	0.282
Na (B)	0.019	0.000	0.000	0.011	0.000	0.000	0.000	0.000	0.000	0.000
(Na+K) (A)	0.007	0.013	0.005	0.204	0.007	0.009	0.005	0.014	0.013	0.005
$Mg/(Mg+Fe^{2+})$	0.565	0.769	0.766	0.609	0.755	0.784	0.606	0.723	0.769	0.708
$Fe^{3+}/(Fe^{3+}Al^{vi})$	0.000	1.000	1.000	0.000	1.000	1.000	1.000	1.000	1.000	1.000
Sum of S2	14.488	14.707	14.700	14.346	14.710	14.733	14.951	14.706	14.703	14.718

Table 4.14 contd: Structural formulae of amphibole in fine-grained amphibolites(sample) from Wonu, Ibadan-Apomu area

	AM7/37	AM7/50	AM7/51	AM7/53	AM7/54	AM7/56	AM7/60	AM7/61	AM7/62	AM7/46
SiO_2	52.18	55.57	55.27	53.61	51.40	52.89	51.82	51.58	52.29	50.31
TiO_2	0.37	0.43	0.47	0.41	0.29	0.89	0.79	0.83	0.88	1.11
Al_2O_3	1.31	1.43	1.38	1.17	1.85	2.72	2.16	2.32	2.27	8.61
Cr_2O_3	0.12	0.14	0.14	0.10	0.10	0.24	0.24	0.23	0.17	0.04
Fe_2O_3	9.27	5.24	7.52	7.16	12.16	0.00	0.00	0.00	0.00	0.00
FeO	14.37	14.86	10.36	15.18	11.72	8.34	9.52	10.04	9.71	11.11
MnO	0.45	0.37	0.38	0.41	0.40	0.23	0.28	0.27	0.25	0.11
MgO	20.82	22.65	24.90	21.26	22.54	15.20	15.53	15.17	15.44	13.97
CaO	1.88	1.97	2.03	1.95	0.97	20.17	19.24	19.07	19.16	11.56
Na_2O	0.04	0.03	0.04	0.04	0.01	0.27	0.32	0.36	0.38	1.83
K_2O	0.01	0.01	0.00	0.00	0.26	0.01	0.00	0.00	0.00	0.97
H_2O*	2.13	2.20	2.22	2.15	2.16	2.14	2.10	2.10	2.12	2.12
Total	102.95	104.90	104.72	103.44	103.85	103.10	102.00	101.97	102.67	101.74
Structural formulae based on 23 oxygens										
Si	7.348	7.561	7.449	7.474	7.152	7.421	7.393	7.378	7.407	7.119
Al ^{iv}	0.217	0.229	0.219	0.192	0.303	0.450	0.363	0.391	0.379	0.881
Al ^{vi}	0.000	0.000	0.000	0.000	0.000	0.000	0.000	0.000	0.000	0.555
Ti	0.039	0.044	0.048	0.043	0.030	0.094	0.085	0.089	0.094	0.118
Cr	0.013	0.015	0.015	0.011	0.011	0.027	0.027	0.026	0.019	0.004
Fe^{3+}	0.983	0.536	0.763	0.751	1.273	0.000	0.000	0.000	0.000	0.000
Fe^{2+}	1.692	1.691	1.168	1.770	1.364	0.979	1.136	1.201	1.150	1.315
Mn	0.054	0.043	0.043	0.048	0.047	0.027	0.034	0.033	0.030	0.013
Mg	4.371	4.594	5.003	4.419	4.675	3.179	3.303	3.235	3.261	2.947
Ca	0.284	0.287	0.293	0.291	0.145	3.032	2.941	2.922	2.908	1.753
Na	0.011	0.008	0.010	0.011	0.003	0.073	0.089	0.100	0.104	0.502
K	0.002	0.002	0.000	0.000	0.046	0.002	0.000	0.000	0.000	0.175
OH*	2.000	2.000	2.000	2.000	2.000	2.000	2.000	2.000	2.000	2.000
Total	17.013	17.010	17.010	17.011	17.049	17.284	17.371	17.375	17.352	17.382
Amphibole group	Fe-Mg-Mn	Fe-Mg-Mn	Fe-Mg-Mn	Fe-Mg-Mn	Fe-Mg-Mn	Ca	Ca	Ca	Ca	Ca
(Ca+Na) (B)	0.284	0.287	0.293	0.292	0.145	3.032	2.941	2.922	2.908	2.000
Na (B)	0.000	0.000	0.000	0.000	0.000	0.000	0.000	0.000	0.000	0.247
(Na+K) (A)	0.012	0.009	0.010	0.010	0.049	0.075	0.089	0.100	0.104	0.430
$Mg/(Mg+Fe^{2+})$	0.721	0.731	0.811	0.714	0.774	0.765	0.744	0.729	0.739	0.691
$Fe^{3+}/(Fe^{3+}Al^{vi})$	1.000	1.000	1.000	1.000	1.000	0.000	0.000	0.000	0.000	0.000
Sum of S2	14.716	14.713	14.707	14.709	14.855	12.177	12.341	12.352	12.340	12.952

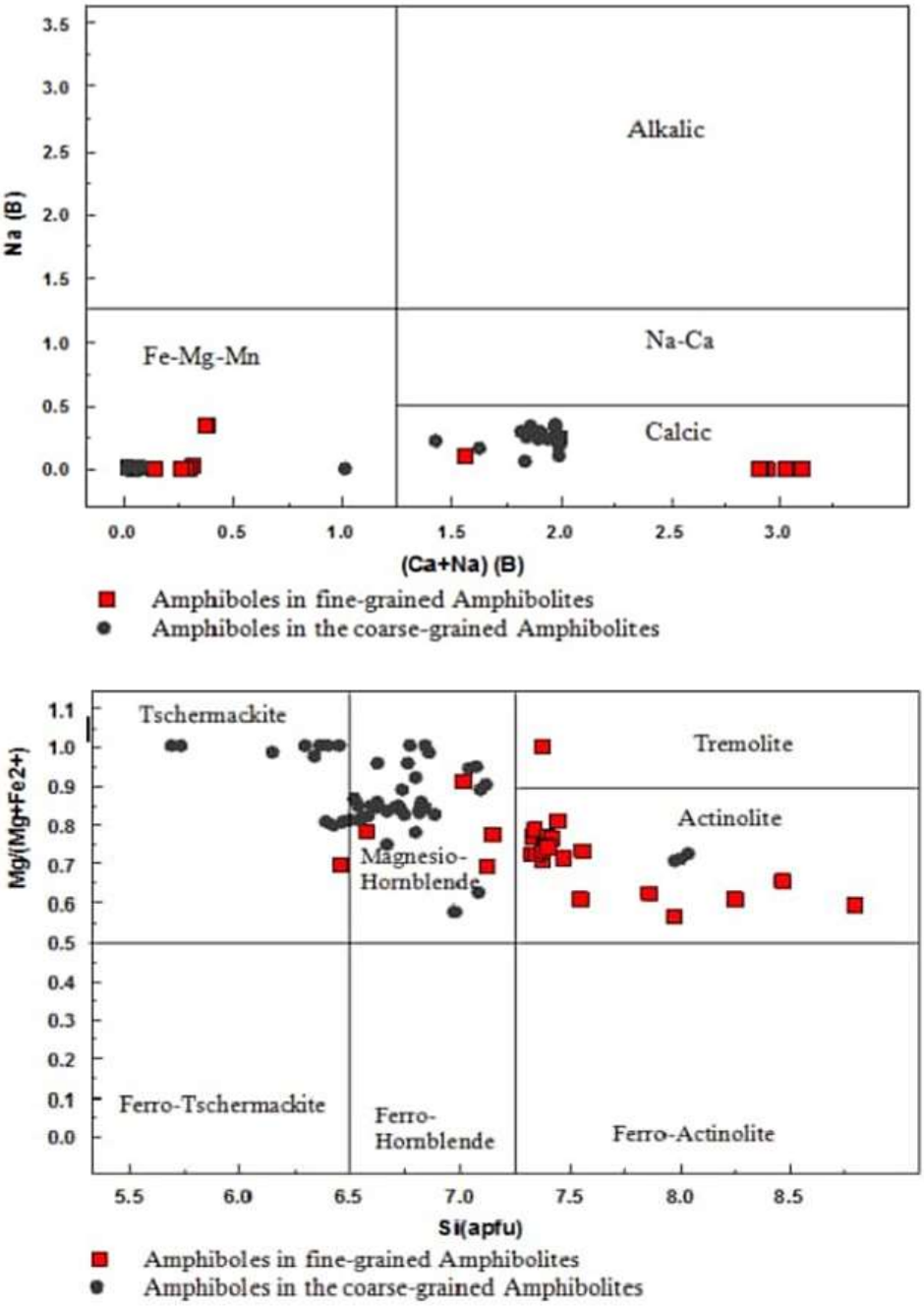

Fig. 4.39: Classification of theamphiboles in the fine-grained amphibolite (red square) of Wonu, Ibadan-Apomu area on (a) as calcic group on the *B (Na)* vs *B (Ca+Na)*of Giret *et al.*(1980), (b) as actinolite, magnesio-hornblende and tremoliteon the X_{Mg} vs Si (apfu) plot of Leake *et al.*(1997).

Biotite

The mineral chemistry of the biotite in the fine-grained amphibolites of Wonu, Ibadan-Apomu area are shown in Table 4.15.

The biotite minerals ranged from Mg-rich biotite to phlogopite, as shown in Fig. 4.40 (Nachit *et al.,* 2005).The TiO_2 of the biotite ranged from low (1.23 %) to high (4.95 %). The Ti percentage in biotites is affirmed to be controlled by the temperature of crystallization of biotite and the oxygen fugacity (fO_2) (Abuquerque, 1973) and also on the volatile component of the magma. A low Ti content corresponds with low temperature of crystallization and decreased oxygen fugacity. Low Ti-bearing Mg-biotites and phlogopites are found mainly in tholeiitic basalts and basaltic komatiites. The $Al_2O_3$is moderate (11.83-13.61 %) while the Mg# ranged from 0.5 to 0.6, which are characteristic of sub-continental lithosphere that has undergone metasomatism.

The classification of the biotites on the Mg - Fe^{3+}+Ti - Fe^{2+}+Mn diagram after Deer (1992)confirmed that they are Mg-rich biotite(Fig. 4.41a).According to Abdel-Rahman(1994; 1996),the chemistry of biotite could be used to discriminatetheir magma source as eitheranorogenic alkaline magma(A), calc-alkaline magma (C) of orogenic suites orperaluminous magma(P)(including S-type). All the biotite in the fine-grained amphibolites plot withinthe field of calc-alkaline magma (C) orogenic suites as depicted on the Abdel-Rahman (1994) $MgO–FeO_{(t)}–Al_2O_3$ tectonomagmatic discrimination diagram (Fig. 4.41b). This corresponds to the aluminium saturation catalog of the rock.

The $FeO_{(t)}$+MnO-10*TiO_2-MgO plot of the biotites showed that the amphibolites contained both primary biotite and reequilibrated primary biotite(Fig. 4.42). This implies that part of the primary biotites formed directly from the fractionation of the primary magmahas been reequilibrated during metasomatismor post-magmatic hydrothermal alteration.

Table 4.15: Mineral Chemistry of biotite in fine-grained amphibolites

	AM7/7	AM7/13	AM7/17	AM7/20	AM7/23	AM7/27	AM7/32	AM7/44	AM9/6	AM9/8
SiO_2	39.73	36.70	38.68	49.36	36.11	36.32	37.88	43.28	38.90	35.80
TiO_2	1.30	4.79	4.78	3.62	4.62	4.95	4.70	1.23	4.95	4.52
Al_2O_3	13.56	12.25	13.61	11.83	12.95	12.41	12.55	12.02	13.40	12.00
FeO	10.72	16.19	14.75	11.58	14.35	14.71	11.38	14.47	16.30	17.10
MnO	0.06	0.04	0.03	0.02	0.05	0.04	0.05	0.17	0.04	0.04
MgO	14.63	15.83	12.84	10.51	14.35	15.61	18.10	18.39	13.00	13.00
CaO	5.96	0.10	0.07	0.55	1.88	0.05	0.03	0.11	0.05	1.42
Na_2O	1.55	0.07	0.06	0.22	0.06	0.09	0.09	0.05	0.06	0.09
K_2O	6.56	9.25	9.49	8.91	9.13	9.48	9.48	7.03	9.37	8.58
Cr_2O_3	0.10	0.01	0.27	0.19	0.23	0.01	0.75	0.08	0.02	0
NiO	0.05	0.08	0.08	0.05	0.09	0.06	0.05	0.07	0.06	0.08
H_2O*	4.05	3.97	4.00	4.28	3.92	3.92	4.05	4.20	4.04	3.83
Total	98.27	99.28	98.66	101.12	97.74	97.65	99.11	101.10	100.19	96.46
Structural formulae based on 22 oxygens										
Si	5.888	5.546	5.801	6.908	5.527	5.554	5.606	6.178	5.777	5.607
Al ^{iv}	2.112	2.182	2.199	1.092	2.336	2.237	2.189	1.822	2.223	2.215
Al ^{vi}	0.257	0.000	0.207	0.859	0.000	0.000	0.000	0.200	0.122	0.000
Ti	0.145	0.544	0.539	0.381	0.532	0.569	0.523	0.132	0.553	0.532
Cr	0.012	0.001	0.032	0.021	0.028	0.001	0.088	0.009	0.002	0.000
Fe	1.329	2.046	1.850	1.355	1.837	1.881	1.409	1.727	2.024	2.240
Mn	0.008	0.005	0.004	0.002	0.006	0.005	0.006	0.021	0.005	0.005
Mg	3.232	3.566	2.871	2.193	3.274	3.558	3.993	3.913	2.878	3.035
Ni	0.006	0.010	0.010	0.006	0.011	0.007	0.006	0.008	0.007	0.010
Ca	0.946	0.016	0.011	0.082	0.308	0.008	0.005	0.017	0.008	0.238
Na	0.445	0.021	0.017	0.060	0.018	0.027	0.026	0.014	0.017	0.027
K	1.240	1.783	1.815	1.591	1.782	1.849	1.790	1.280	1.775	1.714
OH*	4.000	4.000	4.000	4.000	4.000	4.000	4.000	4.000	4.000	4.000
Total	19.620	19.720	19.357	18.550	19.660	19.696	19.640	19.321	19.392	19.624
Y total	4.988	6.172	5.513	4.817	5.688	6.022	6.025	6.011	5.592	5.822
X total	2.632	1.820	1.844	1.733	2.109	1.884	1.820	1.311	1.800	1.980
Al total	2.369	2.182	2.406	1.951	2.336	2.237	2.189	2.022	2.346	2.215
Fe/Fe+Mg	0.291	0.365	0.392	0.382	0.359	0.346	0.261	0.306	0.413	0.425
Luhr et al. 1984	906.3	1091.6	1129.0	1113.5	1126.1	1146.2	1265.3	875.4	1101.7	1052.8

* Luhr *et al.* (1984)

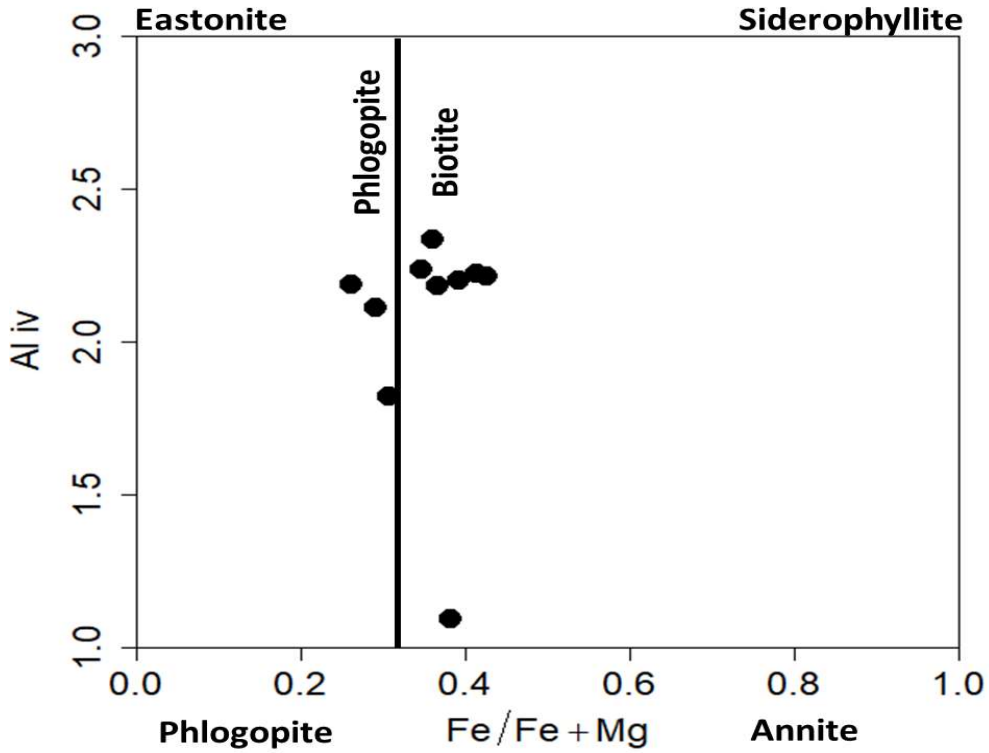

Fig. 4.40: Division of the biotite in fine-grained amphibolite in Wonu, Ibadan-Apomu area (after Nachit *et al.*, 2005).

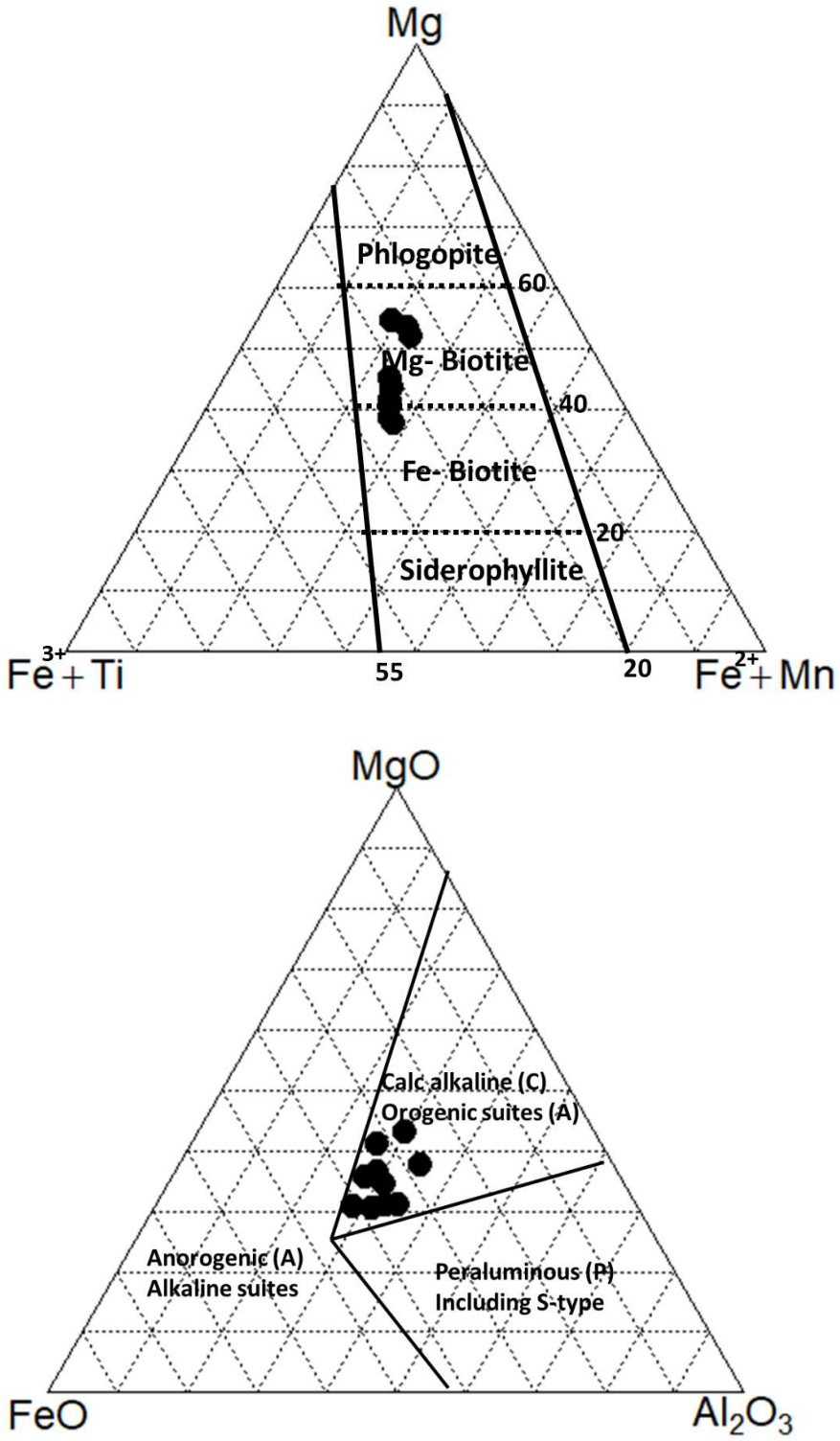

Fig. 4.41: Classification of biotites of the fine-grained amphibolite in Wonu, Ibadan-Apomu area on the (a) Mg - Fe^{3+}+Ti - Fe^{2+}+Mn diagram (after Deer 1992)and (b) MgO–$FeO_{(t)}$–Al_2O_3 tectonic plot.

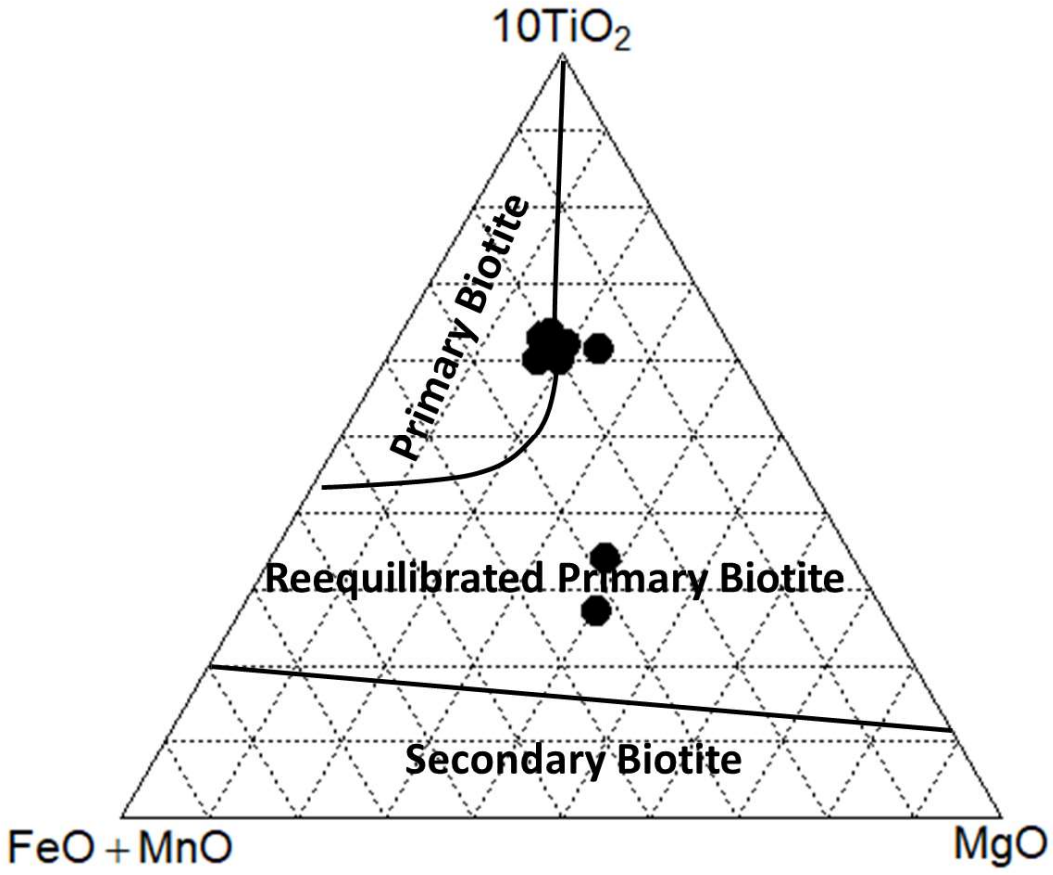

Fig. 4.42: Division of biotite in the fine-grained amphibolite of Wonu, Ibadan-Apomu areas on the FeO(t)+MnO-10*TiO_2-MgO diagram (after Nachit *et al.*, 2005).

Magnetite and Ilmenite

Mineral chemistry of the magnetite and ilmenite in the fine-grained amphibolites of Wonu, Ibadan-Apomu area are presented in Table 4.16. The ilmenite occur as small subhedral grains with low MgO (0.10-0.15 %) and Mn (0.46-0.78 %). They are normal low-Mg ferroilmenite characteristic of basaltic rocks.

The magnetite also occur as small subhedral disseminated grains with the Fe_2O_3:FeO compositional ratio of almost 2:1 (Table 4.16). Alteration of magnetite to haematite should be expected in such metasomatised amphibolite.

Feldspars

Plagioclase and K-felspars occur within the fine-grained amphibolites of Wonu, Ibadan-Apomu area.

Plagioclase feldspars

Theplagioclase crystals are euhedral to subhedral, fragmented and broken with albite twinningand oscillatory zoning.According to Deer *et al*.(1962),only plagioclases with zoned structures have irregular growth (Figs. 4.30 and 4.32).

Representative mineral chemistry of the plagioclase feldspars are shown in Table 4.17. Their compositionsranged from andesine (An_{50-44}) to oligoclase (An_{30-20}) (Fig. 4.43), typical of mafic rocks. Alteration in the form of kaolinization ofplagioclasesandchloritization of ferromagnesian minerals, such as, amphiboles and biotite was very common. Hydrothermal alteration of the olivines, pyroxenes and amphiboles could lead to the release of Na, Ca and Mg, which could crystalise into secondary sodic feldspars (albite) and calcite/dolomite, respectively.

Plagioclase and orthoclase often formed symplectite with hornblende as observed in the thin sections (Figs. 4.30 and 4.32), and also in the SEM-EDS (Figs. 4.33 and 4.34). This intimate association led to the increase in the Ca content of plagioclase as revealed in the three (3) samples that plot outside the field of normal feldspars (Fig. 4.43).

Table 4.16: Mineral chemistry of magnetite and ilmenite in the fine-grained amphibolites

	Magnetite			Ilmenite		
	AM7/2	**AM7/65**	**AM7/66**	**AM7/1**	**AM7/63**	**AM7/64**
SiO_2	0.03	0.03	0.03	0.03	0.02	0.03
TiO_2	0.52	0.46	0.69	49.12	52.55	50.62
Al_2O_3	0.06	0.04	0.05	0.00	0.00	0.00
Cr_2O_3	0.12	0.10	0.09	0.00	0.00	0.00
Fe_2O_3	67.50	68.15	68.26	0.00	0.00	0.00
FeO	31.45	30.74	30.79	48.90	45.18	48.16
MnO	0.00	0.02	0.01	0.72	0.46	0.55
MgO	0.01	0.00	0.02	0.10	0.15	0.10
Total	**99.69**	**99.54**	**99.94**	**98.87**	**98.36**	**99.46**
Formula units based on 4 oxygens				**Formula units based on 3 oxygens**		
Si	0.001	0.001	0.001	0.001	0.001	0.001
Ti	0.015	0.013	0.020	0.959	1.009	0.975
Al	0.003	0.002	0.002	0.000	0.000	0.000
Cr	0.004	0.003	0.003	0.000	0.000	0.000
Fe^{3+}	1.961	1.980	1.973	0.000	0.000	0.000
Fe^{2+}	1.015	0.993	0.989	1.061	0.965	1.032
Mn	0.000	0.001	0.000	0.016	0.010	0.012
Mg	0.001	0.000	0.001	0.004	0.006	0.004
Tot. cat.	3.000	2.993	2.990	2.041	1.990	2.024
Tot. oxy.	4.000	4.000	4.000	3.000	3.000	3.000

Table 4.17: Mineral chemistry of plagioclase feldspars in fine-grained amphibolites

	AM7/6	**AM7/24**	**AM7/26**	**AM7/28**	**AM7/39**	**AM7/42**	**AM7/43**	**AM7/48**	**AM7/57**
SiO_2	62.57	56.39	61.75	64.61	55.17	55.28	63.98	55.56	56.20
TiO_2	0.06	0.09	0.07	0.13	0.09	0.09	0.01	0.10	0.07
Al_2O_3	20.87	27.33	21.52	21.94	27.07	27.04	22.31	27.33	27.58
Cr_2O_3	0.01	0.01	0.00	0.00	0.00	0.00	0.00	0.00	0.00
Fe_2O_3	0.00	0.00	0.28	0.30	0.29	0.22	0.00	0.54	0.00
FeO	0.22	0.27	0.00	0.00	0.35	0.44	0.06	0.00	1.89
MnO	0.01	0.01	0.00	0.01	0.02	0.02	0.01	0.00	0.04
MgO	0.00	0.07	0.03	0.02	0.01	0.03	0.00	0.07	1.19
CaO	5.04	9.78	5.83	3.41	10.10	10.06	4.28	9.78	9.83
Na_2O	8.58	5.80	9.27	8.75	5.70	5.66	8.80	6.03	4.73
K_2O	0.38	0.15	0.11	1.95	0.11	0.16	0.10	0.22	0.20
Total	97.74	99.90	98.86	101.12	98.91	99.00	99.55	99.63	101.73
Structural formula units recalculated based on 8 oxygens									
Si	2.846	2.542	2.762	2.835	2.514	2.518	2.853	2.507	2.507
Ti	0.002	0.003	0.002	0.004	0.003	0.003	0.000	0.003	0.002
Al	1.119	1.452	1.134	1.135	1.454	1.452	1.173	1.453	1.450
Cr	0.000	0.000	0.000	0.000	0.000	0.000	0.000	0.000	0.000
Fe^{3+}	0.000	0.000	0.010	0.010	0.010	0.008	0.000	0.019	0.000
Fe^{2+}	0.008	0.010	0.000	0.000	0.013	0.017	0.002	0.000	0.070
Mn	0.000	0.000	0.000	0.000	0.001	0.001	0.000	0.000	0.002
Mg	0.000	0.005	0.002	0.001	0.001	0.002	0.000	0.005	0.079
Ca	0.246	0.472	0.279	0.160	0.493	0.491	0.205	0.473	0.470
Na	0.757	0.507	0.804	0.744	0.504	0.500	0.761	0.527	0.409
K	0.022	0.009	0.006	0.109	0.006	0.009	0.006	0.013	0.011
Tot. cat.	5.000	5.000	5.000	5.000	5.000	5.000	5.000	5.000	5.000
An	23.98	47.81	25.64	15.81	49.16	49.09	21.06	46.67	52.77
Ab	73.87	51.31	73.78	73.42	50.20	49.98	78.36	52.08	45.95
Or	2.15	0.87	0.58	10.77	0.64	0.93	0.59	1.25	1.28

Table 4.16 contd.: Mineral chemistry of plagioclase feldspars in fine-grained amphibolites

	AM9/3	AM9/4	AM9/11	AM9/12	AM9/14	AM9/15	AM9/16
SiO_2	67.30	64.03	64.71	54.84	62.66	54.23	68.83
TiO_2	0.03	0.01	0.02	0.07	0.08	0.08	0.01
Al_2O_3	20.94	22.94	23.67	27.40	22.46	27.27	18.30
Cr_2O_3	0.00	0.01	0.00	0.01	0.00	0.00	0.01
Fe_2O_3	0.00	0.00	0.00	0.85	0.00	0.00	0.00
FeO	0.62	0.15	0.12	0.00	1.25	4.40	0.64
MnO	0.00	0.00	0.00	0.00	0.00	0.00	0.00
MgO	0.08	0.01	0.00	0.04	0.20	0.27	0.02
CaO	1.86	4.29	4.72	10.21	4.14	5.39	3.40
Na_2O	8.49	9.03	8.59	5.78	7.95	4.46	7.31
K_2O	1.76	0.11	0.12	0.15	1.10	0.20	0.13
Total	101.08	100.58	101.95	99.35	99.84	96.30	98.65
Structural formula units recalculated based on 8 oxygens							
Si	2.969	2.822	2.824	2.487	2.803	2.578	3.158
Ti	0.001	0.000	0.001	0.002	0.003	0.003	0.000
Al	1.089	1.191	1.217	1.465	1.184	1.528	0.990
Cr	0.000	0.000	0.000	0.000	0.000	0.000	0.000
Fe^{3+}	0.000	0.000	0.000	0.030	0.000	0.000	0.000
Fe^{2+}	0.023	0.006	0.004	0.000	0.047	0.175	0.025
Mn	0.000	0.000	0.000	0.000	0.000	0.000	0.000
Mg	0.005	0.001	0.000	0.003	0.013	0.019	0.001
Ca	0.088	0.203	0.221	0.496	0.198	0.275	0.167
Na	0.726	0.771	0.727	0.508	0.689	0.411	0.650
K	0.099	0.006	0.007	0.009	0.063	0.012	0.008
Tot. cat.	5.000	5.000	5.000	5.000	5.000	5.000	5.000
An	9.63	20.66	23.13	48.97	20.87	39.35	20.26
Ab	79.53	78.71	76.17	50.17	72.53	58.92	78.82
Or	10.84	0.63	0.70	0.86	6.60	1.74	0.92

K-feldspars

Mineral chemistry of the K-feldspars in the fine-grained amphibolite are presented in Table 4.18 and those of the perthites in Table 4.19. The K-feldspar crystals are anhedral andexhibit Carlsbad twinning, which indicated that they are orthoclase and not microcline (Fig. 4.30 and 4.32). Some of the K-feldspars are perthitic, with intergrowth of orthoclase and plagioclase as shown in Table 4.19 and (Fig. 4.43).Kaolinization oforthoclase, perthites and sericitization of plagioclases are noted. The presence of sanidine as shown in Fig. 4.43 could not be ruled out because the tholeiitic basalt precursor of the fine-grained amphibolite are volcanic.The presence of sanidine couldfurther suggest rapid quenching of high temperature pillow basalts probably erupted at or near marine environment.

Quartz

Fine-grained anhedral quartz crystals (2-4 %) occur as inclusions in many of the feldspar crystals (Fig. 4.34).Some of these quartz crystals are presumed to be of secondary or metasomatic origin based on their crystal shape, extinction and colour.

Table 4.18: Mineral Chemistry of K-feldspars in Fine-grained amphibolites

	AM7/22	**AM7/14**	**AM7/15**	**AM7/18**	**AM7/38**	**AM9/9**	**AM9/7**	**AM7/25**
SiO_2	60.30	62.20	64.13	64.12	62.51	63.61	61.65	64.69
TiO_2	0.37	0.04	0.08	0.12	0.04	0.06	0.04	0.07
Al_2O_3	16.74	17.21	18.07	17.43	17.65	17.83	17.48	18.22
Cr_2O_3	0.01	0.00	0.01	0.00	0.00	0.00	0.00	0.01
Fe_2O_3	1.24	0.09	0.00	0.00	0.00	0.25	0.25	0.00
FeO	0.00	0.00	0.11	0.22	0.10	0.00	0.00	0.20
MnO	0.02	0.00	0.01	0.00	0.00	0.01	0.00	0.00
MgO	1.22	0.03	0.03	0.11	0.02	0.01	0.01	0.08
CaO	0.27	0.10	0.32	0.11	0.53	0.98	3.11	1.31
Na_2O	1.24	1.44	1.85	1.02	1.34	1.73	1.44	2.19
K_2O	13.68	14.53	13.29	14.77	13.72	13.55	13.41	12.51
Total	95.09	95.64	97.90	97.90	95.91	98.03	97.39	99.28
Structural formula units recalculated based on 8 oxygens								
Si	2.920	2.989	3.010	3.023	3.002	2.984	2.916	2.992
Ti	0.013	0.001	0.003	0.004	0.001	0.002	0.001	0.002
Al	0.955	0.975	1.000	0.969	0.999	0.986	0.974	0.993
Cr	0.000	0.000	0.000	0.000	0.000	0.000	0.000	0.000
Fe^{3+}	0.047	0.003	0.000	0.000	0.000	0.009	0.009	0.000
Fe^{2+}	0.000	0.000	0.004	0.009	0.004	0.000	0.000	0.008
Mn	0.001	0.000	0.000	0.000	0.000	0.000	0.000	0.000
Mg	0.088	0.002	0.002	0.008	0.001	0.001	0.001	0.006
Ca	0.014	0.005	0.016	0.006	0.027	0.049	0.158	0.065
Na	0.116	0.134	0.168	0.093	0.125	0.157	0.132	0.196
K	0.845	0.891	0.796	0.888	0.840	0.811	0.809	0.738
Tot. cat.	5.000	5.000	5.000	5.000	5.000	5.000	5.000	5.000
An	1.44	0.50	1.64	0.56	2.75	4.84	14.34	6.50
Ab	11.93	13.02	17.18	9.45	12.57	15.46	12.02	19.65
Or	86.63	86.48	81.18	89.99	84.68	79.70	73.64	73.85

Table 4.19: Mineral chemistry of Perthites from fine-grained amphibolites

	AM9/2	AM9/13	AM7/19	AM7/34	AM7/35	AM7/40	AM7/58	AM7/4	AM7/16
SiO_2	61.99	61.16	63.81	64.69	61.84	65.37	64.14	63.32	65.04
TiO_2	0.13	0.25	0.04	0.16	0.20	0.14	0.02	0.22	0.13
Al_2O_3	21.17	20.00	19.80	20.12	19.58	19.76	21.12	18.36	19.32
Cr_2O_3	0.00	0.00	0.00	0.00	0.02	0.00	0.00	0.00	0.01
Fe_2O_3	0.20	2.39	0.00	0.00	0.67	0.00	0.16	0.00	0.00
FeO	0.38	0.00	0.30	0.15	0.00	0.15	0.00	0.22	0.26
MnO	0.01	0.01	0.00	0.02	0.00	0.01	0.00	0.02	0.00
MgO	0.03	0.73	0.19	0.00	0.39	0.00	0.01	0.00	0.01
CaO	3.05	2.08	2.82	1.56	1.93	1.14	2.75	0.64	0.99
Na_2O	5.63	5.57	4.96	4.55	4.42	4.20	7.98	3.02	3.95
K_2O	5.85	6.62	7.19	8.50	8.61	9.60	4.76	11.55	9.87
Total	98.44	98.81	99.11	99.75	97.66	100.37	100.94	97.35	99.58
Structural formula units recalculated based on 8 oxygens									
Si	2.838	2.796	2.913	2.940	2.868	2.958	2.821	2.970	2.971
Ti	0.004	0.009	0.001	0.005	0.007	0.005	0.001	0.008	0.004
Al	1.142	1.078	1.065	1.078	1.070	1.054	1.095	1.015	1.040
Cr	0.000	0.000	0.000	0.000	0.001	0.000	0.000	0.000	0.000
Fe^{3+}	0.007	0.085	0.000	0.000	0.024	0.000	0.006	0.000	0.000
Fe^{2+}	0.015	0.000	0.011	0.006	0.000	0.006	0.000	0.009	0.010
Mn	0.000	0.000	0.000	0.001	0.000	0.000	0.000	0.001	0.000
Mg	0.002	0.050	0.013	0.000	0.027	0.000	0.001	0.000	0.001
Ca	0.150	0.102	0.138	0.076	0.096	0.055	0.130	0.032	0.048
Na	0.500	0.494	0.439	0.401	0.397	0.368	0.681	0.275	0.350
K	0.342	0.386	0.419	0.493	0.509	0.554	0.267	0.691	0.575
Tot. cat.	5.000	5.000	5.000	5.000	5.000	5.000	5.000	5.000	5.000
An	15.10	10.38	13.85	7.83	9.56	5.65	12.03	3.22	4.98
Ab	50.43	50.29	44.09	41.35	39.64	37.68	63.17	27.52	35.94
Or	34.48	39.33	42.06	50.82	50.80	56.67	24.80	69.26	59.08

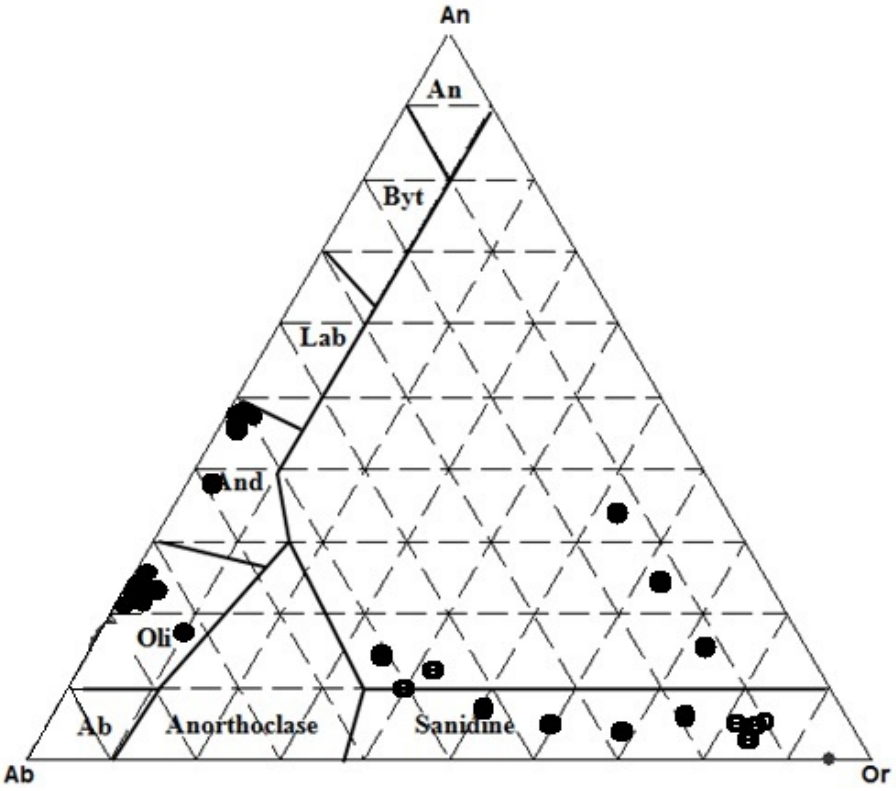

Fig. 4.43:Feldspar varieties in fine-grained amphibolites of Wonu, Ibadan-Apomu area (after Deer *et al.*, 1962).

4.3.1.4 Geochemistry of the fine-grained Amphibolites

The fine-grained amphibolites of the study area were processed for major, traceand rare-earth element components, including the range and average values are shown in Table 4.20. The SiO_2 contents ranged from 44.78 - 50.63%, Al_2O_3 14.01-16.41 %,$Fe_2O_{3(t)}$ 12.27-14.83 %, CaO 8.64 – 10.00 % and MgO 8.08-12.15 %. Other oxides, such as, TiO_2(0.25-1.39 %), MnO (0.07-0.24 %) and P_2O_5(0.01-0.09 %) are less than 1.5 %. These chemical data demonstrated basic composition of mafic rocks.

The Sum Alkalinity (Na_2O+K_2O)versus SiO_2 diagram (after Middlemost 1994) of the fine-grained amphibolite showed that the precursor vary from dominantly basalt to picrobasalt(Fig. 4.44). This clearly indicates the igneous parentage of the fine-grained amphibolites.The basic chemical character and the tholeiitic nature of the amphibolitewas further confirmed on the AFM (Na_2O + K_2O) – Fe_2O_3 – MgO)diagram of Irvine and Barager (1971) (Fig. 4.45a), while the Al_2O_3-MgO-($Fe_2O_{3(t)}$+TiO_2) diagrams of Jenson (1976) showed that the amphibolites are high-Fe tholeiitic basalt(Fig. 4.45b). The CaO-Al_2O_3-MgO plots of the Wonu, Ibadan-Apomu ultramafic-mafic rocks after Viljoen & Viljoen, (1969a, 1969b) (Fig. 4.46) showed possible fractionation of the tholeiitic basaltic protoliths from co-magmatic komatitic magma. The major element composition of the fine-grained amphibolites samples correlates with amphibolites in other parts of Nigeria (Table 4.21). Subtledistinctions observed are probably influenced by crustal materials, metasomatism and metamorphic conditions. The major element composition of the fine-grained amphibolites often indicate a relatively minute differences in constituents.

Fine-grained amphibolites are rich in trace elements such as Ba, Cr, V, Co, Cu, Ni, Rb, Sr, Y, Zr and Zn, though lower in Cr and Ni compared to similar amphibolites from Pakistan, Canada, India and Alabama (USA) (Table 4.21). Trace elements have largevariations, hence they are crucial to the study of petrogenesis. The trace element data and ratios of the fine-grained amphibolites are presented in Table 4.20. Trace element composition reveals average values of Sr (123), Ba (202), Cr (78) and Ni (65), Rb (33), Y(37), Zr (55), Cs(0.7), Th(1.0) ppm.

Table 4.20: Major oxides (%), trace elements and rare-earth (ppm) elements composition of fine-grained amphibolite.

	1	2	3	4	5	6	7	8	9	10	11	12	Average	Range	
SiO_2	50.60	50.03	50.62	48.5	44.78	48.91	50.43	50.63	50.44	49.6	47.50	48.70	49.23	50.63	44.78
TiO_2	0.46	0.25	0.51	0.32	0.88	0.26	0.82	0.56	1.39	0.63	0.42	0.39	0.57	1.39	0.25
Al_2O_3	15.05	14.81	15.26	16.41	14.01	15.11	14.34	14.53	14.04	14.21	15.61	15.33	14.89	16.41	14.01
$Fe_2O_{3(t)}$	12.52	14.1	13.03	12.27	14.62	13.31	12.67	12.69	12.62	13.19	14.83	12.77	13.21	14.83	12.27
MnO	0.09	0.12	0.15	0.07	0.23	0.13	0.14	0.11	0.08	0.19	0.21	0.24	0.15	0.24	0.07
MgO	9.65	8.11	8.08	11.2	12.15	9.84	8.19	8.82	8.78	10.03	9.52	10.93	9.61	12.15	8.08
CaO	8.72	9.45	9.22	9.25	10	9.33	9.54	9.49	8.92	8.84	8.79	8.64	9.18	10	8.64
Na_2O	1.25	1.78	1.56	1.13	1.88	1.52	1.72	1.67	2.35	1.62	1.19	1.82	1.62	2.35	1.13
K_2O	0.99	0.82	0.75	0.46	0.65	0.73	0.85	0.92	0.59	0.61	0.66	0.49	0.71	0.99	0.46
P_2O_5	0.02	0.05	0.01	0.09	0.02	0.04	0.06	0.08	0.06	0.05	0.08	0.09	0.054	0.09	0.01
LOI	0.35	0.32	0.25	0.34	0.28	0.38	0.26	0.37	0.31	0.39	0.29	0.33	0.32	0.39	0.25
Total	99.7	99.84	99.44	100.04	99.5	99.56	99.02	99.87	99.58	99.36	99.1	99.73			
Trace elements (ppm)															
Cr	92	58	65	92	88	80	60	53	90	93	79	89	78.25	93	53
Ni	46	68	24	85	98	47	69	28	82	96	65	67	64.58	98	24
Co	85	76	68	85	40	77	73	64	78	42	71	47	67.17	85	40
Cu	40	35	48	51	66	38	37	47	50	64	48	42	47.17	66	35
Zn	98	120	96	96	80	100	148	94	97	82	96	95	100.17	148	80
V	53	56	72	94	68	55	58	69	92	67	71	57	67.67	94	53
Sc	5	10	7	5	9	11	6	8	5	12	7	10	7.92	12	5
Ga	25	28	26	27	29	24	27	28	25	29	23	28	26.58	29	23
Ba	350	99	86	250	135	340	95	94	240	145	260	330	202	350	86
Rb	38	26	32	29	40	39	25	31	30	40	33	36	33.25	40	25
Sr	125	132	143	106	110	124	132	142	116	112	123	109	122.83	143	106
Y	38	44	26	32	45	37	43	25	31	44	39	38	36.83	45	25
Zr	62	48	57	49	59	61	49	58	46	57	55	53	54.5	62	46
Nb	2	6	9	6	5	5	7	6	5	8	7	6	6	9	2
Cs	0.4	0.6	0.6	0.9	0.8	0.6	0.7	0.9	0.5	0.8	0.7	0.6	0.68	0.9	0.4
Hf	1.1	0.5	0.9	0.8	0.7	0.9	1.0	0.7	0.9	1.1	0.8	0.9	0.86	1.1	0.5
Ta	0.3	0.5	0.4	0.3	0.1	0.2	0.4	0.4	0.1	0.2	0.5	0.5	0.33	0.5	0.1
Th	0.9	0.2	1.0	1.9	0.7	0.9	0.6	1.1	1.6	0.9	1.2	1.0	1	1.9	0.2
U	0.7	0.3	0.5	0.4	0.5	0.7	0.4	1.2	1.4	0.2	0.4	0.8	0.63	1.4	0.2
Rare-Earth elements (ppm)															
La	19.51	14.20	12.15	13.05	11.14	12.81	12.43	6.90	9.27	17.35	13.69	14.38	13.07	19.51	6.9
Ce	33.04	27.91	34.01	25.96	28.92	24.75	31.72	36.3	24.28	34.5	31.65	32.74	30.48	36.3	24.28
Pr	3.05	4.09	4.90	2.88	3.01	2.60	3.15	4.65	2.23	3.83	3.10	2.83	3.36	4.9	2.23
Nd	12.15	14.01	12.38	13.11	11.65	12.74	12.02	18.05	16.59	13.05	13.69	12.11	13.46	18.05	11.65
Sm	2.0	1.96	1.87	1.35	1.10	1.58	1.71	2.95	1.37	1.97	1.12	1.48	1.71	2.95	1.1
Eu	0.69	0.71	1.09	0.80	0.93	1.22	0.12	0.62	0.65	0.72	1.01	0.88	0.79	1.22	0.12
Gd	2.25	2.45	2.17	2.17	1.08	2.71	2.03	2.07	2.65	1.16	2.55	2.19	2.12	2.71	1.08
Tb	0.64	0.47	0.55	0.49	0.21	0.12	0.45	0.86	0.18	0.17	0.64	0.55	0.44	0.86	0.12
Dy	1.69	2.81	3.71	2.38	1.08	2.39	1.17	2.28	2.31	1.98	1.55	2.46	2.15	3.71	1.08
Ho	0.56	0.55	0.87	0.18	0.14	0.13	0.18	0.32	0.15	0.19	0.22	0.22	0.31	0.87	0.13
Er	1.10	1.63	1.53	1.43	1.32	0.94	0.46	0.58	1.29	0.44	1.38	2.05	1.18	2.05	0.44
Tm	0.32	0.30	0.21	0.20	0.18	0.26	0.18	0.19	0.27	0.16	0.33	0.29	0.24	0.33	0.16
Yb	1.66	1.39	1.87	1.11	1.09	1.11	1.09	0.99	0.85	1.02	1.69	1.42	1.27	1.87	0.85
Lu	0.29	0.28	0.21	0.22	0.24	0.22	0.24	0.09	0.07	0.06	0.28	0.23	0.20	0.29	0.06
Rare-Earth Elements ratios															
Eu/Eu*	0.99	0.99	1.65	1.43	2.60	1.80	0.20	0.77	1.04	1.45	1.82	1.49	1.35	0.20	2.60
LaN/YbN	8.00	6.95	4.42	8.00	6.96	7.85	7.76	4.74	7.42	11.58	5.51	6.89	7.17	4.42	11.58
LaN/SmN	6.11	4.54	4.07	6.06	6.35	5.08	4.55	1.47	4.24	5.52	7.66	6.09	5.14	1.47	7.66
CeN/YbN	5.24	5.29	4.79	6.16	6.99	5.87	7.66	9.65	7.52	8.91	4.93	6.07	6.59	4.79	9.65
CeN/SmN	4.00	3.45	4.41	4.66	6.37	3.80	4.50	2.98	4.30	4.24	6.85	5.36	4.58	2.98	6.85
EuN/YbN	1.19	1.46	1.67	2.06	2.44	3.15	0.32	1.79	2.19	2.02	1.71	1.77	1.82	0.32	3.15
Sum_REE	78.95	72.76	77.52	65.33	62.09	63.58	66.95	76.85	62.16	76.60	72.90	73.83	70.79	62.09	78.95

Table 4.21: Correlation of the average constituents in the fine-grained amphibolite of Wonu, Ibadan-Apomu area with other amphibolites

	This study (1)			2	3	4	5	6	7	8	9	10
	Mean	Range		Mean	Mean	Mean	Mean	Mean	Mean	Mean	Mean	Mean
SiO_2	49.23	50.63	44.78	49.03	50.11	49.10	47.72	49.00	50.23	49.30	51.10	49.70
TiO_2	0.57	1.39	0.25	0.63	0.55	0.39	1.06	1.09	1.40	1.49	1.60	1.15
Al_2O_3	14.89	16.41	14.01	22.84	14.75	20.20	14.74	14.80	10.76	17.00	16.20	15.26
$Fe_2O_{3(t)}$	13.21	14.83	12.27	11.48	14.75	11.56	3.85	2.36	14.21	2.00	3.10	-
FeO	-	-	-	-	9.20	-	8.32	8.20	-	6.80	7.60	10.37
MnO	0.15	0.24	0.07	0.04	0.21	0.08	0.23	0.19	0.24	0.10	0.17	0.113
MgO	9.61	12.15	8.08	6.63	8.56	7.85	10.05	6.36	8.02	7.20	6.20	7.60
CaO	9.18	10	8.64	7.83	10.34	8.11	11.20	9.75	9.83	11.70	9.90	10.99
Na_2O	1.62	2.35	1.13	1.55	0.63	1.34	1.80	2.07	2.42	2.70	2.51	2.80
K_2O	0.71	0.99	0.46	0.02	0.20	0.85	0.19	0.25	0.36	0.16	0.70	0.50
P_2O_5	0.054	0.09	0.01	0.01	0.07	0.03	0.25	0.19	0.42	0.16	0.22	0.19
LOI	0.32	0.39	0.25	-	-	0.28	1.83	-	-	-	-	-
Trace elements (ppm)												
Cr	78.25	93	53	-	-	51	**800**	-	**1019**	-	-	**283**
Ni	64.58	98	24	125	85	23	**153**	**150**	**351**	97	85	**142**
Co	67.17	85	40	185	28	53	78	48	83.4	32	39	39
Cu	47.17	66	35	24	185	45	<30	100	-	77	127	81
Zn	100.17	148	80	64	-	62	150	100	-	-	100	86
V	67.67	94	53	-	-	62	-	-	327	-	-	221
Sc	7.92	12	5	-	-	-	-	-	32.3	-	-	-
Ga	26.58	29	23	-	-	66	<10	-		-	-	-
Ba	202	350	86	-	-	144	<30	-	327	-	-	62
Rb	33.25	40	25	-	-	46	<10	-	5	-	-	-
Sr	122.83	143	106	3	45	120	80	124	148	130	400	207
Y	36.83	45	25	18	17	25	39	25	22.9	43	32	-
Zr	54.5	62	46	32	15	66	17	110	104	45		-
Nb	6	9	2	-	-	-	-	-	6.5	-	-	-
Cs	0.68	0.9	0.4	-	-	-	-	-		-	-	-
Hf	0.86	1.1	0.5	-	-	-	-	-	2.25	-	-	-
Ta	0.33	0.5	0.1	-	-	-	-	-	0.33	-	-	-
Th	1	1.9	0.2	-	-	-	-	-	1.79	-	-	-
U	0.63	1.4	0.2	-	-	-	-	-	3.69	-	-	-
Rare-Earth elements (ppm)												
La	13.07	19.51	6.9	-	-	-	-	-	-	-	-	-
Ce	30.48	36.3	24.28	-	-	-	-	-	-	-	-	-
Pr	3.36	4.9	2.23	-	-	-	-	-	-	-	-	-
Nd	13.46	18.05	11.65	-	-	-	-	-	-	-	-	-
Sm	1.71	2.95	1.1	-	-	-	-	-	-	-	-	-
Eu	0.79	1.22	0.12	-	-	-	-	-	-	-	-	-
Gd	2.12	2.71	1.08	-	-	-	-	-	-	-	-	-
Tb	0.44	0.86	0.12	-	-	-	-	-	-	-	-	-
Dy	2.15	3.71	1.08	-	-	-	-	-	-	-	-	-
Ho	0.31	0.87	0.13	-	-	-	-	-	-	-	-	-
Er	1.18	2.05	0.44	-	-	-	-	-	-	-	-	-
Tm	0.24	0.33	0.16	-	-	-	-	-	-	-	-	-
Yb	1.27	1.87	0.85	-	-	-	-	-	-	-	-	-
Lu	0.20	0.29	0.06	-	-	-	-	-	-	-	-	-

1. Average Wonu, Ibadan-Apomu amphibolite (this study)
2. Average Zuru amphibolite NW Nigeria (Danbatta and Garba, 2007)
3. Modal composition of Burum amphibolite, Central Nigeria (Elueze and Okunlola, 2003)
4. Modal composition of Ilesha amphibolite, SW Nigeria (Bolarinwa and Adeleye, 2015)
5. Average Southern amphibolite, Kohistan Arc, N Pakistan (Qasim Jan, 1990)
6. Modal composition of Archaan metabasalt, Canadian Shield (Glikson, 1971)
7. Modal composition of Bethampudi amphibolite, Telangana India (Brahmaiah *et al.,*2019)
8. Modal composition of Oceanic tholeiite (Engel *et al.,*1965)
9. Modal composition of Tholeiitic basalt (Manson, 1967; Prinz, 1967)
10. Modal composition Alabama Pedimont amphibolite (Stow *et al.,* 1984)

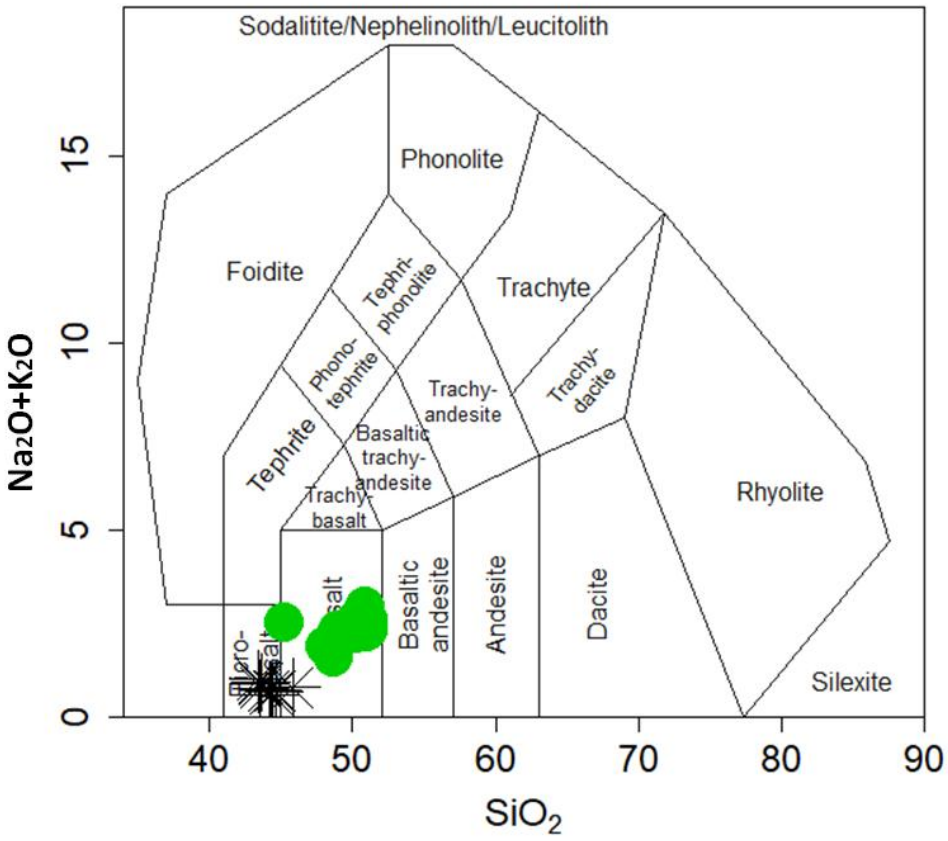

Fig. 4.44:Sum Alkalinity (Na_2O+K_2O)versus SiO_2diagram (after Middlemost 1994) of the fine-grained amphibolite (green) from Wonu, Ibadan-Apomu area showedthat the precursor may vary from dominantly basalt to picrobasalt.

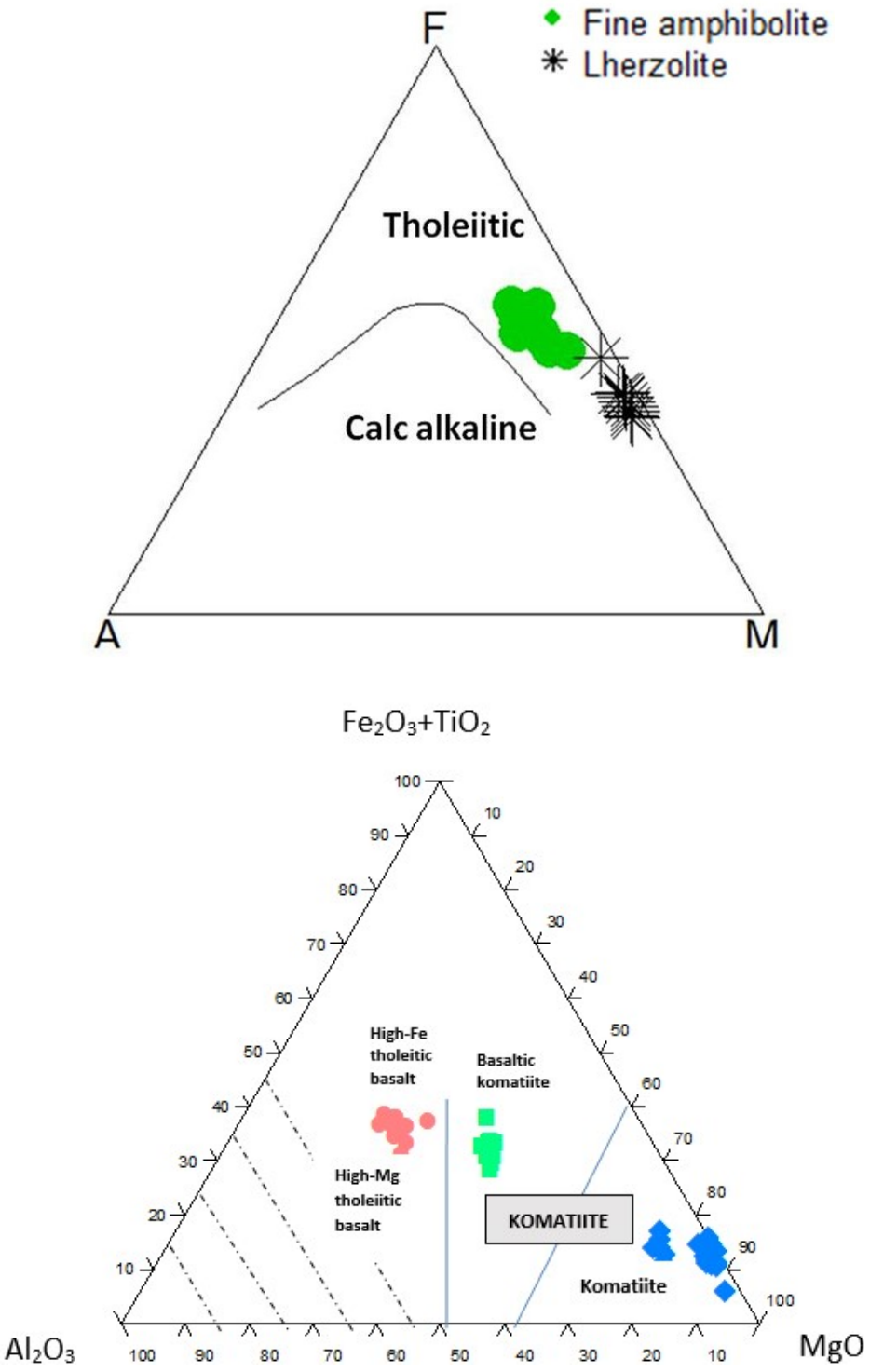

Fig. 4.45: The (a) Al-Fe-Mg diagram and (b) Al_2O_3-MgO-($Fe_2O_{3(t)}$+TiO_2) diagrams of after Jenson (1976) showing the high-Fe tholeiitic nature of the basaltic protolith (red).

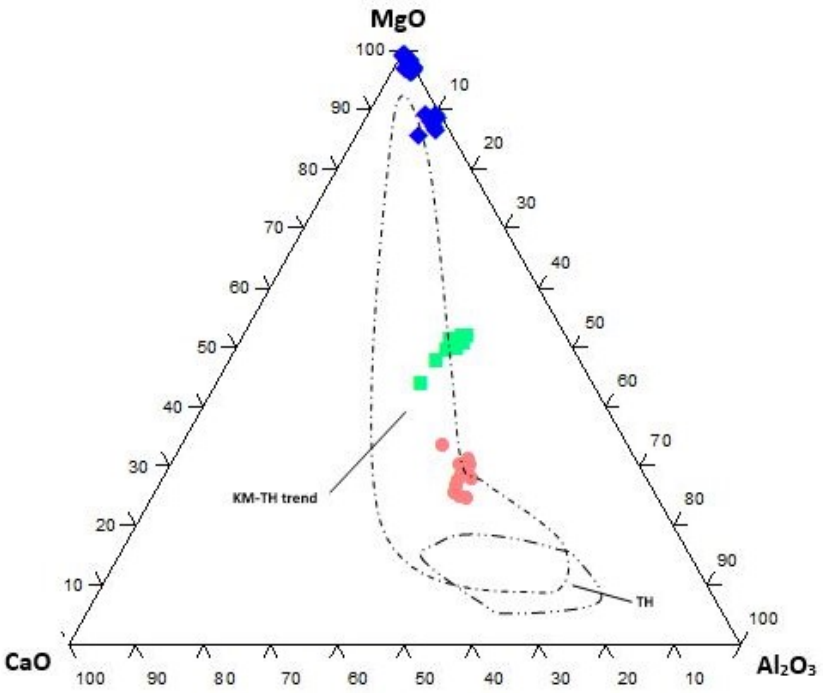

Fig. 4.46: The CaO-Al_2O_3-MgO ternary diagram for Wonu, Ibadan-Apomu ultramafic-mafic rocks (after Viljoen & Viljoen, 1969a, 1969b), showing possible fractionation of the tholeiitic basaltic protoliths from komatitic magma.KM-komatiite, TH-tholeiite.

The Ba (86-350 ppm) concentration is similar to those of other amphibolites in Ilesha, Nigeria and Telangana, India(Table 4.21). The Sr (106-143 ppm) contents are similar to deposits elsewhere in the world except the average oceanic tholeiites, tholeiitic basalts and Alabama amphibolite (Stow*et al.,* 1984), which are higher. Most of the trace elements are not very mobile during alteration and hence are most useful in petro-tectonic studiesof rocks, the V showed an affliation to TiO_2 (Table 4.20). The Harker diagram (Fig. 4.47) showed that the major and trace elements correlate negatively with MgO except TiO_2 and Ni which are positive. Fine-grained amphibolites exhibited higher contents of U and Th compared to other mafic-ultramafic rocks of this study (Fig. 4.48). Rb versus (Y+Nb) diagram showed that they are mantle related magmaerupted in volcanic arc (VAG) setting for the amphibolite(Pearce *et al.,* 1984), (Fig. 4.49).

The rare-earth elements (REEs) of the fine-grained amphibolites are presented in Table 4.18. Rare-earth elements (REEs) are not readily dissolved nor verymobile during fluid movement or hydrothermal alteration and therefore gives a clue to the composition parental melt (Michard, 1989). The chondrite-systemized REE traces for the fine-grained amphibolites of Wonu, Ibadan-Apomu area,presented in Fig 4.50,showed high LREE enrichment, slight HREE depletion with a positive Eu anomaly. The La_N/Sm_N ranged from 0.93 - 3.04 and the ratios Ce_N/Yb_N ranged from 1.84 - 4.23. The Low REE fractionation factor (La_N/Yb_N: 3.04 to 6.14) and the positive Eu anomaly, (Eu/Eu*: 0.22 to 1.36) suggested increase in hornblende, titanite and plagioclase contents, which was corroborated from the mineral chemistry. The positive Eu anomaly and high contents of incompatible elements indicated crystallization of the amphibolites from enriched melts.

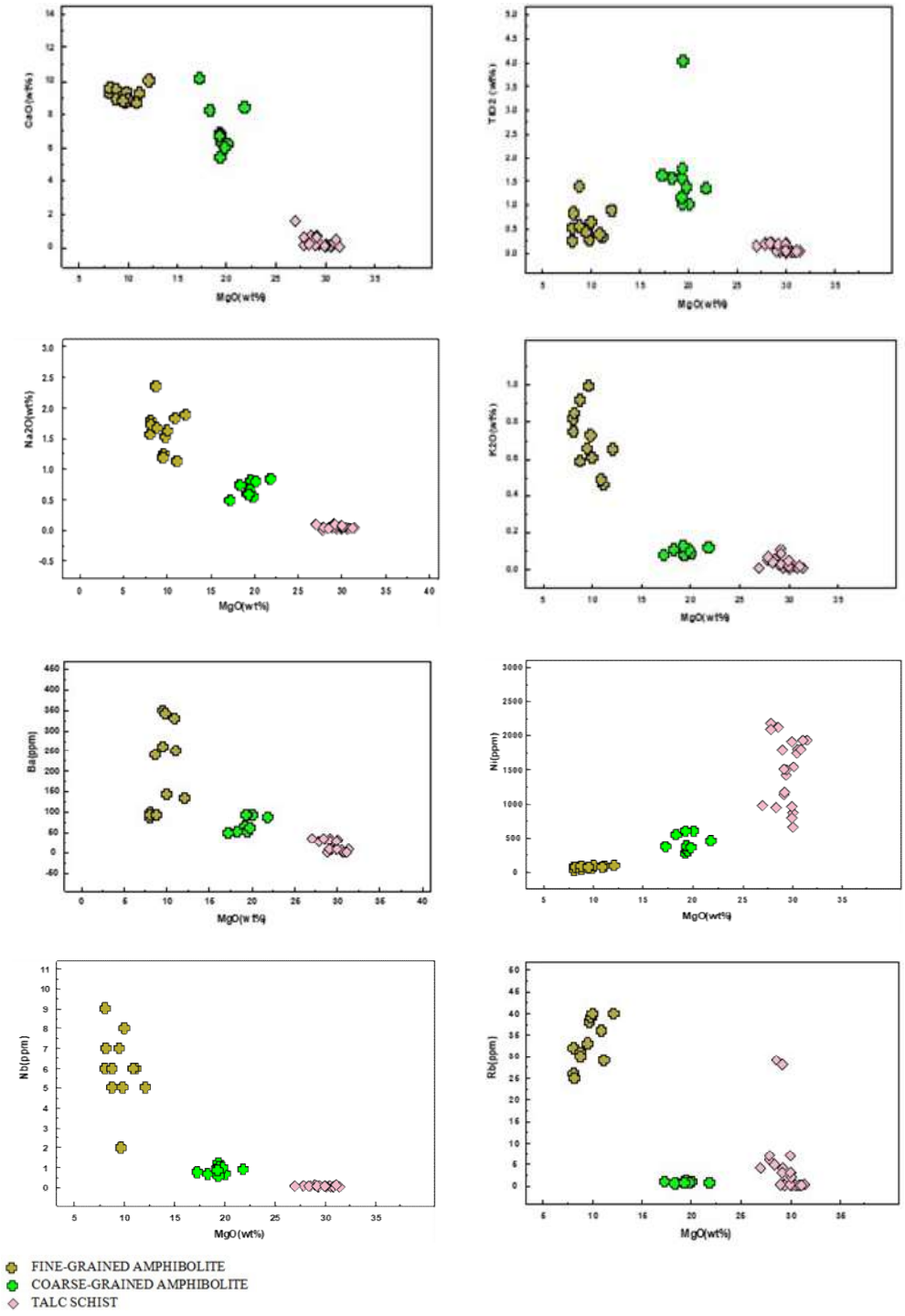

Fig. 4.47: Major oxides and trace elements versus MgO for ultramafic-mafic rocks plots of the Wonu, Ibadan-Apomu area.

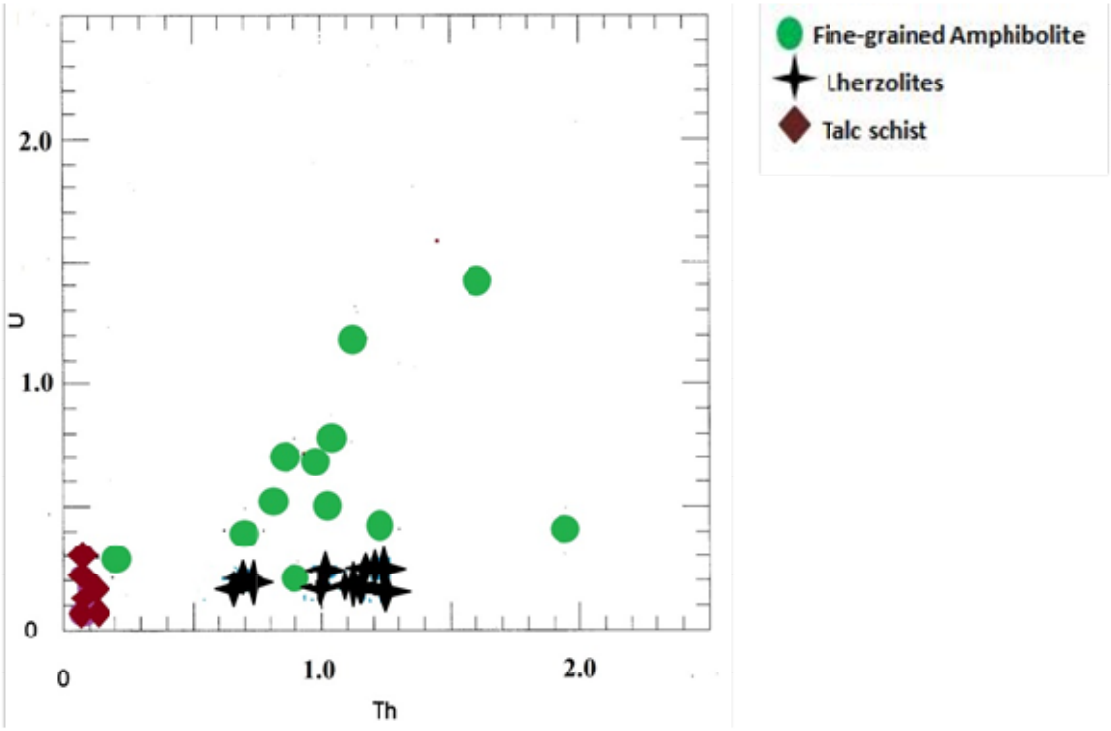

Fig. 4.48:Abundances of U vs Th in mafic-ultramafic rocks of Wonu, Ibadan-Apomu area showing higher contents of U and Th in the fine-grained amphibolites.

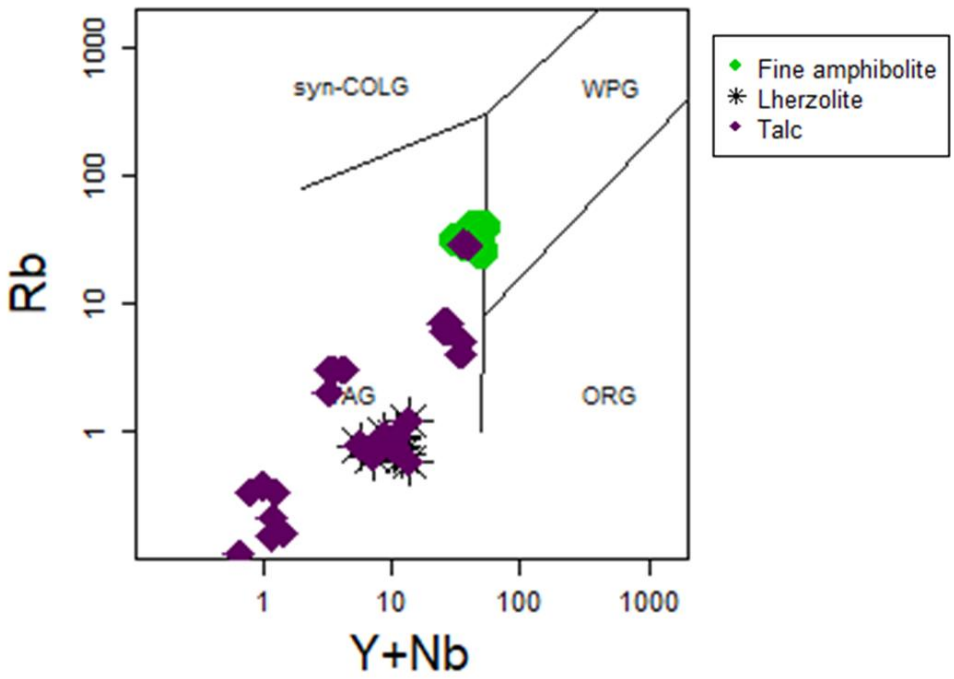

Fig. 4.49: Fine-grained amphibolites, lherzolites and talc schist of Wonu, Ibadan-Apomu area drawn on the Rb versus (Y+Nb) plot (after Pearce et al. 1984). Syn-COLG - syn-collisional granites. WPG - within plate granites, ORG - ocean ridge granites, VAG volcanic arc granites.

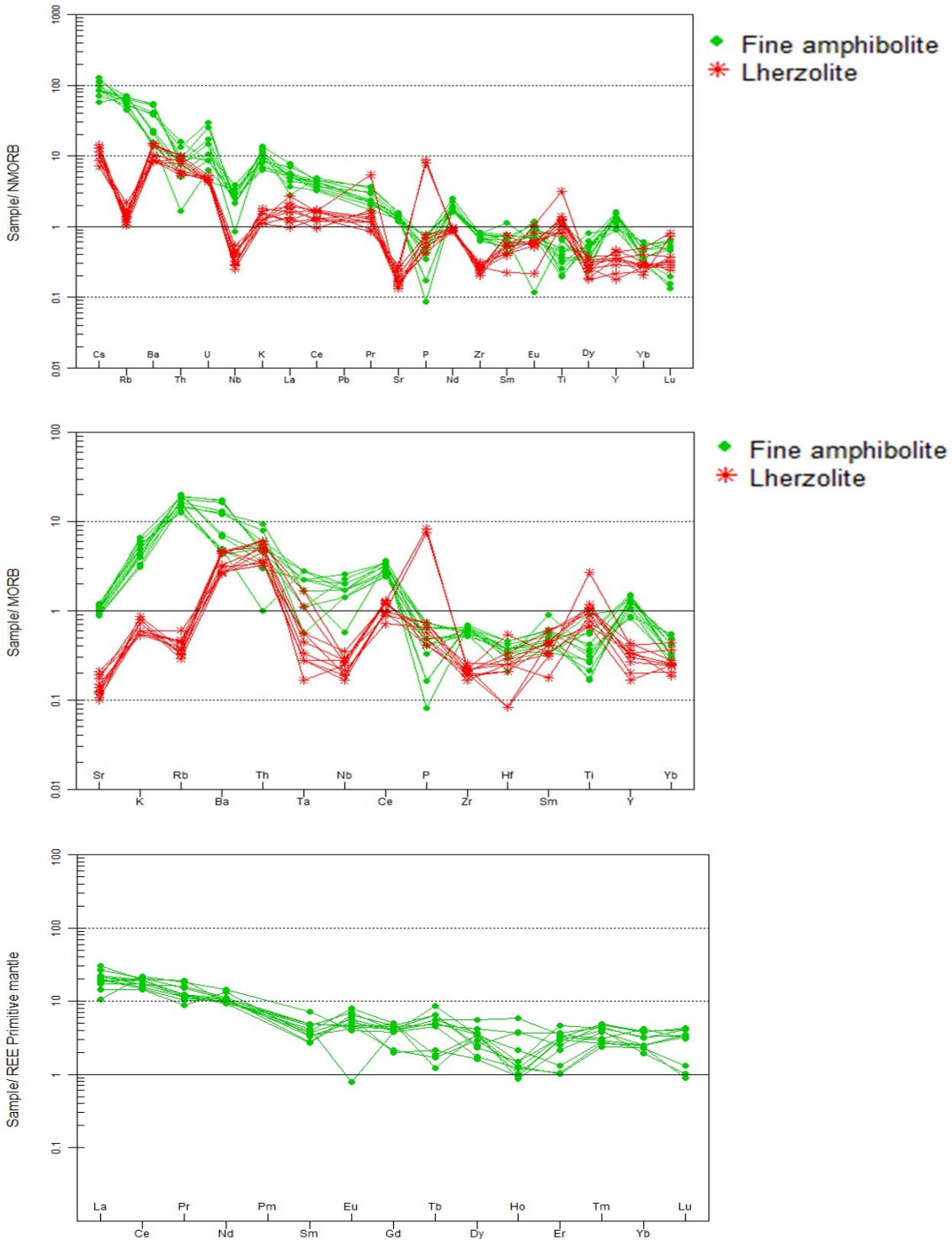

Fig. 4.50: Chondrite systemized (a and b) trace components and rare earth (c) rare earth elements diagram of the fine-grained amphibolitesand lherzolites of Wonu, Ibadan-Apomu area (after Mc Donough and Sun, 1992).

4.3.2 Coarse-grained Amphibolite (Lherzolite)

4.3.2.1 Petrography of the Coarse-grained Amphibolite (Lherzolite)

The outcrops of a rock that was hithertho refered to as coarse-grained amphibolites occur in the southern part of the study area near Olosun village (Fig 4.1). The outcrops are restricted in extent, very smooth, rounded, greenish to dark coloured and very dense. Freshly broken hand specimen (Fig. 4.51) showed that it is inequigranular to coarse-grained, greenish and with some dark patches. The rims of the rock have been altered to shades of reddish brown to black perhaps due to oxidation of iron-bearing, minerals. White,pinkish to light green patches suspected to be serpentine, amesite and chlorite minerals could be seen and identified from their soapy feel, indicating partial alteration of the supposed fresh sample. Crystals of amphibole and plagioclase are observable in hand specimen. Some of the outcrops arecompletely weathered while others showed minor alteration.

Minerals identified under the microscope, include olivines (42-50 %), orthopyroxenes (20-26 %), clinopyroxenes (5-9 %), serpentine (8-11%), amphiboles (6-9 %) and opaque minerals, notably Cr-spinel (1-4 %),magnetite (1-2 %),rutile (1-3 %), sulphides(1 %) and graphite (1 %) (Table 4.22).Metasomatic minerals, such as,kelyphite is developed from the replacement of garnet. Other metasomatic minerals include fine-grained aggregates of secondary orthopyroxene, clinopyroxene, amesite altered spinel and phlogopite (Naemura *et al.,* 2009).

Needles and plates of olivines and pyroxenes, notably orthopyroxenes dominate the mineral assemblage. Most of these olivines and pyroxenes have been retrograded to secondary amphibole and chlorite due to metasomatism. The two types of pyroxenes present were identified as the brighter, Ca-rich phase and a darker Ca-poor phase forming a distinct composite lamellae features in the thin section.The two pyroxenes recorded the same extinction angle suggesting that they are not mutually independent. The amphiboles vary from magnesio-hornblende (major) to tchermakitic-hornblende.Other amphiboles present are tremolitic to actnolite.Serpentine minerals include amesite, clinochlore, antigoriteand chrysotile, which occur as collapsed and stretched, dark mesh microstructure aggregates. Amesite and chrysotile are white to pinkishand occur as fine crystals aligned along fractures and edges of pyroxene crystals.Needle-like specks of rutile are observed in both the thin section and the SEM-EDS.

Fig.4.51: Hand specimens of the coarse-grained amphibolites (lherzolite) from Wonu, Ibadan-Apomu area.

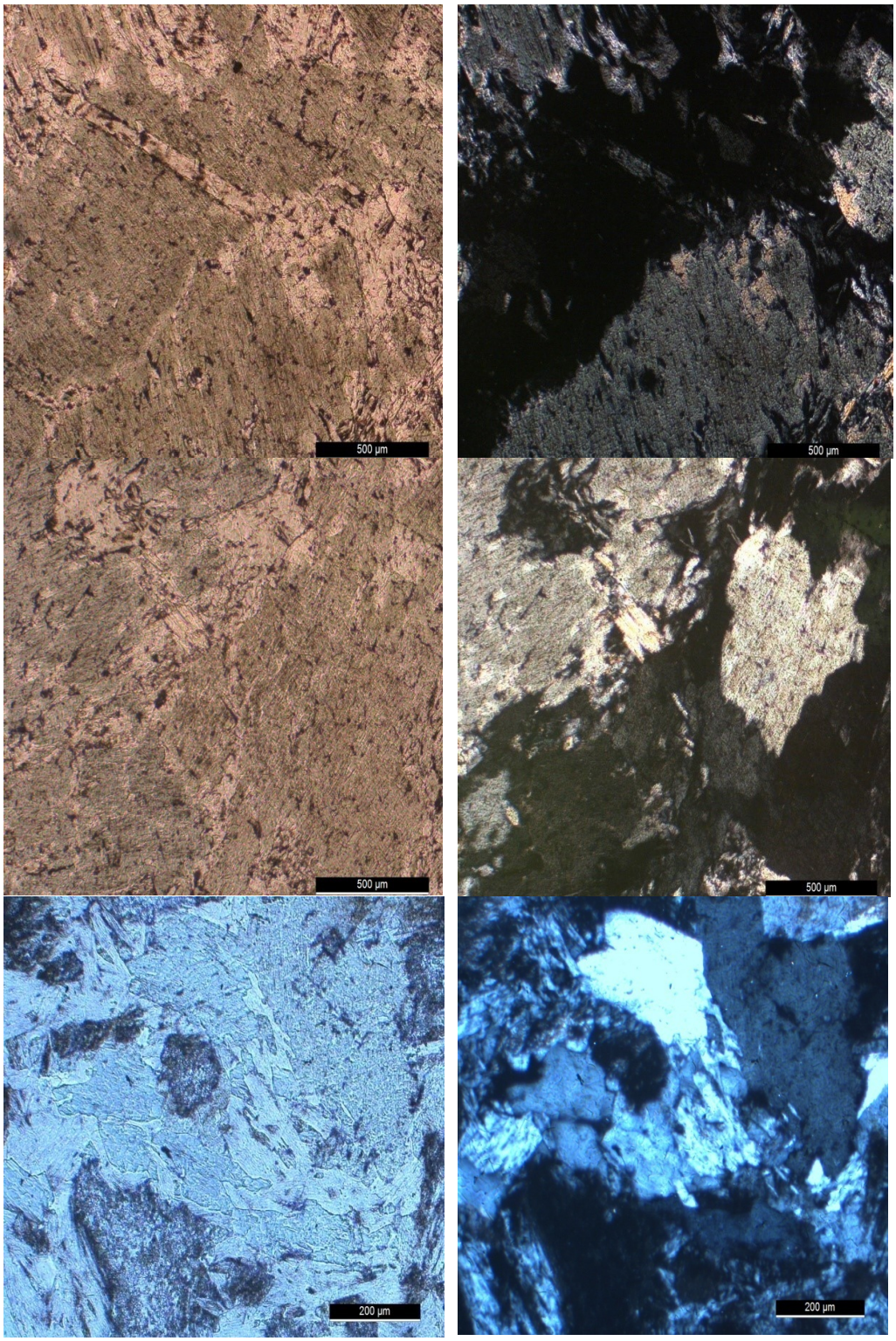

Fig. 4.52: Photomicrograph of coarse-grained amphibolite (lherzolite) of Wonu, Ibadan-Apomu area showing elongated altered olivine crystals surrounded by altered pyroxenes, amesite (serpentine-chlorite group), and Cr- spinel.

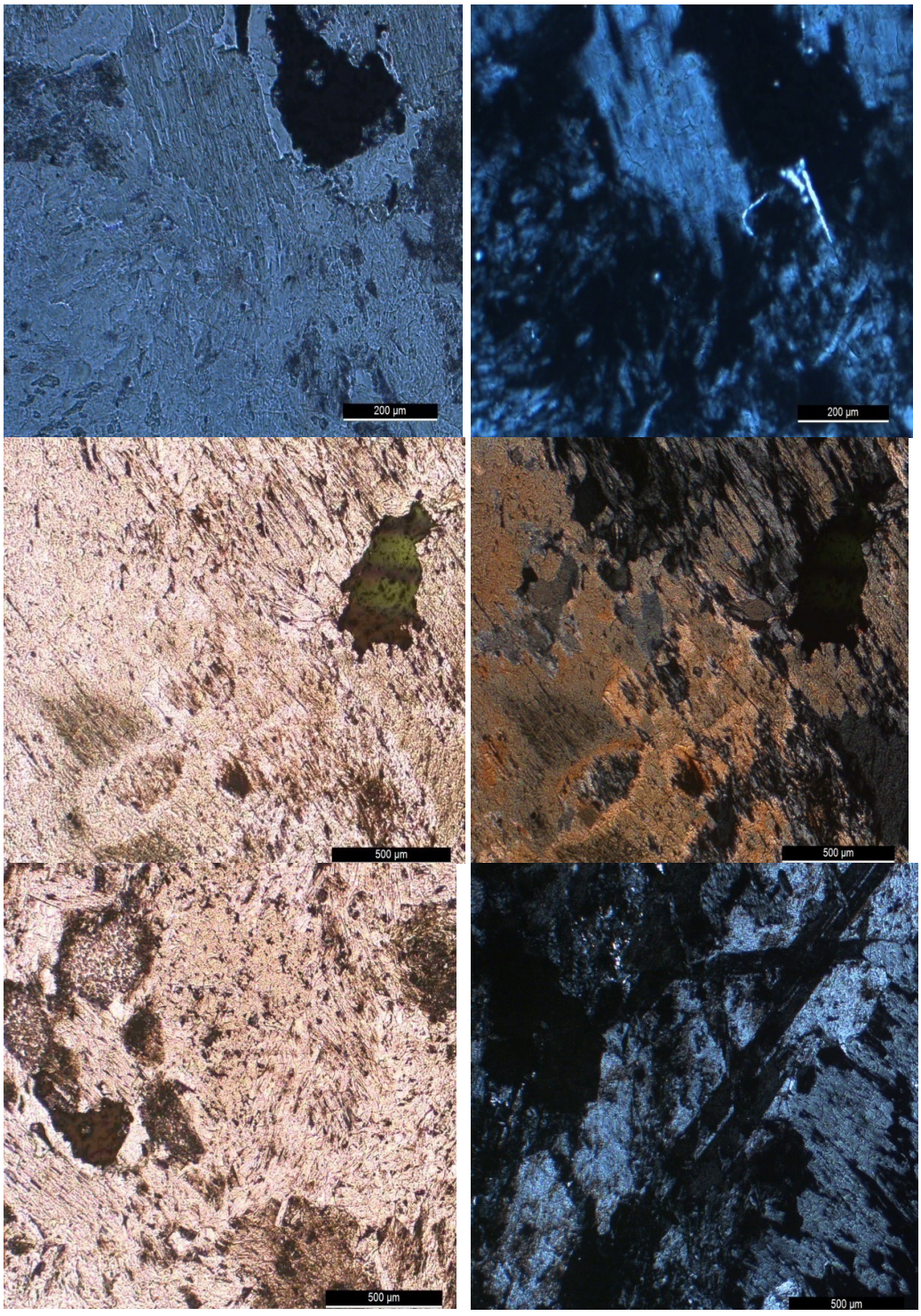

Fig. 4.53: Photomicrograph of coarse-grained amphibolite (lherzolite) of Wonu, Ibadan-Apomu area showing altered olivine, clinopyroxene, rutile, amesite (serpentine-chlorite group mineral) Cr-spinel and tremolite-actinolite minerals.

Table 4.22.Modal composition of coarse- grained amphibolites (lherzolites) of Wonu, Ibadan-Apomu

	1	**2**	**3**	**4**	**5**	**6**	**7**	**8**	**9**	**10**
Olivine	42	50	42	44	45	50	46	45	47	46
Orthopyroxene	25	21	26	22	23	22	20	20	24	21
Clinopyroxene	7	5	6	8	6	6	8	9	5	9
Amesite/Chlorite	9	8	10	9	10	9	10	11	8	10
Amphiboles	7	8	9	9	9	7	8	7	8	6
Cr-Spinel	4	3	2	2	2	1	2	3	1	3
Magnetite	2	2	1	2	2	1	2	1	2	2
Rutile	2	1	2	2	1	2	2	2	3	1
Sulphides	1	1	1	1	1	1	1	1	1	1
Graphite	1	1	1	1	1	1	1	1	1	1
Total	**100**	**100**	**100**	**100**	**100**	**100**	**100**	**100**	**100**	**100**

4.3.2.2 SEM-EDS Images of the Coarse-grained Amphibolites (Lherzolite)

The SEM-EDS of the coarse-grained amphibolite (lherzolite) from Wonu, Ibadan-Apomu area confirmed most of the mineralogy observed in the thin sections under petrography. Olivine, which ranged from forsterite to fayalite are altered in most cases to serpentines, orthopyroxenes, amesite and chlorite, even in the seemingly fresh lherzolite samples. The altered serpentines are dark and mesh-like. The Graphite is also found interstitial between titanium-bearing clinopyroxene (Augite) (Spectrum 14) and amesite (Spectrum 15)that are Al-bearing (Fig. 4.54). The amesite in (Fig. 4.54) belongs to the kaolinite-serpentine group of minerals. The SEM-EDS of coarse-grained amphibolite (lherzolite) (Fig. 4.55) showed needle-like and rounded rutile crystals inclusions (Spectrum 7) within amesite (Spectrum 8) in pyroxenes-amphibole-chlorite groundmass.

The primary pyroxenes are mainly orthopyroxenes with few clinopyroxene (Figs. 4.56 and 4.57). The pyroxenes are also serpentinised as shown in Figs. 4.56 and 4.57. Cr-spinel grains are commonly surrounded by orthopyroxene and clinopyroxene. They also occur as inclusions in olivines. The core of the Cr-spinel is homogeneous in composition with retrograde zoning in the outermost rim. Some coarse-grained spinel serve as a host to graphite. The importance of these COH fluids is in the occurrence of graphite in the rock. Evidence of hydrothermal invasion are observed in Fig. 4.56, leading to the precipitation of sulphides and REE-bearing minerals, such as allanite and monazite, which were recorded in some of the lherzolite samples.

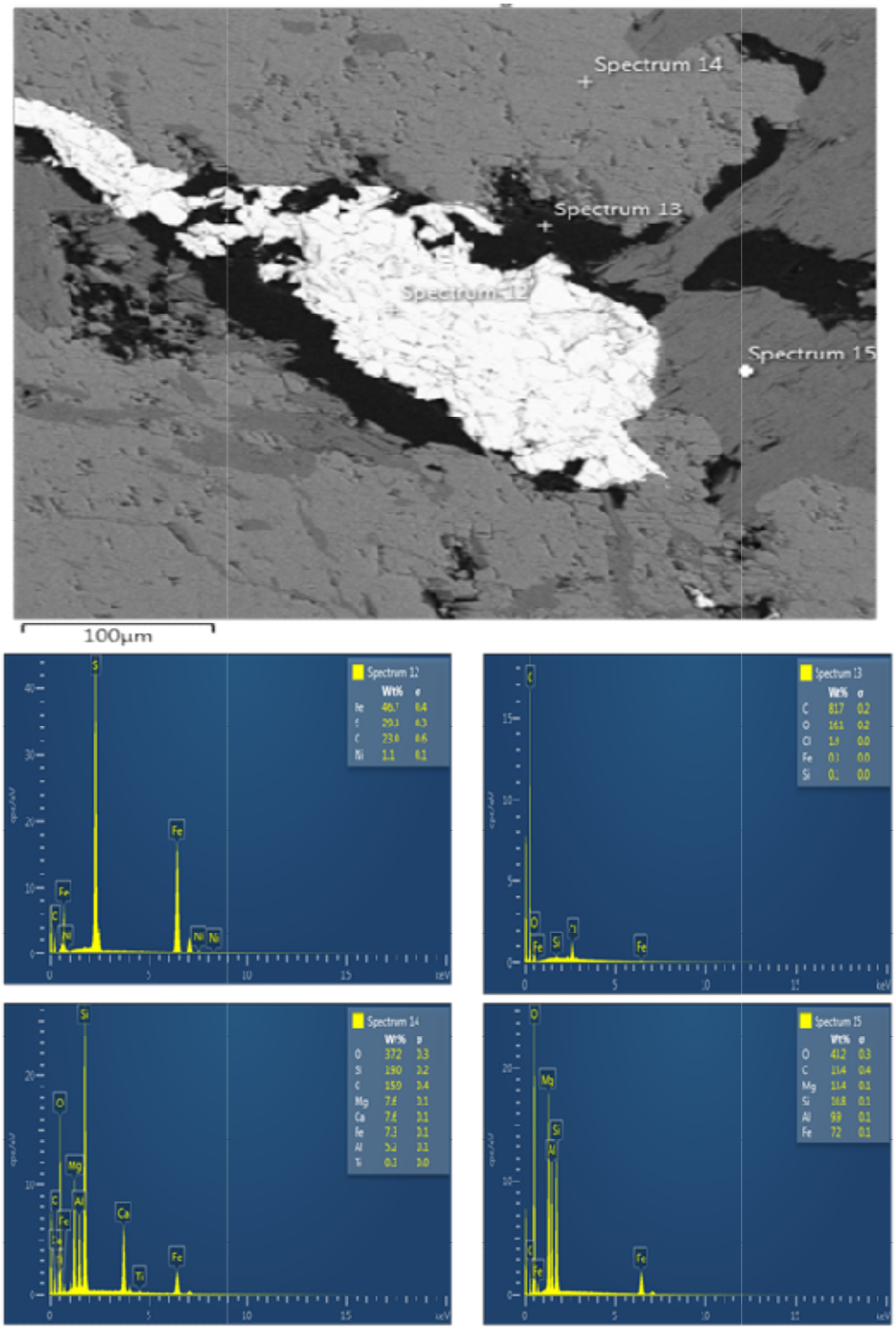

Fig. 4.54:SEM-EDS of coarse-grained amphibolite (lherzolite) from Wonu, Ibadan-Apomuarea showing pyrrhotite and pentlandite (Fe,Ni)in graphite(Spectrum 12), Cl-bearing graphite (dark) surrounding the sulphides (Spectrum 13), titanium-bearing clinopyroxene (Augite) (Spectrum 14) and serpentinised olivine (amesite)in graphite ground mass (Spectrum 15).

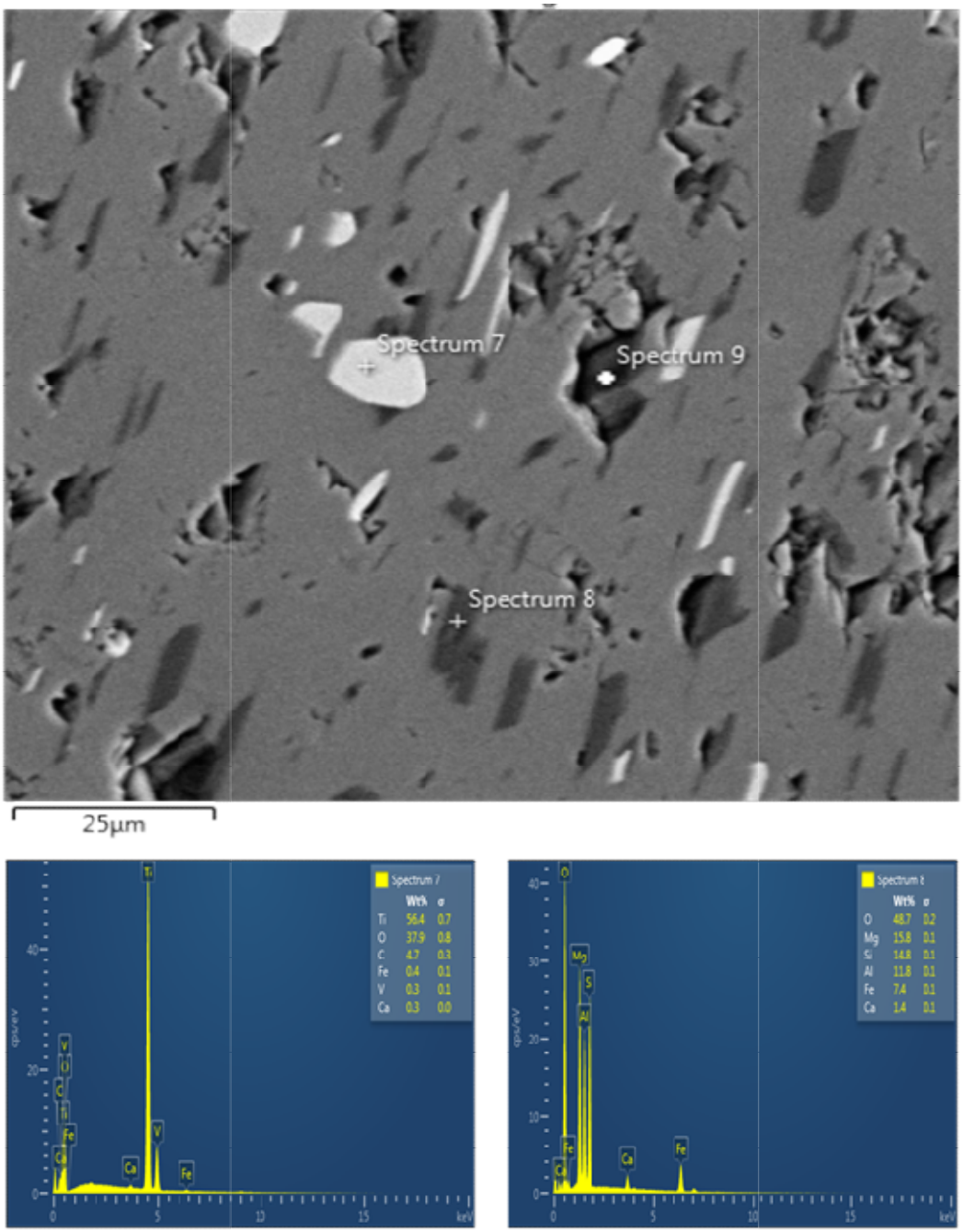

Fig. 4.55:SEM-EDS of coarse-grained amphibolite (lherzolite) from Wonu, Ibadan-Apomu area showing rutile (Spectrum 7), amesite (Spectrums 8and 9) in pyroxenes-amphibole-chlorite groundmass.

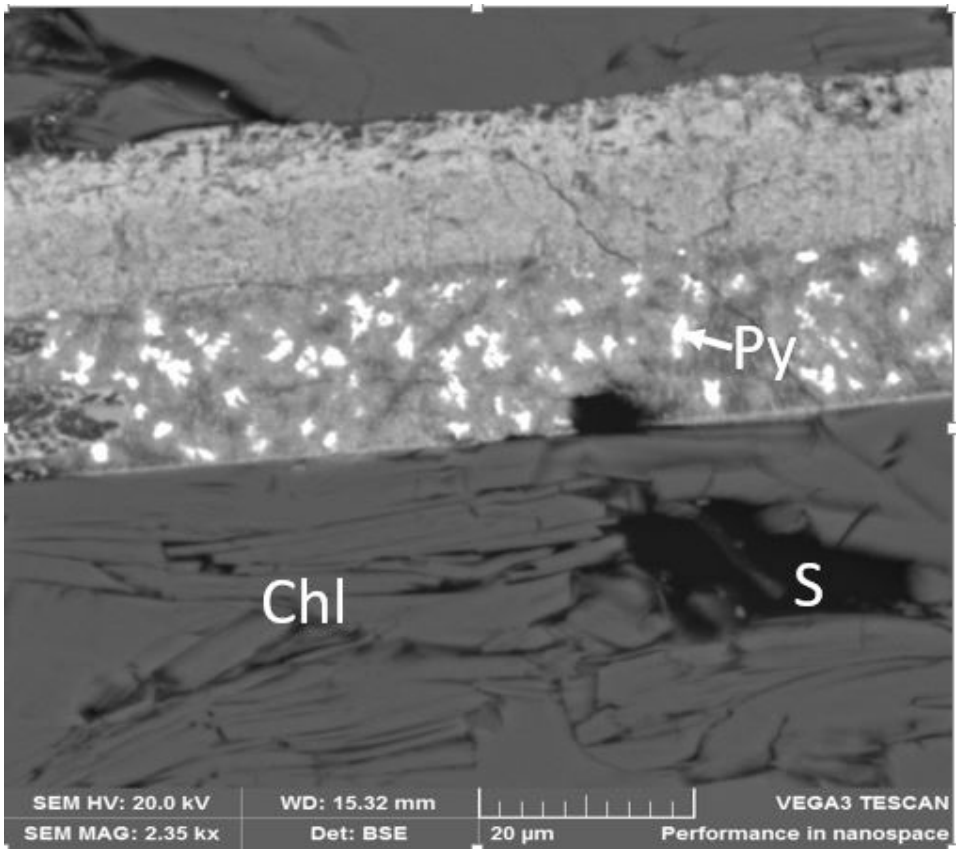

Fig. 4.56: SEM-EDS of coarse-grained amphibolite (lherzolite) from Wonu, Ibadan-Apomu area showing hydrothermal altered band (in sheared contact) containing pyrrhotite (Fe_7S_8) and pentlandite $(Fe,Ni)_9S_8$(white) within chloritic (grey) and serpentinised olivine(amesite) (black).

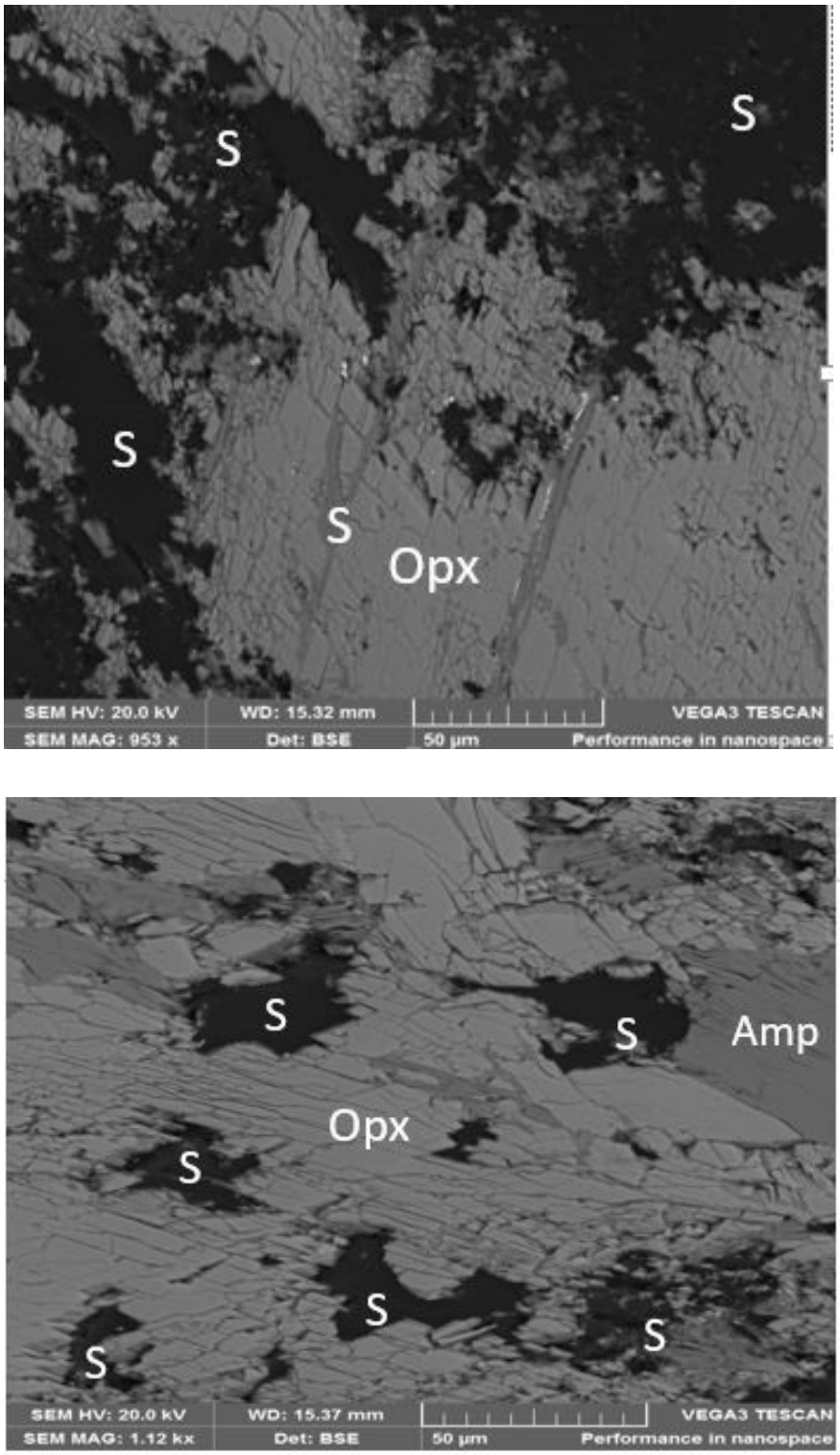

Fig. 4.57: SEM-EDS of coarse-grained amphibolite (lherzolite) from Wonu-Ibadan-Apomu area showing hydrothermally altered olivines, orthopyroxenes and amphiboles to serpentinites (S).

4.3.2.3 Mineral Chemistry of the Coarse-grained Amphibolites (Lherzolite)

Olivine

The olivine minerals in the coarse-grained amphibolites (lherzolite) in Wonu-Ibadan–Apomu area are mainly forsterite. Olivine is the primary component of the earth's upper mantle and a major mineral in lherzolites comprising 40-90%.

Olivine compositions ranged in $100*Mg/(Mg+Fe^{2+})$ (Mg#) from 87 to 90. Representative olivine analyses are presented in Table 4.23. The olivines are mainly forsterite at different stages of alteration leading to a range of compositions. Some of the analyses reflect olivine/orthopyroxene transitional composition suggesting alteration of some of the olivine to orthopyroxene. Both the olivine porphyroclasts and neoblasts are similar in chemical composition. The low Cr (0.01-0.05 %), Ca (0.07-0.12 %) and Ti (0.01-0.02 %) compositions of the olivines are compatible with those of passive continental margin peridotites (Pearce *et al.,* 2000),in the olivine-spinel mantle array (OSMA) that sufferedpartial melting of 5 to 15 % of the Fertile MORB mantle (FMM) according to Arai (1994). The composition of the olivine also supported derivation from fractional crystallization.The Fo content in the olivine (87 to 90) and the modal % of the olivine (< 50 %) suggested Late Precambrian to Early Phanerozoic lherzolite, a view supported by Baer and Glaeser (1998) for the Mallam Tanko ultramafic rocks in the Pan African Basement complex of northwestern Nigeria.

Spinel

Spinel crystals in the lherzolite are Cr-spinel and has a wide range of composition similar to those of ferritchromite. The Mg# of the spinel are very low (<0.30), while the Fe^{2+}# are very high (>0.5-0.9). The Cr# ranged from 0.6 to 0.8 with the most Cr-rich samples in the clinopyroxene-poor samples. On the basis of the high Fe and low Mg contents, the Cr-spinel is classified as ferritchromite. These ferritchromitesaresimilar in composition to those reported for the supra-subduction zone (SSZ) Izu-Bonin peridotites by Parkinson and Pearce(1998). This is also in agreement with the olivine-spinel mantle array (OSMA) and the Fertile MORB mantle (FMM) of Arai (1994). However, the composition indicated that the ferritchromite are metasomatised Cr-spinel, with loss of Al and enrichment of Fe.

Table 4.23: Mineral chemistry of olivine in coarse grained amphibolites (lherzolite)

	1	**2**	**3**	**4**	**5**	**6**
SiO_2	40.56	40.12	41.03	40.21	40.54	40.05
TiO_2	0.02	0.01	0.02	0.01	0.02	0.02
Al_2O_3	0.02	0.03	0.01	0.02	0.03	0.02
Cr_2O_3	0.05	0.04	0.05	0.03	0.02	0.01
Fe_2O_3	0.00	0.50	0.00	1.03	0.00	1.37
FeO	12.12	11.63	9.50	10.42	11.04	9.03
MnO	0.11	0.05	0.12	0.22	0.20	0.14
MgO	47.52	47.35	48.54	48.21	47.89	48.90
CaO	0.09	0.11	0.08	0.07	0.12	0.09
Total	100.49	99.84	99.35	100.22	99.86	99.63
Formula units based on 4 oxygens						
Si	0.999	0.994	1.012	0.990	1.001	0.987
Ti	0.000	0.000	0.000	0.000	0.000	0.000
Al	0.001	0.001	0.000	0.001	0.001	0.001
Cr	0.001	0.001	0.001	0.001	0.000	0.000
Fe^{3+}	0.000	0.009	0.000	0.019	0.000	0.025
Fe^{2+}	0.250	0.241	0.196	0.215	0.228	0.186
Mn	0.002	0.001	0.003	0.005	0.004	0.003
Mg	1.745	1.749	1.785	1.769	1.762	1.796
Ca	0.002	0.003	0.002	0.002	0.003	0.002
tot. cat.	3.000	3.000	3.000	3.000	3.000	3.000
tot. oxy.	4.000	4.000	4.013	4.000	4.002	4.000
End members						
Fo	87.28	87.31	89.90	88.05	88.22	89.23
Fa	12.49	12.50	9.87	11.63	11.41	10.50

Pyroxenes

The pyroxene minerals in the coarse-grained amphibolites (lherzolite) in Wonu, Ibadan-Apomu area include primary orthopyroxene and clinopyroxene.

Orthopyroxene

Orthopyroxene compositions are presented in Table 4.24. They are magnesian in composition with Mg# of 75 to 80. The Al_2O_3contents are low ranging from 0.37-3.23 wt %. Orthopyroxene exsolution lamellae in clinopyroxene have the highest Al_2O_3contents (2.62-3.23 %). Most samples have <1 wt % Al_2O_3contents except one sample and the two exolved samples. These samples contain aluminous mineral phases, such as amphibole or chlorite. The CaO contents ranged between 0.35-1.27%. Compositional zoning are observed within the orthopyroxenes with Al_2O_3, Cr_2O_3 and CaO decreasing towards the rims. The orthopyroxene is enstatite (Fig. 4.58).

Clinopyroxene

The clinoopyroxene compositions are presented in Table 4.25. Primary clinopyroxenes from the lherzolite are all diopsides. The Mg# content vary from 0.7 to 0.8 with Al_2O_3 (0.68-11.22 %), TiO_2(0.05-0.45 %) and Na_2O (0.01-1.23 %) suggesting that the lherzolite contain aluminous amphibole and chlorite equilibrating with the clinopyroxenes. Some large clinopyroxenes have striking compositional zoning reflected in the varied Al and Mg composition. The clinopyroxene with $Al_2O_3$of 4.05 % showed exolution lamellae. Secondary clinopyroxenes, which occur as mantles around the orthopyroxenes and olivines are augites with higher MgO and lower Al_2O_3contents compared with the primary clinopyroxenes. The transition from primary orthopyroxene to secondary clinopyroxene with attendant increasein CaO and Na_2O has been implicated in the crystallization of secondary minerals, such as, calcite and plagioclase, notably albite. Amphiboles, amesite and chlorites are products of such alterations.The low TiO_2 content of the clinopyroxenes (0.05-0.45 wt%) (Table 4.25) indicated high to medium orthopyroxene-clinopyroxene-type cumulate magma generated from high to medium degree of partial melting for the lherzolite. The clinopyroxene in the coarse-grained amphibolites of the Wonu, Ibadan-Apomu areas is augite as presented in Fig. 4.58.

Table 4.24: Mineral chemistry of orthopyroxenes in the coarse grained amphibolites (lherzolite)

	CA11 /39	CA11 /43	CA11 /45	CA11 /46	CA12 /66	CA12 /69	CA12 /106	CA12 /110
SiO_2	63.34	53.67	56.38	56.58	56.29	56.33	56.56	63.39
TiO_2	0.00	0.04	0.02	0.01	0.02	0.00	0.02	0.01
Al_2O_3	3.23	2.62	0.37	0.50	0.95	0.66	0.65	1.15
Cr_2O_3	0.00	0.00	0.00	0.00	0.00	0.00	0.01	0.02
Fe_2O_3	0.00	2.34	0.00	0.00	0.00	0.00	0.00	0.00
FeO	12.34	13.57	17.10	16.88	16.28	16.63	16.96	16.23
MnO	0.00	0.43	0.47	0.46	0.48	0.47	0.48	0.45
MgO	19.82	27.73	25.39	25.39	25.68	25.58	25.54	18.22
CaO	1.27	0.39	0.35	0.35	0.40	0.37	0.67	0.48
Na_2O	0.00	0.06	0.02	0.03	0.05	0.02	0.02	0.02
Total	100.00	100.84	100.10	100.20	100.15	100.06	100.91	99.97
Formula units (based on 6 oxygens)								
Si	2.338	1.915	2.054	2.058	2.042	2.049	2.042	2.382
Ti	0.000	0.001	0.001	0.000	0.001	0.000	0.001	0.000
Al	0.141	0.110	0.016	0.021	0.041	0.028	0.028	0.051
Cr	0.000	0.000	0.000	0.000	0.000	0.000	0.000	0.001
Fe^{3+}	0.000	0.063	0.000	0.000	0.000	0.000	0.000	0.000
Fe^{2+}	0.381	0.405	0.521	0.513	0.494	0.506	0.512	0.510
Mn	0.000	0.013	0.015	0.014	0.015	0.014	0.015	0.014
Mg	1.091	1.475	1.379	1.377	1.389	1.387	1.375	1.021
Ca	0.050	0.015	0.014	0.014	0.016	0.014	0.026	0.019
Na	0.000	0.004	0.001	0.002	0.004	0.001	0.001	0.001
Tot. cat.	4.000	4.000	4.000	4.000	4.000	4.000	4.000	4.000
Tot. oxy.	6.408	6.000	6.062	6.068	6.061	6.062	6.056	6.408
End members								
Wo	3.30	0.76	0.71	0.72	0.82	0.76	1.36	1.25
En	71.67	75.35	72.06	72.31	73.16	72.72	71.87	65.85
Fs	25.03	23.89	27.23	26.97	26.02	26.52	26.77	32.90
Total	100.00	100.00	100.00	100.00	100.00	100.00	100.00	100.00

Table 4.25: Mineral chemistry of clinopyroxenes in the coarse grained amphibolites (lherzolite)

	CA12/89	CA12/90	CA12/96	CA12/97
SiO_2	54.92	47.56	48.82	53.63
TiO_2	0.05	0.42	0.38	0.45
Al_2O_3	0.68	11.22	9.49	4.05
Cr_2O_3	0.00	0.00	0.00	0.00
Fe_2O_3	0.00	0.00	0.00	0.00
FeO	11.30	10.02	9.41	10.20
MnO	0.13	0.13	0.10	0.13
MgO	16.58	14.76	15.71	19.31
CaO	16.76	11.63	11.96	11.61
Na_2O	0.01	1.23	1.01	0.81
Total	**100.43**	**96.97**	**96.88**	**100.19**
Formula units (based on 6 oxygens)				
Si	2.034	1.787	1.835	1.947
Ti	0.001	0.012	0.011	0.012
Al	0.030	0.497	0.420	0.173
Cr	0.000	0.000	0.000	0.000
Fe^{3+}	0.000	0.000	0.000	0.000
Fe^{2+}	0.350	0.315	0.296	0.310
Mn	0.004	0.004	0.003	0.004
Mg	0.915	0.827	0.880	1.045
Ca	0.665	0.468	0.482	0.452
Na	0.001	0.090	0.074	0.057
tot. cat.	4.000	4.000	4.000	4.000
tot. oxy.	6.050	6.003	6.019	6.017
End members				
Wo	34.45	29.08	29.05	25.00
En	47.42	51.36	53.10	57.86
Fs	18.13	19.56	17.84	17.14
Total	**100.00**	**100.00**	**100.00**	**100.00**

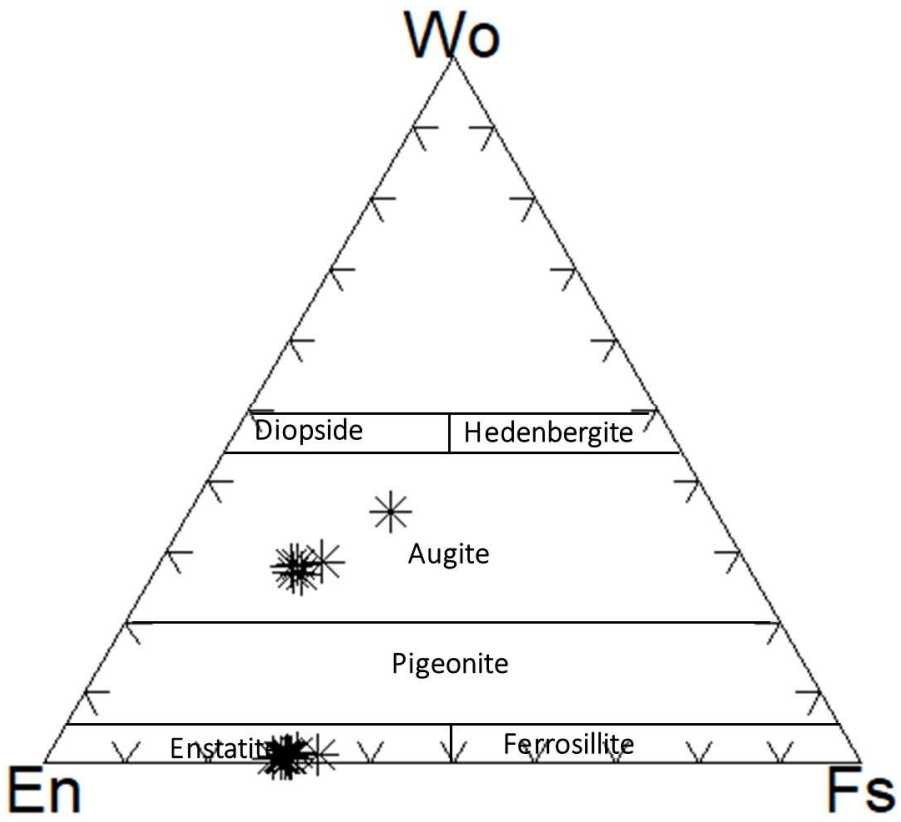

Fig. 4.58: Classification of pyroxenes in the coarse-grained amphibolites of the Wonu, Ibadan-Apomu areas (after Sushevskaya *et al*, 2008).

Amphiboles

Representative chemical analysis of amphiboles in the coarse-gained amphibolites (lherzolite) of Wonu, Ibadan-Apomu area are shown in Table 4.26 (a-c). Other amphibole data (d-f) are in the Appendix. Structural formulae of the amphiboles were calculated basedon 23oxygen atoms per half unit cell, with the general form $A_{0\text{-}1}B_2\ C_5\ T_8\ O_{22}\ (OH)_2$ representing one formula unit.

The amphiboles have Si content which ranged from 5.69 to 8.04 apfu. They magnesia rich, weakly titaniferous and have most of their alumina in tetrahedral site.Based on the classification of Giret *et al*.(1980) depicted on the Na versus (Ca + Na) diagram, the amphiboles ranged from Fe-Mg-Mn to calcic varieties (Fig. 4.42a).According to the IMA nomenclature and Leake *et al*.(1997) classification expressed on the Xmg or Mg# = $Mg/(Mg+Fe^{2+})$ versus Si (apfu) diagram, the amphiboles occupies the tschermackite to magnesio-hornblende field, with one sample in the actinolite field (Fig. 4.39).

The amphiboles are ferroan and calcic rich. In the ferroan samples the Mg content ranges from 4.78 to 5.34 apfu while the Ca content are very low ranging from 0.022 to 1.020 apfu. In the calcic variety the Mg content are lower ranging from 2.12 to 3.76 apfu, while Ca content are higher than those of the ferroan samples, ranging from 1.47 to 1.90 apfu. The Na are very low in all the amphiboles. The calcic amphiboles are more abundant than the Fe-Mg-Mn amphiboles(Table 4.26a-c) and (d-f in the appendix).

On the basis of compositional variations of amphiboles onthe Al^{iv} versus Na + K and Al^{iv} versus Ti (in apfu) diagram the amphiboles are mainly tremolite – actinolite type (Fig. 4.59a and b) (Béziat *et al.,* 2000). The amphiboles have low Al^{iv}, low Na + K and low Ti values. Those few samples with high $Al^{iv}$and Na + K values are alteration products.

Two major types of amphiboles are thus distinguished. The tremolite-actinolite group, which occur in serpentinsed part of the rock forming rims on the clinopyroxene grains and the tschermackite to magnesio-hornblende variety that occur as blades within the clinopyroxene grains. The Al_2O_3 content of the tremolite-actinolite is > 10 % in most samples indicating that they are generally more aluminous than tremolites described in abyssal peridotites (Kimball, 1985).

Table 4.26(a): Mineral chemistry of amphibole in coarse grained amphibolites(Lherzolite)

	CA11/2	CA11/3	CA11/4	CA11/5	CA11/11	CA11/17	CA11/21	CA11/22	CA11/23	CA11/24
SiO_2	47.10	46.60	45.59	47.16	46.98	47.88	45.86	46.41	46.48	45.66
TiO_2	0.49	0.46	0.56	0.44	0.47	0.47	0.54	0.50	0.55	0.54
Al_2O_3	10.89	11.42	12.66	11.19	11.31	10.45	12.59	11.67	11.81	12.48
Cr_2O_3	0.00	0.01	0.00	0.00	0.02	0.02	0.01	0.00	0.01	0.01
Fe_2O_3	5.61	5.64	5.50	5.96	5.95	4.83	5.67	6.21	6.49	6.68
FeO	5.11	5.17	5.81	4.77	4.88	5.48	5.69	4.92	4.72	4.63
MnO	0.12	0.14	0.14	0.12	0.14	0.12	0.11	0.14	0.14	0.12
MgO	14.73	14.49	13.72	14.63	14.54	14.96	13.84	14.44	14.52	14.01
NiO	0.02	0.00	0.03	0.01	0.01	0.02	0.01	0.00	0.00	0.03
CaO	11.82	11.77	11.78	11.62	11.66	11.96	11.80	11.80	11.81	11.59
Na_2O	1.21	1.29	1.39	1.25	1.27	1.09	1.36	1.27	1.33	1.32
K_2O	0.11	0.17	0.19	0.11	0.10	0.11	0.18	0.16	0.12	0.20
H_2O*	2.10	2.09	2.09	2.10	2.10	2.10	2.10	2.10	2.11	2.09
Total	99.31	99.26	99.45	99.37	99.44	99.50	99.75	99.61	100.09	99.36
Structural formulae based on 23 oxygens										
Si	6.738	6.679	6.548	6.731	6.708	6.825	6.561	6.632	6.610	6.545
Al^{iv}	1.262	1.321	1.452	1.269	1.292	1.175	1.439	1.368	1.390	1.455
Al^{vi}	0.574	0.608	0.690	0.614	0.611	0.580	0.684	0.598	0.589	0.653
Ti	0.053	0.050	0.060	0.047	0.050	0.050	0.058	0.054	0.059	0.058
Cr	0.000	0.001	0.000	0.000	0.002	0.002	0.001	0.000	0.001	0.001
Fe^{3+}	0.604	0.609	0.594	0.640	0.640	0.518	0.611	0.667	0.695	0.721
Fe^{2+}	0.611	0.620	0.697	0.570	0.583	0.654	0.680	0.587	0.561	0.555
Mn	0.015	0.017	0.017	0.015	0.017	0.014	0.013	0.017	0.017	0.015
Mg	3.141	3.096	2.937	3.113	3.095	3.179	2.952	3.076	3.078	2.994
Ni	0.002	0.000	0.003	0.001	0.001	0.002	0.001	0.000	0.000	0.003
Ca	1.812	1.807	1.813	1.777	1.784	1.826	1.809	1.807	1.799	1.780
Na	0.336	0.358	0.387	0.346	0.352	0.301	0.377	0.352	0.367	0.367
K	0.020	0.031	0.035	0.020	0.018	0.020	0.033	0.029	0.022	0.037
OH*	2.000	2.000	2.000	2.000	2.000	2.000	2.000	2.000	2.000	2.000
Total	17.167	17.197	17.235	17.143	17.154	17.148	17.219	17.188	17.188	17.183
Amphibole group	Ca	Ca	Ca	Ca	Ca	Ca	Ca	Ca	Ca	Ca
(Ca+Na) (B)	2.000	2.000	2.000	2.000	2.000	2.000	2.000	2.000	2.000	2.000
Na (B)	0.188	0.193	0.187	0.223	0.216	0.174	0.191	0.193	0.201	0.220
(Na+K) (A)	0.167	0.197	0.235	0.143	0.154	0.148	0.219	0.188	0.188	0.183
$Mg/(Mg+Fe^{2+})$	0.837	0.833	0.808	0.845	0.842	0.829	0.813	0.840	0.846	0.844
$Fe^{3+}/(Fe^{3+}+Al^{vi})$	0.513	0.500	0.462	0.511	0.511	0.472	0.472	0.527	0.541	0.524
Sum of S2	13.000	13.000	13.000	13.000	13.000	13.000	13.000	13.000	13.000	13.000
Calculated pressure of formation of the amphiboles in the coarse-grainedamphibolites										
P (kbars)										
Hammarstrom& Zen (1986)	5.3	5.8	6.9	5.5	5.7	4.9	6.8	6.0	6.0	6.7
Hollister et al. (1987)	5.6	6.1	7.3	5.9	6.0	5.1	7.2	6.3	6.4	7.1
Johnson & Rutherford (1989)	4.3	4.7	5.6	4.5	4.6	4.0	5.5	4.9	4.9	5.5
Schmidt (1992)	5.7	6.2	7.2	6.0	6.0	5.3	7.1	6.3	6.4	7.0

Table 4.26(b): Mineral chemistry of amphibole in coarse grainedamphibolites(Lherzolite)

	CA11 /25	CA11 /27	CA11 /29	CA11 /34	CA11 /47	CA11 /48	CA11 /14
SiO_2	47.84	47.18	46.41	45.78	45.64	44.87	44.56
TiO_2	0.42	0.48	0.50	0.53	0.54	0.45	0.54
Al_2O_3	10.48	12.15	11.43	12.82	12.25	12.75	13.69
Cr_2O_3	0.00	0.08	0.00	0.00	0.13	0.03	0.00
Fe_2O_3	8.31	5.08	6.72	5.55	7.47	11.34	5.60
FeO	2.44	6.47	4.41	5.47	3.93	0.00	6.03
MnO	0.13	0.11	0.12	0.14	0.11	0.11	0.14
MgO	15.06	12.65	14.69	13.81	14.26	15.45	13.16
NiO	0.02	0.00	0.01	0.00	0.01	0.02	0.02
CaO	11.77	10.64	11.79	11.69	11.50	10.10	11.69
Na_2O	0.16	1.20	1.29	1.37	1.30	1.25	1.57
K_2O	0.10	0.17	0.12	0.20	0.28	0.13	0.20
H_2O*	2.11	2.08	2.10	2.09	2.10	2.10	2.08
Total	98.83	98.29	99.59	99.45	99.51	98.59	99.28
	Structural formulae based on 23 oxygens						
Si	6.806	6.807	6.629	6.559	6.531	6.408	6.428
Al^{iv}	1.194	1.193	1.371	1.441	1.469	1.592	1.572
Al^{vi}	0.564	0.873	0.553	0.723	0.596	0.554	0.756
Ti	0.045	0.052	0.054	0.057	0.058	0.048	0.059
Cr	0.000	0.009	0.000	0.000	0.015	0.003	0.000
Fe^{3+}	0.889	0.551	0.723	0.598	0.804	1.218	0.608
Fe^{2+}	0.290	0.781	0.527	0.655	0.470	0.000	0.727
Mn	0.016	0.013	0.015	0.017	0.013	0.013	0.017
Mg	3.194	2.721	3.128	2.949	3.042	3.289	2.830
Ni	0.002	0.000	0.001	0.000	0.001	0.002	0.002
Ca	1.794	1.645	1.804	1.794	1.763	1.545	1.807
Na	0.044	0.336	0.357	0.381	0.361	0.346	0.439
K	0.018	0.031	0.022	0.037	0.051	0.024	0.037
OH*	2.000	2.000	2.000	2.000	2.000	2.000	2.000
Total	16.856	17.012	17.183	17.211	17.175	17.045	17.283
Amphibole group	Ca	Ca	Ca	Ca	Ca	Ca	Ca
(Ca+Na) (B)	1.838	1.980	2.000	2.000	2.000	1.871	2.000
Na (B)	0.044	0.336	0.196	0.206	0.237	0.325	0.193
(Na+K) (A)	0.018	0.031	0.183	0.211	0.175	0.045	0.283
$Mg/(Mg+Fe^{2+})$	0.917	0.777	0.856	0.818	0.866	1.000	0.796
$Fe^{3+}/(Fe^{3+}+Al^{vi})$	0.612	0.387	0.566	0.453	0.574	0.687	0.446
Sum of S2	13.000	13.000	13.000	13.000	13.000	13.129	13.000
Calculated pressure of formation of the amphiboles in the coarse-grainedamphibolites							
P (kbars)							
Hammarstrom& Zen (1986)	4.9	6.5	5.8	7.0	6.5	6.9	7.8
Hollister et al. (1987)	5.2	6.9	6.1	7.4	6.9	7.3	8.4
Johnson & Rutherford (1989)	4.0	5.3	4.7	5.7	5.3	5.6	6.4
Schmidt (1992)	5.4	6.8	6.1	7.3	6.8	7.2	8.1

Table 4.26(c): Mineral chemistry of amphibole in coarse grained amphibolites(Lherzolite)

	CA11/35	CA11/8	CA11/44	CA11/18	CA11/19	CA11/20
SiO_2	38.64	39.09	43.25	55.06	56.30	57.04
TiO_2	0.06	0.28	0.05	0.01	0.02	0.01
Al_2O_3	13.95	15.75	11.39	0.30	0.32	0.44
Cr_2O_3	0.02	0.01	0.02	0.01	0.01	0.00
Fe_2O_3	14.34	11.37	11.96	0.00	0.00	0.00
FeO	0.00	0.00	1.14	16.55	16.71	15.75
MnO	0.23	0.09	0.19	0.49	0.47	0.45
MgO	24.16	20.70	23.62	22.22	22.55	23.00
NiO	0.02	0.01	0.03	0.01	0.00	0.00
CaO	0.39	6.53	0.14	0.59	0.46	0.35
Na_2O	0.00	0.50	0.01	0.01	0.01	0.02
K_2O	0.00	0.06	0.01	0.00	0.00	0.01
H_2O*	2.02	2.06	2.04	2.07	2.11	2.13
Total	93.82	96.45	93.86	97.32	98.96	99.20
Structural formulae based on 23 oxygens						
Si	5.738	5.699	6.346	7.979	8.008	8.043
Al ^{iv}	2.262	2.301	1.654	0.021	0.000	0.000
Al ^{vi}	0.179	0.406	0.315	0.031	0.054	0.073
Ti	0.007	0.031	0.006	0.001	0.002	0.001
Cr	0.002	0.001	0.002	0.001	0.001	0.000
Fe^{3+}	1.602	1.247	1.321	0.000	0.000	0.000
Fe^{2+}	0.000	0.000	0.140	2.006	1.988	1.857
Mn	0.029	0.011	0.024	0.060	0.057	0.054
Mg	5.348	4.499	5.166	4.800	4.782	4.835
Ni	0.002	0.001	0.004	0.001	0.000	0.000
Ca	0.062	1.020	0.022	0.092	0.070	0.053
Na	0.000	0.141	0.003	0.003	0.003	0.005
K	0.000	0.011	0.002	0.000	0.000	0.002
OH*	2.000	2.000	2.000	2.000	2.000	2.000
Total	17.232	17.369	17.005	16.995	16.964	16.923
Amphibole group	Fe-Mg-Mn	Fe-Mg-Mn	Fe-Mg-Mn	Fe-Mg-Mn	Fe-Mg-Mn	Fe-Mg-Mn
(Ca+Na) (B)	0.062	1.020	0.022	0.094	0.073	0.058
Na (B)	0.000	0.000	0.000	0.003	0.003	0.005
(Na+K) (A)	0.000	0.153	0.005	0.000	0.000	0.002
$Mg/(Mg+Fe^{2+})$	1.000	1.000	0.974	0.705	0.706	0.722
$Fe^{3+}/(Fe^{3+}+Al^{vi})$	0.899	0.755	0.807	0.000	0.000	0.000
Sum of S2	15.170	14.196	14.978	14.900	14.891	14.863

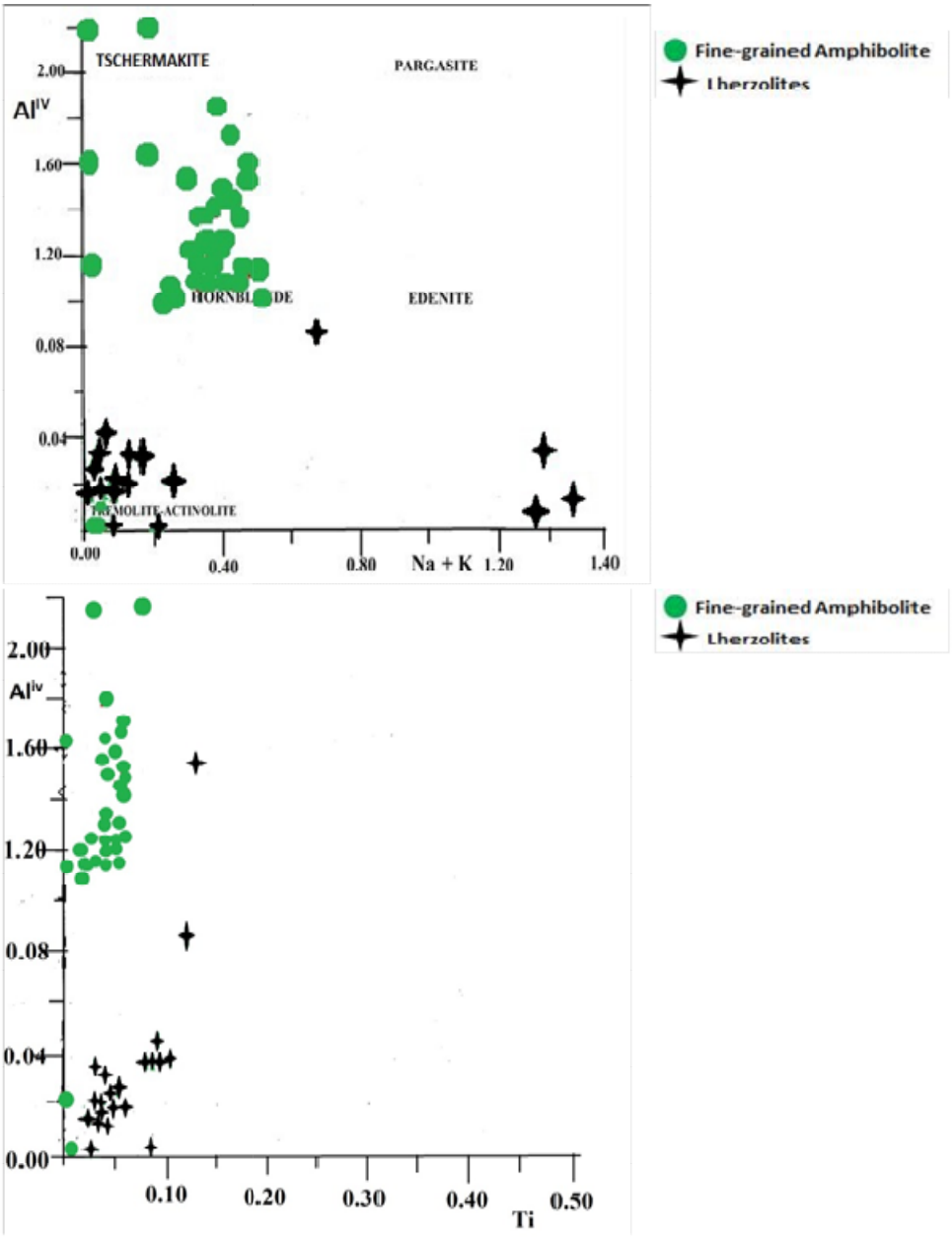

Fig. 4.59:Compositional variation of amphiboles in fine-grained amphibolites and coarse-grained amphibolites(lherzolite) of Wonu, Ibadan-Apomu areaon (a) Al^{iv}versus Na + K and (b) Al^{iv}versus Ti (atoms p.f.u) (Béziat *et al.,* 2000).

Kaolinite-Serpentine Group minerals

Some of the olivines and pyroxenes in the coarse-grained amphibolite (lherzolite) in the Wonu, Ibadan-Apomu area are altered to kaolinite-serpentine group minerals includingamesite-clinochlore-antigorite transitional minerals (Fig. 4.60). Amesite and chlorite, mainly clinochlore occur as white to light-green crystals in the lherzolite. Green titanite (sphene) also occur in purple chromium-bearing amesite (clinochlore). Representative chemical analysis of amesite in the lherzoliteof Wonu, Ibadan-Apomu area are shown in Table 4.27(a-b). Other details are presented in the appendix. The structural formula of the amesite: $(Mg_{3.8}Fe_{0.8}Al_{1.4})(Si_{2.8}Al_{1.2})O_{10}(OH)_8$ showed that the mineral is similar to the ideal composition of clinochlore, which is $Mg_5Al(Si_3Al)O_{10}(OH)_8$. The mineral chemistry also indicated that part of the Mg had been replaced by Fe and Al during exchange reactions accompanying hydrothermal alteration of the lherzolite. This is reflected in the Mg# = Mg/Mg+Fe reduction from > 90 in the olivine and pyroxene to 82 in the amesite/chlorite-serpentine trend shown in Figs. 4.60a and b.

Amesite occurs in an environment of low-grade metamorphism, affecting rocks of high aluminium and magnesium content. It is commonly associated with polytypes of chlorite, antigorite, magnetite, rutile, calcite and diopside. Antigorite is formed at a higher temperature above 250ºC compared to chysotile and lizardite that are low-temperature serpentine minerals (Evans, 2008). The estimated temperature from the mineral chemistry of the chlorite range from 300 to 500 ºC (Fig. 4.61).

Table 4.27: Mineral chemistry of amesite in coarse grained amphibolites (lherzolite)

	CA11/1	CA11/6	CA11/7	CA11/9	CA11/10	CA11/12	CA11/13	CA11/15	CA11/16	CA11/26	CA11/28	CA11/30	CA11/31	CA11/32	CA11/33	CA11/36	CA11/37	CA11/38	CA11/40	CA11/42
SiO_2	28.97	28.21	27.73	28.56	28.31	28.62	28.41	28.61	29.34	28.92	28.68	28.79	29.39	28.39	30.61	28.40	29.35	29.35	29.25	28.80
TiO_2	0.12	0.05	0.10	0.08	0.09	0.08	0.09	0.10	0.11	0.09	0.10	0.09	0.10	0.09	0.11	0.10	0.08	0.11	0.09	0.09
Al_2O_3	21.04	21.71	21.91	22.10	22.10	22.27	22.46	22.22	21.48	21.31	21.67	21.20	20.68	21.97	21.11	22.06	21.82	21.56	20.91	21.70
Cr_2O_3	0.00	0.00	0.00	0.01	0.00	0.01	0.00	0.00	0.01	0.01	0.01	0.02	0.00	0.02	0.01	0.02	0.01	0.03	0.00	0.01
FeO	10.20	10.14	10.42	10.54	10.50	10.50	10.56	10.29	10.40	10.00	10.40	10.34	10.20	10.45	10.23	10.47	10.14	10.49	10.02	10.25
MnO	0.03	0.04	0.05	0.04	0.05	0.04	0.03	0.04	0.04	0.04	0.04	0.04	0.03	0.03	0.05	0.03	0.05	0.06	0.02	0.04
MgO	26.20	23.57	24.23	25.32	25.34	25.46	25.46	24.46	25.39	25.72	25.62	25.87	26.24	25.61	25.46	25.54	25.37	25.33	26.25	25.88
CaO	0.03	0.05	0.01	0.02	0.01	0.03	0.01	0.06	0.01	0.02	0.02	0.02	0.01	0.03	0.05	0.02	0.01	0.04	0.01	0.00
Na_2O	0.00	0.02	0.02	0.00	0.00	0.00	0.00	0.01	0.00	0.01	0.01	0.01	0.00	0.00	0.01	0.01	0.01	0.00	0.01	0.00
K_2O	0.00	0.03	0.01	0.01	0.00	0.00	0.00	0.01	0.00	0.01	0.00	0.00	0.00	0.00	0.03	0.01	0.00	0.00	0.01	0.00
Total	86.59	83.82	84.48	86.68	86.40	87.01	87.02	85.80	86.78	86.13	86.55	86.38	86.65	86.59	87.67	86.66	86.84	86.97	86.57	86.77
	Formula units based on 14 Oxygens																			
Si	2.837	2.849	2.788	2.797	2.783	2.791	2.772	2.824	2.864	2.843	2.812	2.829	2.874	2.784	2.948	2.783	2.858	2.861	2.860	2.814
Al iv	1.163	1.151	1.212	1.203	1.217	1.209	1.228	1.176	1.136	1.157	1.188	1.171	1.126	1.216	1.052	1.217	1.142	1.139	1.140	1.186
Al vi	1.266	1.434	1.385	1.349	1.344	1.352	1.356	1.410	1.336	1.312	1.317	1.285	1.258	1.324	1.345	1.332	1.363	1.338	1.271	1.313
Ti	0.009	0.004	0.008	0.006	0.007	0.006	0.007	0.007	0.008	0.007	0.007	0.007	0.007	0.007	0.008	0.007	0.006	0.008	0.007	0.007
Cr	0.000	0.000	0.000	0.001	0.000	0.001	0.000	0.000	0.001	0.001	0.001	0.002	0.000	0.002	0.001	0.002	0.001	0.002	0.000	0.001
Fe	0.835	0.856	0.876	0.863	0.863	0.856	0.862	0.849	0.849	0.822	0.853	0.850	0.834	0.857	0.824	0.858	0.826	0.855	0.820	0.838
Mn	0.002	0.003	0.004	0.003	0.004	0.003	0.002	0.003	0.003	0.003	0.003	0.003	0.002	0.002	0.004	0.002	0.004	0.005	0.002	0.003
Mg	3.824	3.548	3.630	3.696	3.712	3.701	3.702	3.598	3.694	3.768	3.744	3.788	3.824	3.743	3.655	3.730	3.682	3.679	3.826	3.768
Ca	0.003	0.005	0.001	0.002	0.001	0.003	0.001	0.006	0.001	0.002	0.002	0.002	0.001	0.003	0.005	0.002	0.001	0.004	0.001	0.000
Na	0.000	0.004	0.004	0.000	0.000	0.000	0.000	0.002	0.000	0.002	0.002	0.002	0.000	0.000	0.002	0.002	0.002	0.000	0.002	0.000
K	0.000	0.004	0.001	0.001	0.000	0.000	0.000	0.001	0.000	0.001	0.000	0.000	0.000	0.000	0.004	0.001	0.000	0.000	0.001	0.000
Total	9.940	9.859	9.909	9.921	9.930	9.922	9.930	9.877	9.892	9.917	9.929	9.937	9.927	9.938	9.848	9.936	9.884	9.892	9.929	9.930
Fe/Fe+Mg	0.18	0.19	0.19	0.19	0.19	0.19	0.19	0.19	0.19	0.18	0.19	0.18	0.18	0.19	0.18	0.19	0.18	0.19	0.18	0.18

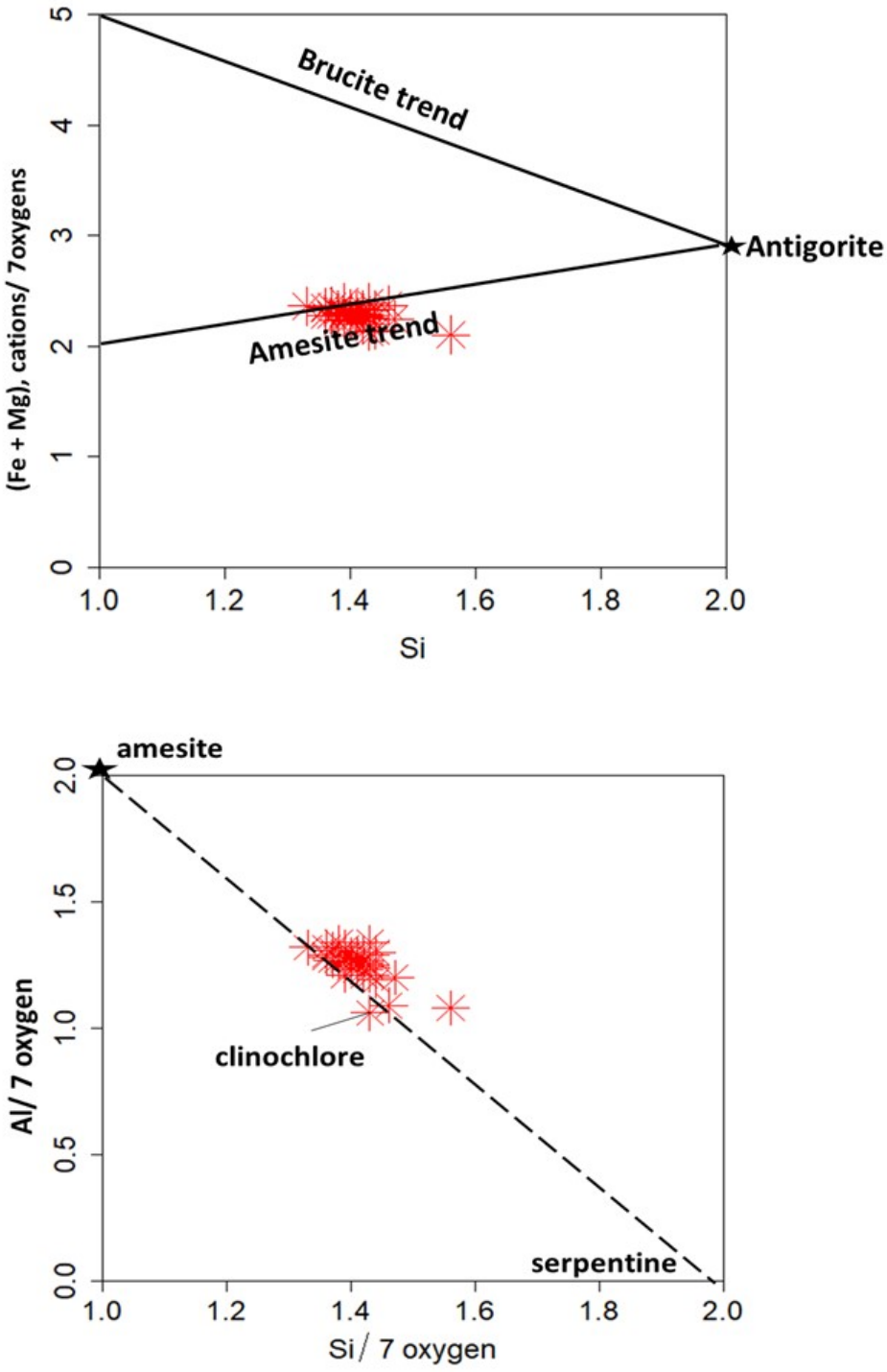

Fig. 4.60:Chemistry of the chlorites(clinochlore) in the lherzolite of Wonu, Ibadan-Apomuarea showing amesite (chlorite)-antigorite (serpentine) trend (after Beard *et al*. 2009).

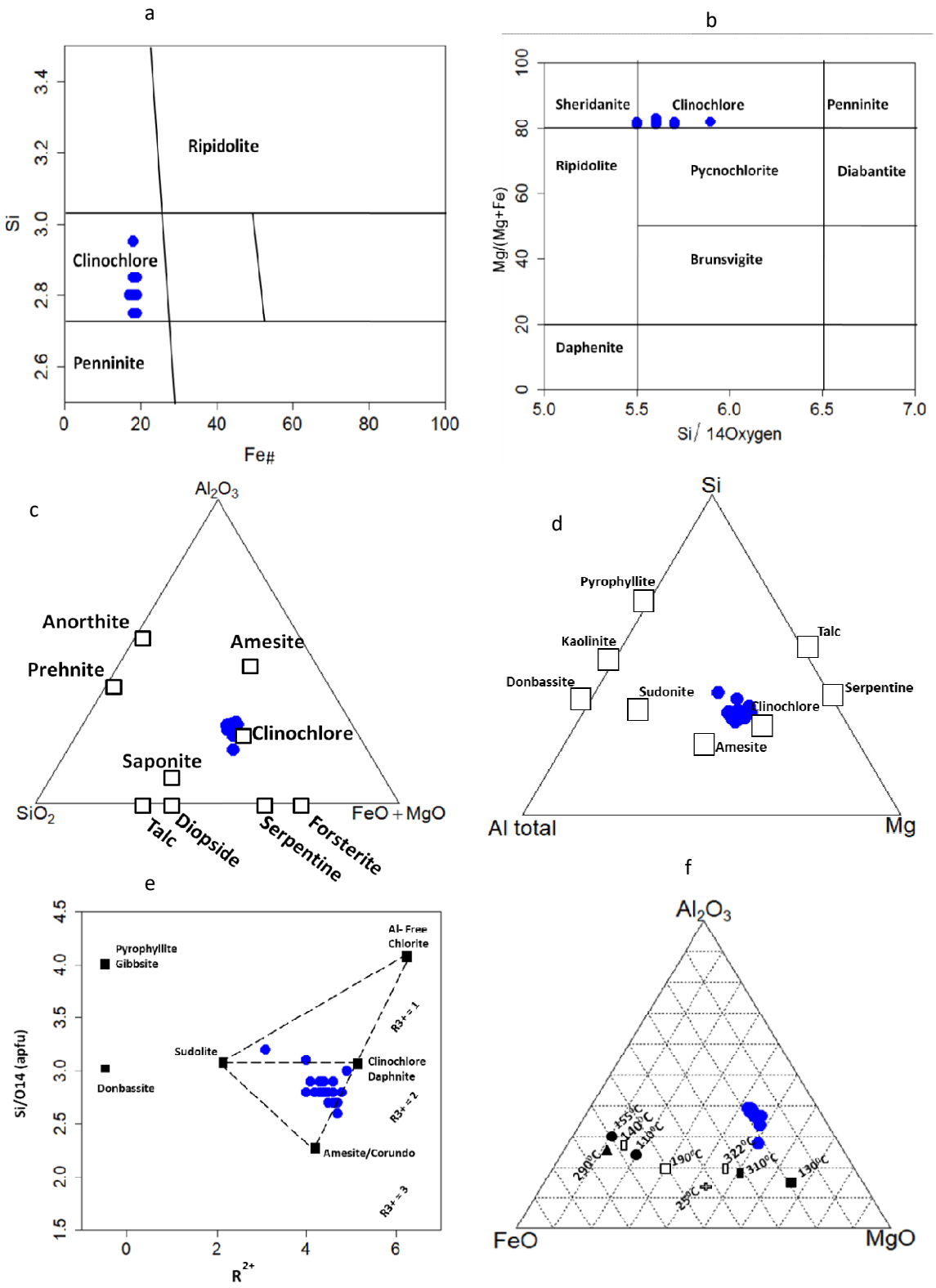

Fig. 4.61:Chemistry of the chlorites (clinochlore) (a-e) and temperature range of (300 to 500 ºC) (f) in the lherzolite of Wonu, Ibadan-Apomu area.

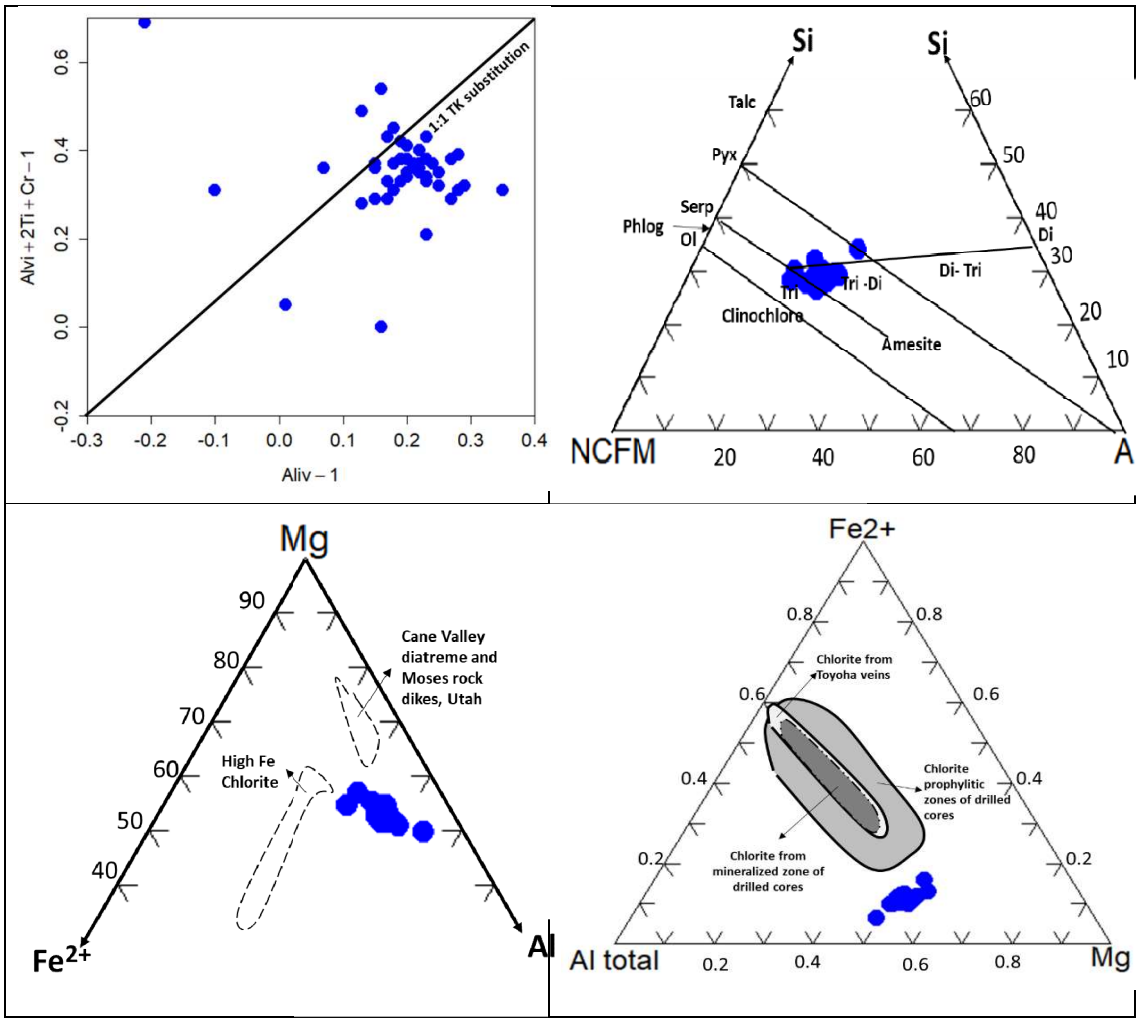

Fig. 4.62:Chemistry of the chlorites (clinochlore) in the lherzolite of Wonu, Ibadan-Apomu area amesite (chlorite)-antigorite (serpentine) trend (after Beard *et al*. 2009; Inoue *et al.* 2010).

Opaques

Opaque minerals include ferrichromite, ilmenite and magnetite, which corresponds to 5 % in the modal volume in some cases. The opaque minerals in the lherzolite in the Wonu, Ibadan-Apomu area are mainly ferritchromite and magnetite, which are alteration products of Cr-spinel. The mineral chemistry of the magnetite in the lherzolites are shown in Table 4.28. The ratio of FeO to Fe_2O_3 vary from 1:2 to 1:3 indicating altered magnetite.

Sulphides

Within thelherzolite,the sulphides appear as interwoven growths of pentlandite-magnetite and magnetite-pyrrhotite occurring as substantial quantity of shredded grains. The pentlandites have a high Ni content of between 25-35% similar to those of spinel lherzolite xenoliths from South Africa (Bishop *et al.,* 1975).

Table 4.28: Mineral chemistry of magnetite in the lherzolites

	CA11/49	CA12/88	CA12/93
SiO_2	0.63	0.02	0.02
TiO_2	0.02	0.01	0.00
Al_2O_3	0.18	0.01	0.00
Cr_2O_3	0.01	0.00	0.00
Fe_2O_3	74.28	74.66	67.04
FeO	24.51	25.17	32.32
MnO	0.00	0.00	0.00
MgO	0.05	0.00	0.00
Total	**99.68**	**99.87**	99.38
Formula units based on 4 oxygens			
Si	0.024	0.001	0.001
Ti	0.001	0.000	0.000
Al	0.008	0.000	0.000
Cr	0.000	0.000	0.000
Fe^{3+}	2.109	2.132	1.964
Fe^{2+}	0.773	0.799	1.052
Mn	0.000	0.000	0.000
Mg	0.003	0.000	0.000
Tot. cat.	2.917	2.933	3.017
Tot. oxy.	4.000	4.000	4.000

4.2.2.4 Geochemistry of the Coarse-grained Amphibolites (Lherzolite)

The mean and range values of the main and minor component concentrations of the lherzolite are shown in Table 4.29. As observed the SiO_2 concentration ranged 41.66 – 43.65%, Al_2O_3 of 11.67 – 13.90%,$Fe_2O_3$of 12.10 – 20.75%,and MgO of 17.29 – 21.87%.The CaO (5.39 – 10.39 %) contents vary widely among the samples. Generally, komatities are characterized by high MgO contents (20-30wt%) with high CaO and Al_2O_3 concentration.The results of major elements of the lherzolites showed similarities with komatiites. The high Al_2O_3 content of 11.67 - 13.90% indicated that they are Al-enrichedkomatiites, which implies both the components of the parental rocks and also the liquefying temperatures\pressures gave rise to the eventual whole rock formations. The MnO (0.17%) content is low, while the $TiO_2$of 1.01 to 4.03% is relatively higher in the lherzolite than those of the fine-grained amphibolites.The K_2O (0.08 –0.13 %) values are low. Usually, K_2O is often found in orthoclase feldspar and sanidine-bearing mafic-ultramafics. The Na_2O varies from 0.49 – 0.84% while the P_2O_5 values ranged from 0.05 – 1.02 %. The loss on ignition (LOI) value are low (0.25 - 0.39%), suggesting low fluid in the crystal lattice of the lherzolite.

The Sum Alkalinity (Na_2O+K_2O) versus SiO_2 diagram (after Middlemost 1994) of the lherzoliteshowed that the precursor varies from dominantly basalt to picrobasalt (Fig. 4.63).The basic chemical character and thekomatitic nature of the lherzolite was confirmed on the AFM ($Na_2O + K_2O$) – Fe_2O_3 – MgO) diagram of Irvine and Barager (1971) (Fig. 4.64), while the Al_2O_3-MgO-($Fe_2O_{3(t)}$+TiO_2) diagrams of Jenson (1976) showed that the amphibolites are basaltic komatiite (Fig. 4.45b, green). The CaO-Al_2O_3-MgO plots of the Wonu, Ibadan-Apomu ultramafic-mafic rocks after Viljoen & Viljoen, (1969a, 1969b) (Fig. 4.46, green) showed fractionation of the basaltic komatiites protoliths from Dunitic magma at a deeper level.Harker diagrams of the major and trace elements versus MgO for the amphibolite and lherzolite (Fig. 4.65), indicate transition from lherzolite to amphibolite characterised by enrichment of Na_2O, K_2O, Ba, Nb and Rb in the amphibolite, with increasing fractionation. This is further demonstrated by the abundances of Al_2O_3 vs MgO and FeO*/MgO versus SiO_2diagram (after Miyashiro, 1974), showing differentiation from high MgO-rich dunitic magma to FeO-rich tholeiitic magma(Figs. 4.47 and 4.66).

Table 4.29: Major oxides(%), minor components and rare earth (ppm) components composition in coarse grained amphibolite (Lherzolite).

	1	2	3	4	5	6	7	8	9	10	Average	Range	
SiO_2	43.04	43.65	42.5	42.35	41.78	43.55	41.89	43.35	42.81	41.66	42.66	43.65	41.66
TiO_2	1.58	1.77	4.03	1.01	1.35	1.02	1.56	1.62	1.37	1.15	1.65	4.03	1.01
Al_2O_3	12.22	11.67	12.21	13.15	13 90	12.36	11.81	11.97	12.34	12.67	12.27	13.15	11.67
$Fe_2O_{3(t)}$	13.63	13.81	12.1	12.23	20.75	12.38	13.55	12.7	13.11	13.19	13.75	20.75	12.1
MnO	0.17	0.18	0.18	0.19	0.16	0.18	0.19	0.18	0.17	0.15	0.18	0.19	0.15
MgO	19.27	19.4	19.5	20.11	21.87	19.4	18.36	17.29	19.87	19.33	19.44	21.87	17.29
CaO	6.81	6.71	6.3	6.23	8.4	5.39	8.21	10.11	5.99	6.68	7.08	10.11	5.39
Na_2O	0.59	0.57	0.81	0.79	0.84	0.66	0.73	0.49	0.55	0.59	0.66	0.84	0.49
K_2O	0.09	0.09	0.09	0.09	0.12	0.08	0.11	0.08	0.11	0.13	0.10	0.13	0.08
P_2O_5	0.06	0.06	0.09	0.92	1.02	0.09	0.05	0.08	0.05	0.07	0.25	1.02	0.05
SO_3	1.05	0.96	0.66	0.61	0.63	1.3	0.31	0.35	0.99	0.88	0.77	1.3	0.31
LOI	2.48	2.2	2.88	2.04	2.75	2.82	2.97	2.45	2.91	3.32	2.68	3.32	2.04
Total	100.99	101.07	101.4	99.72	99.67	99.23	99.74	100.67	100.27	99.82			
Trace elements (ppm)													
Cr	40	46	175	254	293	261	253	645	236	171	237.4	645	40
Ni	267	331	311	599	458	376	542	367	353	596	420	599	267
Co	79	108	150	125	145	116	107	78	76	120	110.4	150	76
Cu	64	70	58	124	143	145	87	64	131	55	94.1	145	55
Zn	73	103	51	42	35	40	31	57	63	109	60.4	109	31
V	80	78	92	72	86	196	198	135	98	93	112.8	198	72
Sc	11.8	12.2	11	14	24	20	16	11	12	13	14.5	24	11
Ga	7.85	8.28	6.9	16	24	9	13	15	7	9	11.603	24	6.9
Ba	65.1	54.8	53	93	88	95	53	52	62	92	70.79	95	52
Rb	0.87	0.72	1.2	0.91	0.65	0.77	0.58	0.93	0.64	0.75	0.802	1.2	0.58
Sr	16.5	14.6	12.8	25	21	23	15	18	14	12	17.19	25	12
Y	9.9	9.1	12.3	10	11	5	13	8	6	10	9.43	13	5
Zr	15.0	19.1	17.6	21	19.5	20	17.4	16.6	18.9	23	18.81	23	15
Nb	0.97	1.23	1.03	0.67	0.91	0.58	0.66	0.75	0.98	0.86	0.864	1.23	0.58
Cs	0.09	0.08	0.06	0.05	0.09	0.10	0.08	0.07	0.08	0.06	0.076	0.1	0.05
Hf	0.6	0.7	0.2	0.2	0.6	1.3	0.5	0.5	0.8	0.6	0.6	1.3	0.2
Ta	0.08	0.1	0.3	0.1	0.2	0.05	0.05	0.06	0.05	0.03	0.102	0.3	0.03
Th	1.01	0.64	1.10	1.03	1.20	0.68	0.74	0.92	0.68	1.21	0.921	1.21	0.64
U	0.22	0.25	0.23	0.20	0.25	0.21	0.23	0.20	0.22	0.25	0.226	0.25	0.2
Rare-Earth elements (ppm)													
La	6.71	5.31	4.6	4.03	4.81	2.43	2.90	3.37	3.01	4.06	4.123	6.71	2.43
Ce	12.25	11.93	8.85	9.91	12.72	9.72	9.53	7.11	12.91	12.35	10.728	12.91	7.11
Pr	1.69	1.53	1.54	1.13	1.20	1.55	2.01	2.22	1.80	7.15	2.182	7.15	1.13
Nd	7.07	6.53	7.11	6.91	6.31	6.47	6.15	6.46	6.58	6.29	6.588	7.11	6.15
Sm	1.51	1.45	1.02	1.44	0.58	1.11	1.95	1.37	1.97	1.09	1.349	1.97	0.58
Eu	0.63	0.58	1.07	0.83	0.22	0.65	0.52	0.61	0.52	0.54	0.617	1.07	0.22
Gd	1.61	1.54	1.76	1.48	0.71	1.02	1.77	1.01	1.46	1.52	1.388	1.77	0.71
Tb	0.24	0.24	0.29	0.11	0.12	0.17	0.36	0.26	0.23	0.22	0.224	0.36	0.11
Dy	1.54	1.47	1.31	1.28	1.69	1.17	1.05	1.14	0.81	0.85	1.231	1.69	0.81
Ho	0.32	0.31	0.49	0.24	0.13	0.18	0.32	0.25	0.29	0.33	0.286	0.49	0.13
Er	0.92	0.89	1.76	1.38	1.32	0.88	0.96	0.58	0.66	0.84	1.019	1.76	0.58
Tm	0.13	0.13	0.39	0.12	0.12	0.16	0.11	0.09	0.12	0.11	0.148	0.39	0.09
Yb	0.88	0.83	1.49	1.24	0.63	0.83	0.94	0.82	0.69	0.85	0.92	1.49	0.63
Lu	0.14	0.13	0.37	0.17	0.33	0.15	0.11	0.12	0.17	0.13	0.182	0.37	0.11
Rare-Earth Elements ratios													
Eu/Eu*	0.65	0.73	0.61	0.89	0.87	0.83	0.60	0.52	0.54	0.64	0.73	0.63	0.68
LaN/YbN	13.95	22.64	23.14	7.16	22.63	12.08	6.59	14.63	12.05	15.12	19.25	33.69	16.91
LaN/SmN	4.89	6.13	2.18	6.13	4.24	2.62	2.98	1.24	1.68	1.86	6.53	4.08	3.71
CeN/YbN	3.32	6.06	6.29	1.55	6.82	5.73	1.86	6.50	5.67	5.98	2.82	8.21	5.07
CeN/SmN	1.17	1.64	0.59	1.32	1.28	1.24	0.84	0.55	0.79	0.73	0.96	1.00	1.01
EuN/YbN	1.61	2.10	4.77	0.93	4.30	2.72	0.92	3.44	1.85	2.66	1.36	4.30	2.58
Sum_REE	11.35	14.56	11.61	13.95	13.31	14.97	11.17	11.62	13.79	9.70	13.40	14.11	12.80

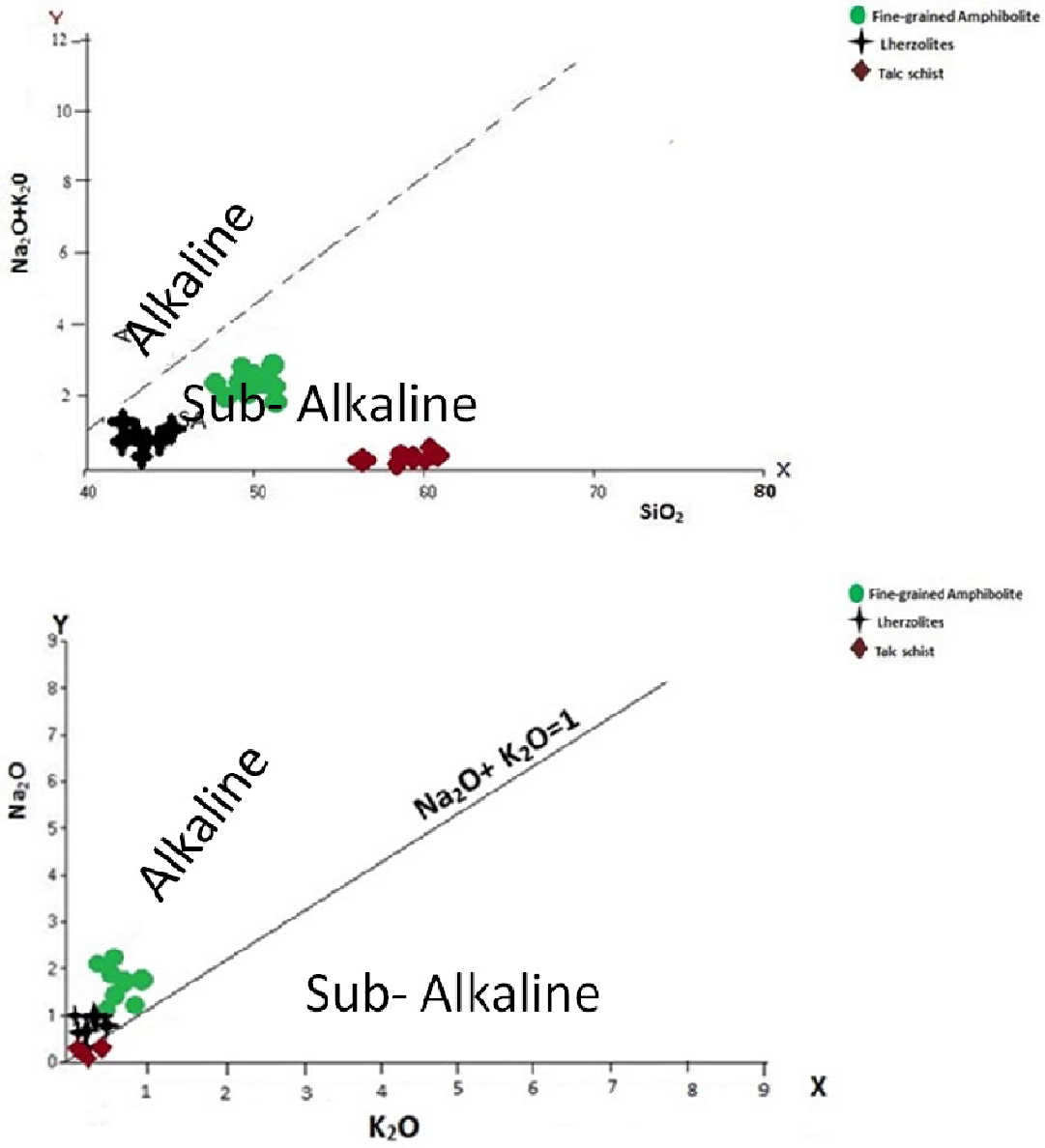

Fig. 4.63: (a) Total Alkalis (TAS) (Na_2O+K_2O) versus SiO_2 and (b) K_2O versus Na_2O diagrams (after Middlemost 1994) of the ultramafic-mafic rocks of Wonu, Ibadan-Apomu area.

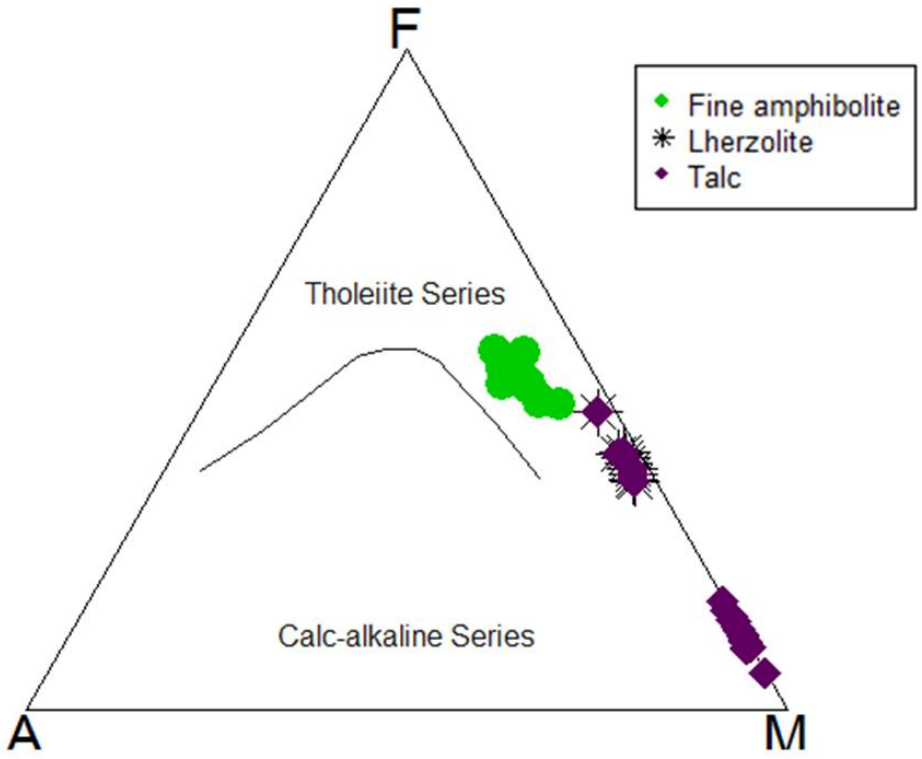

Fig. 4.64: The Al-Fe-Mg diagram (adapted from Irvine and Barager, 1971) indicating the tholeiitic nature of the fine-grained amphibolite(green), the komatitic nature of the lherzolite (purple star) and the dunite talc precursor (purple lozenge).

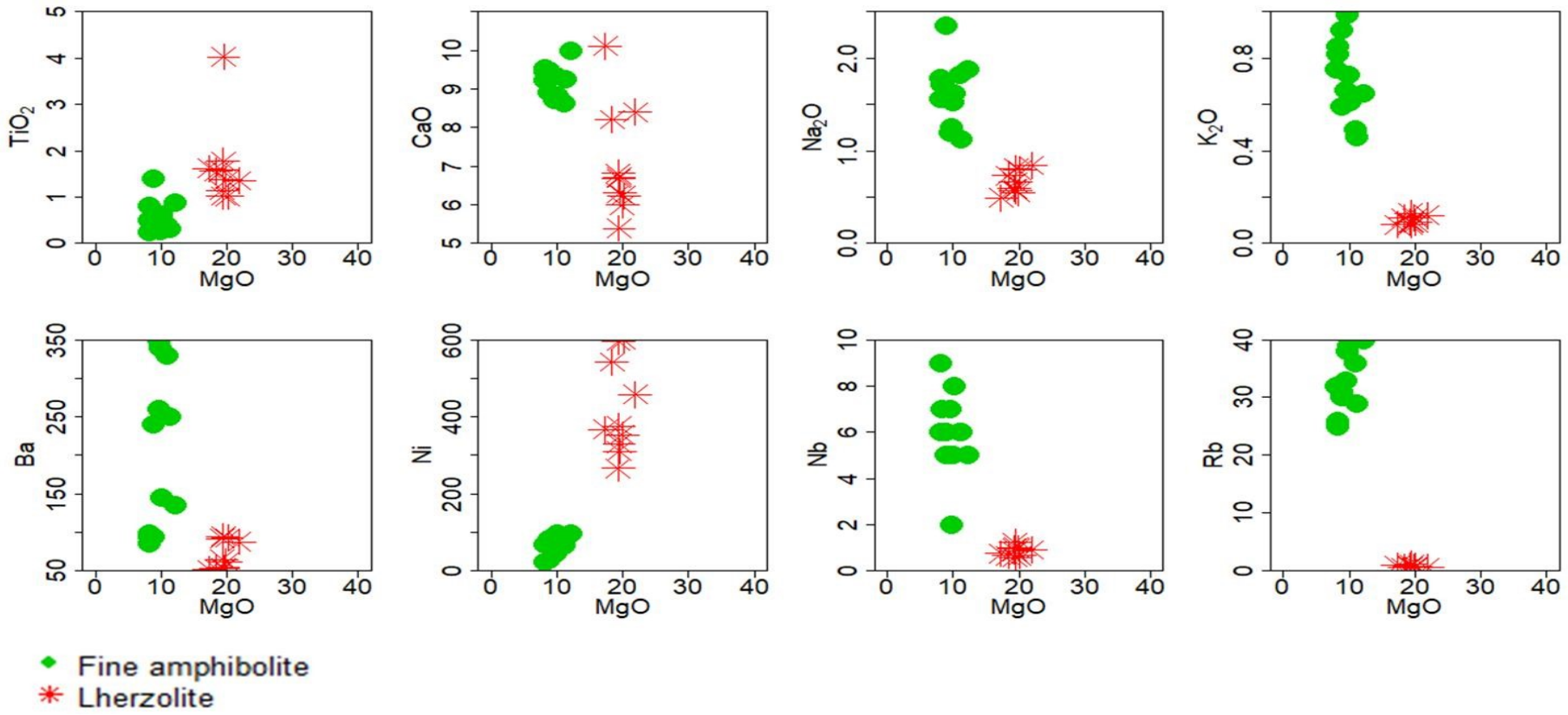

Fig. 4.65:Plots of major oxides and trace components versus MgO for amphibolite and lherzolite in Wonu, Ibadan-Apomu area, indicating transition, with enrichment in Na_2O, K_2O, Ba, Nb and Rb, from lherzolite to amphibolite.

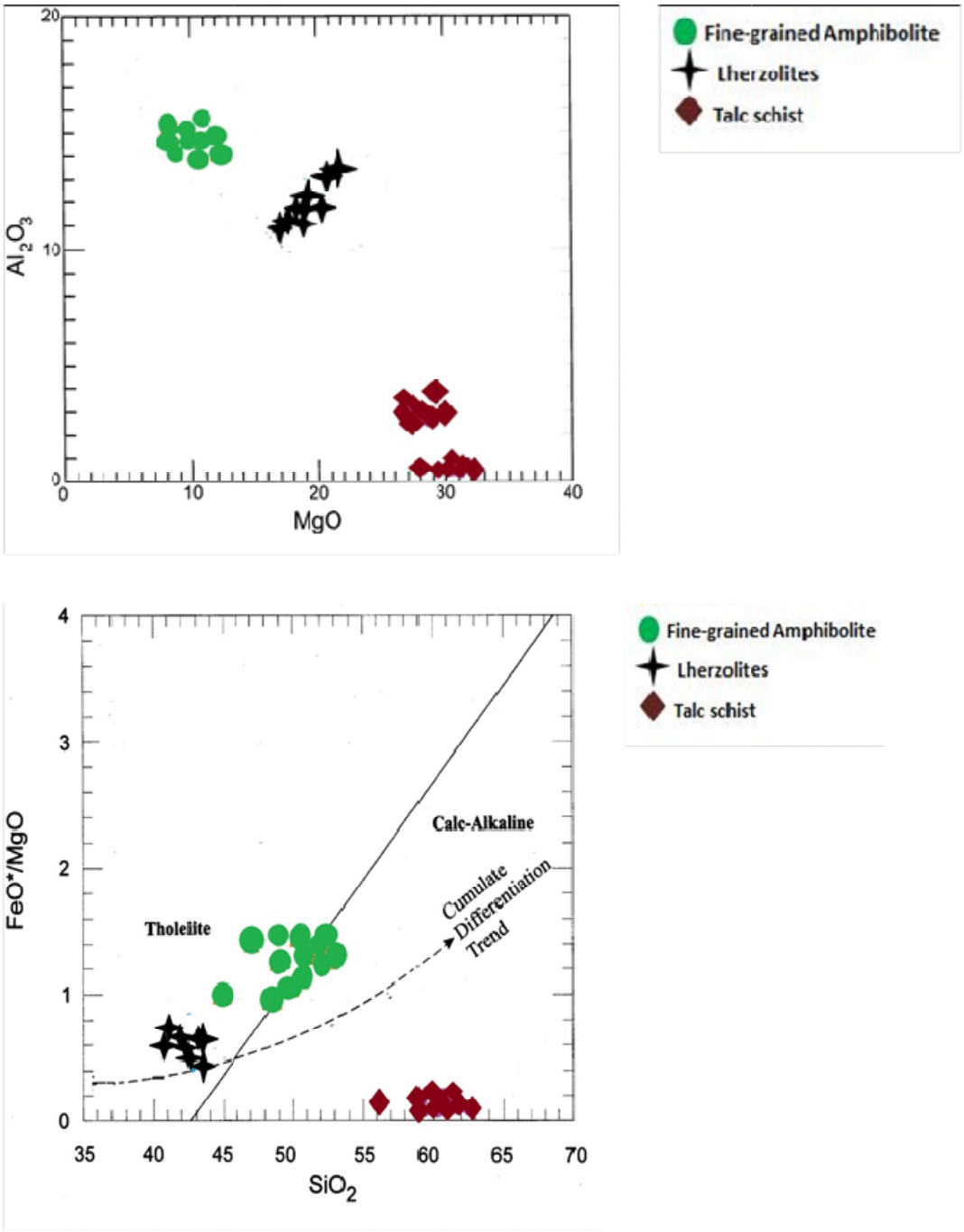

Fig. 4.66:Abundances of (a) Al_2O_3 vs MgO and FeO*/MgO vs SiO_2 plot showing the composition of the ultramafic rocks in Wonu, Ibadan-Apomu area in relation to cumulate differentiation trend (after Miyashiro,1974).

The trace elements data of the lherzolite (Table 4.15) indicated average values of Rb (1), Sr (17),Cr (237), Y (9), Zr (19) and Ba (71). The Th (<1) and U (0.23) ppm are lower compared to those of amphibolites (Fig. 4.48). The Cr of 237,Co of 110, Ni of 420, Cu of 94 and V of 113ppm. The lherzolites have marked depletion in the high-field elements (HFSE), such as, Ta (0.03 – 0.2ppm)and Nb (0.58 – 1.23ppm), which are characteristic of metasomatised ultramafic rocks. These geochemical features are typical of island arc lavas (Fig. 4.67a) (Pearce and Stern, 2006) indicating a significant input of a subduction component into the mantle source material generating the lherzolite. The major and trace element whole-rock geochemistry aptly supported the mineralogy of a serpentinised peridotite composed of olivine, tremolite, actinolite, chlorite, antigorite, Cr-spinel and magnetite.The Ni versus Ba diagram for the ultramafic-mafic rocks of Wonu, Ibadan-Apomu area showed low partial melting and fractional crystallization of the lherzoliteinto the amphibolite (Fig. 4.67b) (after Cocherie, 1986; De-Souza et al, 2007).

The chondrite-normalized REE patterns for the lherzolite in Fig. 4.68, is generally flat between 1.0 and 10.0. The concentrations of of the REE are Ce(7.11-12.91), Gd (0.71-1.77), Er (0.58-1.76) and Lu (0.11-0.37) ppm.The lherzolite showed slightly high LREE enrichment, slight HREE depletion having a positive Eu anomaly. Theyhave flat REE traces characteristic of komatiites and dunites. They showed positive Eu-anomaly indicating retention of feldspar in the melt after partial melting. The L_{aN}/Yb_N ratios of the lherzolite ranged from 1.99-5.19, while La_N/Sm_N ranged from 0.93-2.83 and the ratios Ce_N/Yb_N ranged from 1.56-5.32. The positive Eu anomaly (Eu/Eu*) ranged from 0.85-2.44 which is far higher than that of the fine-grained amphibolites, which ranged from 0.22 to 1.36, indicating retention of feldspar in the melt after crystallization. Conclusively, the major oxides and trace components of the lherzolite indicate a residual origin, although they are strongly metasomatised.

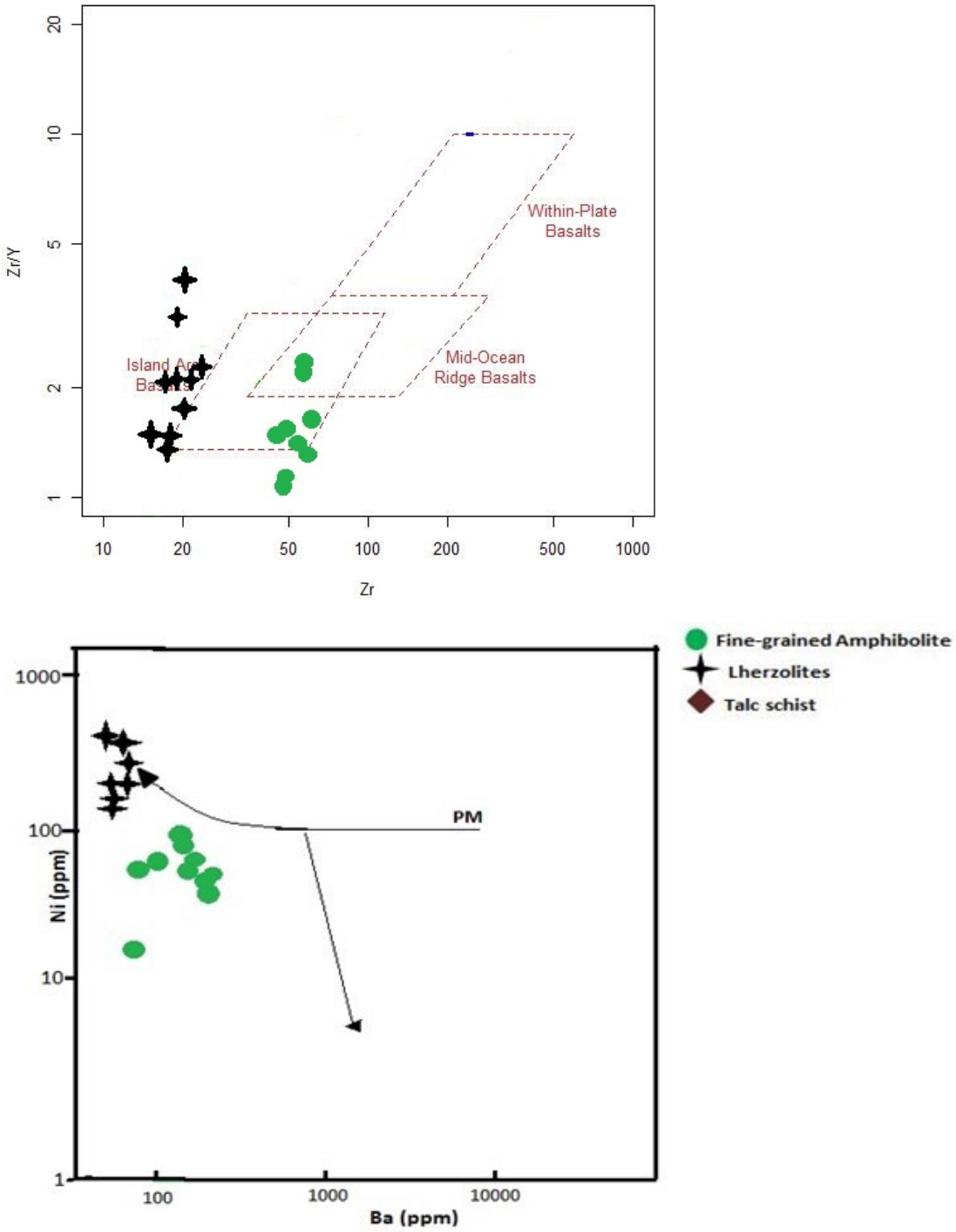

Fig. 4.67:(a) Zr/Y versusZr for the lherzolites and amphibolites of Wonu, Ibadan-Apomu area (b) Ni versus Ba for the ultramafic-mafic rocks of Wonu, Ibadan-Apomu area showing the effect of partial melting and fractional crystallization of the lherzolite (after Cocherie, 1986).

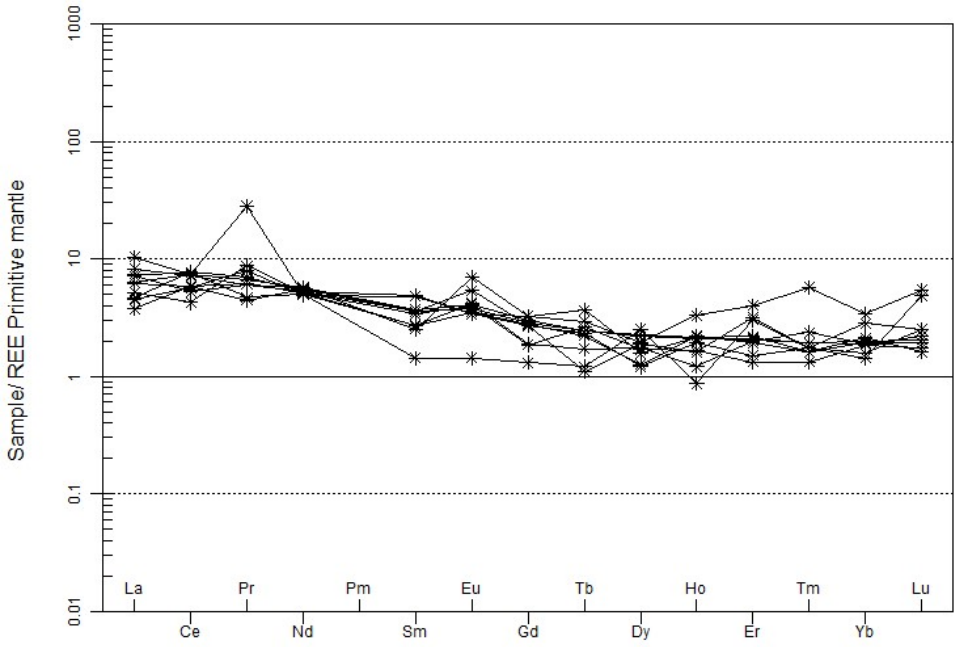

Fig. 4.68: Concentration of the rare earth components in lherzolite of Wonu, Ibadan-Apomu area (after McDonough and Sun, 1995).

4.4 Talc Schist

4.4.3.1 Petrography of the talc shist

Talc bodies occur as narrow discontinuous lensesparallel to the regional foliation. Discontinuous ring structures of the occurrences of the talc schist of about 1.5m and a maximum width of 300m (Fig. 4.69),within amphibolites and lherzolites is hereby interpreted as a sheet that was domed in the centre and then eroded. Other rock types around the talc schist include quartzite, quartz schist and granitoids. The largest occurrences is a mining site between Wonu and Pagbo (Fig. 4.70). The talcose bodies possess a strong soapy feel, greyish white to a tint of green in colour, while the weathered outcrops are brownish. In hand specimen the samples appear foliated, as defined by fine to platy aggregates of talc. With increase in chlorite content a greenish tint colour is observed.

Under the microscope talc and talc-chlorite constitute up to about 80% with lesser proportions of saponite, tremolite, actinolite, anthophyllite, antigorite, ferritchromite, magnetite and olivine (Table 4.30). The talc schists in thin section occur as platy, fibrous talc and mottled talc.Some crystals occur as foliated mass, coarse to fine platelets or acicular aggregates (Fig 4.71 and Fig 4.72).The talc mineral is white and radiating in texture. Chlorite crystals vary from white through light green to pink indicating the presence of amesite, diabantite (clinochlore) and saponite. Greenish plate-like crystals of chlorite occur within the talc matrix. It is strongly pleochroic from shades of green to brown. Some anhedral porphyroblastic olivine crystals are strained while other small acicular grains are strain-free and euhedral to subhedral. These are common features of recrystallised olivine.Prismatic crystals of anthophyllite exhibit parallel extinction within the radiating matrix of talc (Fig 4.71 and Fig 4.72). Tremolite occurs as fibrous aggregates and rosettes around fine-grained matrix of flaky talc. Actinolite areobserved as spindle-like crystals alongside tremolite.

Serpentine minerals present include antigorite, amesite and small amount of chrysotile (Fig. 4.71 and 4.72).Altered Cr-spinel (ferritchromite), magnetite and sulphides occur as opaque minerals.Antigorite occurs as collapsed, dark mesh-like structure defining a continuous dark band around relict olivine. Pods and lenses of Cr-spinel in the parent rock have been altered to ferritchromite and magnetite in the talc schists. This ferritchromite occurs as common accessory mineral in all the talc samples with a range of 1-3 %.

Fig. 4.69: Field photograph of talc schist at Wonu, Ibadan-Apomu area.

Fig. 4.70: A talcose rock mining site at Wonu, Ibadan-Apomu area.

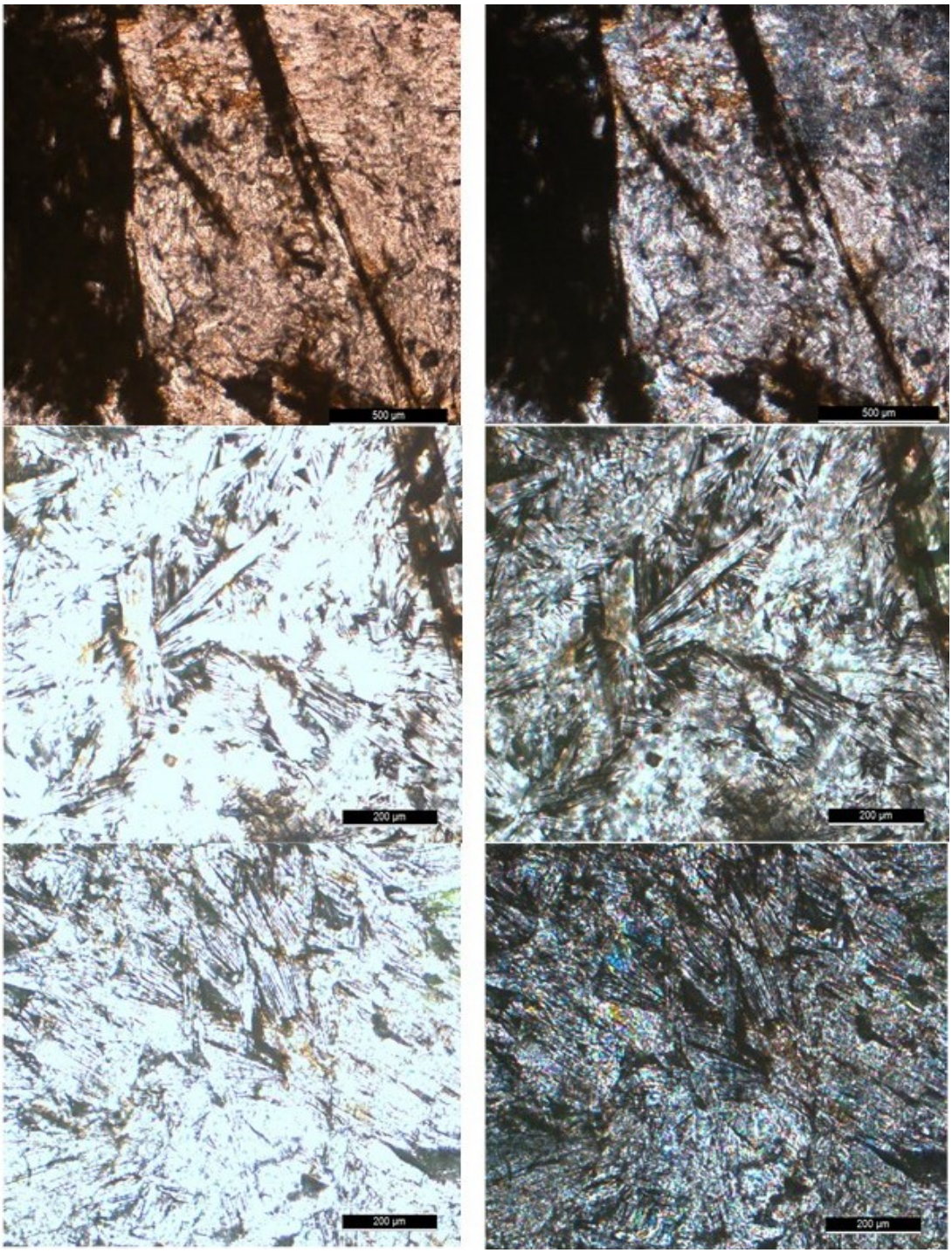

Fig. 4.71: Photomicrograph of talc schist from Wonu, Ibadan-Apomu area showing olivine and pyroxene alteration to antigorite/chrysotile, tremolite - asbestos (top) and talc-chlorite (bottom). Note the complete replacement of original matrix mass by antigorite (± chlorite) on the left. Under one direction polarization of light (left) and cross-polarised light (right).

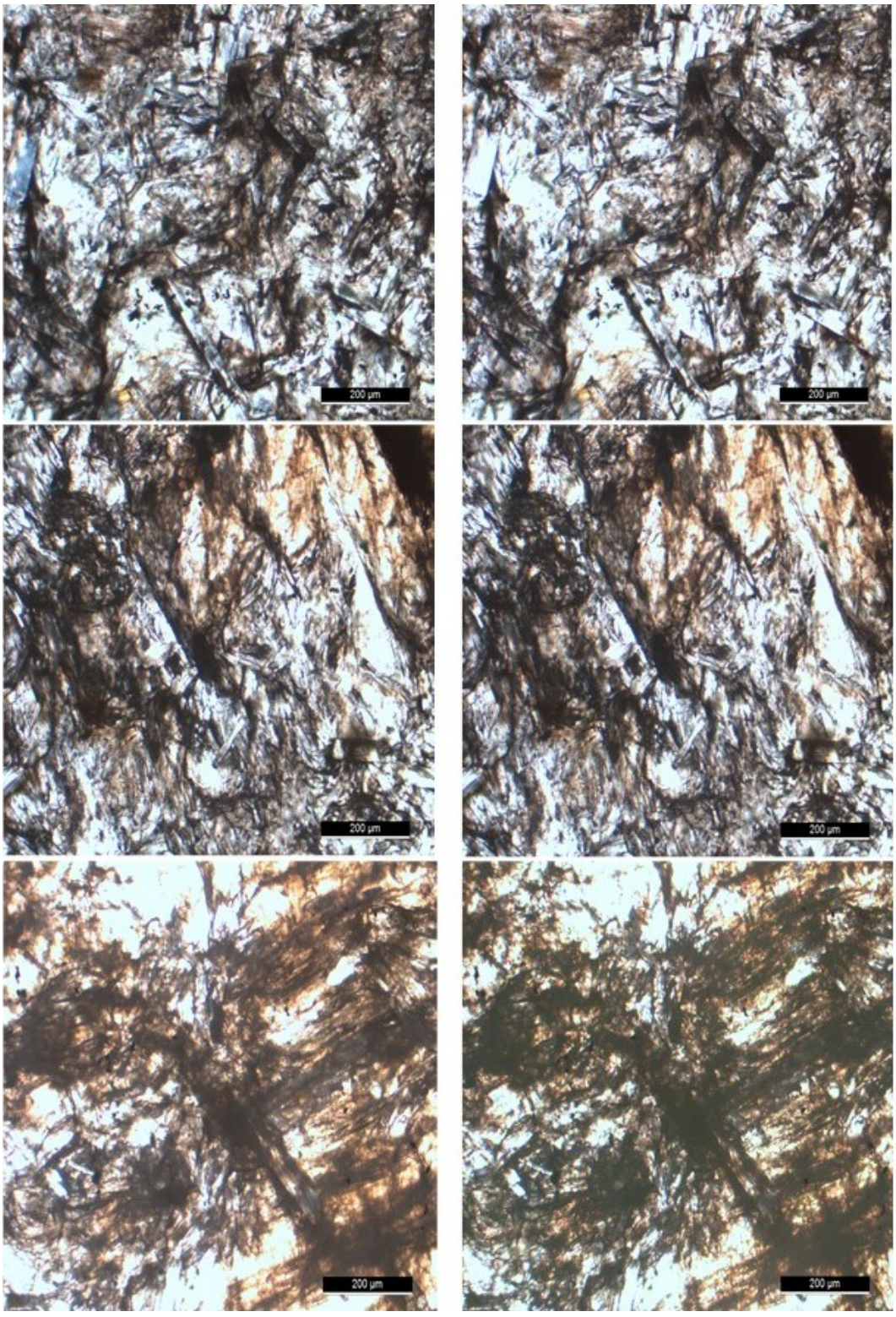

Fig. 4.72: Photomicrograph of talc schist from Wonu, Ibadan-Apomu area showing olivine and pyroxene alteration to talc-chlorite-antigorite/chrysotile-tremolite schist (top) and serpentinized (black-mesh) talc (bottom) in plane-polarized of light and cross-polarized light.

Table 4.30: Modal composition (vol.%) of minerals in talc schist from Wonu, Ibadan-Apomu area from petrography, SEM, XRD and EMPA

Minerals	1	2	3	4	5	6	7	8	9	Average
Talc	50	52	51	44	46	60	50	65	60	61
Talc-chlorite	18	20	20	25	26	18	23	16	20	22
Saponite/Diabantite	10	12	11	5	5	10	12	9	10	10
Anthophyllite	8	8	10	10	10	7	9	3	-	-
Tremolite/Actinolite	3	3	2	9	8	2	1	2	5	2
Ferritchromite	5	2	3	3	1	1	2	3	2	2
Magnetite	3	2	3	2	1	1	2	1	2	2
Antigorite/Chrysotile	3	1	1	2	1	1	1	1	1	1
Total	100	100	100	100	100	100	100	100	100	100

4.3.3.2 SEM-EDS Images of the Talc Schist

The SEM-EDS of talc schist from Wonu, Ibadan-Apomu area showed the presence of olivine (forsterite) and ferritchromite (Spectrum 2)(Fig. 4.73). White ferritchromite inclusions occur within the altered olivine crystals. Needle-like antigorite and flames of nickel sulphide (NiS) were observed in some samples (Fig. 4.74). As shown in (Fig. 4.74) the talc schist showed different stages of hydrothermal alteration of olivine (forsterite) (Spectrums 12, 13 and 14), releasing Nickel (Spectrum 12 and 14) to form pentlandite and Ca to form secondary $CaCO_3$ (Spectrum 12 and 13). The hydrothermal fluid is probably more of magmatic source given the presence of H_2O, CO_2, F and Irasite (Fig. 4.74). Plates of talc schist with tremolite, serpentine (antigorite/chrysotile) and nickel sulphide (NiS) are conspicuously displayed in the SEM of the Wonu, Ibadan-Apomu area (Fig. 4.75).The SEM-EDS of the talc schist showed manganese-bearing ferrichromite in aluminosilicate matrix (Spectrum 16), some unaltered olivine (Forsterite) (Spectrum 17), in graphite-bearing chloritic groundmass (Fig. 4.76).

Chromite is ubiquitous accessory mineral in all the talc samples with an average mode of 1-3 %. Pods and lenses of chromite are aligned, revealing foliation in the talc schist. Ferritchromite occurs as distinct and highly reflective rim around chromite with or without, an outer rim of magnetite. The boundary between chromite and ferritchromite is commonly sharp, just as the boundary between ferritchromite and magnetite.

The SEM-EDS of talc schist from Ibadan-Apomu area showed the presence of magmatic fluid rich in allanite (Spectrum 1) and monazite (Spectrum 2),which altered olivine (Forsterite) (Spectrum 3) and pyroxenes to produce amesite, chlorite, diabantite, saponite, tremolite, actinolite, anthophyllite, ferritchromite, magnetite and secondary carbonate (Fig. 4.77). The pervasive nature of the fluid was observed in the almost complete destruction of the olivines, pyroxenes and other primary minerals and replacement with REE-bearing minerals, such as, monazite and allanite. This led to the enrichment of the ultramafic rocks of dunitic composition with REEs, as reported in the whole-rock geochemistry. The petrography and SEM clearly showed the possibility of two parent sources for the talc bodies. The talc-rich purer variety with extensive carbonates might be sourced from the metasedimentary schist, while those with higher impurities are probably derived from the alteration of the Fe-rich tholeiitic and komatitic rocks.

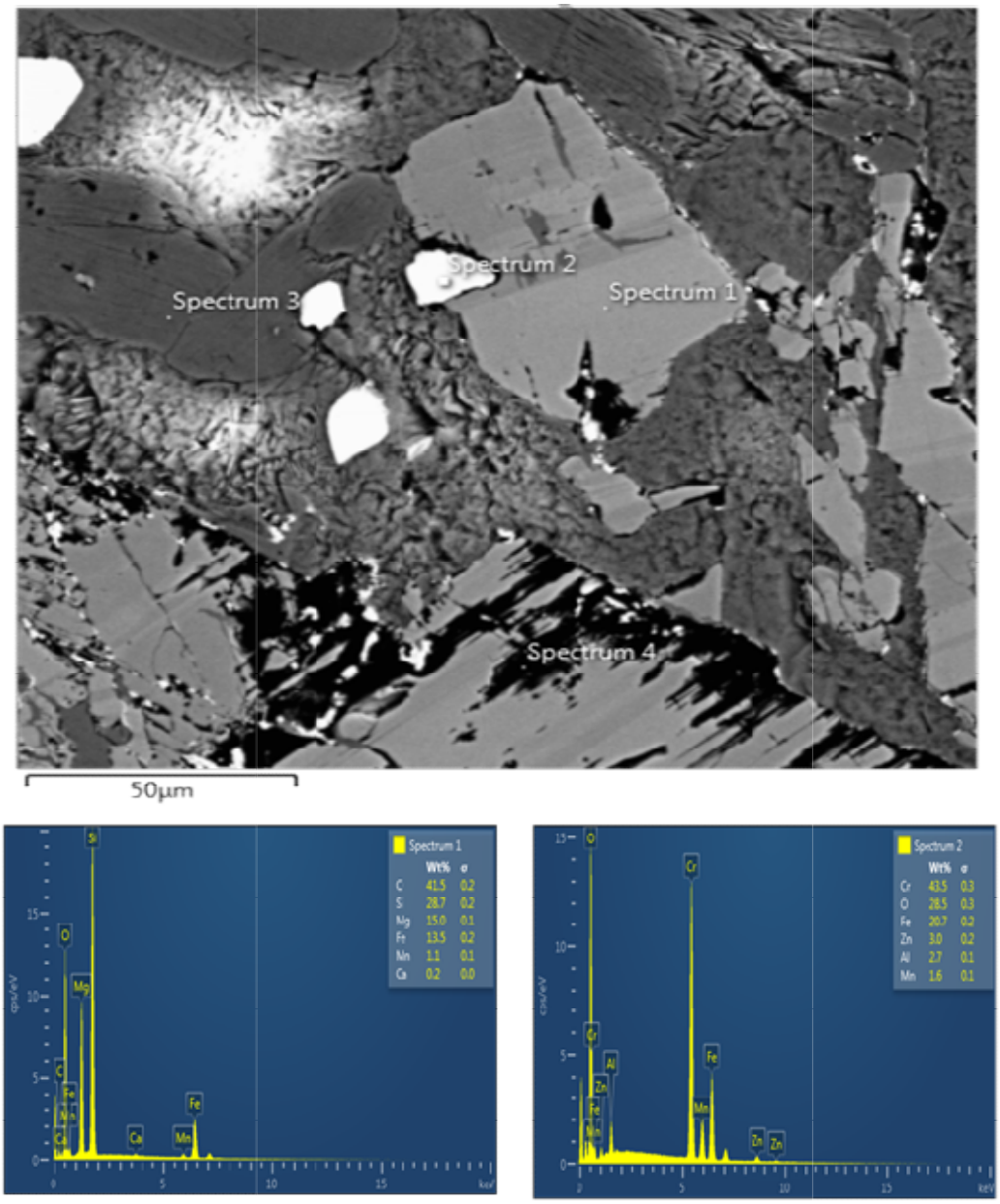

Fig. 4.73: SEM-EDS of talc schist from Wonu, Ibadan-Apomu area showing olivine (Forsterite) (Spectrum 1), Ferritchromite (Spectrum 2), olivine (Forsterite).

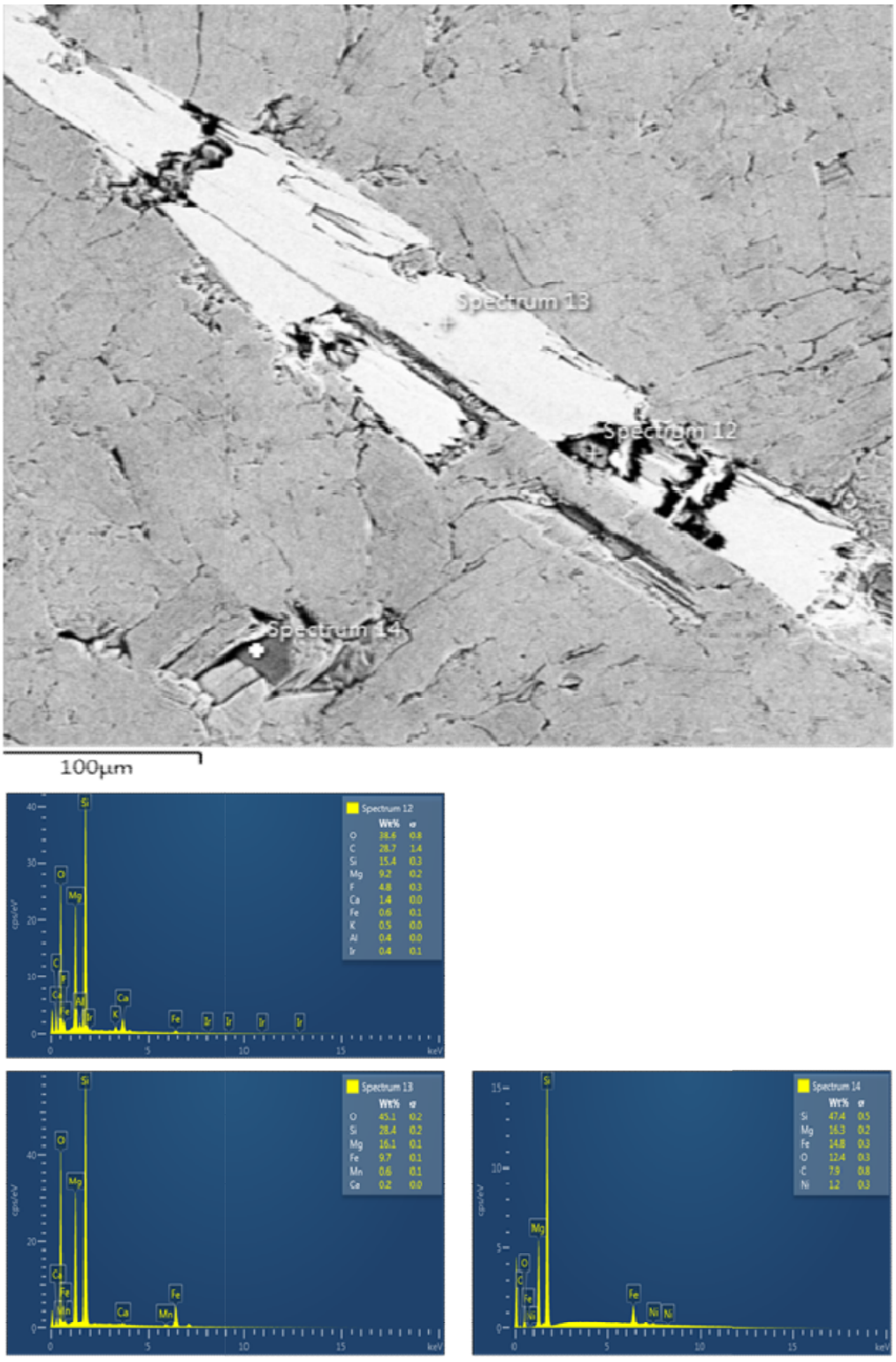

Fig. 4.74: SEM-EDS of talc schist from Wonu, Ibadan-Apomu area showing different stages of hydrothermal (H_2O-CO_2-F) altered olivine (forsterite) (Spectrums 12, 13 and 14), releasing Irasite and Nickel (Spectrum 12 and 14), and Ca to form secondary $CaCO_3$(Spectrum 12 and 13).

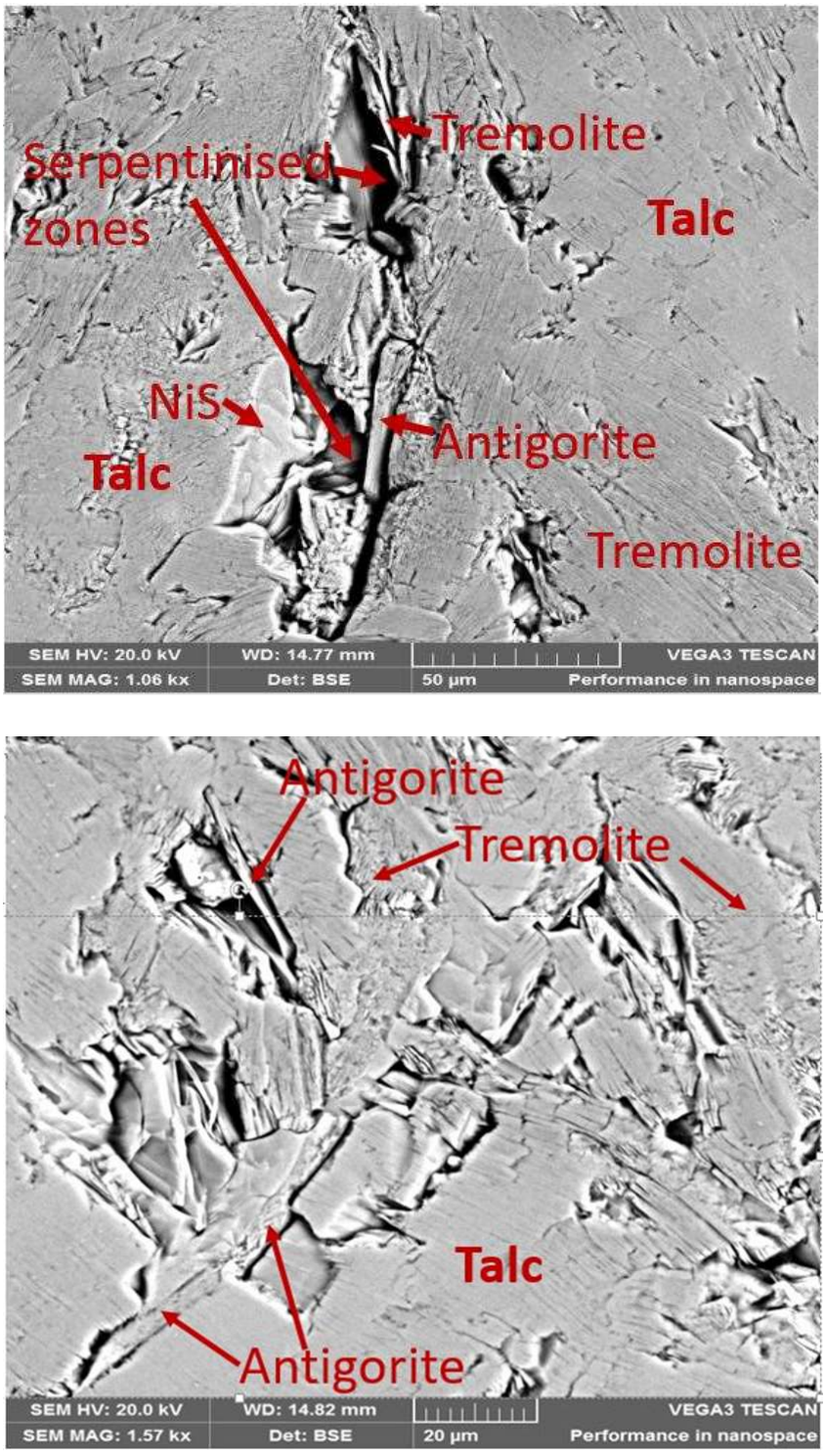

Fig. 4.75: Plates of talc schist with tremolite, serpentine (antigorite/chrysotile)and nickel sulphide (NiS) in the Wonu, Ibadan-Apomu area.

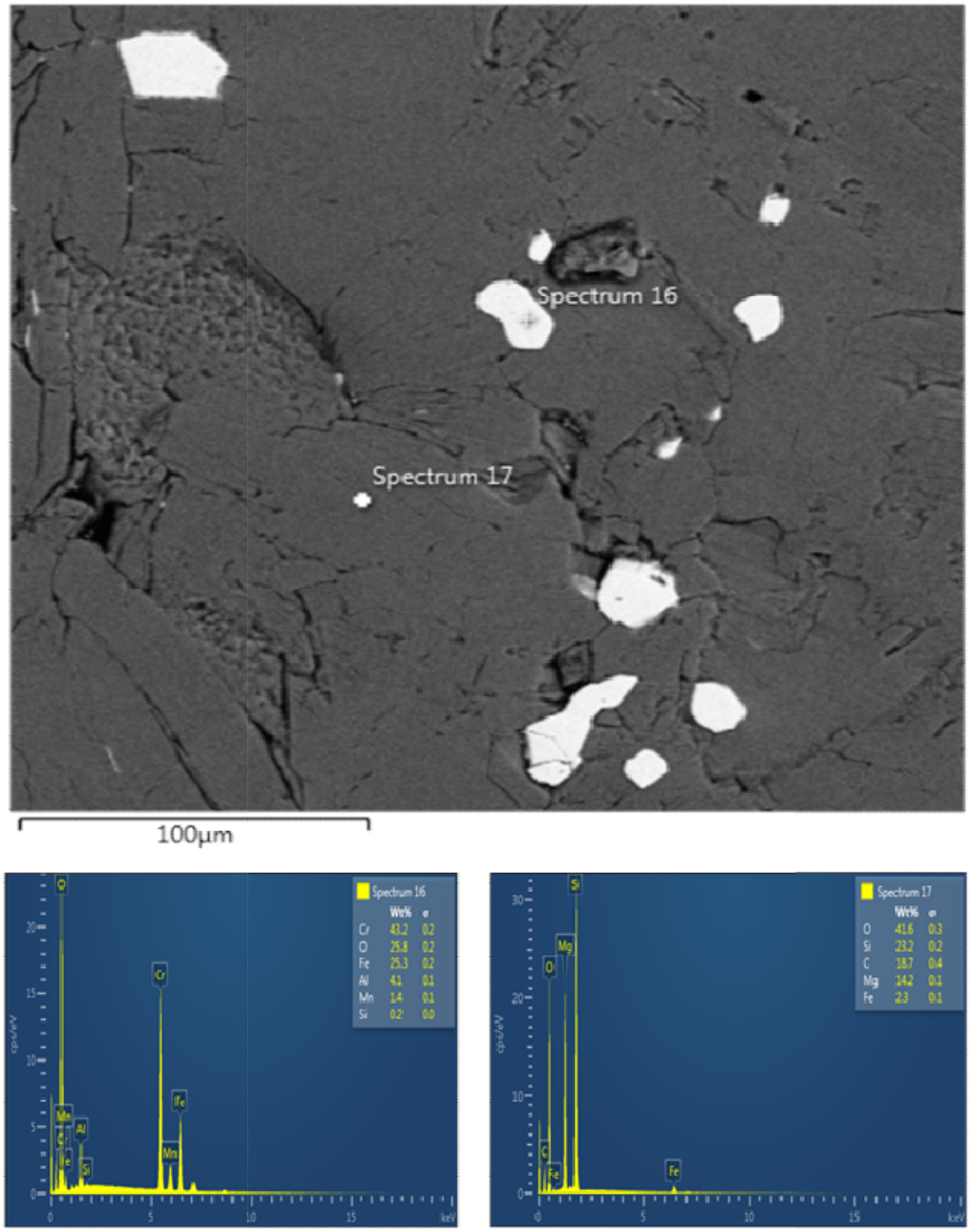

Fig. 4.76:SEM-EDS of talc schist from Wonu, Ibadan-Apomu area showing manganese-bearing ferrichromite in aluminosilicate matrix (Spectrum 16), unaltered olivine (Forsterite) (Spectrum 17), in graphite-bearingchloritic groundmass.

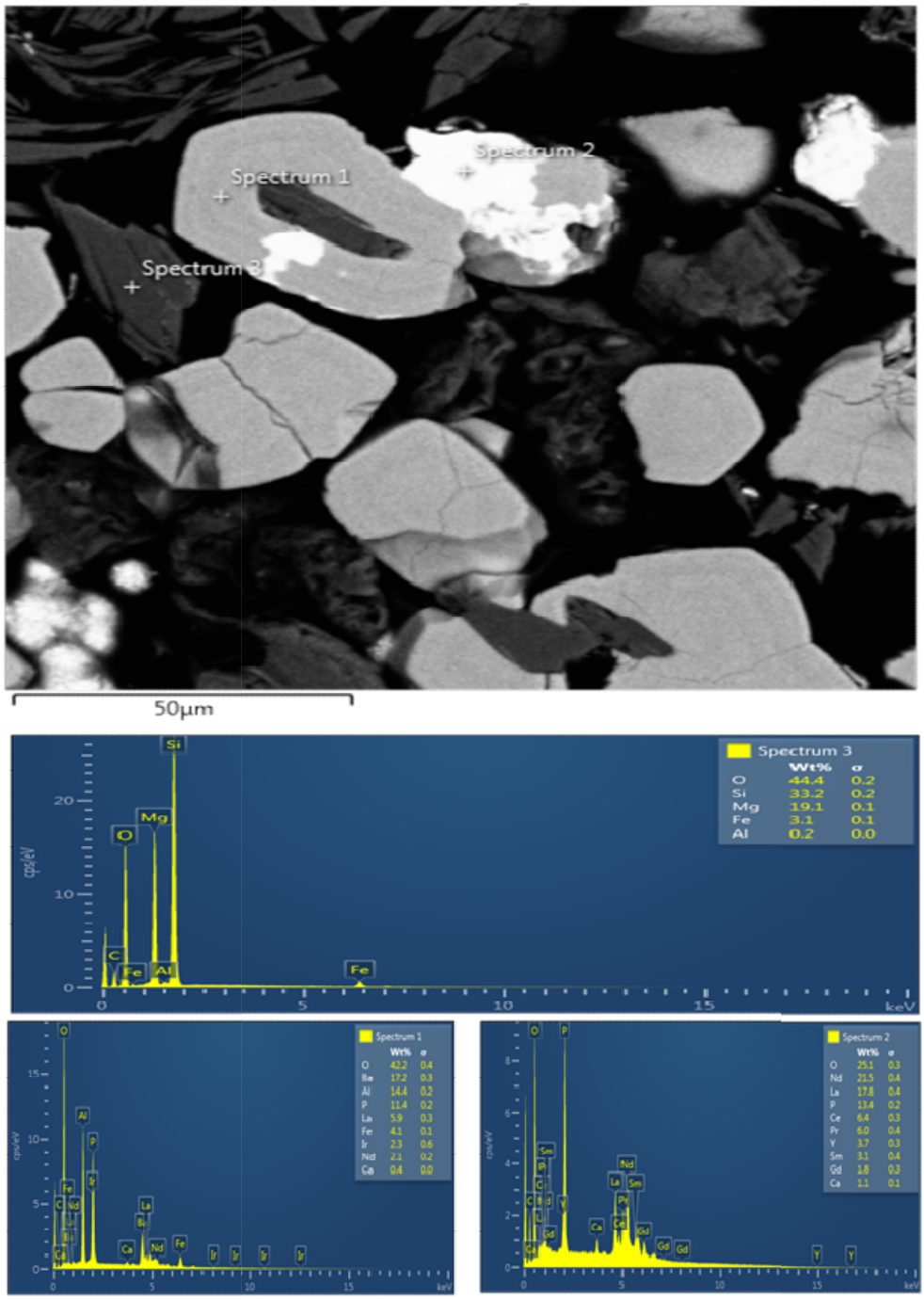

Fig. 4.77: SEM-EDS of talc schist from Wonu, Ibadan-Apomu area showing allanite (Spectrum 1), monazite (Spectrum 2), altered olivine (Forsterite) (Spectrum 3) and secondary carbonate.

4.3.3.3 Mineral identification of talc by XRD

The X-ray diffraction patterns of the talc schists in Wonu, Ibadan-Apomu area are presented in Tables 4.31 to 4.32; and Figs. 4.79 to Fig. 4.80.Minerals identified include talc, amesite, chlorite (clinochlore), saponite, anthophyllite, serpentinite and quartz.

Talc was identified at 9.33,3.11, 1.87, and 1.56Å. (Figs. 4.78 to Fig. 4.80). Saponite, a trioctahedral mineral of the smectite group, was identified at 18.51 and 18.61 Å. It is a soft, plastic soapstone derived from serpentinised olivine and pyroxene that formed talc(Fig. 4.72). Anthophyllite peaks occur at 3.22 and 8.25 Å, and with peaks denoted as pyrophylliteat 3.04, 4.50 and 4.67Å.

Chlorite, mainly clinochlore was identified at 14.22, 7.11, 4.75, 3.56 and 2.74 Å. Chlorite is a hydrous silicate of aluminum, iron and magnesium (Mg, $Fe)_5Al(AlSi_3)O_{10}(OH)_9$ while clinochlore with chemical composition $(Mg,Fe, Al)_6$ $(Si,Cr)O_{10}$ $(OH)_8$ is a monoclinic crystal, whichis distinctly biaxial and optically positive as earlier observed under the petrological microscope. The chromium-bearing clinochlore was abundant in the talc schist, with composition of between 16-26%. This is responsible for the greenish colour of the samples. The broad regions on the X-ray traces between 6.20 to 7.63 Å is serpentine, ferritchromite and magnetite. Quartz was identified at 2.59 Å (Fig. 4.78 and 4.79). Saponite and serpentine are however not present in the XRD in Fig. 4.80.

Anthophyllite is an orthorhombic amphibole while tremolite is a monoclinic amphibole. Anthophyllite is stable only at low temperature. When heated to about 400^oC, it may alter to a monoclinic amphibole, such as, tremolite or actinolite. The heat for the conversion of the anthophyllite to tremolite might have been provided by the granitic intrusives around the talc bodies.

Though the overall mineralogical data based on peak height of the XRD did not totally agree with the modal composition on Table 4.30, they are however similar. I estimated that the talc samples are composed of about 50% talc, 20 % chlorite, 10 % anthophyllite and pyrophyllite, 7 % saponite, 5 % serpentineand quartz 2 % (Table 4.30). The XRD of the talcose rock of Wonu, Ibadan-Apomu area are of two typesbased on the mineralogical composition. The XRD of the sample in Fig. 4.78 possess the highest impurities while those in Fig. 4.80 has the least indicating possible derivation of the former from mafic-ultramafic and the later from lenses of metacarbonates.

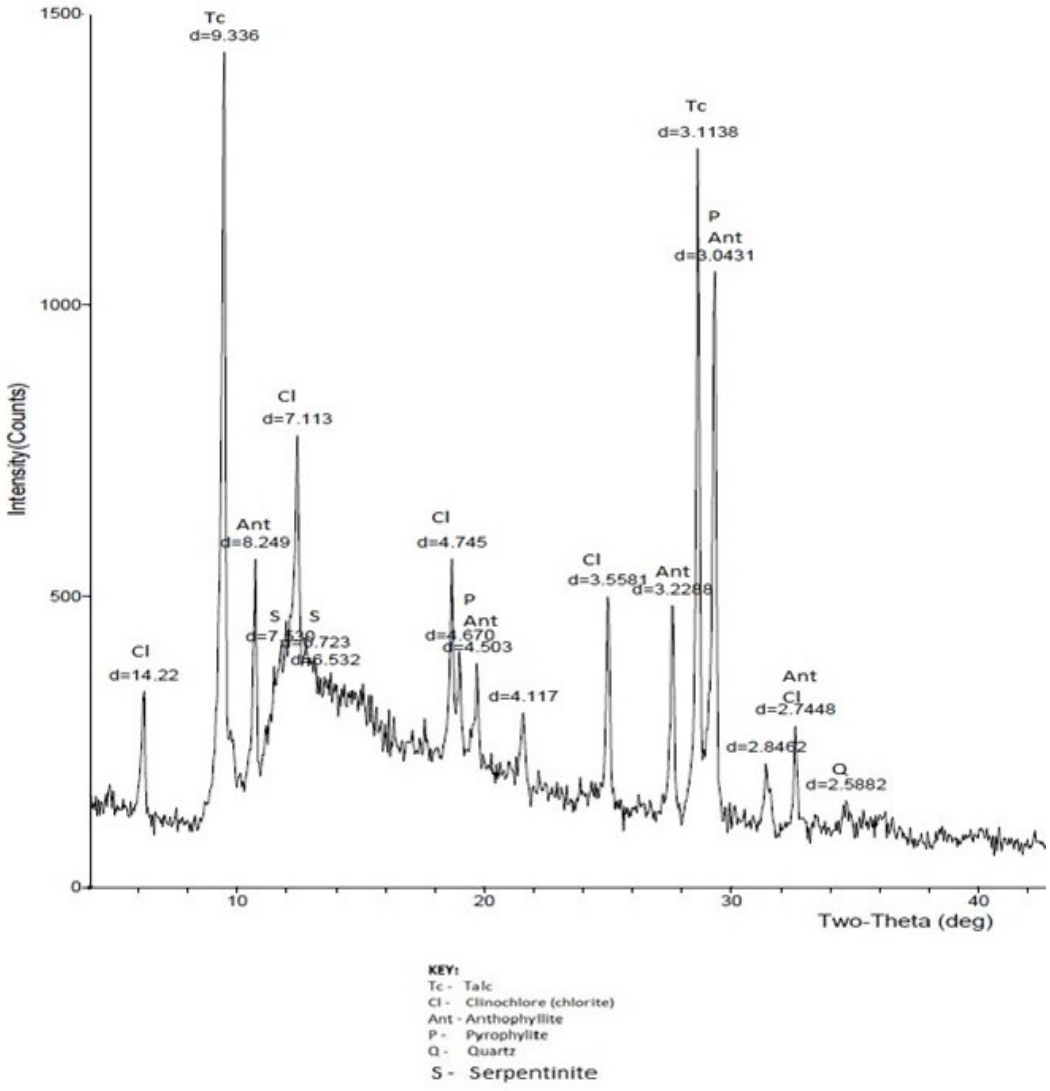

Fig. 4.78: X-ray diffraction patterns of the serpentinised talcoce rocks from Wonu, Ibadan-Apomu area.

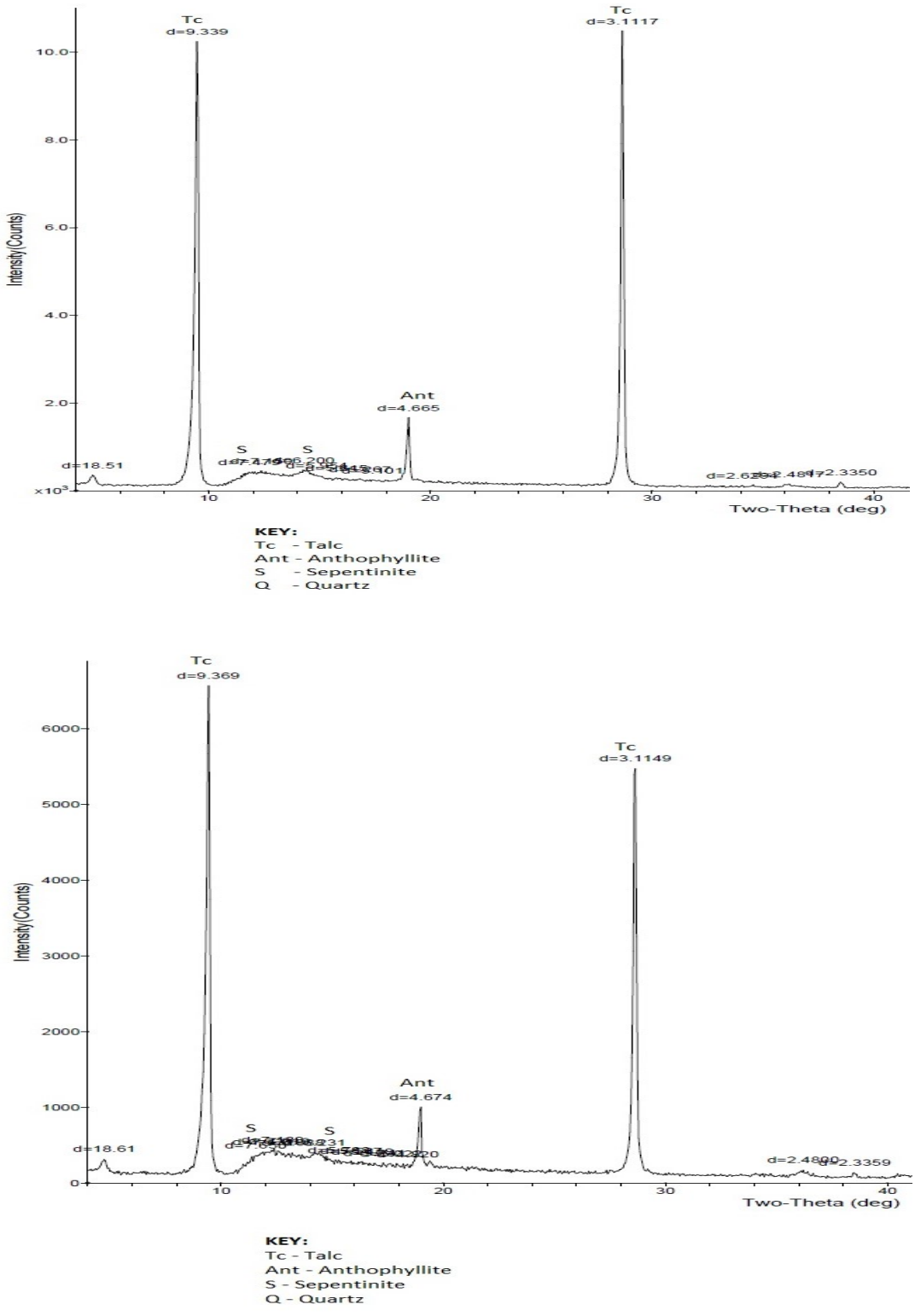

Fig. 4.79: X-ray diffraction patterns of the serpentinised talcose rocks from Wonu, Ibadan-Apomu area.

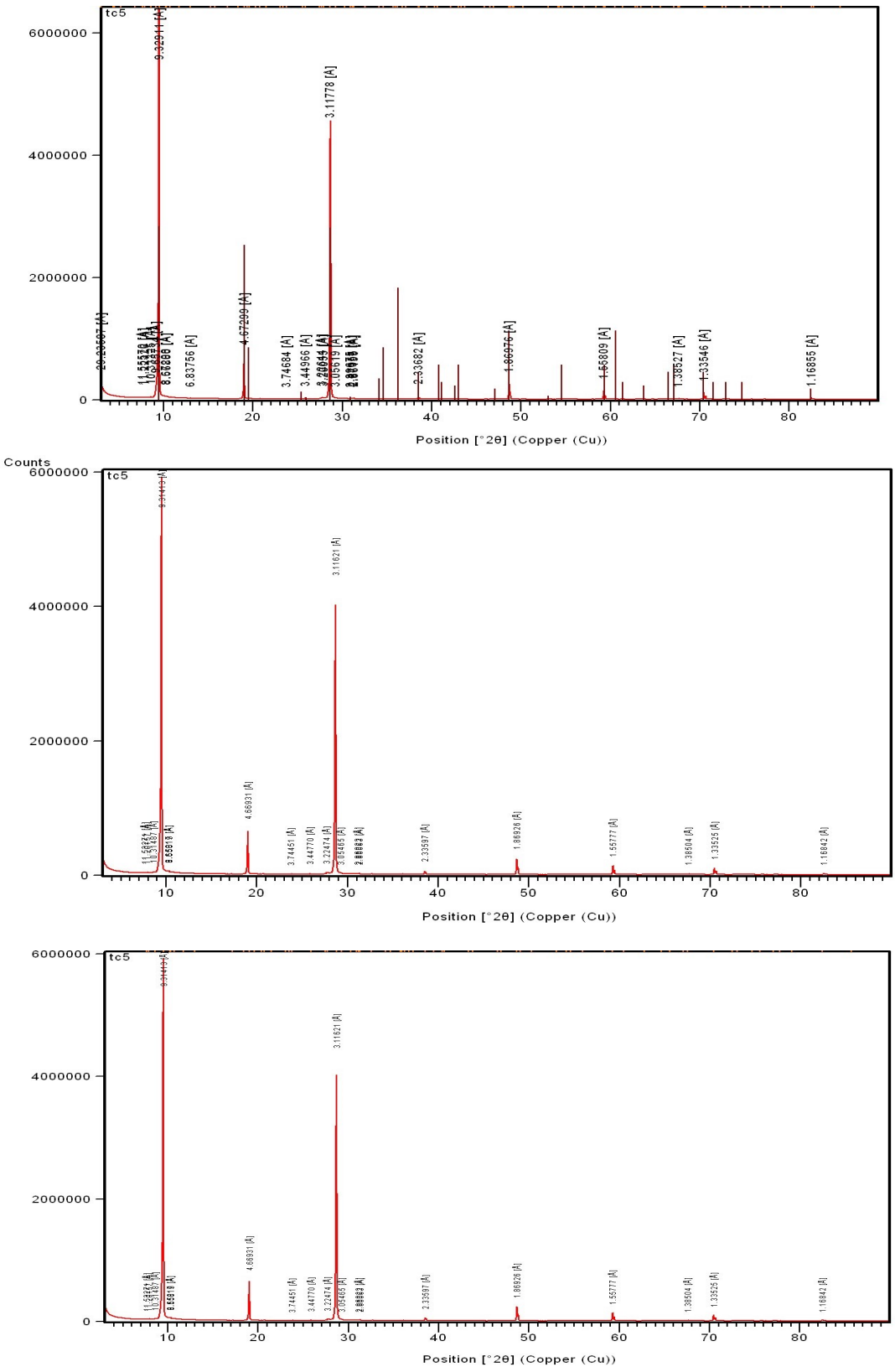

Fig. 4.80: X-ray diffraction patterns of the talc rocks from Wonu, Ibadan-Apomu area.

4.3.3.4 Mineral Chemistry of the Talc Schist

The mineral chemistry of talc, saponite and ferritchromite in the talc schist of Wonu, Ibadan-Apomu area are discussed in this section because of their importance in the determination of the genesis, evolution and tectonic setting of the talc bodies. Other minerals present such as olivine, chlorite, serpentine (antigorite and chrysotile are also discussed due to their geodynamic importance.

Olivine

The olivine in the talc schist of Wonu, Ibadan-Apomu area is mainly fosterite as observed in the SEM. Olivine-spinel geothermometry is usually 700-750 ºC. Olivine is not stable below 620 ºC in the presence of water hence olivine and Cr-spinel only occurred as altered accessory mineral in the talc schist.Olivine was not subjected to microprobe studies.Estimation of the mineral chemistry was carried out using the SEM-EDS data of partially altered olivine (Fig. 4.77).

Talc-chlorite-saponite

Representative mineral chemistry of the talc schist of Wonu, Ibadan-Apomu are presented in Table 4.31a and b. More detailed results of the talc are in the appendix. The talc composition ranged from pure talc to talc-chlorite, talc-chlorite-saponite and talc-chlorite-saponite-antigorite-chrysotile.

Two major groups of talc schists are distinguished. They are, the talc-chloritewith FeO of 2.86-4.69 wt.%; $Mg/(Mg+Fe_{total})$ of 0.92-0.95 (Table 4.31a-e) and the second one which is the talc-magnesian saponite with FeO of 11.51-14.01 wt.%; $Mg/(Mg+Fe_{total})$ of 0.77-0.79 (Table 4.32). The structural formula of saponite calculated for sample TC4/28 is: $Ca_{0.5}(Mg_{4.8}Fe_{1.2})Si_8O_{22}(OH)_4$.The low TiO_2 content of the talc and saponite (0.00-0.02 wt%) (Tables 4.31 and 4.32) are characteristic ofdunite-type magma. The talc bodies are associated with pyrrhotite, pentlandite and chromite ores.

Table 4.31(a): Mineral chemistry of talc sample TC3 of Wonu, Ibadan-Apomu area

	TC3/1	TC3/2	TC3/3	TC3/4	TC3/5	TC3/6	TC3/7	TC3/8	TC3/9	TC3/10
SiO_2	61.25	62.69	62.26	61.21	62.36	60.98	60.55	61.22	62.13	63.30
TiO_2	0.01	0.02	0.01	0.00	0.01	0.02	0.02	0.00	0.01	0.00
Al_2O_3	0.35	0.32	0.38	0.32	0.30	0.38	0.41	0.36	0.29	0.38
FeO	3.21	3.29	3.21	3.17	3.23	3.22	3.13	3.17	3.23	3.12
MnO	0.03	0.02	0.02	0.02	0.02	0.02	0.03	0.02	0.03	0.02
MgO	27.92	28.48	26.72	28.14	28.77	29.90	28.99	28.12	27.38	27.93
CaO	0.04	0.00	0.02	0.03	0.01	0.01	0.01	0.03	0.02	0.00
Na_2O	0.04	0.04	0.03	0.04	0.04	0.04	0.04	0.05	0.01	0.03
K_2O	0.04	0.00	0.03	0.02	0.00	0.00	0.01	0.05	0.02	0.00
Cr_2O_3	0.07	0.07	0.09	0.07	0.09	0.08	0.11	0.08	0.09	0.11
NiO	0.21	0.22	0.22	0.22	0.24	0.21	0.22	0.2	0.22	0.18
H_2O	4.57	4.67	4.58	4.58	4.67	4.64	4.58	4.58	4.60	4.68
Total	97.74	99.82	97.57	97.82	99.74	99.50	98.10	97.88	98.03	99.75
	Formula units based on 22 $(O, OH)_2$)									
Si	8.029	8.042	8.149	8.018	8.013	7.880	7.926	8.015	8.104	8.104
Al iv	0.000	0.000	0.000	0.000	0.000	0.058	0.063	0.000	0.000	0.000
Al vi	0.054	0.048	0.059	0.049	0.045	0.000	0.000	0.056	0.045	0.057
Ti	0.001	0.002	0.001	0.000	0.001	0.002	0.002	0.000	0.001	0.000
Cr	0.007	0.007	0.009	0.007	0.009	0.008	0.011	0.008	0.009	0.011
Fe	0.352	0.353	0.351	0.347	0.347	0.348	0.343	0.347	0.352	0.334
Mn	0.003	0.002	0.002	0.002	0.002	0.002	0.003	0.002	0.003	0.002
Mg	5.456	5.446	5.213	5.495	5.511	5.759	5.657	5.488	5.324	5.330
Ni	0.022	0.023	0.023	0.023	0.025	0.022	0.023	0.021	0.023	0.019
Ca	0.006	0.000	0.003	0.004	0.001	0.001	0.001	0.004	0.003	0.000
Na	0.010	0.010	0.008	0.010	0.010	0.010	0.010	0.013	0.003	0.007
K	0.007	0.000	0.005	0.003	0.000	0.000	0.002	0.008	0.003	0.000
OH*	4.000	4.000	4.000	4.000	4.000	4.000	4.000	4.000	4.000	4.000
TOTAL	17.947	17.933	17.823	17.960	17.964	18.090	18.041	17.963	17.871	17.865
Y total	5.896	5.881	5.659	5.924	5.940	6.142	6.039	5.923	5.758	5.754
X total	0.022	0.010	0.015	0.018	0.011	0.011	0.013	0.025	0.009	0.007
Al total	0.054	0.048	0.059	0.049	0.045	0.058	0.063	0.056	0.045	0.057
Fe/Fe+Mg	0.061	0.061	0.063	0.059	0.059	0.057	0.057	0.059	0.062	0.059

Table 4.31(b): Mineral chemistry of talc sample TC4 of Wonu, Ibadan-Apomu area

	TC4/1	TC4/2	TC4/3	TC4/4	TC4/5	TC4/6	TC4/7	TC4/8	TC4/9	TC4/10
SiO_2	60.87	61.29	61.36	59.51	63.50	62.95	61.99	63.50	62.93	63.93
TiO_2	0.00	0.02	0.00	0.01	0.02	0.00	0.01	0.01	0.00	0.00
Al_2O_3	1.62	0.36	0.34	0.33	0.35	0.24	0.39	0.36	0.08	0.31
FeO	3.26	3.19	3.30	3.31	3.37	3.25	3.23	3.25	3.13	3.27
MnO	0.02	0.02	0.03	0.02	0.02	0.02	0.03	0.02	0.01	0.02
MgO	26.58	28.23	28.36	30.95	25.37	28.60	28.10	27.88	29.16	26.77
CaO	0.00	0.02	0.01	0.00	0.01	0.00	0.03	0.01	0.00	0.01
Na_2O	0.03	0.04	0.04	0.04	0.04	0.02	0.03	0.03	0.01	0.03
K_2O	0.01	0.01	0.00	0.01	0.01	0.00	0.01	0.00	0.00	0.01
Cr_2O_3	0.06	0.1	0.06	0.08	0.08	0.05	0.11	0.06	0.01	0.08
NiO	0.26	0.25	0.28	0.26	0.27	0.26	0.28	0.25	0.27	0.28
H_2O	4.56	4.59	4.60	4.60	4.60	4.69	4.63	4.70	4.70	4.67
Total	97.27	98.12	98.38	99.12	97.64	100.08	98.84	100.07	100.30	99.38
	Formula units based on 22 (O, $OH)_2$)									
Si	8.005	8.007	8.001	7.752	8.282	8.053	8.035	8.110	8.034	8.204
Al iv	0.000	0.000	0.000	0.051	0.000	0.000	0.000	0.000	0.000	0.000
Al vi	0.251	0.055	0.052	0.000	0.054	0.036	0.060	0.054	0.012	0.047
Ti	0.000	0.002	0.000	0.001	0.002	0.000	0.001	0.001	0.000	0.000
Cr	0.006	0.010	0.006	0.008	0.008	0.005	0.011	0.006	0.001	0.008
Fe	0.359	0.349	0.360	0.361	0.368	0.348	0.350	0.347	0.334	0.351
Mn	0.002	0.002	0.003	0.002	0.002	0.002	0.003	0.002	0.001	0.002
Mg	5.211	5.498	5.512	6.010	4.933	5.454	5.430	5.308	5.549	5.121
Ni	0.028	0.026	0.029	0.027	0.028	0.027	0.029	0.026	0.028	0.029
Ca	0.000	0.003	0.001	0.000	0.001	0.000	0.004	0.001	0.000	0.001
Na	0.008	0.010	0.010	0.010	0.010	0.005	0.008	0.007	0.002	0.007
K	0.002	0.002	0.000	0.002	0.002	0.000	0.002	0.000	0.000	0.002
OH*	4.000	4.000	4.000	4.000	4.000	4.000	4.000	4.000	4.000	4.000
TOTAL	17.871	17.964	17.975	18.224	17.691	17.929	17.933	17.863	17.961	17.773
Y total	5.856	5.942	5.963	6.409	5.395	5.872	5.884	5.744	5.925	5.558
X total	0.009	0.015	0.012	0.012	0.013	0.005	0.013	0.009	0.002	0.010
Al total	0.251	0.055	0.052	0.051	0.054	0.036	0.060	0.054	0.012	0.047
Fe/Fe+Mg	0.064	0.060	0.061	0.057	0.069	0.060	0.061	0.061	0.057	0.064

Table 4.32: Mineral chemistry of saponite in the talc samples of Wonu, Ibadan-Apomu area

	TC4/27	TC4/30	TC4/33	TC3/20	TC4/28	TC4/29	TC3/30
SiO_2	57.23	55.29	55.80	52.75	58.68	53.18	55.25
TiO_2	0.01	0.00	0.10	0.00	0.00	0.01	0.01
Al_2O_3	0.22	0.47	1.85	0.20	0.26	0.37	12.35
FeO	14.01	12.70	12.91	3.14	11.51	4.69	3.26
MnO	0.89	0.82	0.55	0.01	0.75	0.02	0.02
MgO	26.61	25.11	27.49	31.75	24.29	29.37	17.68
CaO	0.43	0.36	0.23	0.01	0.37	0.00	0.06
Na_2O	0.03	0.06	0.06	0.02	0.02	0.02	0.06
K_2O	0.00	0.01	0.00	0.00	0.00	0.00	0.16
Cr_2O_3	0.08	0.05	0.06	0.04	0.06	0.04	0.04
NiO	0.12	0.15	0.15	0.23	0.16	0.19	0.16
H_2O*	0.00	4.38	0.00	4.25	4.49	4.22	4.41
Total	99.63	99.40	99.20	92.40	100.59	92.11	93.46
Formula units based on 22(O, OH)							
Si	7.509	7.565	7.318	7.435	7.828	7.550	7.510
Al iv	0.034	0.076	0.286	0.033	0.041	0.062	0.490
Al vi	0.000	0.000	0.000	0.000	0.000	0.000	1.489
Ti	0.001	0.000	0.010	0.000	0.000	0.001	0.001
Cr	0.008	0.005	0.006	0.004	0.006	0.004	0.004
Fe	1.537	1.453	1.416	0.370	1.284	0.557	0.371
Mn	0.099	0.095	0.061	0.001	0.085	0.002	0.002
Mg	5.204	5.122	5.374	6.671	4.831	6.215	3.582
Ni	0.013	0.017	0.016	0.026	0.017	0.022	0.017
Ca	0.060	0.053	0.032	0.002	0.053	0.000	0.009
Na	0.008	0.016	0.015	0.005	0.005	0.006	0.016
K	0.000	0.002	0.000	0.000	0.000	0.000	0.028
OH*	4.000	4.000	4.000	4.000	4.000	4.000	4.000
Total	18.473	18.403	18.534	18.549	18.151	18.419	17.519
Y total	6.862	6.692	6.883	7.073	6.223	6.802	5.467
X total	0.068	0.070	0.048	0.007	0.058	0.006	0.052
Al total	0.034	0.076	0.286	0.033	0.041	0.062	1.979
Fe/Fe+Mg	0.228	0.221	0.209	0.053	0.210	0.082	0.094
Luhr *et al*. 1984	811.2	810.7	816.2	810.7	810.7	812.2	812.8

A plot of the amesite, saponite and talc and saponite composition on the triangular diagram of Alt *et al.* (1998) and Nimis *et al.* (2004) (Fig. 4.81) showed gradual decrease in MgO content from amesite to talc through Mg-saponite (Fig. 4.81).The chemistry of the Mg-saponite and talc in the talc schist of Wonu, Ibadan-Apomu area (Fig. 4.82) showed that they are ore associated saponites and olivine and pyroxene associated saponites derived from hydrothermal alteration of ultramafic rocks. As shown in Fig. 4.83 the talc bodies vary from talc-chlorite to diabantite, which is also a variety of chlorite. The plot of amesite of the lherzolite on this same diagram of Hey (1954), showed that the talc bodies are probably products of hydrothermal upflow-zones similar to those of Izu-Bonin (Fig. 4.83).

Several deformation episodes affected the dunitic and peridotitic rocks in this area as observed on the field during field mapping and the geological map produced. In this type of polymetamorphic setting, chlorites could be formed in two different situations. Those that syn-crystallised with amphiboles as pseudomorphs of clinopyroxenes and orthopyroxenes, that is, formed contemporaneously with amphiboles at temperatures below 500 ºC, and those that grew after spinel. Their relative high degree of tschermakite substitution indicates conditions of retrograde amphibolite to greenschist facies metasomatism corresponding to greenschist facies and temperature of about 500 ºC.

$$2NaCa_2Mg_4AlA_{l2}Si_6O_{22}(OH)_2 + 8SiO_2 = CaMg_5Si_8O_{22}(OH)_2 + Ca_2Mg_3Al_2Al_2SiO_6O_{22}(OH)_2 + 2NaAlSi_3O_8$$

Pargasite Quartz Tremolite Tschermakite Albite

Primary minerals in the amphibolite and lherzolite, notably olivine, pyroxene, amphibole and Cr-spinel are altered to chlorite, saponite, talc and serpentine. Antigorite is formed from olivine while talc is formed from orthopyroxene. The presence of greenschist hornblendes, tremolites and actinolites indicated that hydrous episodes are responsible for the serpentinisation of the peridotite (Agrinier *et al.,* 1993). Deformation episodes led to shearing of rocks and provision of permeable zones. Occurrence of tremolites are related to these fracturing events. A few tremolites have a characteristic outwardform within clinopyroxenes with chemical composition identical with those formed from hydrous fluids with which they are contemporaneous.

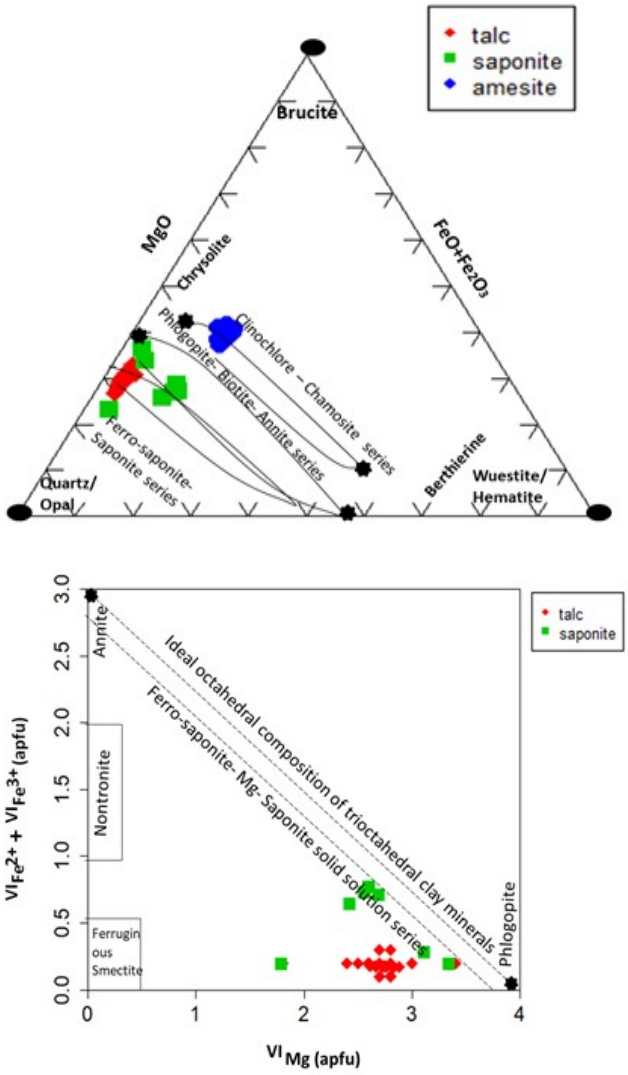

Fig. 4.81: Mineral chemistry of the chlorite, Mg-saponite and talc within altered lherzolite ofWonu, Ibadan-Apomu area (after Nimis*et al.* 2004).

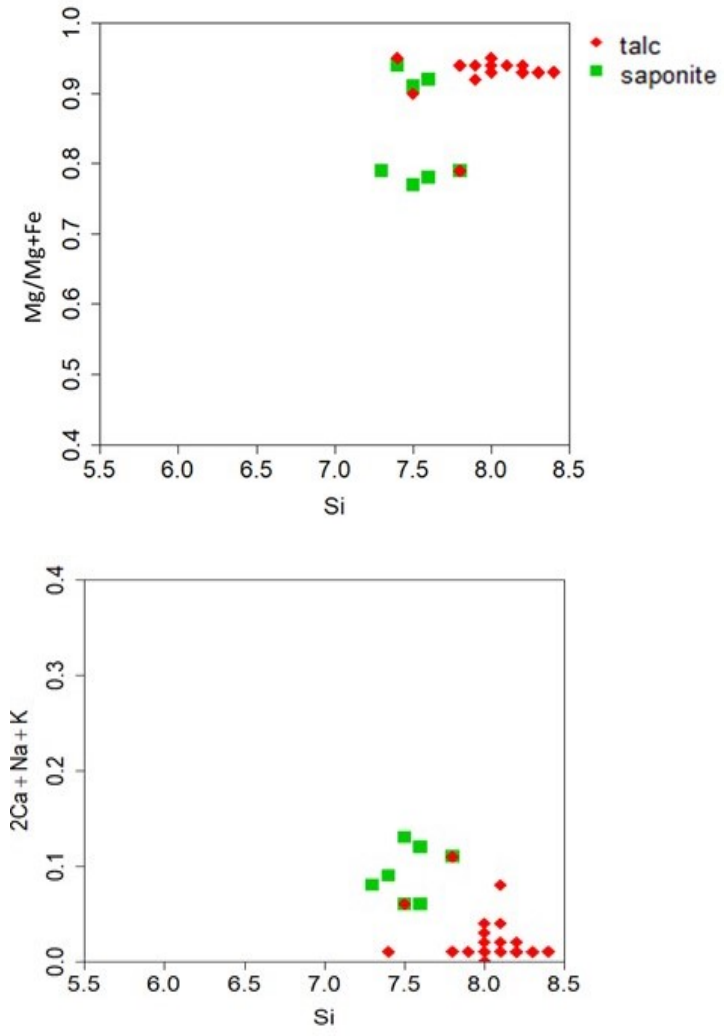

Fig. 4.82: Mineral chemistry of the Mg-saponite and talc within altered lherzolite of Wonu, Ibadan-Apomu area indicating ore associated saponites, and olivine and pyroxene associated saponites of hydrothermally altered ultramafic rocks of arc and boninitic affinity (after Alt *et al.* 1998; Nimis *et al.* 2004).

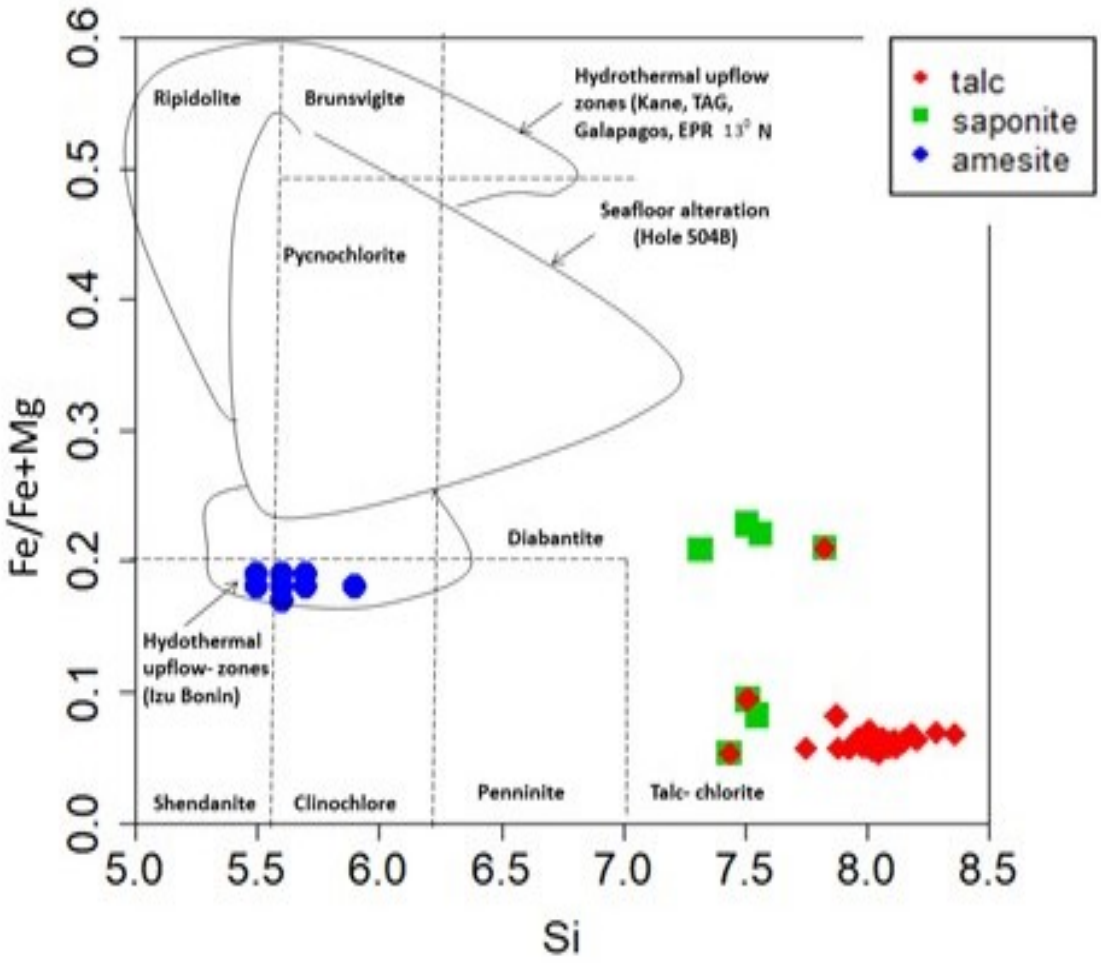

Fig. 4.83: Chemistry of amesite, Mg-saponite and talc in the Wonu, Ibadan-Apomu area showing hydrothermal alteration of the amphibolite and lherzolites of boninitic composition (Hey 1954; Nimis *et al.* 2004).

The precipitation of the tremolites occurred before the faulting that took place along with serpentinisation. The tremolitic amphibolesobserved from this study are productsof the influence of hydrothermal fluids during the mantle upwelling of the peridotic rocks. The presence of H_2O, CO_2 and HCl indicated that the hydrothermal fluid was partly derived from both magmatic and seawater-derived fluid, as exemplified by the presence of allanite and monazite, and microbial activities in the fine-grained amphibolite.

Chromites in the talc schist

Mineral chemistry of selected ferritchromite in talc samples are presented in Table 4.33 and plotted in several discrimination diagrams of Figs. 4.84-4.88. The range of oxides (wt %) in the chromite grains are: Cr_2O_3 (44.33–60.85), Al_2O_3 (5.63–16.72), FeO (25.39–34.02) and MgO (0.09–8.92), while the TiO_2, CaO, NiO, SiO_2, Na_2O and K_2O are below 1%. The MnO content ranged from 1.04-1.83. The high content of the FeO (> 25 wt%), low MgO (< 10 wt%) and lowto moderate Al_2O_3 (ca. 6-17 wt%) indicated alteration of Cr-spinel to ferritchromite. The ferritchromite in the talc schist is characteristic of stratiform chromite as depicted on the Cr# versus Fe^{2+}# binary diagram (Fig. 4.84a and b). The Cr_2O_3 versus Al_2O_3 diagram (Fig. 4.84c) further indicated a dominant stratiform chromitite. It could be observed that the chromites are Cr- and Fe-rich with Cr_2O_3 content greater than 50 wt % and FeO that ranged from 25.29 - 34.02 wt %. The Al_2O_3, on the other hand ismostly below 15 wt %. The TiO_2content is generally higher than 0.3 wt %, which is typical of stratiform chromites (Table 4.33).

The importance of this is that the primary spinels in the ultramafic rocks that produced the talc schist have been altered to metamorphic ferritchromite formed in a boninitic tectonic setting (Fig. 4.85). Chromite composition is quite critical because it gives an inference to parental rock and tectonic environment.

Table 4.33: Mineral chemistry of chromite in talc samples of Wonu, Ibadan-Apomu area

	TC1/3	TC1/4	TC1/5	TC1/6	TC3/39	TC3/40	TC3/41	TC4/45	TC4/46	TC4/47
SiO_2	0.09	0.13	1.16	0.13	0.14	0.06	0.09	0.04	0.06	0.05
TiO_2	0.05	0.04	0.05	0.03	0.03	0.89	0.02	0.04	0.03	0.04
Al_2O_3	7.04	5.89	5.72	5.77	5.63	16.72	5.13	7.83	16.70	9.44
Cr_2O_3	57.00	58.82	57.49	58.66	59.23	44.33	60.85	53.26	47.26	53.26
Fe_2O_3	0.00	0.00	0.00	0.00	0.00	6.79	0.00	3.78	0.74	3.40
FeO	29.31	28.83	28.77	28.56	26.28	21.42	25.39	30.62	32.44	30.96
MnO	1.40	1.27	1.75	1.66	1.81	0.21	1.83	1.04	1.25	1.60
MgO	0.43	0.44	0.09	0.46	0.55	8.92	0.53	0.50	0.52	0.54
Total	95.32	95.42	95.03	95.27	93.67	99.34	93.84	97.11	99.00	99.29
Formula units (based on 4 oxygens)										
Si	0.003	0.005	0.044	0.005	0.005	0.002	0.003	0.001	0.002	0.002
Ti	0.001	0.001	0.001	0.001	0.001	0.022	0.001	0.001	0.001	0.001
Al	0.312	0.262	0.256	0.257	0.255	0.643	0.233	0.340	0.681	0.398
Cr	1.694	1.756	1.725	1.754	1.802	1.143	1.854	1.550	1.294	1.505
Fe^{3+}	0.000	0.000	0.000	0.000	0.000	0.167	0.000	0.105	0.019	0.091
Fe^{2+}	0.921	0.910	0.913	0.903	0.846	0.584	0.818	0.943	0.939	0.926
Mn	0.045	0.041	0.056	0.053	0.059	0.006	0.060	0.032	0.037	0.048
Mg	0.024	0.025	0.005	0.026	0.032	0.434	0.030	0.027	0.027	0.029
Tot. cat.	3.000	3.000	3.000	3.000	3.000	3.000	3.000	3.000	3.000	3.000
Tot. oxy.	4.007	4.015	4.036	4.012	4.035	4.000	4.048	4.000	4.000	4.000
Cr#	84.4	87.0	87.1	87.2	87.6	64.0	88.8	82.0	65.5	79.1
Mg#	2.54	2.67	0.54	2.80	3.64	42.6	3.54	2.78	2.80	3.04

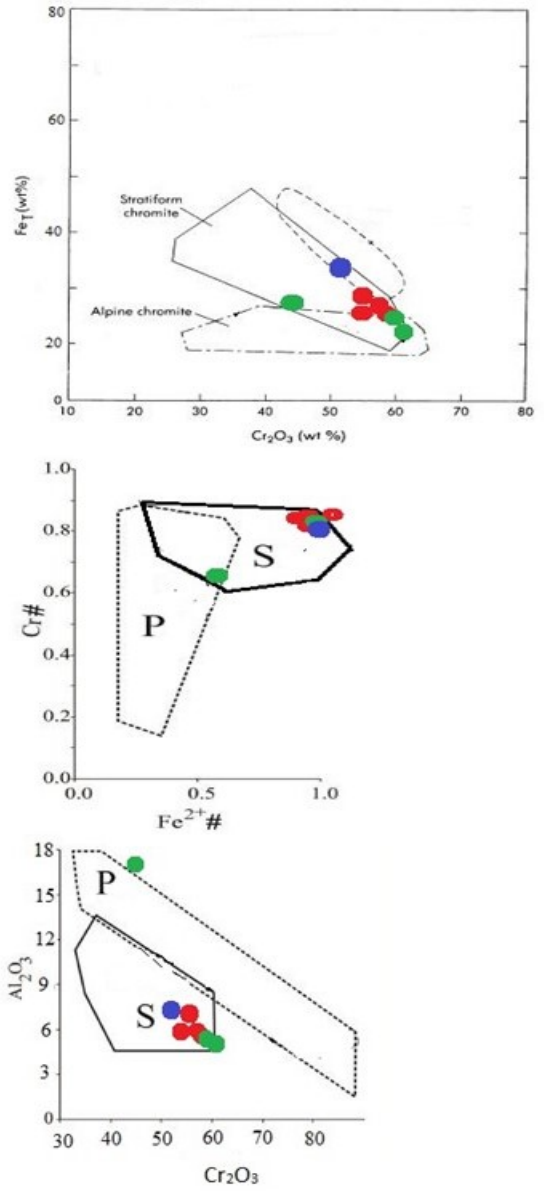

Fig. 4.84:(a) Total Fe versus Cr_2O_3 of the ferritchromites in the talc schist from Wonu-Ibadan Apomu area. (b)the Cr# versus Fe^{2+}# binary diagram (c) Cr_2O_3 versus Al_2O_3 diagram.

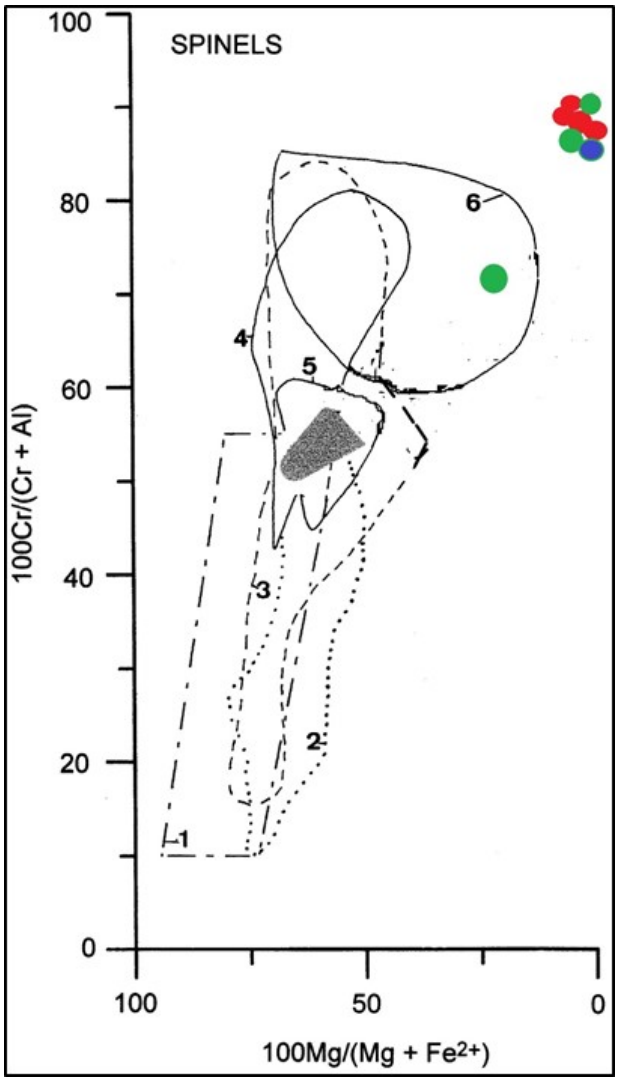

Fig. 4.85: The diagram of the stratiform Cr-spinel in 6 showingalteration to ferritchromite in the talc schist of Wonu, Ibadan-Apomu area (after Beziat et al 2000).

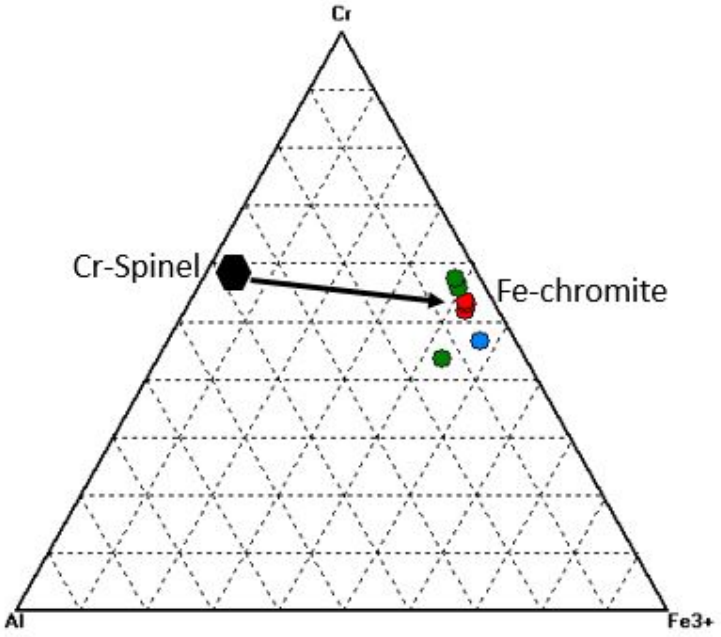

Fig. 4.86:Typical alteration of Cr-spinel to ferritchromite as depicted in the Wonu, Ibadan-Apomu talc schists (black- normal field of Cr-Spinel before alteration).

Generally, Al-rich chromites are inferred to be formed either at the mid-ocean ridge or in a back-arc basin, while Cr-rich chromites are mainly formed in the mantle sequence of ophiolites mostly occurring in supra-subduction zone (SSZ) (Zaccarini *et al*, 2011). The presence of Cr-rich chromites with high Fe and low Al in the Wonu, Ibadan-Apomu talc schist, could be interpreted to result from exhumation and fractional precipitation during differentiation of a single batch of magma, with an initial high-Cr of boninitic composition, characteristic of a supra-subduction zone.

The composition of the ferritchromites in the Wonu, Ibadan-Apomu ultramafics indicated that they are altered metamorphic stratiform chromite in depleted peridotites (Figs. 4.85 and 4.86). The alterations may be produced from percolation of melts, in subduction or areas adjacent to supra-subduction zone, within depleted peridotitc rocks.

The origin of the ultramafic-maficrocks can be inferred partly from their chromite composition in the talc schist as metamorphic stratiform chromite asshown in Fig. 4.87. In the plot of TiO_2 versus Al_2O_3(Fig. 4.88a), samplesoccupythefieldofchromite generated fromor adjacent to supra-subduction zone (SSZ).As shown in Fig.4.88b,thechromites are low in Ti, which is characteristic of Island Arc Basalts (IAB) that are reminiscent of modern boninites.It could be suggested that the chromites are formed around a supra-subduction zone from a single batch of magma with an initial high-Cr of boninitic composition, which was later differentiated in the mantle above the Moho transition zone.

On the basis of the chromite-melt relationships (Fig. 4.85), most of the analysed chromites from the talc schist in the study areacould be derived from Island Arc-related melts of boninitic composition. Moreso, the chromites follow a definite trend from Al_2O_3-poor to Al_2O_3-rich compositions, indicating differentiation of a single melt in an Island Arc tectonic environment. The derivation of both SSZ and IAB is an indication of syn-collision above a mantle wedge.

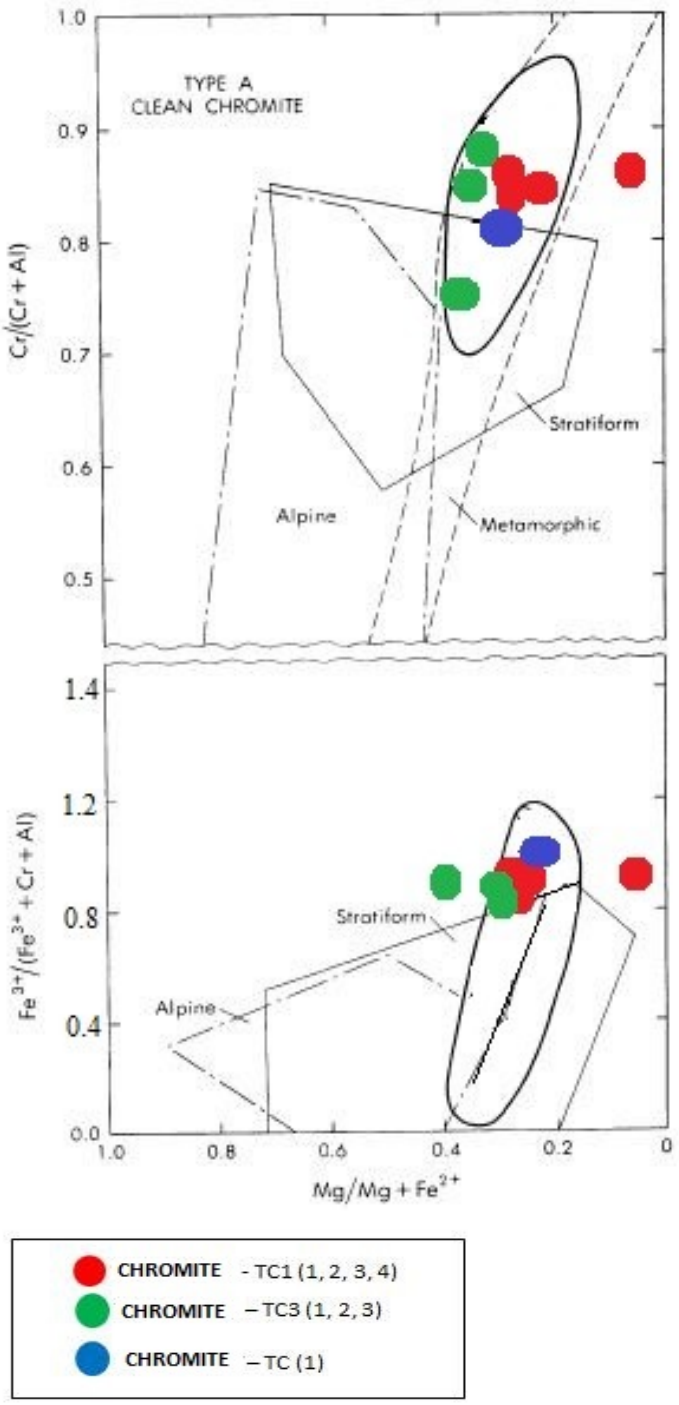

Fig. 4.87:Ferritchromites within talc schists of Wonu, Ibadan-Apomu area indicating metamorphic stratiform chromite composition.

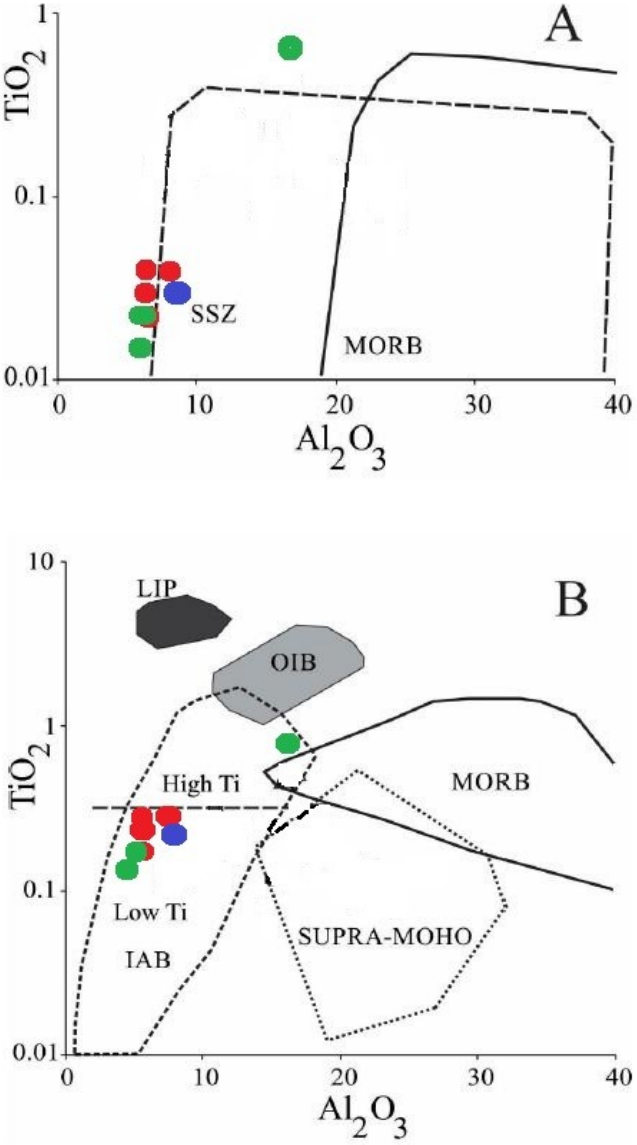

Fig. 4.88: TiO_2-Al_2O_3 of altered spinels in the talc schist of Wonu- Ibadan-Apomu area showing (a) the ferritchromites produced from the alteration of spinels plotted in supra-subduction zone (Kamenetsky *et al*, 2001); (b) the ferrichromites plots in the low-Ti zone, which indicates that it is boninitic.

4.3.3.5 Geochemistry of theTalcose Rocks

The whole-rock geochemistryof the talc schist of the Wonu, Ibadan-Apomu area are shown in Table 4.34. The majoroxides showed that the average value of SiO_2 is 60.51 %.The MgO contents ranged between 28.99-31.49 %.The Al_2O_3 (0.76-3.77 %),Fe_2O_3 (3.27-6.43 %) and CaO (0.05-1.62 %) contents showed a wider range within samples. The MnO, Na_2O, K_2O, TiO_2 and P_2O_5 are generally low (<0.05%) and are not strikingly varied within samples; while loss on ignition (LOI) do not generally exceed 5.0%.

The Sum Alkalinity (Na_2O+K_2O) versus SiO_2 diagram (after Middlemost 1994) of the talc schist showed that it is low in alkalis but high in silica (Fig. 4.63). The high silica is interpreted as SiO_2 contribution by the invading hydrothermal fluid. The AFM ($Na_2O + K_2O$) – Fe_2O_3 – MgO) diagram of Irvine and Barager (1971) (Fig. 4.64) confirmed the basic chemical character and the komatitic nature of the talc schist. The Al_2O_3-MgO-($Fe_2O_{3(t)}$+TiO_2) diagrams of Jenson (1976) showed that the talc schist are basaltic komatiite (Fig. 4.45b, blue). The CaO-Al_2O_3-MgO plots of the Wonu, Ibadan-Apomu ultramafic-mafic rocks after Viljoen & Viljoen, (1969a, 1969b) (Fig. 4.46, blue) showed fractionation of the Mg-rich basaltic komatiites protoliths from parental magma believed to be the source from which the talc schist was derived. Harker diagrams of the major and trace elements versus MgO for the talc schist (Fig. 4.89), indicated that there are two types of talc with one overlapping the composition of the lherzolite from which it was possibly derived. The other talc richer in CaO, Na_2O and Rb are interpreted to be related to pillow basalts from which the amphibolite was derived. The precursor of the talc is Mg-rich as demonstrated by the abundances of Al_2O_3 vs MgO and FeO*/MgO versus SiO_2 diagram (after Miyashiro, 1974), showing differentiation from high MgO-rich dunitic magma to FeO-rich tholeiitic magma (Figs. 4.62a). This is supported by the Harker diagram in Fig. 4.89, which clearly demonstrated transition from Mg-rich talc precursor to lherzolite and amphibolite.

The trace elements data in Tables 4.34 indicated an average concentrations of 1135, 1736, 66 and 80 ppm for Cr, Ni, Zn and Co respectively. Others, such as, Ba,Co, Cu, Ga, Rb, Sr, V, Y, Th, U and Zr are generally low and do not show any marked distribution trend in the samples.

Table 4.34: Major oxides (%), trace elements and rare earth (ppm) elements composition of talc schist

	1	2	3	4	5	6	7	8	9	10	Average	Range	
SiO_2	61.56	60.93	60.22	60.28	60.09	59.25	61.11	60.56	61.23	59.88	60.51	61.56	59.25
TiO_2	0.04	0.03	0.04	0.03	0.02	0.03	0.02	0.03	0.03	0.03	0.03	0.04	0.02
Al_2O_3	0.44	0.47	0.06	0.53	0.9	0.86	0.79	0.08	0.05	0.46	0.46	0.9	0.05
$Fe_2O_{3(t)}$	3.91	4.76	5.01	3.70	4.39	5.16	2.03	4.63	5.31	3.95	4.29	5.31	2.03
Cr_2O_3	0.19	0.16	0.20	0.18	0.15	0.15	0.17	0.19	0.16	0.2	0.18	0.20	0.15
NiO	0.27	0.24	0.25	0.26	0.23	0.24	0.29	0.25	0.28	0.25	0.26	0.29	0.23
MnO	0.03	0.09	0.12	0.05	0.07	0.10	0.11	0.08	0.07	0.09	0.08	0.12	0.03
MgO	30.62	30.19	29.41	31.49	30.54	29.48	30.89	29.96	28.99	31.15	30.27	31.49	28.99
CaO	0.05	0.15	0.23	0.02	0.08	0.24	0.32	0.07	0.12	0.48	0.18	0.48	0.02
Na_2O	0.02	0.03	0.02	0.03	0.03	0.04	0.03	0.02	0.03	0.03	0.03	0.04	0.02
K_2O	0.02	0.04	0.02	0.01	0.02	0.01	0.01	0.02	0.03	0.02	0.02	0.04	0.01
P_2O_5	0.03	0.03	0.04	0.01	0.03	0.03	0.02	0.04	0.02	0.02	0.03	0.04	0.01
LOI	3.02	2.32	4.30	3.49	3.50	4.20	4.25	4.08	3.44	3.07	3.57	4.30	2.32
Total	100.2	99.44	99.92	100.08	100.05	99.79	100.04	100.01	99.76	99.63	99.89	100.2	99.44
Trace elements (ppm)													
Cr	1028	521	1326	1152	1055	980	1577	1133	1625	950	1135	1625	521
Ni	1795	1545	1418	1937	1746	1494	1790	1906	1797	1935	1736	1937	1418
Co	65	66	79	76	66	97	83	87	95	88	80.2	97	65
Cu	2.9	3.5	5.2	6.1	4.5	5.0	5.3	2.9	3.6	2.8	4.18	6.1	2.8
Zn	101	75	52	101	69	52	31	47	74	59	66.1	101	31
V	3.33	2.51	7.75	2.57	3.13	7.16	6.42	3.22	5.43	4.02	4.55	7.75	2.51
Sc	0.55	1.66	0.54	0.65	0.89	1.31	5.44	3.76	0.82	0.65	1.62	5.44	0.54
Ga	0.69	0.66	0.55	0.38	0.67	0.70	1.16	0.58	0.69	0.78	0.68	1.16	0.38
Ba	3.28	32.6	10.2	9.3	6.5	10.3	0.6	8.8	1.67	0.7	8.39	32.6	0.6
Rb	0.11	0.02	0.33	0.37	0.15	0.03	0.16	0.21	0.33	0.05	0.17	0.37	0.02
Sr	0.22	0.38	0.34	0.68	0.47	0.55	0.56	0.76	0.24	0.33	0.45	0.76	0.22
Y	0.61	1.13	0.76	0.95	1.10	2.25	1.38	1.11	1.12	0.99	1.14	2.25	0.61
Zr	0.06	0.07	0.06	0.35	0.09	0.04	0.05	0.07	0.08	0,06	0.09	0.35	0.04
Nb	0.03	0.04	0.03	0.03	0.05	0.05	0.03	0.06	0.13	0.12	0.05	0.13	0.03
Cs	0.01	0.01	0.02	0.01	0.01	0.01	0.02	0.02	0.01	0.01	0.01	0.02	0.01
Hf	0.02	0.01	0.01	0.02	0.02	1.3	0.02	0.01	0.01	0.02	0.14	1.3	0.01
Ta	0.02	0.01	0.03	0.01	0.02	0.02	0.01	0.01	0.02	0.03	0.02	0.03	0.01
Th	0.05	0.05	0.03	0.04	0.03	0.06	0.08	0.02	0.08	0.05	0.05	0.08	0.02
U	0.02	0.04	0.10	0.03	0.07	0.04	0.12	0.32	0.17	0.22	0.11	0.32	0.02
Rare-Earth elements (ppm)													
La	2.47	3.99	2.36	2.65	2.99	3.55	3.28	2.15	4.01	3.11	3.06	4.01	2.15
Ce	1.27	3.45	1.15	3.12	5.11	4.35	2.82	2.47	3.66	3.18	3.06	5.11	1.15
Pr	0.76	1.16	0.78	0.86	1.20	1.32	1.11	1.10	1.21	0.99	1.05	1.32	0.76
Nd	2.70	4.10	3.91	5.06	4.29	3.43	3.61	3.50	2.98	2. 77	3.73	5.06	2.7
Sm	0.47	0.71	0.88	0.76	0.69	0.85	1.02	1.09	1.12	1.05	0.86	1.12	0.47
Eu	0.10	0.16	0.15	0.15	0.08	0.09	0.07	0.12	0.11	0.13	0.12	0.16	0.07
Gd	0.31	0.49	0.65	0.70	0.68	0.58	0.33	0.46	0.35	0.37	0.49	0.7	0.31
Tb	0.04	0.06	0.13	0.05	0.14	0.06	0.08	0.17	0.18	0.22	0.11	0.22	0.04
Dy	0.19	0.30	0.32	0.15	0.08	0.09	0.11	0.24	0.71	0.20	0.24	0.71	0.08
Ho	0.03	0.05	0.03	0.03	0.07	0.05	0.04	0.04	0.05	0.04	0.04	0.07	0.03
Er	0.08	0.14	0.04	0.08	0.22	0.14	0.09	0.11	0.15	0.17	0.12	0.22	0.04
Tm	0.01	0.02	0.01	0.02	0.03	0.02	0.01	0.02	0.03	0.02	0.02	0.03	0.01
Yb	0.07	0.15	0.09	0.10	0.12	0.10	0.16	0.10	0.17	0.14	0.12	0.17	0.07
Lu	0.01	0.02	0.01	0.02	0.03	0.01	0.02	0.02	0.02	0.02	0.02	0.03	0.01
Rare-Earth Elements ratios													
Eu/Eu*	0.80	0.83	0.61	0.63	0.36	0.39	0.37	0.52	0.54	0.64	0.57	0.36	0.83
LaN/YbN	24.01	18.10	17.85	18.03	16.96	24.16	13.95	14.63	16.05	15.12	17.89	13.95	24.16
LaN/SmN	3.29	3.52	1.68	2.18	2.72	2.62	2.01	1.24	2.24	1.86	2.34	1.24	3.52
CeN/YbN	4.78	6.06	3.36	8.21	11.21	11.45	4.64	6.50	5.67	5.98	6.79	3.36	11.45
CeN/SmN	0.65	1.18	0.32	1.00	1.80	1.24	0.67	0.55	0.79	0.73	0.89	0.32	1.80
EuN/YbN	4.09	3.05	4.77	4.30	1.91	2.58	1.25	3.44	1.85	2.66	2.99	1.25	4.77
Sum_REE	8.51	14.80	10.51	13.75	15.73	14.64	12.75	11.59	14.75	9.64	12.67	8.51	15.73

Table 4.34Contd: Major oxides (%), trace elements and rare earth (ppm) elements composition of talc schist

	1	2	3	4	5	6	7	8	9	10	11	12	Ave	Range	
SiO_2	57.29	58.43	59.23	60.15	60.01	55.62	59.19	57.67	56.77	60.09	59.91	57.92	58.52	60.15	55.62
TiO_2	0.19	0.20	0.18	0.20	0.02	0.16	0.18	0.19	0.17	0.18	0.03	0.13	0.15	0.20	0.02
Al_2O_3	3.16	3.30	3.62	0.84	0.77	2.74	3.12	3.21	3.77	0.93	0.76	2.87	2.42	3.77	0.76
$Fe_2O_{3(t)}$	4.34	3.83	3.27	3.94	3.75	6.43	3.29	4.90	5.09	3.76	3.83	5.33	4.31	6.43	3.27
Cr_2O_3	0.11	0.13	0.09	0.09	0.10	0.12	0.12	0.16	0.14	0.09	0.08	0.09	0.11	0.16	0.08
NiO	0.21	0.21	0.15	0.08	0.06	0.11	0.20	0.09	0.11	0.09	0.07	0.06	0.12	0.21	0.06
MnO	0.14	0.13	0.15	0.48	0.05	0.19	0.12	0.14	0.16	0.49	0.05	0.21	0.19	0.49	0.05
MgO	28.59	27.89	29.18	30.04	30.06	29.15	27.9	28.42	29.16	30.01	29.99	27.01	28.95	30.06	27.01
CaO	0.70	0.17	0.59	0.06	0.05	0.71	0.60	0.22	0.62	0.07	0.08	1.62	0.46	1.62	0.05
Na_2O	0.04	0.01	0.11	0.03	0.03	0.04	0.05	0.02	0.09	0.04	0.07	0.09	0.05	0.11	0.01
K_2O	0.06	0.05	0.11	0.01	0.02	0.03	0.07	0.04	0.09	0.02	0.05	0.01	0.05	0.11	0.01
P_2O_5	0.03	0.03	0.03	0.01	0.01	0.02	0.03	0.02	0.01	0.02	0.01	0.02	0.02	0.03	0.01
LOI	4.42	4.65	3.21	3.81	4.79	4.58	4.43	4.66	3.19	3.22	4.61	4.20	4.15	4.79	3.19
Total	99.28	99.03	99.92	99.74	99.72	99.90	99.30	99.74	99.37	99.01	99.54	99.56	99.51	99.92	99.01
Trace elements (ppm)															
Cr	1182	1321	970	938	1094	1265	1230	1629	1445	993	836	972	1156	1629	836
Ni	2115	2180	1512	867	659	1136	2092	948	1164	957	796	968	1283	2180	659
Co	69	69	83	71	73	87	68	97	75	73	85	68	76.5	97	68
Cu	3	6	3	3	5	3	6	5	3	5	5	4	4.25	6	3
Zn	7	64	62	45	71	53	66	61	45	71	63	56	55.33	71	7
V	1	8	6	5	5	4	7	6	5	5	8	6	5.5	8	1
Sc	7	2	1	4	2	3	1	1	1	2	2	2	2.33	7	1
Ga	2	3	3	2	2	3	4	3	3	3	4	2	2.83	4	2
Ba	32	30	37	9	10	31	29	36	9	10	30	37	25	37	9
Rb	29	6	4	3	2	28	7	5	3	3	7	4	8.41	29	2
Sr	10	12	9	2	2	11	11	8	2	2	11	8	7.33	12	2
Y	34	25	33	2	2	38	24	34	2	3	26	34	21.41	38	2
Zr	17	14	13	8	8	16	13	13	8	8	14	13	12.08	17	8
Cs	<0.1	<0.1	<0.1	<0.1	<0.1	<0.1	<0.1	<0.1	<0.1	<0.1	<0.1	<0.1	<0.1		
Hf	1.0	1.1	1.0	1.2	1.2	1.3	1.2	1.3	1.0	1.2	1.3	1.1	1.16	1.3	1
Ta	<0.1	<0.1	<0.1	<0.1	<0.1	<0.1	<0.1	<0.1	<0.1	<0.1	<0.1	<0.1	<0.1	0	0
Nb	1.3	1.4	1.1	1.3	1.2	1.3	1.5	1.3	1.5	1.2	1.3	1.6	1.33	1.6	1.1
Th	0.1	0.2	0.1	0.15	0.5	0.6	0.4	0.04	0.3	0.5	0.6	0.4	0.32	0.6	0.04
U	<0.1	<0.1	<0.1	<0.1	<0.1	<0.1	<0.1	<0.1	<0.1	<0.1	<0.1	<0.1	<0.1		
Rare-Earth elements (ppm)															
La	3.28	4.99	3.06	4.21	3.99	3.55	3.00	2.15	3.01	3.11	5.94	4.95	3.77	5.94	2.15
Ce	2.02	3.45	2.15	2.35	3.11	4.35	2.19	2.47	3.66	3.18	2.25	3.12	2.86	4.35	2.02
Pr	0.55	1.16	0.78	0.61	1.15	1.32	0.52	1.10	1.21	0.99	0.76	0.86	0.92	1.32	0.52
Nd	3.61	3.10	3.15	4.19	2.94	3.43	2.99	3.50	2.98	4. 70	2.79	3.06	3.25	4.19	2.79
Sm	0.42	0.51	0.88	0.43	0.59	0.85	0.63	1.09	1.12	1.05	0.57	0.76	0.74	1.12	0.42
Eu	0.09	0.11	0.15	0.13	0.18	0.19	0.10	0.12	0.11	0.13	0.10	0.15	0.13	0.19	0.09
Gd	0.43	0.41	0.65	0.46	0.68	0.58	0.41	0.46	0.35	0.37	0.31	0.70	0.48	0.7	0.31
Tb	0.08	0.06	0.13	0.09	0.14	0.06	0.07	0.17	0.18	0.22	0.04	0.05	0.10	0.22	0.04
Dy	0.45	0.30	0.32	0.45	0.08	0.09	0.43	0.24	0.71	0.20	0.19	0.15	0.30	0.71	0.08
Ho	0.05	0.10	0.05	0.12	0.11	0.07	0.09	0.04	0.05	0.04	0.03	0.03	0.06	0.12	0.03
Er	0.10	0.15	0.09	0.34	0.12	0.14	0.32	0.11	0.15	0.17	0.08	0.08	0.15	0.34	0.08
Tm	0.05	0.03	0.05	0.08	0.07	0.08	0.06	0.02	0.03	0.02	0.05	0.03	0.04	0.08	0.02
Yb	0.16	0.15	0.09	0.40	0.12	0.20	0.31	0.10	0.17	0.14	0.21	0.10	0.18	0.4	0.09
Lu	0.06	0.04	0.06	0.09	0.03	0.06	0.05	0.05	0.06	0.08	0.08	0.07	0.06	0.09	0.03
Rare-Earth Elements ratios															
Eu/Eu*	0.65	0.73	0.61	0.89	0.87	0.83	0.60	0.52	0.54	0.64	0.73	0.63	0.68	0.52	0.89
LaN/YbN	13.95	22.64	23.14	7.16	22.63	12.08	6.59	14.63	12.05	15.12	19.25	33.69	16.91	6.59	33.69
LaN/SmN	4.89	6.13	2.18	6.13	4.24	2.62	2.98	1.24	1.68	1.86	6.53	4.08	3.71	1.24	6.53
CeN/YbN	3.32	6.06	6.29	1.55	6.82	5.73	1.86	6.50	5.67	5.98	2.82	8.21	5.07	1.55	8.21
CeN/SmN	1.17	1.64	0.59	1.32	1.28	1.24	0.84	0.55	0.79	0.73	0.96	1.00	1.01	0.55	1.64
EuN/YbN	1.61	2.10	4.77	0.93	4.30	2.72	0.92	3.44	1.85	2.66	1.36	4.30	2.58	0.92	4.77
Sum_REE	11.35	14.56	11.61	13.95	13.31	14.97	11.17	11.62	13.79	9.70	13.40	14.11	12.80	9.70	14.97

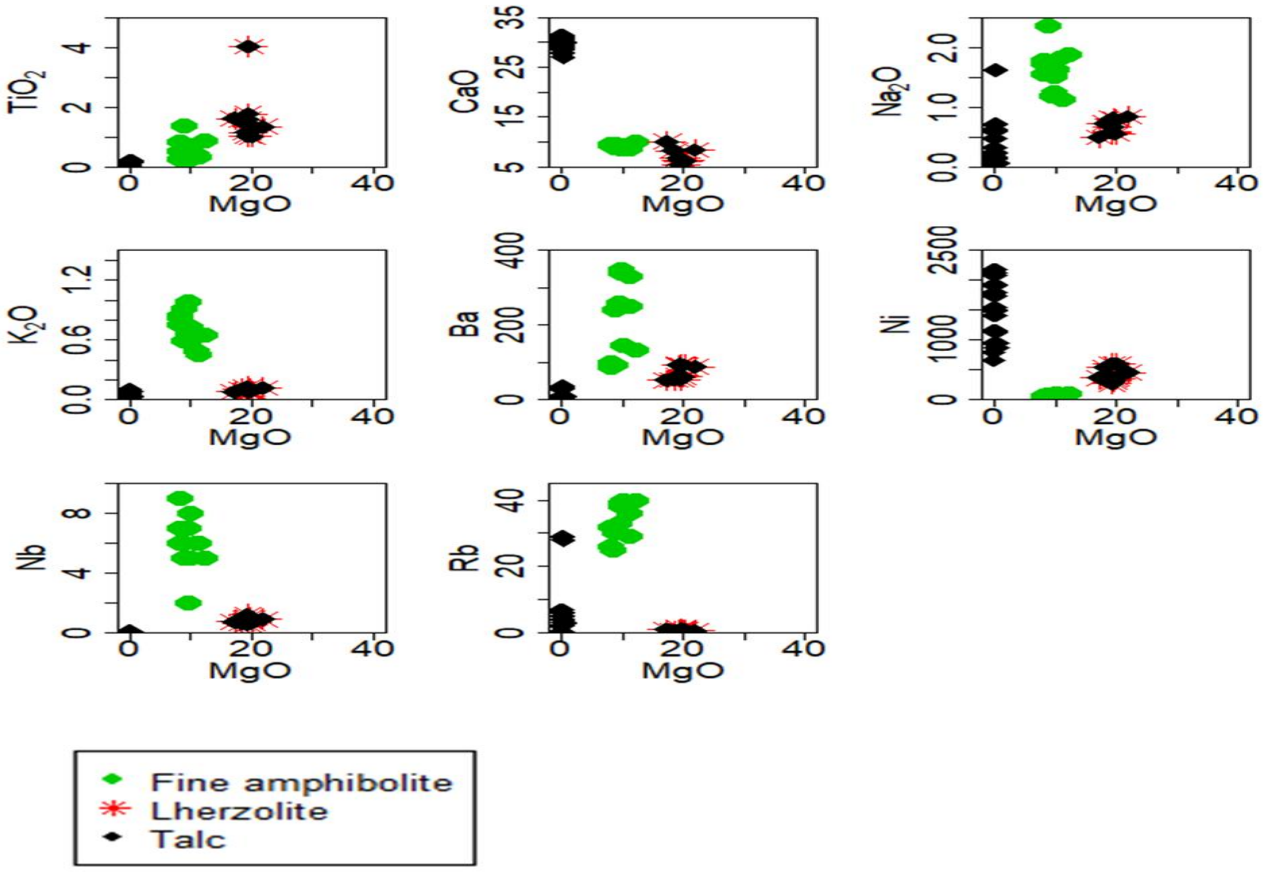

Fig. 4.89:Diagrams of major oxides and trace elements versus MgO for amphibolite and lherzolite and talc in Wonu, Ibadan-Apomu area.

The chondrite-systemized REE patterns for the talc schist in the study area are given Fig. 4.90. The talc schist showed light rare-earth element (LREE) enrichment than the middle rare-earth element (MREE) and heavy rare-earth element (HREE) due to REE contribution from hydrothermal fluid. In the talc schist, La yielded the highest concentration, with values ranging from 2.15-5.94 ppm, followed by Ce (1.15- 4.35), Gd (0.31-0.70), Er (0.04-0.34) and Lu, which is0.02-0.09 on the average. The talc schist showed LREE depletion in relation to the fine-grained amphibolite and lherzolites. Chondrite-normalized REE patterns showed a negative Eu anomaly instead of a positive or no anomaly characteristic of mafic-ultramafic rocks as a result of the hydrothermal fluid interaction, which led to the recrystalisation of secondary plagioclasefeldspar, the fractionation of which led to negative anomaly. The fine-grained amphibolites and the lherzolites, on the other hand showed the characteristic positive Eu anomaly (Eu/Eu*), which ranged from 0.52-0.89. The La_N/Yb_N ratios ranged from 1.99-5.19; while the La_N/Sm_Nranged from 0.93-2.83 and the ratios Ce_N/Yb_N ranged from 1.56-5.32.

Talc could be formed from or by fluid induced metamorphism of mafic-ultramafic rocks in subduction zones, precipitation of talc could occur at great depths and at higher temperatures 800 ºC than other rock units 400-650 ºC. Percolating hydrothermal fluids transports the trace element contents and sometimes initiates partial melting of contact rocks. Rocks formed may not undergo decarbonification during subduction, which may be important to carbon recycling in the mantle.

As shown in Fig. 4.90, the trace element composition of the talc is similar to that of the lherzolite but different from that of the amphibolite indicating that the amphibolite is more differentiated. The chemostratigraphy observed in the rocks is reminiscent of the stratigraphy observed in modern subduction or subduction initiation/collision settings with a transition from komatitic rocks at the base overlain by rocks of tholeiitic, boninitic and calc-alkaline compositions.

The MgO+Fe+CaO against SiO_2+Al_2O_3 diagram indicated a predominantly Al-enriched mantle,mafic-ultramafic-derived talc rather than carbonate-derived one (Fig. 4.91). The chemical data supported a metasomatised residual to cumulate magma with 40 % fractionation of the parent, Late Pan-African to low-Ca Phanerozoic- boninitic-komatitic magma (Figs. 4.92 and 4.93).

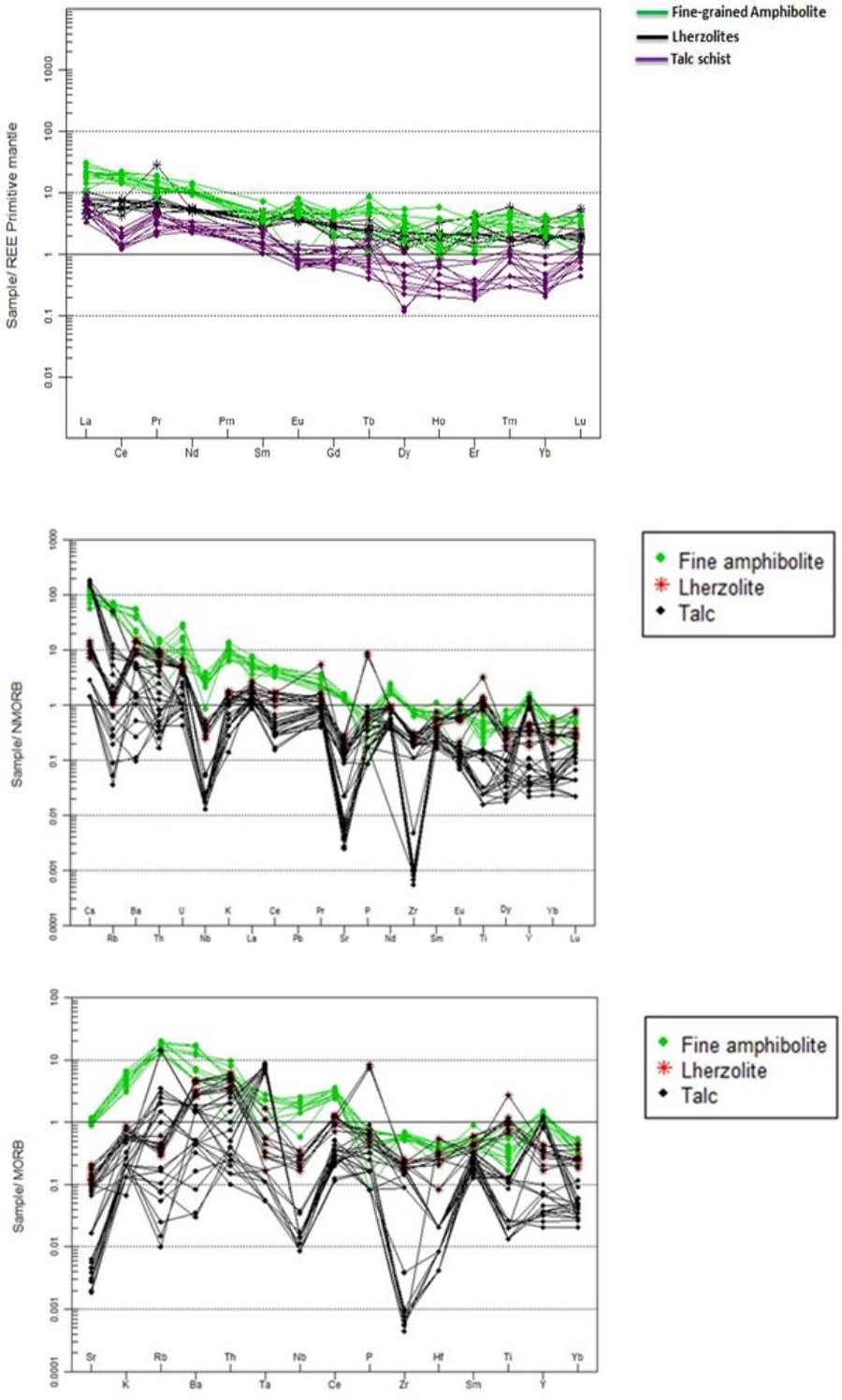

Fig. 4.90: Chondrite-normalized rare earth components and minor components of the ultramafic-mafic rocks of Wonu, Ibadan-Apomu area(a, b and c).

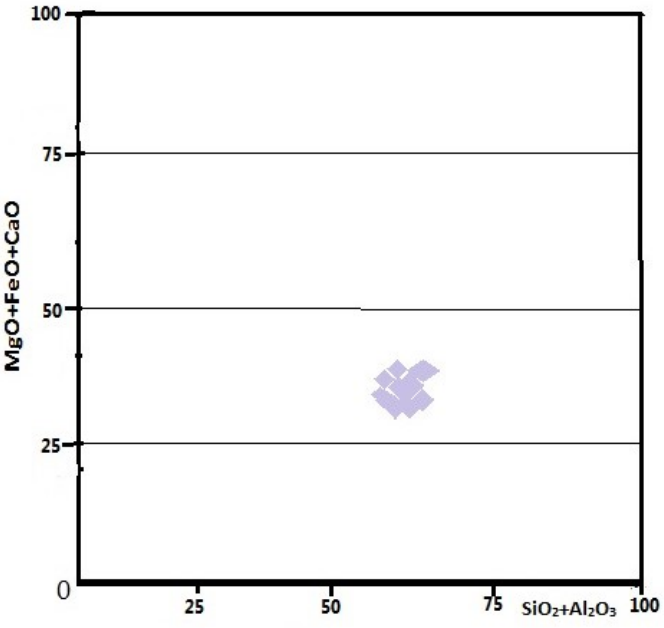

Fig. 4.91: Major oxides of silicate-rich whole-rock talc samples of Wonu, Ibadan-Apomu area indicating mafic-ultramafic source.

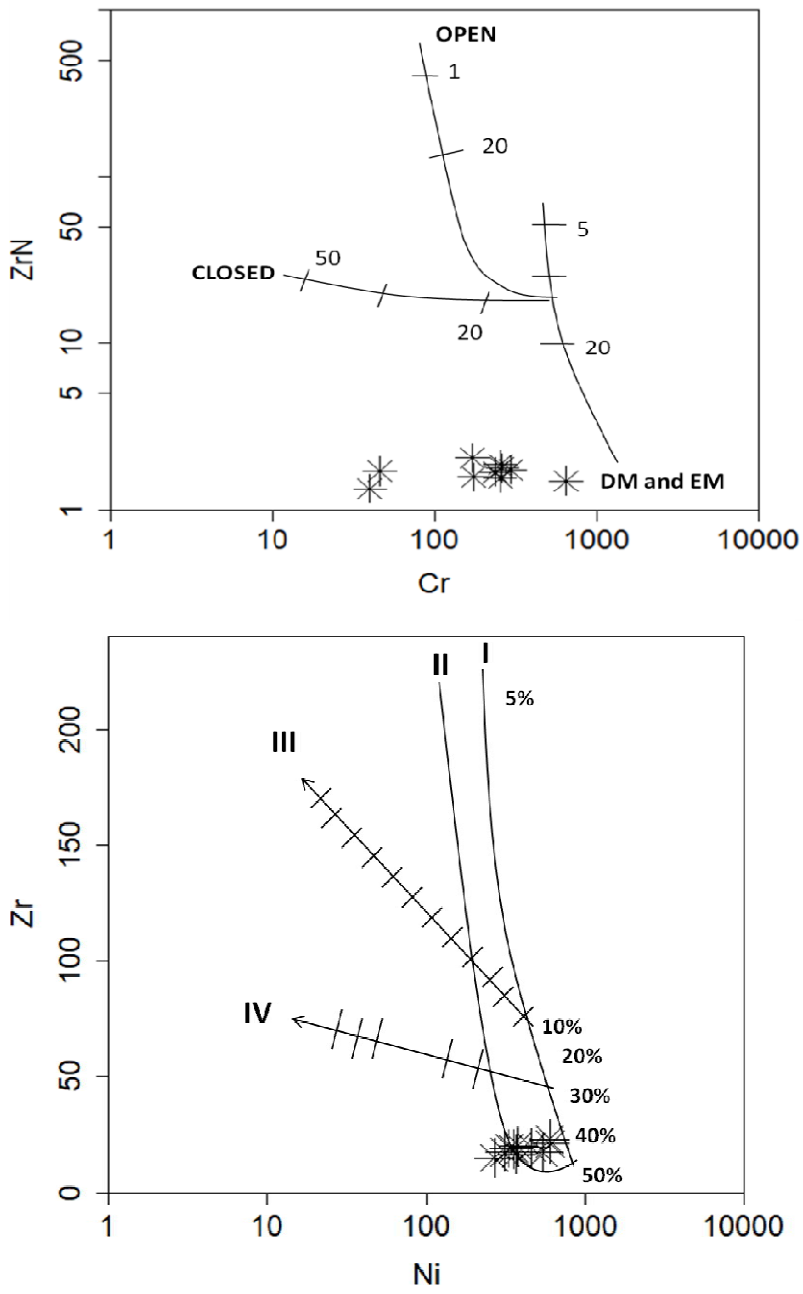

Fig. 4.92:A model for petrogenesis of the the whole-rock talc samples of Wonu, Ibadan-Apomu area based on (a) compatible (Cr) and (Zr_N) elements for high-Mg mafic rocks with the trace elements showing depleted and enriched mantle sources (after McDonough *et al.* 1992) and (b) Ni and Zr diagram showing 40 % partial melting (after Rajamani *et al.* 1985).

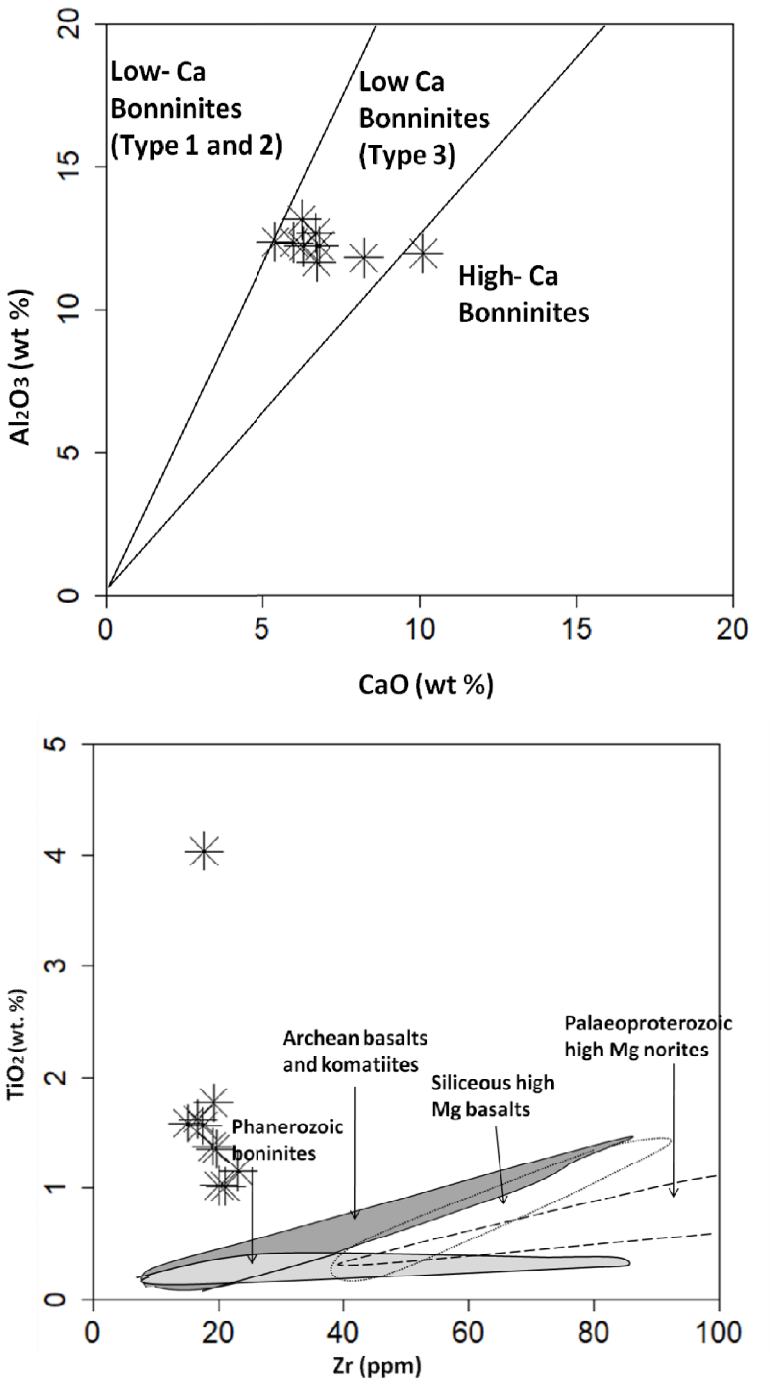

Fig. 4.93:(a) Al_2O_3 versus CaO diagram of the talc samples of Wonu, Ibadan-Apomu area showing low Ca boninites, (b) TiO_2 versus Zr showing Phanerozoic boninites (Smithies, 2002).

4.4 Discussion

4.4.1 Petrogenesis of the Wonu, Ibadan-Apomu rocks

Discrimination diagrams have been used to classify the tectonic settings of the granitic and mafic-ultramafic rocks of Wonu, Ibadan-Apomu area.The Na_2O versus K_2O and the Alkalinity-Silica diagrams (Le Bas and Streckeisen, 1991)(Figs. 4.94a &b) and the AFM diagram (Irvine and Barager, 1971) (Fig. 4.95) for the rocks of Wonu, Ibadan-Apomu area showed that the granitic rocks are subalkaline/calc-alkaline while the mafic-ultramafic rocks are tholeiitic to komatitic in composition. As shown in Figs. 4.94 and 4.95, the rock sequences in the study area are divided into three principal types: (1) The low-K_2O, low-Na_2O mafic-ultramafic subalkaline rocks (2)Thelow-K_2O, high-Na_2Ogranite to granodiorite and (3) The high-K_2O, high-Na_2O migmatite and pegmatite.

The Proterozoic rocks of Nigeria contain both tholeiitic and calc-alkaline assemblages (Hirdes *et al.,* 1996). Abouchami *et al.* (1990) and Sylvester and Attoh, (1992) , proposed that ultramafic-mafic assemblages in the paleoproterozoic rocks of West Africa are associated with tholeiitic basalts, whereas the granitic rocks are associated with calc-alkaline suite. In southwestern Nigeria, tholeiitic suites of ultramafic-mafic bodies occur mainly in the schist belts that occupied a synclinorial trough within the migmatite-gneiss complex.

In the ultramafic-mafic assemblage, the crystallization sequence is olivine-chromite followed by orthopyroxene, clinopyroxene, amphibole and biotite. Thehigh Mg-number of both clinopyroxene (0.95-0.75) and orthopyroxene (0.68–0.55) in the amphibolite and 0.80-0.75 and 0.80-0.70, respectively in the clinopyroxene and othopyroxene of the lherzolite reflects thefact that they followed olivine very closely on theliquidus, before the magma was depleted in Mg(Elthon *et al.,* 1982). The first phase crystallizing afterolivine in a cumulate sequence is determined bythe degree of partial melting of the mantlesource (Jaques and Green, 1980). The presence of plagioclase in the amphibolite correspond to low degree of partial melting,clinopyroxene to medium, and orthopyroxene tohigh. High TiO_2 (0.6–0.8 wt%) occurs in clinopyroxenes of plagioclase-type cumulates,moderate TiO_2 (0.4 wt%) in clinopyroxene-type cumulates and low TiO_2 (0.1 wt%) in those of orthopyroxene-type cumulates (Ishiwatari, 1985). The CaO/Al_2O_3 and the Fe_2O_3/MgO ratios of the lherzolite showed an Al-undepleted komatiites with olivine and clinopyroxene fractionation.

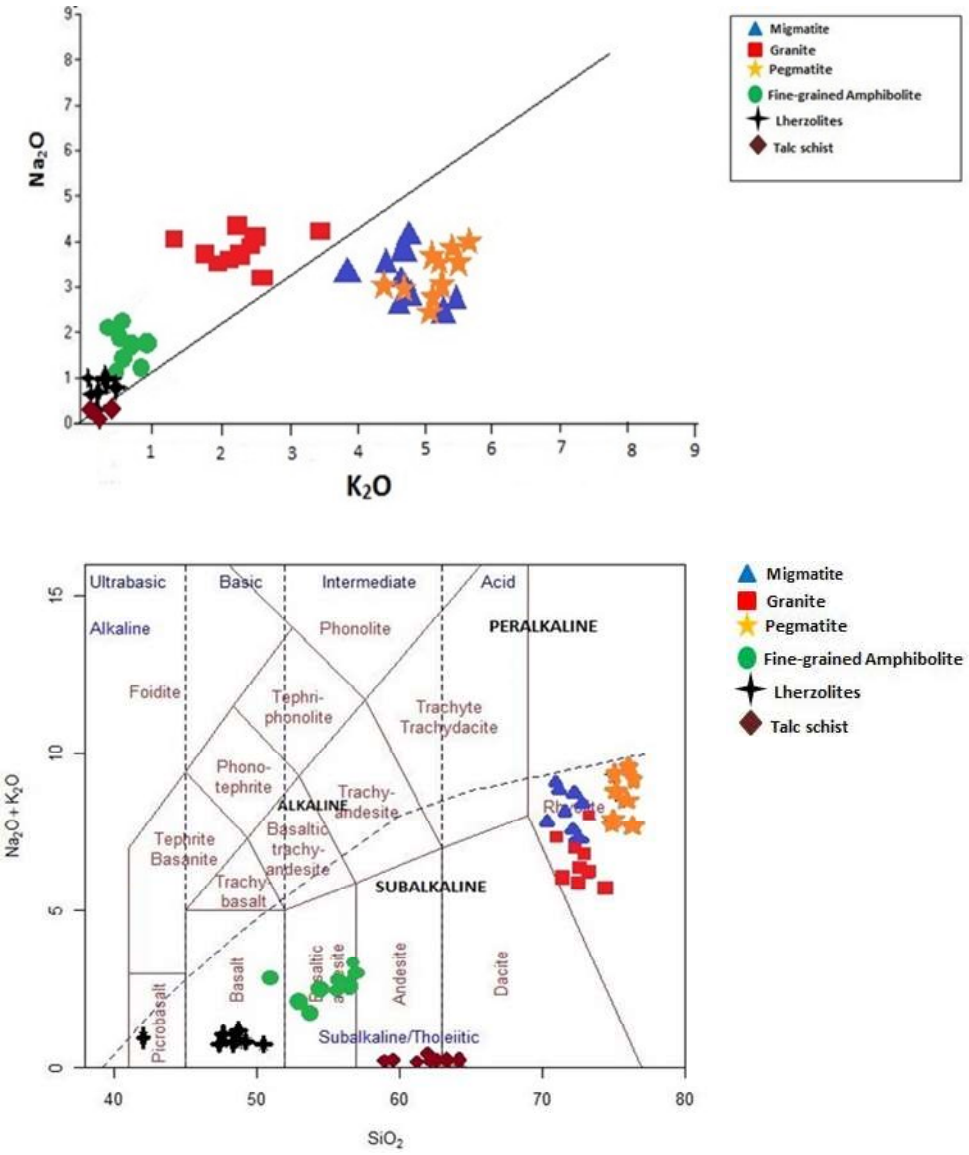

Fig. 4.94: Classification of protolith lavas of the Wonu, Ibadan-Apomu rocks using (a) Na_2O versus K_2O and (b) the IUGS-recommended Alkalnity-Silica diagramof Le Bas and Streckeisen (1991)indicating the subalkaline related granitoids and the basaltic precursor.

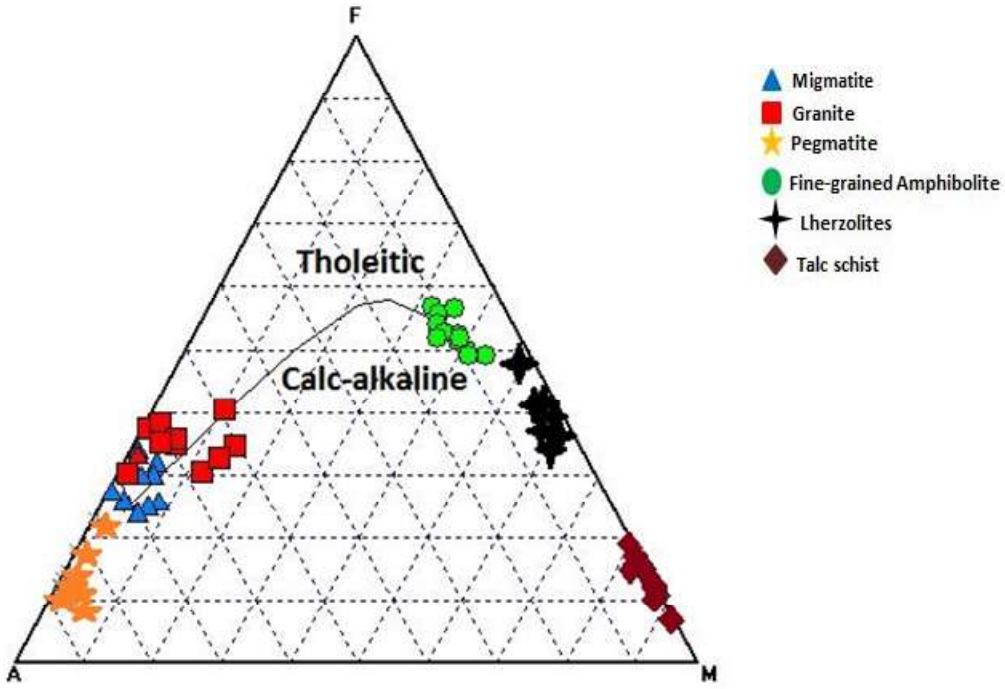

Fig. 4.95: Classification of protolith lavas of the Wonu, Ibadan-Apomu rocks using (a) on the AFM plot showing the calc-alkaline related granitoids and the tholeiitic to komatitic mafic-ultramafics.

Crystallization of both pyroxenes in the lherzolite and the low to moderate TiO_2 content of clinopyroxene(0.05-0.45 wt%) is consistentwith the parental magma generated bya high to moderate degree of partial melting of 10 to 15 % in the amphibolite and lherzolite and 40 % in the talc. The high TiO_2 content of clinopyroxene (0.79-0.89 wt%) in the amphibolite is consistent with the presence of plagioclase and low degree of partial melting. The low, heavy REE, Y and Sc contents of the ultramafic-mafic rocks (Tables 4.20 and 4.29) could result from high degrees of melting of anAl-undepleted source (Baker *et al.,* 1994).

The crystallizationpressures is estimated from crystallizationof aluminous chromite (Al_2O_3 5.13-16.72 %) (Table 4.33) from the talc parent magma, and clinopyroxene (Al_2O_3 0.68-11.22 %) (Table 4.25) from the lherzolite. According to Dick and Bullen (1984), partition coefficientsfor Cr in spinel decrease significantlywith increasing pressure, leading to lower Crcontents in spinels formed athigh pressure. In addition, Irvine (1967) suggestedthat, at pressures above the olivine-plagioclase stability field (>8 kbar), a basaltic liquidwill crystallize aluminous spinel and pyroxenerather than plagioclase. The high Cr:(Cr+Al) ratios (0.64–0.84), with the higher value of 0.84 being dominant in the earliest crystallized spinels from the Wonu, Ibadan-Apomu area and the presence of olivine-plagioclaseassemblages may therefore be indicativeof crystallization at low pressures (<8 kbar). Moreover,the low Mg contents of chromite grains trappedin olivine and the zonation inchromite-ferritchromite-magnetite, olivine and pyroxene crystals are indicativeof extensive subsolidus reequilibrationduring slow cooling of the complex at low pressures.

Evidence of primary crystallization of brownamphibole is demonstrated by the postcumulus phase enclosing olivine grains and the Cr, Ti and alkalis-rich characteristics, similar to those reported in the layeredsequences and gabbros inOman and Alaska (Lippard *et al.,* 1986, DeBari and Coleman,1989), in picritic rocks of northwest Scotland and in lower crustal xenoliths from island arcs(Tarney and Weaver, 1987). The presence of primary magmatic amphiboleand biotite (Green, 1982), and the latecrystallization of plagioclase (Allanand Carmichael, 1984) indicate hydrous partial melting of a mantlesource affected by previous metasomatic events.The mineralogy and chemical composition of the rocks strongly suggest that they are products of fractional crystallization (Fig. 4.99).

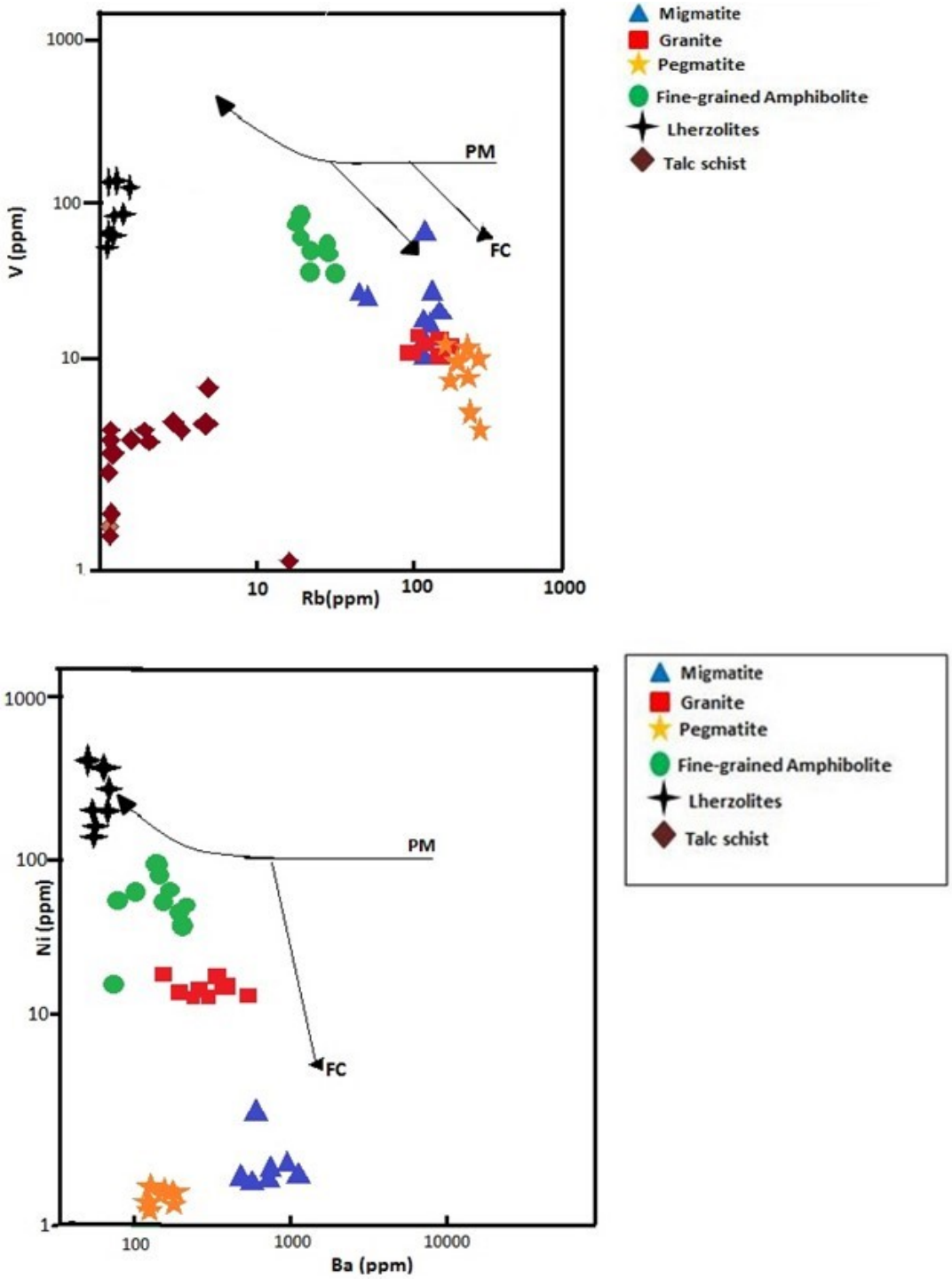

Fig. 4.96:Discrimination diagram of (a) V versus Rb and (b) Ni versus Ba for the rocks of Wonu, Ibadan-Apomu area indicating fractional crystallization and the distinctive ultramafic nature of the lherzolite from which other rocks differentiated (after Cocherie, 1986).

4.4.2Tectonic Settings of the Wonu, Ibadan-Apomu rocks

The Th-Hf/3-Ta concentrations of ultramafic-mafic rocks of Wonu, Ibadan-Apomu area are plotted in the diagram (Fig. 4.97) of Wood *et al.* (1979), which has been utilized to distinguish the tectonic settings of both ultramafic-mafic rocktypes. The fine-grained amphibolites rocks plotted dominantly within the volcanic arc basalts (field D) and within plate alkaline basalts (field C), while the lherzolite plot mainly within the volcanic arc basalts (field D). Some samples of both rocks plot at the transitional zones between the volcanic arc basalts, E-type mid-ocean ridge basalts (E-type MORB) and within plate alkaline basalt fields (Fig. 4.97a), indicating magma suites formed along subduction related destructive plate margins. The mafic-ultramafic rocks could be a dismembered ophiolite. The granitic rocks in the area plot within the syn-collisional granites (Syn-COLG), while the lherzolite plot within thevolcanic arc granites (VAG) field,indicating mantle plume-ridge interaction (Hofmann 1997). The talc schist straddle the lherzolite in the VAG field indicating derivation of the talc schist from the ultramafic rocks(Fig. 4.97b).

4.4.3 Parental magma and Magma source

Mineral chemistry of the Wonu, Ibadan-Apomu rocks indicated that they were not crystallized at pressures and temperatures typical of a shallow igneous intrusion. Typical ultramafic cumulate rocks of oceanic crust crystallize at shallow depths, with plagioclase crystallizing early in the sequence, directly after olivine and spinel. In the Bushveld complex, layered ultramafic-mafic rocks in which orthopyroxene is the major phase and clinopyroxene a minor phase, interstitial plagioclase are present in the lower zone (Hatton and Von Gruenewaldt, 1990). So, the Wonu, Ibadan-Apomu mafic-ultramafic rocks are neither typical layered intrusion nor typical ocean crust ophiolite.

Saunders and Tarney (1991) proposed a Ce/Nb versus Ce (Fig. 4.98a) and Ce/Nb versus Th/Nb (Fig. 4.98b) diagrams to characterise basaltic rocks.They distinguished ocean ridge basalts (N-type and E-type MORB), island arc basalt (IAB), back-arc basalt (BAB),ocean island basalts (OIB) andwithin plate basalts(Fig. 4.98b). TheWonu, Ibadan-Apomu mafic-ultramafic rocks clearly showed IAB for the lherzolite and BAB for the fine-grained amphibolite. The talc schist, on the other hand, reflect crustal contamination of OIB (Fig. 4.98b).

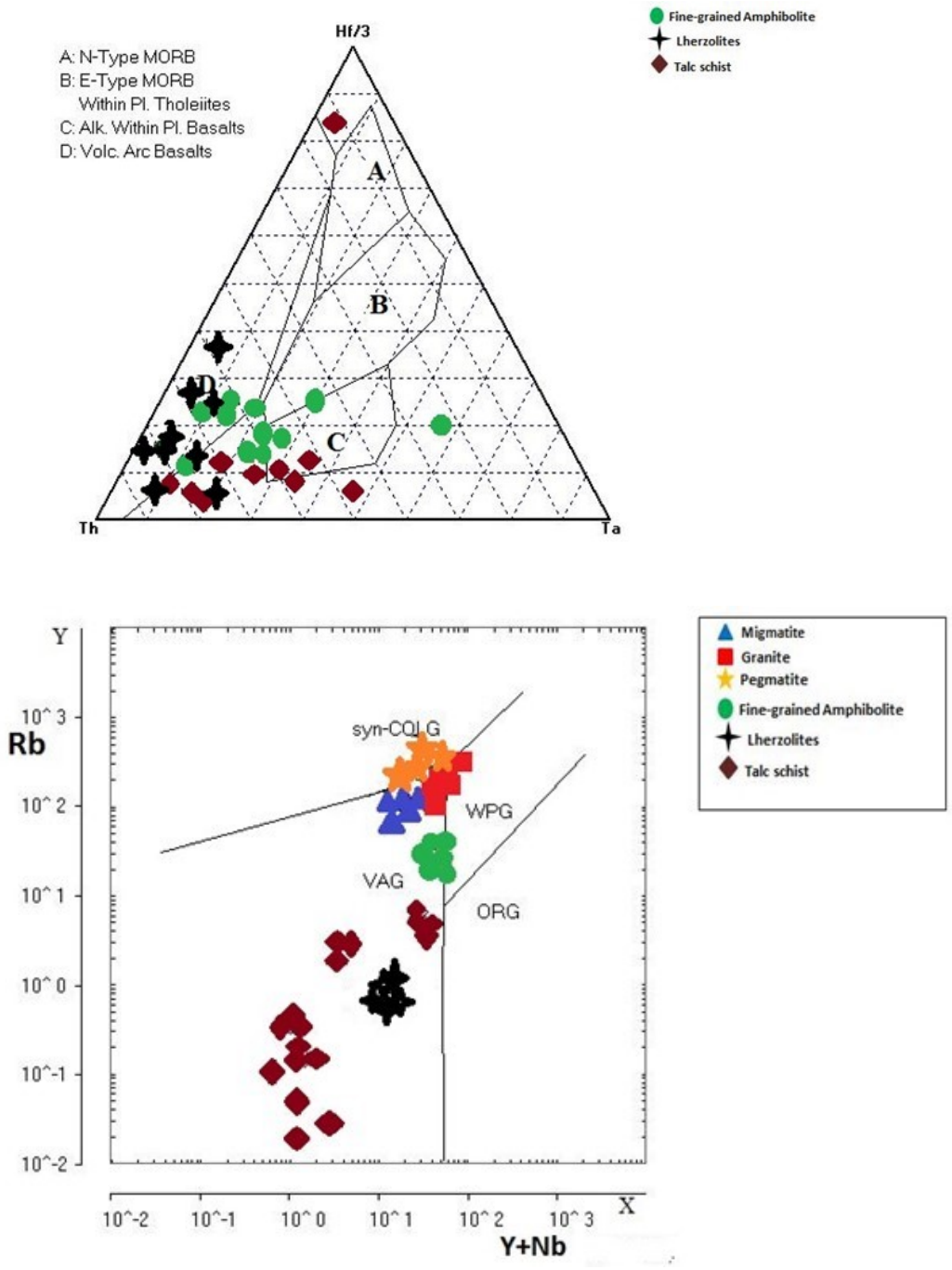

Fig. 4.97. (a) The Th-Hf-Ta plot after Wood *et al.* (1979).and (b) The Rb vs (Y+Nb) discrimination diagram (after Pearce *et al*. 1984) of the rocks of Wonu, Ibadan-Apomu area.

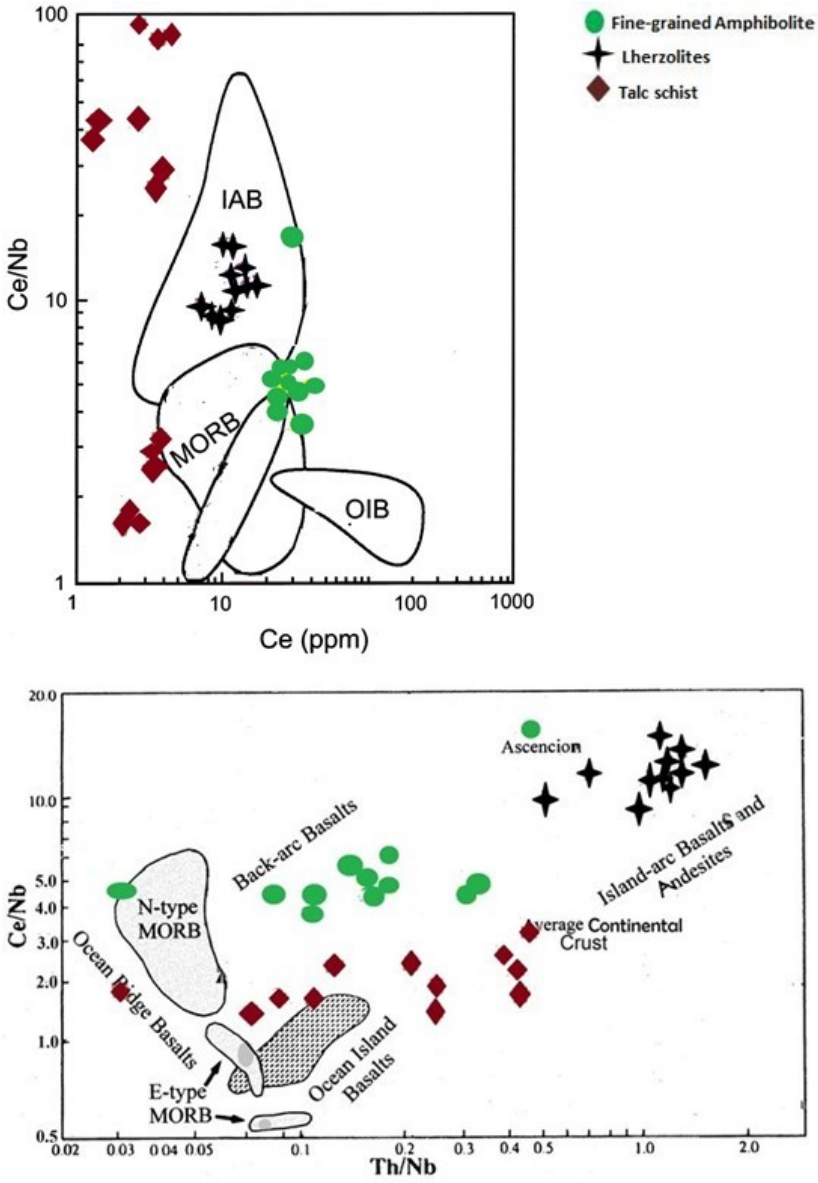

Fig. 4.98: The plot of (a) Ce/Nb vs Ce and (b) Ce/Nb vs Th/Nb of the ultramafic-mafic rocks of Wonu, Ibadan-Apomu area (after Saunders and Tarney (1991).

As shown in Fig. 4.99, the lherzolites are sourced from hydrated mantle (HM), while the amphibolite is sourced from enriched mantle (EM) and the talc schist depicted both enriched mantle (EM) and hydrated enriched mantle (HM) sources (Fig. 4.99). The presence of hydrated mantle and enriched mantle geochemical characteristics implied magma formation in different arc settings, notably back arc settings and fore arcsettings by hydrous melting of depleted mantle wedge source. The enriched mantle are products of decompression and melting of a lower crust-upper mantle plume magma with evidence of crustal contamination (Condie, 2015). The presence ofhydrated mantle material and the low-Ti suggested that convergent margin processes contributed to the petrogenesis of the rocks in Wonu, Ibadan-Apomu area.

4.4.4. Geothermobaromery of the Wonu, Ibadan-Apomu area rocks

Geothermometry determinations were based on the compositions of coexisting minerals. The methods of Balhaus *et al.*(1991) on the olivine and spinel Fe-Mg exchange, the Wells (1977) and Brey and Köhler (1990) based on two pyroxenes and on the Ca-in-orthopyroxene thermometry were used to estimate the range of temperature.

Temperature for coexisting olivine and Cr-spinel for the amphibolite after Balhaus *et al.* (1991) ranged between 700 and 800 ºC; and the lherzolite 900-1100 ºC. The low temperatures estimated for these amphibolite is due to the presence of amphibole and chlorite. The Fe-Mg exchange two pyroxene thermometers yield estimated temperatures of equilibration of between 700 and 1100 ºC. Difference of 200-400 ºC in temperature is not uncommon and may result from degrees of deformation and grain size variation within the samples. Deformation leads to grain size reduction and engender sub-solidus re-equilibration, which according to Kramer and Seifert (1991) reduces temperature. On the other hand, coarse grained samples record higher temperatures, sometimes above 1000ºC. Exolution textures in porphyroclastic pyroxenes indicate that higher temperatures of formation, greater than 1000 ºC, could also be achieved.

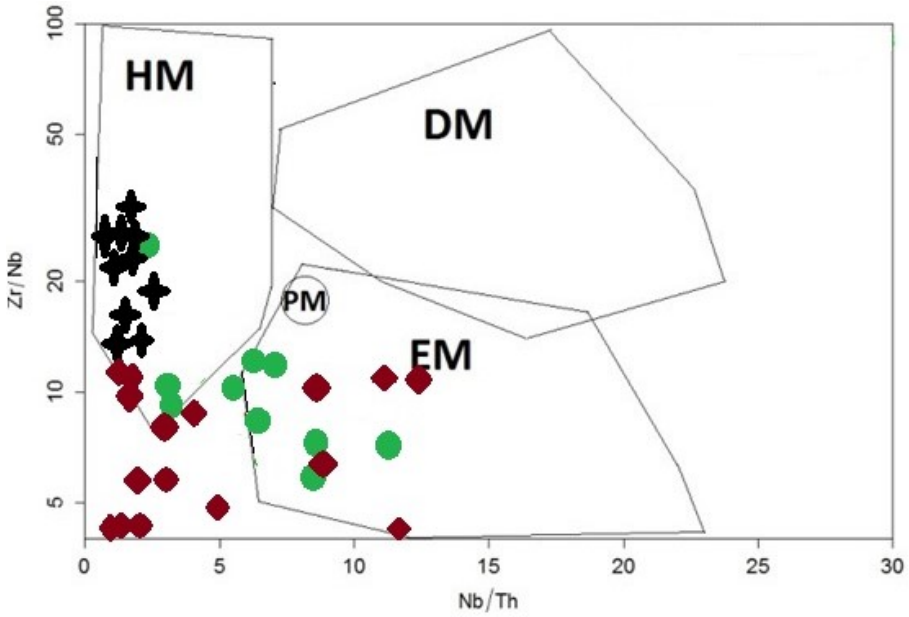

Fig. 4.99: The Zr/Nb versus Nb/Th diagram of theultramafic-mafic rocks of Wonu, Ibadan-Apomu area showing the compositional fields of the precursor rocks.

The temperature of 700 to 1100 ºC and the Cr# of greater than 0.8 are similar to values obtained in the oceanic arc peridotites of the Izu-Bonin forearc (Parkinson *et al.,* 1998). The average temperature calculated for the SSZ peridotites by Parkinson and Pearce (1998) was 647 ºC, which involved calculations from deformed peridotites.

Pressure estimation available for Cr-spinel peridotite is the Ca-in-olivine barometer (Köhler and Brey, 1990). With Ca-in-olivine apfu of 0.002-0.003 and the absence of plagioclase in the lherzolite, the rock must have been recrystallized at P > 6 kbar (Seyler and Mattson, 1989). The presence of Cr-spinel and the absence of garnet suggested that the pressure is less than 20 kbar within the stability field of spinel. With the presence of garnet-clinopyroxene symplectite in the fine-grained amphibolite, it is suggested that the magma may have crystalised at depth corresponding to >20 kbar but uplifted to higher level of < 10 kbar during crustal extension and later eruptions along deformed structures.

4.4.5Geodynamic significance

The lherzolites have high values of MgO (20-30 wt. %) and high CaO and Al_2O_3 concentrations. From the parameters of CaO-Al_2O_3-TiO_2 relationships,the lherzolite of Wonu, Ibadan-Apomu area are members of the Al-rich basaltic komatiites probably erupted from a not too deep mantle melts from subduction zones.These basaltic Komatitic rocks was proposed to originate through subduction processes(Allegre, 1982).

The mafic-ultramafic rocks of Wonu, Ibadan-Apomu area were generated in a same magmatic environment, which include both tholeiitic and calc-alkaline types.The presence of both tholeiitic and calc-alkaline magma could indicate a progressive change of the primitive magma type, reflecting the variable contribution of a slab-derived fluid component to the mantle wedge and the corresponding melting processes. There are some striking similarities in composition and mineralogy between plutonic rocks in island arcs and the rocks of the Wonu, Ibadan-Apomu area.

The ultramafic-mafic rocks of the study area with relatively low La/Nb and U/Nb ratios is similar to magmas formed from ocean island basalts(OIB) and normal (depleted) mid-ocean ridge basalts(N-MORB) sources (Fig. 4.100).

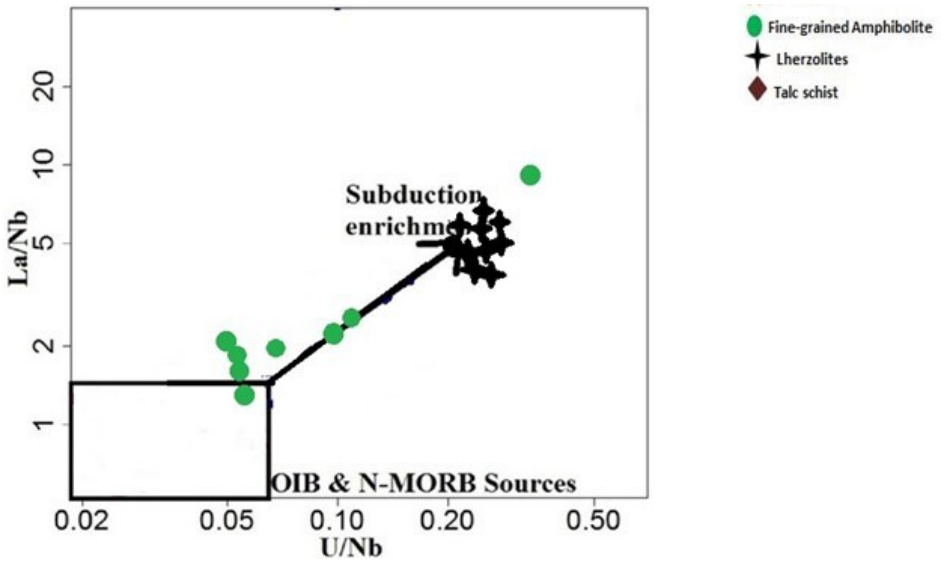

Fig. 4.100: La/Nb versus U/Nb ratios showing subduction enrichment of the Wonu, Ibadan-Apomu ultramafic-mafic rocks.

Geochemical variations in ultramafic-mafic rocks of Wonu, Ibadan-Apomu area indicate parental melts derived from a single primitive mantle source,hydrated for the lherzolites and the talc schist and enriched for the fine-grained amphibolites. The diagram in Fig. 4.101, showed the tectonic environment of the ultramafic-mafic rocks of Wonu, Ibadan-Apomu area after Pearce (2008).

Thebinary plots of trace element indicated that the fine-grained amphibolites are similar to those of the enriched mid-ocean ridge basalts (E-MORB), and the lherzolites, normal (depleted) mid-ocean ridge basalts (N-MORB). The talc schist occupiedboth the subducting sediment and the N-MORB zones. These chemical variations might be in line with derivation of the Wonu, Ibadan-Apomu rocks from multiple lithospheric mantle sources.

The mafic-ultramafic rocks of Wonu, Ibadan-Apomu area could be a dismembered ophiolite derived from the subduction of the lower oceanic crust, between eastern Ghana, Togo-Benin Republic and the gneissic terrain of southwestern Nigeria.

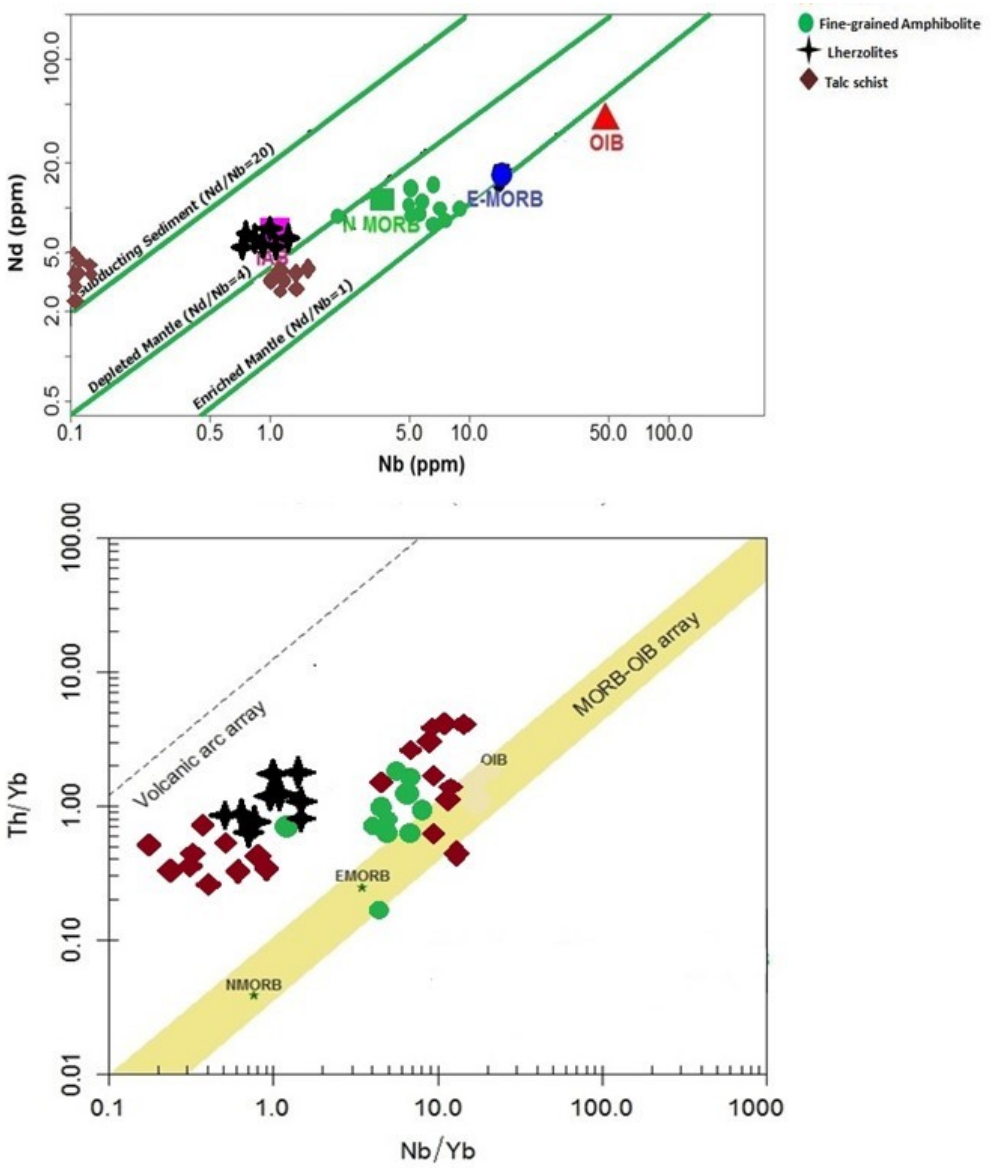

Fig. 4.101: Nd (ppm) versus Nb (ppm) and other trace elements binary plots of tectonic environment in the ultramafic-mafic rocks of Wonu, Ibadan-Apomu area.

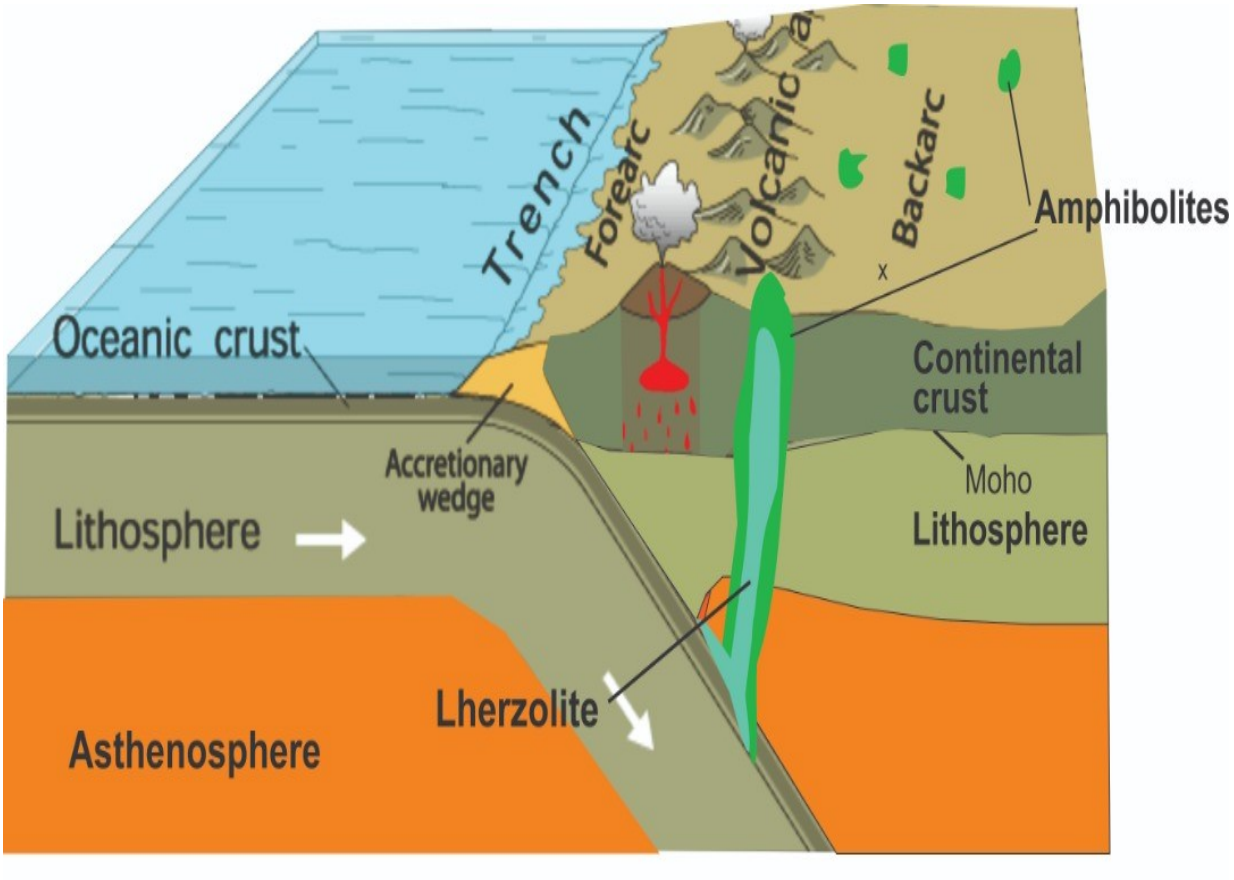

Fig. 4.102: Schematic diagram of the tectonic evolution model of mafic-ultramafic rocks of Wonu, Ibadan-Apomu area: showing ancient subduction zone and adjoining paleo mid-oceanic ridge setting.

CHAPTER FIVE

CONCLUSIONS

5.1 Conclusions

The Precambrian basement complex rocks of Wonu, Ibadan-Apomu area are migmatites, amphibolites, lherzolites and talc schists intruded by granites, pegmatites and quartz veins.The migmatites,granites, pegmatitesand quartz veins are felsic rocks while the amphiobolites, lherzolites (earlier referred to as coarse-grained amphibolites) and talc schists are ultramafic-mafic rocks.Cumulates and fracture-filling lenses of these amphibolites and lherzolites, which altered to talc schists occur as N-S, NE-SW and NW-SE mafic-ultramafic bodies within the dominantly gneissic terrain. NE-SW trending quartzite and veins occur within this gneiss-granite terrain. The amphibolite is fine-grained composed of actinolitic-hornblende, clinopyroxene, orthopyroxene and olivine. Biotite, chlorite, oligoclase, andesine and K-feldspars were <10%. Ilmenite, magnetite, garnet, and quartz were <5%. Disintegration of orthopyroxene to clinopyroxene-plagioclase symplectite, as well as, the presence of carbonate, graphite and chlorine reflected the serpentinisation of the amphibolite. The lherzolite, previously called coarse-grained amphibolites, is a lherzolite containing dominantly of olivines that altered to secondary orthopyroxenes.Other major minerals include primary orthopyroxenes with subordinate clinopyroxenes, tchermakitic-hornblende, magnesio-hornblende, garnet and spinel, alteration minerals include serpentine, amesite, talc, clinochlore and ferritchromite. Ferritchromite, ilmenite, pyrite, magnetite and plagioclase (bytownite) were <5% each. The talc schist is composed of talc, anthophyllite, Cr-bearing clinochlore, olivine, tremolite, amesite, serpentine, ferrichromite and magnetite.

The textural relationships (mineral morphology) and mineral phase chemistry deduced from SEM-EDS and the mineral chemistry (EPMA) data indicated magma crystallization at elevated pressures (6.0 - 8.4 kbar). The parental magma of the ultramafic-mafic rocks had been formed from an average to high degree of partial melting of a mantle source affected by previous metasomatic events above a subducted oceanic slab.

Ultramafic-mafic rocks of Wonu, Ibadan-Apomu area were metamorphosed under amphibolite facies conditions, with pressure of about 6 Kb and temperature of about 575°C (Sawyer, 1986). Evidence for this is the widely preserved prograde mineral zonation patterns found in the ultramafic-mafic rocks. A greenschist-facies metamorphism has overprinted the rocks of the Wonu, Ibadan-Apomu area to varying degrees.

The chromites within the talc schist in the study area had been locally precipitated to ferritchromite and the biotite had been altered to chlorite. The Cr/(Cr+Al) versus Fe^{2+} / (Fe+Mg) and the Al_2O_3 versus Cr_2O_3 of the ferichromite in the talc schist of the study area indicated stratiform source Cr-spinel that have been subjected to metasomatism. The Cr-TiO_2plot for the tectonised ultramafic rocks are found to be of almost the same characteristics as those of the supra-subduction zone (SSZ) of the Tethyan ophiolites.

The granitic rocks in the study area are of the calc-alkaline suite. The Al_2O_3-Fe_2O_3+TiO_2-MgO ternary plot, of the ultramafic-mafic rocks indicated Fe-rich tholeiitic basalt for the amphibolite, basaltic komatiite for the lherzolite and komatiite protoliths for the talc-schist.The amphibolites are tholeiitic suites, while the lherzolites and the talc schist are of komatitic progenitor. However, talc schistsdo plot within calc-alkaline suites due to silicification (> 60 % SiO_2), associated with the alteration by hydrothermal fluids sourced from the felsic intrusions (granites, pegmatites and quartz veins) within the ultramafic-mafic rocks.

The Ce/Nb versus Ce plot and the Ce/Nb versus Th/Nb plot of the trace element data of the ultramafic-mafic rocks indicated that the amphibolites originated from back-arc-basalts (BAB), the lherzolites island-arc-basalt (IAB) and the talc schist ocean ridge basalts (ORB) indicating lower oceanic to upper mantle sources.The-Hf-Ta discrimination diagram showed that the lherzolites and the amphibolites are volcanic arc basaltsaffected by post-subduction eruption of mantle or melted lower crust material.The Rb versus Y + Nb diagram of the granitic rocks in the area suggested syn-collision at subduction plate boundary.

The amphibolite is from an enriched (primordial/primitive) mantle while the lherzolite is from hydratedenriched(primordial/primitive) mantle. The talc schists occurred in the two zones. Some of the talc schist plotted in the subducting sediment zone and the others in the depleted mantle, island arc basalts (IAB). Hence the conclusion that the talc schist in the Womu-Ibadan-Apomu area is of two parent sources (metaigneous and metasedimentary).

The La/Nb versus U/Nb of the lherzolites indicated subduction enrichment. The Th/Yb versus Nb/Yb and Nd vs Nb diagrams of both the amphibolites the lherzolites suggested enriched mid-ocean ridge magma that suffered crustal contamination during ascent while talc schistsare hydrothermal alteration products of both the lherzolite and the amphibolite, thus indicating two protoliths for the talc schists.

The geochemical characteristics, especially the hydrated mantle source of the ultramafic-mafic rocks of Wonu, Ibadan-Apomu area, supports the conclusion that subduction processes had insignificant imput in the petrogenesis of the rocks. This also suggested that the parent rocks of the ultramafic-mafic rocks originated from heterogeneous mantle sources; a single primitive enriched source for the amphibolite and a hydrated enriched source for the lherzolite. The Zr/Nb versus Nb/Thand the Zr/Y versus Zr coroborates the above conclusion.The amphibolites showed a geochemical affinity to the mid-ocean ridge basalts, while the lherzolite showed that of an island-arc environment, indicating variable composition based purely on the level of contamination related to the evolving tectonic setting.

The overall geochemical characteristics of the ultramafic-mafic rock of Wonu, Ibadan-Apomu area can be summarised from the Nd versus Nb, La/Nb versus U/Nb, Th/Yb versus Nb/Yb and the Zr/Nb versus Nb/Th discrimination diagrams. These plots illustrate conciselythe most likely tectonic setting for the development of Archean to Proterozoic mantle heterogeneity, which is responsible for the generation of the ultramafic-mafic rocksin Wonu, Ibadan-Apomu area.

A greenschist-facies metamorphism associated with Late Pan-African events has overprinted the previous rocks.The hydrothermal fluids associated with this late stage granitic intrusions invaded the ultramafic-mafic rocks and altered the primary minerals, notably olivine, orthopyroxene, clinopyroxene and amphibole to secondary minerals, such as, serpentine, chlorite, amesite, saponite and talc. In somelocations the effects of hydrothermal alteration are minor, while in others they are pervasive. In the southeastern part of the Wonu, Ibadan-Apomu area the greenschist-facies metamorphism has virtually obliterated all evidence of the earlier amphibolite facies event. The intensity of retrogression in the area is spatially affliated to the Late Pan-African event that has obliterated the imprints of the Eburnean and older rocks. The schematic diagram of the tectonic evolution of

the mafic-ultramafic rocks of the study area (Fig. 4.102) indicated an ancient subduction zone and an adjoining paleo mid-oceanic setting.

5.2 Recommendations

It is recommended that isotope and fluid inclusion studies be carried out to determine the radiometric age and further information on temperature, pressure and the composition of the hydrothermal fluids. Radiometric dating would help resolve the issue of whether the lherzolite is of the same age with the amphibolites and whether the two rocks are Proterozoic. Also, platinum group elements (PGE) analysis is recommended in further studies to be able to determine the level and sequence of economic mineralisation. The study ofkomatiite-bearing ophiolites are usually supported by deep drilling to unravel the stratigraphy and the order of geologicalor tectonic events in the area. This could only be carried out with adequate financial support.

It is recommended that epidemiological investigation be carried out inthe talc mining sites in order to determine the possible effects of talc dust exposure to humans and the environment.

5.3 Contribution to knowledge

The contribution to knowledge in this work includes:

1. Modification of the geological map of Wonu, Ibadan-Apomu area, southwestern Nigeria to reflect the newly identified rock type (Lherzolite).
2. Determination of the petrogenesis of the granitic, mafic and ultramafic rocks in the study area, which varies from cal-alkaline through tholeiitic to komatitic protholiths, respectively.
3. Identification and determination of the mineral chemistry of some ore minerals,notably ferritchromite and metasomatic minerals, such as, amesite and saponite, which were used in the geothermobarometry and metasomaticalteration studies.
4. The genesis of the talc bodies was determined with the critical study of the altered transitional phases from primary mafic and ultramafic rocks.
5. Determination of the tectonic setting of the rocks to be syn-collisional, with island arc basaltic material, deposited near a supra-subduction zone.

REFERENCES

Abaa, S.J. 1983. The structure and petrography of alkaline rocks of the Mada Younger Granite Complex, Nigeria.*Journal of African Earth Science* 2:107-133

Abdel Rahman A.M.,1996 *"Pan-Africanvolcanism"*, petrology and geochemistry of theDokhan Volcanic suite in the northern NubianShield. Geol. Mag. 133 17-31.

Abdel-Rahman M. (1996).Geotechnical behaviour of shell foundations.Ph.D Thesis.Department of Civil Engineering, Concordia University, Montréal, Canada.

Abdel-Rahman, A. M. (1994). Nature of biotites from alkaline, calc-alkaline, and peraluminous magmas. *Journal of Petrology*35, 525–541.

Abdelsalam, M. G., Ligeois J. P., Stern, R. J., 2002. The Saharan metacraton, journal of African Earth Sciences 34 (3-4), 119-136.

Abiona, M..A. 1988. The petrography of rocks in Mokuro-Itagunmodi areas, Ife-Ilesha schist belt, Southwestern Nigeria, *Unpublished B.sc Thesis Obafemi Awolowo University, Ile-Ife.*62p

Abouchami, W., Boher, M., Michard, a. and Albarede, F. 1990. A major 2.1Ga event of mafic magmatism in West Africa: An early stage of crustal accretion. *Journal of Geophysical Research* 95: 0148-02

Abuquerque C. A.,1973 *"Geochemistry of biotites from granitic rocks, northern Portugal"*, Geochim.cosmochim. Acta 37, 1779- 1802.

Adekoya, J. A. 1988. Precambrian Iron-formation of northwestern Nigeria. *Precambrian Geology of Nigeria*. P. O. Oluyide, W. C. Mbonu, A. E. Ogezi, I. G. Egbuniwe, A. C. Ajibade and A. C. Umeji. Eds. Geological Survey of Nigeria Special Publication.195-210.

Adekoya, J.A., Kehinde-Phillips, O.O. and Odukoya, A.M.. 2003. Geological distribution of mineral resources in southwestern Nigeria. In: Elueze, A.A. (Ed.); *Prospects for Investment in Mineral Resources of Southwestern Nigeria*. Nigerian Mining and Geosciences Society Publication, pp. 1 – 13.

Adeola, A.J. 1988. Petrography of rocks around Ifewara area, southwestern Nigeria.*Unpublished B.Sc Thesis Thesis Obafemi Awolowo University Ife*, 62p.

Adetunji, A. Olarewaju, V. O., Ocan, O. O., Ganev, V. Y. and Macheva, L. 2015. Geochemistry and U-Pb zircon geochronology of the pegmatites in Ede area, southwestern Nigeria: a newly discovered oldest Pan-African rock in southwestern Nigeria. *Journal of African Earth Sciences* 115:177-190.

Adetunji, A. Olarewaju, V. O., Ocan, O. O., Macheva, L. and Ganev, V. Y. 2018. Geochemistry and U-Pb zircon geochronology of Iwo quartz potassic syenite southwestern Nigeria: constraints on petrogenesis, timing of deformation and terrane amalgamation. *Precambrian Research* 307:125-136.

Affaton, P., Rahaman, M.A., Trompette, R. and Sougy, J. 1991. The Dahomeyide Orogen: tectonothermal evolution and relationships with Volta Basin. In: Dallmeyer, R.D. and Lecorche. J.P. (Ed.). The *West African Orogens and Circum-Alantic Correlatives, Spinger-Verlag, Berlin,* pp 107-122.

Aggarwal, P.K. and Nesbitt, B.E. 1984. Geologgy and geochemistry of the Chu Chua massive sulfide deposit, British Columbia: *Economic Geology*, v. 79:815-825.

Agrinier P., Mever C., Bosch D., Javoy M., (1993) Earth and Planetary Science.

Ahmed, M.M., Ibrahim, G.A. and Hassan, M. M.A.2011.Beneficiation of talc Ore.*Journal of Earth and Enviromental sciences.*11:241-272.

Ajayi, T.R. 1980. On the geochemistry and origin of amphibolites in Ife-Ilesa area, southwestern Nigeria.*Journal of Mining and Geology,* 17 (2): 177 – 196.

Ajibade, A.C. and Fitches, W.R. 1988. The Nigerian Precambrian and the Pan-African Orogeny. In: Oluyide, P.O. (Ed): *Precambrian Geology of Nigeria,* Geological Survey of Nigeria, pp. 45 – 52.

Ajibade, A.C., Rahaman, M.A. and Woakes, M., 1987.Proterozoic crustal development in the Pan-African regime of Nigeria.in Proterozoic lithospheric evolution (Kroner, A., 3e.), American Geophysical Union 17, pp. 259-271

Akin-Ojo, O.A., (1992): Compositional and industrial studies of talc bodies in the Precambrian domain of South Western Nigeria, Ibadan, Nigeria. *Unpublished Ph.D Thesis, Universtiy of Ibadan, Nigeria.* 215p.

Allan J. F., Carmichael, I. S. E. 1984. Lamprophyric lavas in the Colima graben, SW Mexico.

Alt JC. Teagle DAH, Brewer T. Shanks WC III, Halliday A (1998) Alteration and mineralization of an oceanic forearc andthe ophiolite-ocean crust analogy. J Geophys Res 103:12365-12380.

Anderson, M.R., Rankin, A.H., Spiro, B. 1992. Fluid mixing in the generation of mesothermal gold minelisation in the ransval Sequence, Transval, South Korea.*Eur. J. Mineral*. 5, 933-948.

Andreola, F., Castellili, E., Ferreira, J., Olhero, S. and Romagnoli, M., 2006b, "Effect of sodium hexametaphosphate and ageing on the rheological behavior of kaolin dispersions", Applied Clay Science, Vol. 31, pp. 56–64.

Andreola, F., Castellili, E., Manfredini, T. and Romagnoli, M., 2006a, "The role of sodium hexametaphosphate in the dissolution process of kaolinite and kaolin", Journal of the European Ceramic Society, Vol. 24, pp. 2113–2124.

Andrew M. McCaig, Sofya S. Titarenko, Ivan P. Savov, Robert A. Cliff, David Banks, Adrian Boyce and Samuel Agostini, No Significant boron in the hydrated mantle of most subducting slabs*, Article doi: 10.1038/s4146-018-07064-6, Nature Communication.*

Andrews, A.J (1980) Saponite and celadonitc in Layer 2 Basalts, DSDP Leg 37.*Contrib Mineral* Petrol 73:323-340.

Andrews, P.R.A. 1985. "Laboratory study of the flotation circuit at Baker talc Inc. high water, Quebec".*CIM Bulletin,* Vol. 78

Andrews, P.R.A., 1989, "Pilot-plant treatment of Quebec talc ore", CIM Bulletin, Vol. 82, No. 932, pp. 76–81.

Annor, A. E. 1995. U-Pb zircon age for Kabba-Okene granodiorite gneiss: implication for Nigeria's basement chronology. *African Geoscience Review* 2.1:101-105.

Arai , S. 1994. Characterization of spinel peridotites by olivine-spinel compositional relationships: Review and interpretation. *Chemical Geology* 113(3-4):191-204.

Arai, S.; Miura, M. Podiform chromitites do form beneath mid-ocean ridges. Lithos 2015, 232, 143–149.

Arribas, A. Jr., Cunningham, C.G., Rytuba, J.J., Rye, R.O., Kelly, W.C., Podwysocki, M.H., McKee, E.H. and Tosdal, R.M. 1995. Geology, geochronology, fluid inclusions, and isotope geochemistry of the Rodalquilar gold alunite deposit, Spain.*Econ. Geol*. 90: 795–822.

Artemieva, I. M. (2003). Lithospheric structure, composition, and thermal regime of the East European Craton: implications for the subsidence of the Russian Platform. Earth and Planetary Science Letters, 213, 429-444.

Astolfi, A., Belluso, E., Ferraris, G., Fubini, B., Giamello, E., and Volante, M.(1991) Asbestiform minerals associated with chrysotile from Western Alps(Piedmont-Italy): Chemical characteristics and possible related toxicity. InR.C Brown, LA. Hoskists, and N.E. Johnson, Eds., Mechanisms in Fiber Carcinogenesis, 223, p. 269—283. NATOASI Series A: Life Sciences, Plenum Press, New York.

Asubiojo, O.I. and Ige, O.A., 1992. Rare earth element patterns in ultramafic rocks of the Schist Belt of south-western Nigeria by instrumental neutron activation analysis. J. Radioanal. Nucl. Chem vol. 158,1:193-200.

Baer, H.P. and Glaeser, R., 1998. The Mallam Tanko serpentines: Late-orogenic ultramafic intrusions on Pan-African Basement Complexes of NW-Nigeria. Precambrian Geology, Geological Survey of Nigeria, Kaduna: pp.165-173.

Bafor, B.E. 1998. Serpentinized Ultramafic photolytic in the Precambrian of N.W, Nigeria.In Metallogeny of basic and ultrabasic rocks. *Theophrastus publ. Athens* pp 121-135.

Baker, M.B., Grove, T.L., Price, R., 1994. Primitive basalts and andesites from the Mt Shasta region, N. California: products of varying melt fraction and watercontent. *Contrib. Mineral.Petrol*. 118, 111–129.

Balhaus, C., Berry, R. F. and Green, D. H. 1991. High pressure experimental calibration of the olivine-orthopyroxine-spinel oxygen geobarometer: implications for the oxidation state of the upper mantle. *Contrib. Mineral. Petrol.* 107: 27-40.

Ballantyne, P., 1992. Petrology and geochemistry of the plutonic rocks of the Halmahera ophiolite, eastern Indonesia, an analogue of modern oceanic forearcs. In: Parson, L.M., Murton, B.J., Browning, P. (Eds.), Ophiolites and their modern oceanic analogues. Geol. Soc. Spec. Pub. 60, 179–202.

Balliarano, P., Andreozzi, G. B., Belardi, G. 2008. Crystal chemical and structural characterization of fibrous tremolite from Susa Valley, Italy, with comments on potential harmful effects on human health. American Mineralogist, 93, 1349-1355.

Barnes, S. J., & Often, M. (1990). Ti-rich komatiites from northern Norway. Contributions to Mineralogy and Petrology, 105, 42-54.

Barnes, S.J.; Roeder, L.P. The range of spinel compositions in terrestrial mafic and ultramafic rocks. J. Petrol. 2001, 42, 2279–2302.

Baumgartner,R.J.;Zaccarini,F.;Garuti,G.;Thalhammer,O.A.R.Mineralogical and geochemical investigation of layered chromitites from the Bracco-Gabbro complex, Ligurian ophiolite, Italy. Contrib Mineral. Petrol. 2013, 165, 477–493.

Beard, B.L., Handler, R.M., Scherer, M.M., Wu, L. 2010. Iron isotope fractionation between acqueous ferrous iron and goethite. Earth and Pianetary Science.

Beccaluva, L., & Serri, G. (1988). Boninitic and low-Ti subduction-related lavas from intraoceanic arc back arc systems and low-Ti ophiolites – a reappraisal of their petrogenesis and original tectonic setting. Tectonophysics, 146, 291-315.

Beccaluva, L., Coltorti, M., Giunta, G., & Siena, F. (2004). Tethyan vs Cordilleran ophiolites: a reappraisal of distinctive tectonomagmatic features of supra-

subduction complexes in relation to the subduction mode. Tectonophysics, 393, 163-174.

Bedard, J. H., Harris, L. B., & Thurston, P. (2013). The hunting of the snArc. Precambrian Research, 229, 20-48.

Bernhard, F. and Gerd, F.T. 1997. Guide to literates of the Jos Plateau/ Petrographic and geochemical aspect of some selected laterites from Jos Plateau Central Nigeria. *Geol. Pal. Inst. U. Museum University of Hamburg Germany.*Pp 145.

Betrand, J.M.I. and Caby, R. 1978. Geodynamic Evolution of Pan-African orogenetic belt.A new interpretation of the Hoggar Shield (Algeria Sahara), *Geol. Rundsh*. 67: 357 – 388.

Bevins, R. E., Robinson, D., and Rowbotham, G. (1991) Compositional variations in mafic phyllosilicates from regional low-grade metabasites and application of the chlorite geothermometer: *J. Metam. Geol.* 9, 711-721.

Beziat, D., Bourges, F., Debat, P., Lompo, M., Martin, F. and Tollon, F. 2000. A paleoproterozoic ultramafic-mafic assemblage and associated volcanic rocks of the Boromo greenstone belt: Fractionates originating from island-arc volcanic activity in the West African craton. Precambrian Research. 101.

Bhatia, M.R. 1983. Plate tectonics and geochemical composition of sandstones.*Geology*, 91: 611 – 627.

Bigeleisen, J. and Mayer, M.G. 1947. Calculation of equilibrium constants for isotopic exchange reactions. 15:261-267.

Bigeleisen, J., Perham, M.L. and Prosser, I.C. 1952. Conversion of hydrogenic materials to hydrogen for isotopic analysis: *Analytical Chemistry*, V. 2: 1356-1357.

Bignon, L., Broehard, P., and Pairon, L.C. (1996) Mesothelioma: causes and fiber-related mechanism. In I. Aisner, MC. Perry, and MR. Green, Eds,, Comprehensive textbook of thoracic oncology, p. 735—756. t.ippincott, Williams, and Willcins, Baltimore.

Bishop, W. W., Pickford, M. and Hill, A. 1975. New evidence regarding the Quaternary geology, archeology and hominids of Chesowanja, Kenya. *Nature*.

Bjerkgard, T. and Bjorlykke, A. 1996. Sulfide deposits in Folldal, southern Trondheim region Caledonides, Norway: Source of metals and wall-rock alterations related to host rocks: *Economic Geology*, v. 91: 676-696.

Black, R. 1980.Precambrian of West Africa Episodes 4, 348.

Bodnar, R.J. 1993.Revised equation and table for determining the freezing point depression of H_2O-NaCl solution *Geochim.Co*smochim. Acta 57: 683-694.

Bodnar, R.J. 1995. Fluid-inclusion evidence for a magmatic source for metals in porphyry copper deposits. In: Thompson, J.F.H. _Ed.., *Magmas, Fluids, and Ore Deposits. Mineral. Assoc.* Can., Short Course Series, vol. 23: 139–152.

Bodnar, R.J., Reynolds, T.J., Kuehn, C.A. 1985.Fluid-inclusion systematics in epithermal systems. In: Berger, B.R., Bethke, P.M. _Eds.., Geology *and Geochemistry of Epithermal Systems.* Reviews in Economic Geology, Society of Economic Geologists, 2: 73–97.

Bodnar, R.J., Sterner, S.M. and Hall, D.L. 1989. SALTY: a fortran program to calculate compositions of fluid inclusions in the system NaCl-KCI-H_2O. *Computers & Geosciences* 15: 19-41.

Boghdady.G.Y., Ahmed, M.M., Ibrahim, G.A. and Hassan, M.M.A. 2005."Petrographical and Geochemical characteristics of some Egyptian talc samples for possible industrial applications".*Journal of Engineering Science Assuit University.*33 (3): 1001- 1011.

Boher, M., . Abouchami, W., Michard, A., Albarade, F. and Arndt, N. T. 1992. Crustal growth in West Africa at 2.1 Ga. *Journal of Geophysical Research: Solid Earth.* 97 (1): 345-369.

Boiron, M.C., Essarraj, S., Sellier, E., Cathelineau, M., Lespinasse, M. and Poty, B. 1992. Identification of fluid inclusions in relation to their host microstructural domains in quartz by cathodoluminescence.*Geochim.Cosmochim*. Acta 56: 175–185.

Bolarinwa, A. T. and Adepoju, A. A. 2017. Geochemical characteristics and tectonic setting of amphibolites in Ifewara area, Ife-Ilesha Schist Belt, southwestern Nigeria. Earth Science Research. 6 (1): 43-54.

Bolarinwa, A.T. 2001. Composition and industrial evaluation of talc bodies of Oke-Ila area, Ilesha Schist Belt, southernwestern Nigeria.*Mineral wealth*, 118, 48-52. pp.

Bolarinwa, A.T. and Adeleye, M.A. 2015a. Nature and origin of the amphibolites in the Precambrian basement complex of Iseyin and Ilesha Schist belts, southwestern Nigeria.*Journal of Geography and Geology*.7 (2): 6-17.

Bolarinwa, A.T. and Adeleye, M.A. 2015b. Petrogenesis and functional applications of talcose rocks *in* Wonu-Apomu and Ilesha areas, southwestern, Nigeria.*R.M.Z –materials and geoenvironment*.6.2. (2): 81-93.

Boulos, T.R., 2004, "Transforming upgrading of talc for different industrial application", Final Report supmeted to the Egyptian Academy for Scientific Research and Technology, pp. 1–54.

Boynton, W.V. (1984). Cosmochemistry of the rare earth elements; meteorite studies. *In: Rare earth element geochemistry. Henderson, P. (Editors), Elsevier Sci. Publ. Co., Amsterdam. 63-114.*

Brahmaiah T., Ch. Ravi, Imran Basha U., Sai Prasad K. S., 2019. Geochemistry and Tectonic Environments of Amphibolites Bethampudi Anorthosite Complex, Khammam Schist Belt, Telangana, India. WSN 126 (2019) 65-87.

Brey, G. P. and Kohler, T. 1990. Geothermobarometry in four-phase Lherzolites II. New thermobarometers, and practical assessment of existing thermobarometers. Petrology. Oxfordjournals. Org. 1354-1378.

Brown, G.C. 1982: Calc-alkaline intrusive rocks: their diversity, evolution, and relation to volcanic arcs. In Thorpe, R.S. (ed.) Orogenic andesites and related rocks. John Wiley, London, 437-61.

Buddington A.F., Lindsley D.H., "*Iron-titanium oxide minerals and synthetic equivalents*", J. Petrology 5 (1964) 310-357.

Burke, K.C. and Dewey, J.F. 1972.Orogeny in Africa in *African Geology*, edited by Desauveagie, T. F. J., and Whiteman, A.J Univ. Ibadan, pp 583-608.

Burnham, C.W., 1979. The importance of volatile constituents. In: Yoder, H.S. (Ed.), The evolution of the igneous rocks. Fiftieth Anniversary Perspectives, pp. 439–482.

Burns, L.E., 1985. The Border Ranges ultramafic and mafic complex, south-central Alaska: cumulate fractionates of island-arc volcanics. Can. J. Earth Sci. 22, 1020–1038.

Cabral, A.R., Wiedenbeck, M., Rios, I.J., GomesJr, A.A.S., Filho, O.G.R. and Jones, R.D. 2012.Talc mineralization associated with soft hematite ore, Gongosoco deposit, Minas Gerais, Brazil: Petrography, mineral chemistry and boron-isotope composition of tourmaline.*Miner Deposita.* 47:411-424.

Caby, R. 1989. Precambrian terrains of Benin, Nigeria and Northwest Brazil and Late Proterozoic South Atlantic fit, *Geological Society of America Special Paper,* 230:145 – 158.

Caby, R. and Boesse, J.M. 2001. Pan-African nappe system in southwest Nigeria: the Ife-Ilesha Schist belt. *Journal African Earth Sciences* 33: 21.

Cameron, W. E., McCulloch, M., & Walker, D. A. (1983). Boninite petrogenesis: chemical and Nd-Sr isotopic constraints. Earth and Planetary Science Letters, 65, 75-89.

Campbell, A.R. and Robinson-Cook, S. 1987. Infrared fluid inclusion microthermometry on coexisting wolframite and quartz.Econ. Geol. 82: 1640–1645.

Campbell, A.R., Hackbarth, C.J., Plumlee, G.S. and Petersen, U. 1984. Internal features of ore minerals seen with the infrared microscope. *Econ. Geol*. 79: 1387–1392.

Campbell, A.R.and Panter, K.S. 1990. Comparison of fluid inclusions in coexisting _cogenetic?.wolframite, cassiterite, and quartz from St. Michael's Mount and Cligga Head, Cornwall, England. *Geochim.Cosmochim. Acta* 54: 673–681.

Castaing, C., Feybesse, J.L., Thieblemont, D., Triboulet, C., Chevremont, P. 1993. Palaeogeographical reconstructions of thePan-African/Brasiliano orogen: closure of an oceanic domain or intracontinental convergence between major blocks? Precamb. Res., 69(1-4): 327-344.

Cathelineau, M. (1988). Cation site occupancy in chlorites and illites as a function of temperature: *Clay Miner.* 23, 471-485.

Cathelineau, M. and Nieva, D. (1985) A chlorite solid solution geothermometer. The Los Azufres (Mexico) geothermal system: *Contrib. Mineral. Petrol.* 91, 235 – 244.

Chalokwu, C. I., and Kuehner, S. M. (1992) Mineral Chemistry and thermobarometry of a southern Appalachian amphibolite with epidote plus quatzsympletite. *American Minerologist*, 77, 617 630.

Chang, L.L.Y., 2002, "Industrial mineralogy", Prentice Hall, New Jersey, pp. 398–407.

Chiaradia, M., Muntener, O., & Beate, B. (2011). Enriched basaltic andesites from mid-crustal fraction crystallization, recharge, and assimilation (Pilavo volcano, Western Cordillera of Ecuador). *Journal of Petrology*, 52, 1107-1141.

Claesson, L.A. 1985: The geochemistry 01 Early Proterozole metavolcanic rocks hosting massive sulphide deposits in the Skellelte district, northern Sweden. *J. Geol. Soc.* London 142. 899-909.

Clayton, R.N. and Mayeda, T.K. 1963. The use of BrF_5 in extraction of oxygen from oxides and silicates for isotope analysis: *Geochimical et Cosmochimica Acta*, 27: 43-52.

Clifford, T.N. 1970. *The Structural framework of Africa*. In Clifford, T.N and Gas, I.G. (eds). Oliver and Boyd, London.

Cocherie, A. 1986. Systematic use of trace element distribution patterns in log-log diagrams for plutonic suites. *Geochemical et Cosmochimica Acta* 50, 2517-2522.

Coleman**,** R.G. and Peteran**,** Z.E.1975. Oceanic plagiogranite. *Journal of Geophysical Research* (1896-1977).

Condie, K. (2015). Changing tectonic settings through time: indiscriminate use of geochemical discriminant diagrams. *Precambrian, research, 266* ,587-591.

Condie, K. C., & Kroner, A. (2013). The building blocks of continental crust: evidence for a major change in the tectonic setting of continental growth at the end of the Archean. *Gondwana Research*, 23, 394-402.

Condie, K.C. 1987: Early Proterozoic volcanic regimes in southwestern North America. In Pharaoh. T.C., Beckinsale, RD. & Rickard, D. (eos.) Geochemistry and Mineralization of Proterozoic Volcanic Suites. *Geol. Soc. Spec. Publ.* 33, 211-218.

Constantopoulos, SB., Saratzis, NA., Kontogiannis, D., Karantanas, A., Goudevenos, IA., and Katsiotis, 1'.(1987) Tremolite whitewashing and pleural calcifications.Chest, 92, 709—7 12.

Cooray, P.G. 1972. Note on the charnockitic of the Ado-Ekiti area, Western Nigeria. In *African Geology Ibadan* 1970.Eds. Dessauvagie and Whiteman Geol. Dept. Univ. Ibadan, Nigeria pp. 45-54.

Cooray, P.G. 1974. Some aspects of the Precambrian of Nigeria.A review.*Journal of mining and Geology.* Vol., 8 pp 17-43.

Corte, M. 1938. Reecherches sur l'optigue Am physique 10:33-405.

Cox, K.G., et al. (1979) The Interpretation of Igneous Rocks. Allen and Unwin, London, 450 p. .*Journal of Geophysical Research* (1896-1977) 80, 8, 1099-1108.

Crawford, A. J., Falloon, T. J. and Green, D. H. (1989) Classification, petrogcnesis and tectonic setting of boninites. *Boninites and Related Rocks* (Crawford, A. J., ed.), 1-49, Unwin Hyman, London.

Dada, S. S., Tubosun, I. A., Lancelot, J. R. and Lar, A. U. 1993. Late Archaean U-Pb age for the reactivated basement of northeastern Nigeria. *Journal of African Earth Sciences* 16:405-412.

Dada, S.S. 2006.Proterozoic evolution of Nigeria. In: Oshi, O (ed) *The basement complex of Nigeria and its mineral resources*. (A tribute to Prof M.A.O. Rahaman) Akin Jinad & Co. Ibadan pp 29-44.

Danbatta U. A. and Garba M. L. 2007. Geochemistry and Petrogenesis amphibolites in the Zuru schist belt, northwestern Nigeria. *Journal of Mining and Geology Vol. 43(1), pp. 23-30.*

Danbatta, U.A. 2003.The lithogeochemical framework underlyingthe geotectonic evolution of the Kazaure Schist Belt, NWNigeria.*The Nigerian Journal of Scientific Research*, 4(1): 1-13.

Darling, R.S. 1991. An extended equation to calculate NaCl contents from final clathrate melting temperatures in H_2OCO_2-NaCl fluid inclusions: Implications for P-T isochore location. *Geoschim.Cosmochim.*Acta 55: 3869-3871.

Date, A.R. and Hutchinson, D. 1987.The determination of trace elements in geochemical exploration samples by ICP-MS, *Spectrochim Acta* 41B: pp 175-181.

DeBari, S. M., Coleman, R.G., 1989. Examination of the deep levels of an island arc: evidence from the Tonsina ultramafic-mafic assemblage, Tonsina, Alaska*. J. Geophys. Res*.

DeBari, S. M., Kay, R. W., Kay, R. W. 1987. Ultramfic xenoliths from Adagdak Volcano, Adak, Aleutian Islands, Alaska: deformed igneous cumulates from the Moho of island arc. *J. Geol.* 95, 329-341

Deer, W.A., Howie, R. A., &Zussman, J. (1992). *An introduction to the rock-forming minerals.* 2nd ed. Harlow, Essex, England : New York, NY: Longman Scientific & Technical.

Deer, W.A., Howie, R.A. and Zussman, J. 1962.*An introduction to rock forming minerals*, Longman, London. 528p.

Depaolo, D.J. and Wasserburg, G.J. 1979b. Neodymium isotopes in flood basalt from the Siberian platform and inferences about their mantle sources, *Proceedings of the Natural Academy of Sciences U.S.A*, 76:3056-3060.

Derco, J. and Nemeth, Z., 2002, "Obtaining of high quality talc from talcose rocks: a case study from the Sinec Kokava deposits (Slovakia)", *Boletin Paranaense de Geociencias*, No. 50, pp. 119–130

De-Souza,Z., Martin, H., Peucat, J., Jardin de Sa, E.F. and Macedo, M.H. 2007.Calc-alkaline magmatism at the Archean- Proterozoic transition: The Caico complex basement (NE Brazil), *Journal ofPetrology* 48: 2149-2185.

Dick, H.J.B., Bullen, T., 1984. Chromian spinel as a petrogenetic indicator in abyssal and alpine- type peridotites, and spatially associated lavas. Contrib. *Mineral. Petrol*. 86, 54–76.

Dilek, Y., & Furnes, H. (2011). Ophiolite genesis and global tectonics: geochemical and tectonic fingerprinting of ancient oceanic lithosphere. *Geological Society of America Bulletin*, 123, 387-411.

Doherty, W.1989. An internal standerisation procedure for the determination of ytterium and the rare earth elements in geological materials by inductively coupled plasma mass spectrometry. *Spectrochim Acta* 44B: 263-280.

Egbuniwe, I.G. 1982. Geotectonic evolution of the Maru Belt, NW Nigeria.*Unpublished Ph.D.Thesis, University of Wales, Aberystwyth*, 411p.

Eggleton, R. A., Foudoulis, C., and Varkevisser, D. (1987) Weathering of basalt: Changes in rock chemistry and mineralogy: *Clays&ClayMinerals* 35, 16 1—169.

Ekwueme, B. N. and Kroner, A. 1997. Zircon evaporation ages and chemical composition of migmatitic schist in the Obudu Plateau: evidence for Palaeoproterozoic (ca 1789) components in the Basement Complex of southeastern Nigeria. *Journal of Mining and Geology* 33.2:81-88.

El-Sharkaway, M.F.2000. Talc mineraization of ultramafic affinity in the Eastern Desert of Egypt. *Mineralium Deposita*, 35: 346-363.

Elthon, D., Casey, J. F., Komor, S. 1982. Mineral chemistry of ultramfic cumulates from the North Arm Mountain massif of Bay of Islands ophiolite: evidence for high pressure crystal fractionation of oceanic basalts. *J. Geophys. Res.* 87, 8717-8734.

Elueze, A.A. 1977. Geological and geochemical studies in the Ilesa Schist belt in relation to gold mineralization. *Unpublished M. Phil Thesis,University of Ibadan, Ibadan, Nigeria,* 282p.

Elueze, A.A. 1981. Petrographic studies of metabasic rocks and meta-ultramafites in relations to mineralization in Nigerian schist belt. *Journal of Mining and Geology,* 18 (1): 31-36.

Elueze, A.A. 1982. Mineraology and chemical nature of meta-ultamafites in Nigerian schist belt.*Journal of Mining and Geology,* 19 (2): 21 – 29.

Elueze, A.A. 1985. Petrochemical and petrogenetic characteristicsof Precambrian amphibolites of the Alawa District, NWNigeria.*Chem. Geol*. 48: 29-41.

Elueze, A.A. 1988.Geology of the Precambrain Schist belt of Ilesa area, southwestern Nigeria. In: Oluyide, P.O. (Ed); *Precambrian Geology of Nigeria.* Geological Survey of Nigeria, pp. 77-82.

Elueze, A.A. and Akin-Ojo, O.A. 1993.Functional characteristics of talc bodies in South Western Nigeria.*Mineral Wealth*, Vol. 55: 7-14.

Elueze, A.A. and Dosumu, O.O. 1987.Preliminary investigation of industrial properties of magnesite-bearing rocks in TuganBako district, Tegina area NW Nigeria.*Nigerian Journal of Science,* 21:133-139.

Elueze, A.A. and Emofurieta, W.O. 1995. Field relationships, petrography and geochemistry of mafic units in Igbeti district, S.W Nigeria, in relation to their origin. *Nigerian Journal of Pure and Applied Sciences.* 10: 335-345

Elueze, A.A. and Kehinde-Phillips, O.O. 1992. Mineralogical and Geochemical feature of lateritic profiles above anthophyllitic Schist, Ita-Osun S.W. Nigeria. *Journ. Min. Geol.* 29 (2): 18.

Elueze, A.A. and Ogunniyi, S.O. 1985. Appraisal of talc bodies of the Ilesa district, southwestern Nigeria, and their potential for industrial applications. *Natural Resources and Development,* 21: 26 – 34.

Elueze, A.A. and Okunlola, O.A. 2003.Geochemical features and petrogenetic affinity of Precambrian amphibolites of Buum area, Central Nigeria.*Journal of Minnin and Goeology,* 39 (2): 71-78

Elueze, A.A., Bolarinwa, A.T. (2004). Petrochemistry and petrogenesis of granitic gneisses of Abeokuta area, southwestern Nigeria.*Journal of Mining and Geology*.40(1):1-8.

Engel, A. E. J., Engel, C. G. and Havens, R. G. 1965.Chemical characteristics of oceanic basalts and the upper mantle.*Geol. Soc. Am. Bull.* 76, pp. 719-734.

Engel, A.E.J. and Wright, L.A. 1960. "Talc and Soapstone" In Gillson, J.L, (Ed), Industrial Minerals and Rocks, *The American Inst. of mining, metallurgical and pet. Engineering (AIME)*, New York, 3rd ed., pp. 835-850.

Ersoy, B., Dikemen, S., Yildiz, A., Goren, R. and Elitok, O. 2013. Mineralogical and physiochemical properties of talc from Emirdag, Afyonkarahisar, Turkey.*Turkish Journal of Earth Sciences* 22: 1112-1114.

Eugster, O., Niedermann, S., Thalmann, C., Frei, R., Kramers, J., Kraehenbuehl, U., Liu, Y.Z., Hofmann, B., Boer, R.H., Reimold, W.U. and Bruno, L. 1995.Noble gases, K, U, Th, and Pb in native gold.*J. Geophys. Res*. B 100: 24677–24689.

Evans, B. W. (2008). Control of the products of sepentrinization by the Fe^{2+} Mg exchange potential of olivine and orthopyroxene.*Journal of petrology* 49, 1873-1887.

Falconer, J. D. 1911. The geology and geography of northern Nigeria. Macmillian London, 295. *Universal Journal of Geoscience* 2(3): 93-103.

Falloon, T. J. and Crawford, A. J. (1991) The petrogenesis of high-calcium boninite lavas dredged from the northern Tonga Ridge. *Earth Planet.Sci. Lett.* 102, 375-394.

Faure, G. 1977. *Principles of Isotope Geology*, Newyork.Wiley, 464p.

Feng, D. and Aldrich, C. 2004. Effect of ultrasonication on the flotation of talc", *Ind. Eng. Chem.,* Vol. 43, pp. 4422–4427.

Ferre, E. C., Deleris, J., Bouchez, J. L., Lar, A. U. and Peucat, J. J. 1996. The Pan-African reactivation of contrasted Eburnean and Archaean provinces in Nigeria: Structural and isotopic data. *Journal of Geological Society of London* 153:719-728.

Frantsesson, E. V. (1970) *The petrology of kimberlites.* Translated by D.A. Brown, Department of Geology Publication No. 150, Australian National University, Canberra.

Fubini B. (1993) *The possible role of surface chemistry in the toxicity of inhaled fibers.* In D.B. Wshreit, Ed., Fiber Toxicology, 11, p. 229—257. Academic Press, San Diego.

Fubini B. (1996) *Physico-chemical and cell free assays to evaluate the potential carcinogenicity of fibres.* In A.B. Kane, P. Boffetta, R.Saracci, and 3.Wilboum, Eds., Mechanisms of fiber carcinogenesis, IARC Scientific Publication 140.International Agency for Research on Cancer, Lyon.

Furnes, H., 2008. Oceanic pillow lavas and hyaloclastites as habitats for microbial life through time – A review. In: Dilek, Y, Furnes, H. Muehlenbachs, K. (eds) Links between geological processes, microbial activities and evolution of life. *Springer Science + Business Media,* pp 1-68.

Gale, N.H. 1981.Mediterranean Obsidian source characterization by strontium isotope analysis, *Archaeometry*. 23: 41-51

Gale, N.H. 1981.Mediterranean Obsidian source characterization by strontium isotope analysis, *Archaeometry.* 23: 41-51.

Gandu, A.H., Ojo S.B.and Ajakaiye D.E. 1986. A gravity study of the Precambrain rocks in the Malumfashi area of Kaduna State, Nigeria *Tectonophysics* 126:181-194.

Garba, I. 2000. Origin of Pan-African mesothermalgoldmineralisation at Bin Yauri, Nigeria *Journ.of African EarthSciences,* 31: 433-449.

Garrels, R.M. and Mackenzie, F.F. 1971. *Evolution of sedimentary rocks.*Published by W.W. Norton & co. Inc.New York, 394p.

Garuti,G.;Pushkarev,E.V.;Thalhammer,O.A.R.;Zaccarini,F.ChromititesoftheUrals: Overview of chromite mineral chemistry and geo-tectonic setting (part 1). *Ofioliti* 2012, 37, 27–53.

Gazzano, E., Turci, F., Riganti, C., Tomatis, M., Fubini, B., Bosia. and Ghigo, D. 2007. La tremolite nelle alpi occidental; test cellulari con prospettive tossicologiche. Workshop "Anfiboli fibrosi: nuove problematiche relative al rischio ambientale e sanitario. " *Roma.* 27-28, Abstracts, 73-74. (in Italian).

Gianfagna, A., Andreozzi, GB.,Baflirano, P., Mazziotti-Tagliani, S., and Bruni, B.M. (2007) Structural and chemical contrasts between prismatic and fibrous fluoro-edenite from Biancavilla, Sicily, Italy. *Canadian Mineralogist*, 45,249—262.

Gianfagna, A., Ballirano, P., Belistreccia, F., Bruni, B.M., Psoletti, L., and Oberti, It (20O3) Characterization of amphibole fibers linked to mesothelioma in the area of Biancavilla, Eastern Sicily, Italy. *Mineralogical Magazine*, 67,1221—1229.

Gill, T. 1981: Orogenic Andesites and Plate Tectonics. *Springer Verlag,* 390 pp.

Gilmour,P. S.,Brown,D.M.,Beswik,E. B.,Mscnee,W. ,Rahmsn, L. andDonaldson, K. (1997) Free radical activity of industrial fibers: Role of iron in oxidative stress and activation of transcription factors.*Environmental Health Perspectives,* 105 Suppl. 5, 1313—1317.

Giret, A., Bonin, B., Leger, J. M. 1980. Amphibole compositional trends in oversaturated and undersaturatedalkaline plutonic ring complexes. *Can. Mineral*. 18, 481-495.

Gleeson, S.A., Wilkinson, J.J., Boyce, A., Fallick, A.E. and Stuart, F.M. 1997b.On the occurrence and wider implications of anomalously low dD fluids in quartz veins, south Cornwall, England.*Chem. Geol*. 160: 161–173.

Glikson, A. Y. 1971. Primitive Archaen element distribution patterns: chemical evidence and geotectonic significance. *Earth Planet. Sci. Lett.* 12, pp. 309-320.

Graham, C.M. 1976. Petrochemistry and tectonic significance of Daldrian metabasaltic rocks of Scottish High lands.*Journal of Geological Society of London,* Vol. 132: 61 – 84.

Graham, C.M., Powel, R. 1984. A garnet-hornblende geothermometer calibration testing and application to the Pelone schist, Southern California.*J. Met. Geol.* 2, 13-33.

Grant, N. K. 1970. Geochronology of Precambrian basement rocks from Ibadan, southwestern Nigeria. *Earth and Planetary Science Letters* 10:29-38.

Green, T.H., 1982. *Anatexis of mafic crust and high pressure crystallization of andesite*. In: Thorpe, R.S. (Ed.), Andesites: Orogenic Andesites and Related Rocks. Wiley, New York, pp. 465–488.

Gunter, A. E., Buzon M. E., and McNamee, B. D. 2018. Current issues with purported "asbestos" content of talc: Asbestos nomenclature and examples in metamorphic carbonate and ultramafic hosted talc ores. *Transactions of the Society for Mining, Metallurgy & Exploration*, Vol. 344, pp. 15-24.

Gunter, M.E., Belluso, E., and Mottana, A. (2007) Amphiboles: Environmental and health concerns. In F.C. Hawthome, R. Oberti, G. Dells Ventura, and A. Mottana, Eds., Amphiboles: Crystal Chemistry, Occurrence, and Health Issues, 67, p. 453—516. *Reviews in Mineralogy and Geochemistry, Mineralogical Society of America*, Chantilly, Virginia.

Gurenko, A. A., & Kamenetsky, V. S. (2011). Boron isotopic composition of olivine-hosted melt inclusions from Gorgona komatiites, Colombia: new evidence supporting wet komatiite origin. *Earth and Planetary Science Letters,* 312, 201-212.

Hamiton, P.J., Evenson, N.M., O'Nions, R.K. and Tarney, J. 1979.Sm-Nd systematic of Lewisian gneiss: implications for the origin of granulites.*Nature* 277: 25-28.

Harley, S.L. 1989. The origin of granulites: a metamorphic perspective *Geol. Mag*. 126:215-247.

Hastie, A. R., Mitchell, S. F., Kerr, A. C., Minifie, M. J., & Millar, I. L. (2011). Geochemistry of rare high-Nb basalt lavas: are they derived from a mantle wedge metasomatized by slab melts? *Geochimica et Cosmochimica Acta*, 75, 5049-5072.

Hatton, C. J., Von Gruenewaldt, G. 1990. *Early Precambrian layered intrusions*. In: Hall, R. P., Hughes, D. J. (eds) Early Precambrian Basic Magmatism. 56-82.

Hedequist, J.W. and Henley, R.W. 1985. The importance of CO_2in freezing point measurements of fluid inclusions; evidence from active geothermal systems and implications for epithermal ore deposition.*Econ. Geol*. 80: 1379-1406.

Heinrich, C. A., Ryan, C. G., Mernagh, T. P. and Eadington, P. J. 1992. Segregation of ore metals between magmatic brine and vapor; a fluid inclusion study using PIXE microanalysis. *Econ. Geol*. 87: 1566–1583.

Heinrich, C.A., Bain, J.H.C., Fardy, J.J. and Wring, C.L. 1993. Br/Cl geochemistry of hydrothermal brines associated with proterozic metasediment-hosted copper mineralized at mount Isa, northern Australia. *Geochin.Cosmochim*. Acta 57: 2991-3000.

Hey, M. H. 1954. A new review of the chlorite. *Mineral. Mag.,* 30:227-292.

Hill, I. G., Worden, R. H. and Meighan, I. G. 2000. Geochemical evolution of a paleolaterite: the Interbasaltic Formation, Northern Ireland. *Chemical Geology* 166: 65-84.

Hirdes, W., Davis, D. W., Ludke, G., Konan, G. 1996. Two generations of Birimian (Paleoproterozoic) volcanic belts in northeastern Cote d'Ivoire (West Africa): consequences for the 'Birimian controversy'. *Precambrian Research*. 80, 173-191.

Hofmann, A. W. 1997. Mantle geochemistry: the message from oceanic volcanism. *Nature* 385: 219-229.

Holland, T., Blundy, J. 1994. Non-ideal interactions in calcic amphiboles and their bearing onamphibole-plagioclase thermometry. *Contr. Mineral. and Petrol.* 116, 433–447.

Holt, R., Egbuniwe, I.G., Fitches, W.R. and Wright, J.B. 1978. The relationships between Low-Grade metasedimentary belts, Calc-Alkaline Volcanism and the Pan African Orogeny in N.W. Nigeria.41 *Geol. Rundsch*.Ed. 67. Heft 2, Seite 631-646.

Honkamo, M. 1987. Geochemistry and tectonic setting of earlyProterozoic volcanic rocks in Northern OshuthotriaFinland,In: Pharaoh T.C., Beckingsale R.D., Richard D. (Eds.)Geochemistry and mineralisation of Proterozoic volcanic suites.*Geol. Soc. Spec. Publ.38, 231.*

Hooker, P.J., O'Nions, R. K. and Pankhurst, R. J. 1975.Determination of rare earth elements in USGS standard rocks by mixed solvent ion exchange and mass-spectrometric isotope dilution *Chem. Geol. 16,* pp 189-199

Hubbard, F.H. 1975. Precambrian crustal development in WesternNigeria; indications from the Iwo region.*Geol. Soc. Am. Bull.*86, pp. 548-554.

Huston, D.L., Bolgar, C., and Cozens, G. 1993. A comparison of mineral deposits at the Gecko and White Devil deposits: Implications for orc genesis in the Tennant Crock district, Northern Territory, Australia.*Economic Geology*, v. 88., p. 1198-1225.

Ige, O. A. and Holness, M.B. 2002.Parageneses, conditions and timing of metamorphism of the metapelitic rocks in the Ilesa schist belt, southwestern Nigeria. *Journal of Mining and Geology*, 38: pp. 71-79.

Ige, O. A., Okrusch, M., Schussler, U., Schmadicke, E. and Cook, N., (1998).The metamorphic mafic ultramafic rocks of Mokuro.Ilesa schist belt.African *Journal of Earth Sciences.*

Ige, O.A. 1888. Mineralogical and industrial properties of some Wonu Apomu talcs, western Nigeria. *Nigerian Journal of Science,* Vol. 19, pp. 121 – 130.

Ige, O.A. 1988. Mineralogical and geochemical studies of some talc bearing ultramafic and associated mafic rocks in the Apomu and Ife-Ilesha areas of southwestern Nigeria. *Unpublished Ph.D, Thesis, Univesity of Ile-Ife* 247 pp.

Ige, O.A. and Asubiojo, O.I. 1991. Trace element geochemistry and petrogenesis of some meta-ultramagites in Apomu and Ile-Ilesha areas of southwestern Nigeria.*Chemical Geology* 91 pp 19 -32.

Ige, O.A., Durotoye, B. and Oluyemi, A.E. 2005.Mineralogy and geochemistry of lateritic weathering profiles on ultramafic rock bodies around Mokuro in Ile-Ife area, Southwestern Nigeria.*Journal of Mining and Geology*. Vol. 41, No. 1, p. 11-18.

Ilgren, E. B., & Hoskins J. A. (2018b). Anthophyllite Asbestos: The Role of Fiber Width in Mesothelioma Induction Part 2: Further epidemiological studies of occupational, domestic and environmental exposure to Finish Anthophyllite asbestos. *Environment and Pollution,* 7(1), 24-35.

Ilgren, E. B., & Hoskins J. A. (2018c). Anthophyllite Asbestos: The Role of Fiber Width in Mesothelioma Induction Part 3: Studies of American and Japanese Anthophyllite Asbestos – Additional Supportive Evidence. *Environment and Pollution,* 8(2).

Ilgren, E. B., & Hoskins, J. A. (2018a). Anthophyllite Asbestos: The Role of Fiber Width in Mesothelioma Induction Part 1: Epidemiological Studies of Finnish Anthophyllite Abestos. *Environment and Pollution,* 7(1), 9-23.

Ilgren, E. B., Van Orden, D. R.., Lee, R. J., Kamiya, Y. M., & Hoskins, J. A. (2015). Further Studies of Bolivian Crocidolite - Part IV: Fibre Width, Fibre Drift and their relation to Mesothelioma Induction: Preliminary Findings. *Epidemiology, Biostatistics and Public Health, 12(2),* e1167 pp. 1-11.

Ingram, M.G. and Chupka, P. 1953. Surface ionisation source using multiple filaments. *Rev. Sci. Instrum,* 24, 518-20.

Inoue, A., Kurokawa, K. and Hatta, T. 2010. Application of chlorite geothermometry to hydrothermal alteration in Toyoha geothermal system, southweastern Hokkaido, Japan. *Resource Geology.* 60 (1) 52-70.

Irvine, T. N. 1967. Chromian spinel as a petrogenetic indicator. Part. 2. Petrographic applications. *Can. J. Earth Sci*. 4, 71–103.

Irvine, T. N. and Baragar, W.R. A. 1971.A guide to the chemical classification of the common volcanic rocks.*Canadian journal of Earth Sciences, 8,* 523-548.

Irvine, T.N. 1965. Chromian spinel as a petrogenetic indicator. Part I. Theory. *Can. J. Earth Sci.* 1965, 2, 648–672.

Irvine, T.N. 1967. Chromian spinel as a petrogenetic indicator. Part II. Petrological application. *Can. J. Earth Sci*. 4, 71–103.

Ishiwatari, A. 1985. Igneous petrogenesis of Yakuno ophiolite (Japan) in the context of the diversity of ophiolites. *Contributions to Mineralogy and Petrology*. 89, 155-167.

Ishizuka, O., Yuasa, M., Tamura, Y., Shukuno, H., Stern, R. J., Naka, J., Joshima, M., & Taylor, R. N. (2010). Migrating shoshonitic magmatism tracks Izu-Bonin-Mariana intra-oceanic arc rift propagation. *Earth and Planetary Science Letters,* 294, 111-122.

Janousek, V., Vrana, S., Erban, V., Vokurkak, Milano (2009) Metabasic rocks in the varied group of the Moldanubian Zone, Southern Bohemia – their petrology, geochemical character and possible petrogenesis.

Jaques, A. L., Green, D. H., 1980. Anhydrous melting of peridotite at 0–15 kb pressure and the genesis of tholeiitic basalts. *Contrib. Mineral. Petrol*. 73, 287–310.

Jarvis, K.E. 1989. Determination of rare-earth elements in geological samples by inductively coupled plasma mass spectrometry*J. Anal.Atom. Spectrom* 4 pp. 563-570.

Jarvis, K.E., Gray, A.L and Houk, R.S. 1992.*Handbook of the inductively Coupled Plasma Mass Spectrometry,* Blackie, Glasgow and London.

Javis, K.E. 1988. ICP-ins: a new technique for the rapid, ultra-trace determination of rare earth elements in geological materials. *Chem. Geol*. 68, pp 31-39.

JCPDS, 1974. Selected powder diffraction data for minerals 1st edition, (Ed. L.G. Berry), *Joint Committee on Powder Diffraction Standard*, Philadelphia,833p.

Jenkin, G.R.T., Craw, D. and Fallick, A.E. 1994. Stable isotopic andfluid inclusion evidence for meteoric fluid penetration into an active mountain belt; Alpine Schist, New Zealand.*J. Metamorphic Geol*. 12, 429–444.

Jenner, F. E., Bennett, V. C., Nutman, A. P., Friend, C. R. L., Norman, M. D., & Yaxley, G. (2009). Evidence for subduction at 3.8 Ga: geochemistry of arc-like metabasalts from the southern edge of the Isua Supracrustal Belt. *Chemical Geology*, 261, 83-98.

Jenson, L. S. 1976. A new cation ploy for classifying subalkalic volcanic rocks: Ontario Deprtment of Mines, Miscellaneous Paper 66.

Kamenetsky, V.S.; Crawford, A.J.; Meffre, S. 2001. Factors controlling chemistry of magmatic spinel: An empirical study of associated olivine, Cr-spinel and melt inclusions from primitive rocks. *J. Petrol.* 2001, 42, 655–671.

Kehinde Philips, O.O. and Tiez, G.F. 1995. The Mineralogy and Geochemistry of the weathering profiles over amphibolites and talc-schist in the Ilesha Schist belt, Southwestern Nigeria. *Journ. Min. Geol*. 31 (1) pp 59-62.

Kelmm, D.D., Schneider, W. and Wagner, B. 1978.Geological and geochemical investigations of the metasedimentary belts of Ife-Ilesa area of S.W. Nigeria. (abstr) *Conf. on African Geology.*Univ.of Ibadan, July 1978.

Kennedy W.G. 1966. *The structural differentiation of Africa in the Pan African Tectonic episode*.8th Annual Representative Research Trust.African Geological Society of London Geology Leeds, 48-50.

Kho, C.J. and Sohn, H.J., 1989, "Column flotation of talc", *International Journal of Mineral Processing,* Vol. 27, pp. 157–167.

Khraisheh, M., Holland, C., Creany, C., Harries, P. and Parolis, L., 2005, "Effect of molecular weight and concentration of the adsorption of CMC onto talc at different ionic strengths"*, International Journal of Mineral Processing,* Vol. 75, pp. 197–206.

Kilik, J. (1997) Geological characteristics from talc deposit GemerskaPoloma-DlhaDolina. *ActaMontanisticaSlovaca* 2: 71-80.

Kimball, K. L. 1985. Compositional variations in spinels from hydrothermally altered abyssal ultramafics. *Trans. Am. Geophys. U*. 66:432.

Klemm, D.D, Schneider, W. and Wagner, B. 1984.The Precambrian meta-volcano-sedimentary sequence east of Ife-Ilesa, southwestern Nigeria.A Nigerian "greenstone belt"?*Journal of African Earth Sciences,* Vol. 2, No. 2, pp. 161-176.

Knoper, M. W. and Condie. K. C. (1988) Geochemistry and petrogenesis of Early Proterozoic amphibolites, West-Central Colorado, U.S.A. *Chem*. *Geol*. 67, 209-225.

Kontinen, A. 1987: An Early Proterozoic ophiolite - the Jormua malic-ultramalic complex, northeastern Finland. *Precamb. Res*.• 313-341.

Kramer, M. J. and Seifert, K. E. 1991. Strained enhanced diffusion in feldspars: Diffusion, atomic ordering, and mass transport. *Springer* 286-303.

Kusky, T. M., & Polat, A. (1999). Growth of granite-greenstone terranes at convergent margins and stabilization of Archean cratons. *Tectonophysics*, 305, 43-73.

Kusky, T. M., Windley, B. F., Safonova, I., Wakita, K., Wakabayashi, J., Polat, A., & Santosh, M. (2013). Recognition of ocean plate stratigraphy in accretionary orogens through Earth history: a record of 3.8 billion years of sea floor spreading, subduction and accretion. *Gondwana Research* 24, 501-547.

Laird, J. and Albee 1981.High pressure metamorphism in mafic schist from Northern Vermont.*Am. J. Sci.* 281, 97-126.

Laird, J., 1988. Chlorites: metamorphic petrology. In Bailey, S. W. (Ed.) Hydrous Physllosilocates.*Mineral Soc. Am.*, Paul H. Ribbe Ser., 19: 405-453.

Lattanzi, P. 1991. Applications of fluid inclusions in the study and exploration of mineral deposits.*Eur. J. Mineral*. 3, 689–701.

Le Bas, M. J.and Streckeisen, A. L. (1991): The IUGS systematics of igneous rocks. *Journal of the Geological Society* 148(5):825-833.

Le Bas, M. J. (2000) IUGS reclassification of the high-Mg and picritic volcanic rocks.*J. Petrol*. 41, 1467-1470.

Le Maitre. R. W. (2002) *Igneous Rocks:A Classification and Glossary of Terms*. 2nd ed., Cambridge Univ. Press, Cambridge, 236 Pp.

Leake, B; Woolley, A.; Arps, C; Birch, W.; Gilbert, C; Grice, J.; Hawthorne, F.; Kato, A.; Kisch, H.; Vladimir, K.; Linthout, K.; Laird, J.; Mandarino, J.; Maresch, W.; Nickel, E.t; Rock, N.; Schumacher, J.; Smith, D.; Stephenson, N.; Guo, Y. 1997. Nomenclature of amphiboles; Report of the Subcommittee on Amphiboles of the International Mineralogical Association, Commission on New Minerals and Mineral Names.*American Mineralogist* .82(2): 1019-1037.

Lee, S.H and Choi, G.J.1994. Phase equilibrium between co-existing minerals in the talc ores and process of talc formation in the Daeheung talc deposits, Korea, J. *Petrol. Soc. Korea* 3,3 156-170 (In Korean).

Lemen. (2015. Conference presentation: Asbestos fiber toxicities" (available on request).

Leslie, R. A. J., Danyushevsky, L. V., Crawford, A. J., & Verbeeten, A. C. (2009). Primitive shoshonites from Fiji: geochemistry and source components. *Geochemistry, Geophysics, Geosystems,* 10.

Lichte, F.E., Meler, A.L. and Crock, J.G. 1987.Determination of rare earth elements in geological materials by ICP-MS, *Anal. Chem*. 59, pp 1150-1157.

Linder, D.A, Wylic, A.G. and Candela, P.A. 1992. Mineralogy and origin of the Statc linc talc deposit, Pennsyvannia: *ECONOMIC GEOLOGY*, v. 87, p. 1607-1615.

Lippard, S.J., Shelton, A.W., Gass, I.G., 1986. *The Ophiolite of northern Oman*. Geological Society of London, Memoir 11, Blackwell, Oxford.

Liu, W., Emst, J.D., and Bmsddus, V.C. (2000) Phagncytosis ofcrocidolite asbestosinduces oxidstive stress, DNA damage, and apoptosis in mesothelial cells.American *Journal of Respiratory Cell and Molecular Biology,* 23, 371—378.

Longerich, H.P., Fryer, B.J. and Strong, D.F. 1987.Determination of lead isotope ratios by inductively of rare earth elements by ICP-MS, *Spectrochim. Acta* 43B, pp 75-93.

Lugli, S., Morteani, G., Blamart, G. 2002.Petrographic, REE, fluid inclusion and stable isotope study of magnesite from the upper Triassic Burano Evaprites (Secchia valley, northern Apennines): contribution from sedimentary, hydrothermal and metasomaticsources. *Mineralium Deposita*. 37:480-494

Luthers, V., Gutzmer, J. and Beukes, N.J. 1999. Fluid inclusion studies in cogenetic hematite, hausmannite, and gangue minerals from high-grade manganese ores in the Kalahari manganese field, South Africa. *Econ. Geol*. 94, 589–596.

Malachovsky P, Turanova L, Dianiska I (1992*) Final report of mineral exploration from GemerskaPoloma.*Slovak Geological Survey, Spisska Nova Ves (Archive), pp 1-132.

Malomo, S., 2004. *National Geological Map of Nigeria, 1:2,000,000*. Nigerian Geological Survey Agency, Abuja, Nigeria.

Manikyamba, C., Kerrich, R., Khanna, T. C., Keshav Krishna, A., & Satyanarayanan, M. (2008). Geochemical systematics of komatiite-tholeiite and adakitic-arc basalt associations: The role of a mantle plume and convergent margin in formation of the Sandur Superterrane, Dharwar craton, India. *Lithos,* 106, 155-172.

Manikyamba, C., Kerrich, R., Khanna, T. C., Satyanarayanan, M., & Keshav Krishna, A. (2009). Enriched and depleted arc basalts, with Mg-andesites and adakites: A potential paired arc- back-arc of the 2.6 Ga Hutti greenstone terrane, India. *Geochimica et Cosmochimica*Acta, 73, 1711-1736.

Manikyamba, C., Kerrich, R., Polat, A., Raju, K., Satyanarayanan, M., & Krishna, A. K. (2012). Arc picrite-potassic adakitic-shoshonitic volcanic association of the Neoarchean Sigegudda greenstone terrane, western Dharwar craton: transition from arc wedge to lithospheric melting. *Precambrian Research,* 212-213, 207-224.

Manson, V. 1967.*Geochemistry of basaltic rocks: major elements*. In: Hess H. H. and Poldervaart, A. (eds.) Basalts 2 Interscience New York, pp. 15-39.

Marine, M., Allan, H. W., Gelu, C., Yong, Y., Jullieta Enone Lum, Shao-Yong Jiang, Fred Jourdan, Gordon Chunnett and Mihaela-Elena Cioaca, The Mafic-Ultramafic Dykes in the Yanbian Terrane (Sichuan Prrovince, SW China): Record of Magma Differentiation and Emplacement in the Emeishan Large Igneous Province, *Journal of Petrology*, 2017, Vol. 58, No. 3, 513-538.

Martuzzi, M., Comba, P., De Santis, M., Lavarone, I., Di Pi, M., Mastrantonio, M., and Pirastu, R. (1999)Asbestos-related lung cancer mortality in Piedmont,Italy.*American Journal of Industrial Medicine*, 33, 565—570.

Mastrantonio,M.,Belli,S.,Binazzi,A.,Cssboni,M.,Comba,P., Fusco, P., Grignoli,M., Lavarone, I., Marsuzzi, M., Nessi, M., Trines, S., and Uccelli, I. T.(2002) IstitutoSuperiore di SanisI. La morsslitd per tumorcmaligno dells pleura neicomuniitaliani (1988—1997) Rapporti ISTISAN 02/12,27 p. (in Italian).

Maurel, C.; Maurel, P. Étude experimental de la distribution de l′aluminium entre bain silicate basique et spinel chromifere. Implications pétrogenetiques: Tenore en chrome des spinelles. *Bull. Mineral.* 1982, 105, 197–202. (In French).

Mavrogenes, J.A., Bodner R.J., Anderson, A.J., Bajt, S., Sutton S.R. and Rivers, M.L. 1995a. Assessment of the uncertainties and limitations of quantitative elemental analysis of individual fluid inclusion using synchrotron X-ray fluorescence (SXRF).*Geochim.Cosmochim.* Acta 59, 3987-3995.

Mavrogenes, J.A., Bodner, R.J., Graney, J.R., Mc Queen, K.G. and Burilinson, K. 1995b. Comparison of decrepitation, microthermometric and compositional characteristics of fluid inclusions in barren and auriferous mesothermal quartz veins of the Cowra Greek gold district, new South Wales, Australia. J. *Geochem. Explor.* 54, 167-175.

McCarthy, E. F., Genco, N. A., and Reade, E. H. Jr., 2006, "*Talc",Industrial Minerals and Rocks,* J. E. Kogel, N.C., Trivedi, J.M. Barker and S. T. Krukowski, eds., Society for Mining, Metallurgy & Exploration, Englewood, CO, pp. 971-986.

McCurry, P. 1970.The geology of Degree sheet 21 (Zaria) in Thesis, Ahmadu Bello University, Nigeria. (unpublished).

McCurry, P. 1973. Geology of degree sheet 21, Zaria, Nigeria.*Overseas Geology Mineral Research*. 45:1-30.

McCurry, P. 1976. *The geology of the Precambrian to lower Palezoic rocks of northern Nigeria* – a review. In: Kogbe, C.A. (ed): Geology of Nigeria, Elizabethan Publishing Co., Lagos, pp. 15 – 39.

McDonough, W. F., & Sun, S. S. (1995). The composition of the Earth. *Chemical Geology*, 120, 223-253.

McDonough, W. F., Sun. S.-S., Ringwood, A. E., Jagoutz. E. and Hofmann, A. W. (1992) K, Rb and Cs in the earth and moon and the evolution of the earth's mantle.*Geochim*.*Cosmochim*.*Acta* 56, 1001-1012.

McGctchin, T. R., Nikhanj, Y. S. and Chodos, A. A. (1973) Carbonatite-kimberlite relations in the Cane Valley Diatreme, San Juan County, Utah. *Journal of Geophysical Research,* 78, 1854—1.869.

McLoughlin, N. Furnes, H. Banerjee, N.R. Muehlenbachs, K. Staudigel, H. 2009. Ichnotaxonomy of microbial trace fossils in volcanic glass. *Journal of the Geological Society* 166: 159-169.

McNamee, B. D., & Gunter, M. E. (2014). Compositional Analysis and Morphological Relationships of Amphiboles, Talc and Other Minerals Founds in the Talc Deposits from the Gouverneur Mining District, New York (Part 2 of 2). *The Microscope,* 62(1), 3-13.

Meeker, GE, Bern, A.M., Brownfield, 1K., Lowers, HA., Susley, 5.3., Boefen, T.M., and Vance, J.S. (2003) The composition and morphology of amphiboles from the Rainy Creek Complex, near Libby, Montana. *American Mineralogist*, 88, 1955—1969.

Meen, J. K. (1989). Formation of shoshonites from calcalkaline basaltic magmas: geochemical and experimental constraints from the type locality. *Contributions to Mineralogy and Petrology,* 97, 333-351.

Melcher, F.; Grum, W.; Simon, G.; Thalhammer, T.V.; Stumpfl, F.E. Petrogenesis of the ophiolitic giant chromite deposits of Kempirsai, Kazakhstan: A study of solid and fluid inclusions in chromite. *J. Petrol.* 1997, 38, 1419–1438.

Michard, A. 1989. Rare earth element systematics in hydrothermal fluids, *Geochimica et CosmochimicaActa*, 53, 3, 745-750.

Middlemost, E.A.K .1994. Naming materials in magma/igneous rocksystem.*Earth Sci* Rev 37:215–224

Middleton, E.V. 1960. *Chemical composition if sandstone.*Bulletin geological society of America*,* Vol(7), pp.1011-1026.

Milodowski, A.E., Gillespie, M.R., Naden, J., Fortey, N.J., Shepherd, T.J., Pearce, J.M.and Metcalfe, R. 1998. The petrology and paragenesis of fracture mineralization in the Sellafield area, west Cumbria.*Proc. Yorkshire Geol. Soc*. 52, 215–241.

Mints, M. V., Belousova, E. A., Konilov, A. N., Natapov, L. M., Shchipansky, A. A., Griffin, W. L., Kaulina, T. V. (2010). Mesoarchean subduction processes: 2.87 Ga eclogites from the Kola Peninsula, Russia. *Geology*, 38, 739-742.

Mitchell, R. S. and Giardini, A. A. (1977) Some mineral inclusions from African and Brazilian diamonds: their nature and significance. *American Mineralogist.*62, 756—762.

Miyashiro, A. 1974.Volcanic rock series in island arcs and active continental margins. *America journal of science.*274, pp. 321-355.

Moine, B., Fortune, J.P., Morcau, P. and Viguier, F. 1989. Comparative mineralogy, geochemistry, and conditions of formation of two metasomatic talc and chlorite deposits Trimouns (Pyrcnccs, France) and Rabenwald (Eastern Alps, Austria): *Economic Geology*, v. 84, p. 1398-1416

Montanez, I.P. 1996. Application of cathodoluminescent cement stratigraphy for delineating regional diagenetic and fluid migration events associated with Mississippi Valley-type mineralization in the Southern Appalachians. In: Sangster, D.F. (Ed), Carbonate-hosted Lead–Zinc Deposits. *Society of Economic Geologists*, Special Publication, vol. 4, pp. 432–447.

Moores, E. M., & Vine, F. J. (1971*). The Troodos massif, Cyprus, and other ophiolites as oceanic crust: evaluation and implications*. Philosophical Transactions of the Royal Society of London Series A, 268, 443-466.

Morimoto, N. (1998). Nomenclature of Pyroxenes. *Mineralogy and Petrology* 39, 55–76.

Morimoto, N., Fabries, J., Ferguson, A. K., Ginzburg, I. V., Ross,M., Seifert, F. A., Zussman, J., Aoki, K. &Gottardi, G. 1981. Nomenclature of pyroxenes. *American Mineralogist* 73,1123-1133.

Mucke A. 2005.The Nigeria manganese-rich iron-formations and their host rocks-from sedimentation to metamorphism.*Journal Africa Sciences* 41, pp. 407-436.

Mucke, A. and Woakes, M., 1986. Pyrophanite: a typical mineral in the Pan-African Province of Western and Central Nigeria. *Journal of African Earth Sciences* 5., p. 675-689.

Mucke, A., 2003. Magnetite, ilmenite and ulvite in rocks and ore deposits: petrograph, microprobe analyses and genetic implications. *Mineralogy and Petrology* 77, pp. 215-234.

Nachit, H., Ibhi, A., Abia, E. H. and Ohoud, M. B. 2005. Discrimination between primary magmatic biotites, requilibrated biotites and neoformed biotites. *C.R. Geoscience*, 337, 1415-1420.

Naemura, K., Hirajima, T., Svojtka, M. (2009). The Pressure – Temperature Path and the Origin of Phlogopite in Spinel – Garnet Peridotites from the lansky

Les Massif of the Moldanubian Zone, Czech Republic. *Journal of Petrology* 50, 1795-1827.

Naldrette, A.J. 1966. Talc-carbonate alteration of some serpentinised ultramafic rocks South of Timmins, Ontario, *Journ petrology* 7, 160-164.

Nasr, B.B. and Masoud, M.S. 1999. "Geology and genesis of Wadi Alaqi talc deposit South Eastern desert, Egypt". *Annal Geol. Survey*.Egypt , Vol. XXII, pp. 309-317.

Nesbitt, B.E. and Muchlenbachs, K. 1994. Palcohydrology of the Canadian Rockies and origin of brines, Pb-Zn deposit and dolomittization in the Western Canada sedimentary basin: *Geology*, v. 22, p. 243-246.

Nesbitt, H.W. and Bricker, O.P. 1978 .Law temperature alteration processes affecting ultramafic bodies. *Geochim.et.Cocmochim.Acta*. 42, pp403-409.

Neumann, E.R., AbuEl-Rus, M.A., Tiepolo, M., Oholin, L., Vannucci, R., and Whitehouse, M (2015) Serpentinization and Deserpentinization reactions in the Upper Mantle beneath Fuerteventure revealed by periodite xenoliths with fibrous orthopyroxene and mottled olivine. *Journal of petrology*, 56(1), 3-31.

Nimis, P., Tesalina, S. G., Omenetto, P., Tartarotti, P. and Lerouge, C.2004. Phyllosilicate minerals in the hydrothermal mafic-ultramafic-hosted massive-sulphide deposit of Ivanovka (southern Urals): comparison with modern ocean seafloor analogues. *Contrib. Mineral Petrol*. 147: 363-383.

Noack, Y., Decarrcu, A., and Manccu, A. 1986. Spectroscopic and oxygen isotopic evidence for low and high temperature origin of talc: *Bulletin Mincralogic*, v, 109, p. 253-263.

Obaje, N.G. 2009.*Geology and Mineral resources of Nigeria*. Lecture Notes in Earth sciences Springer.

Ocan, O. O. 1991. The petrology of rocks around Idanre area, southwestern Nigeria. *PhD Thesis*. Department of Geology, Obafemi Awolowo University, Ile-Ife. xxii+397p.

Odeyemi, I.B. 1981.A review of orogenic events in the Precambrian basement of Nigeria, West Africa.*Geologische Rundschan*, 70 (3), 897-090.

Ogezi, A. E. O., 1977. .E. 1977. Geochemistry and geochronology of basement rock from northwestern Nigeria. *Unpublished Ph.D. Thesis, University ofLeeds.* 259 pp.

Ogezi, A. E. O., 1988. *Geochemistry and origin of ensialic Alpine-type serpentinite associations from Mallam Tanko (Shemi) and Ribah (Wasagu), Northwestern Nigeria.* Precambrian Geology, Geological Survey of Nigeria, Kaduna, pp. 257-276.

Okonkwo, C.T. and Winchester, J.A. 1996. Geochemistry and geotectonic setting of Precambrian amphibolitesand granitic gneisses in the Jebba area, Southwestern Nigeria.*J.Min. Geol*. 32(1), pp. 1-18.

Okunlola, O.A., Akintola, A.J. and Egbeyemi, R.O. 2007.Geological setting, petrochemistry and petrogenetic affinity of Precambrian amphibolite of Lema-Ndeji area, central, Nigeria.*Mineral wealth* 144pp 47-554 .

Okunola, O.A., Ogedengbe, O. and Ojutalayo, A., 2003."Composition features and industrial appraisal of the Babe Ode talc occurrence, South Western Nigeria", *Global Journal of Geological Science*, Vol. 1, No, 1, pp. 63-72.

Olabaniyi, S.B. and Annor, A. E., 2003.Petrology and age implication of ultramafic schist in the Isanlu area of the Egbe-Isanlu schist belt, southwestern Nigeria. *Journal of Mining and Geology* 39, pp.

Olade, M.A. and Elueze, A.A.1979. Petrochemistry of the Ilesaamphibolites and Precambrian crustal evolution in the Pan-African domain of southwestern Nigeria.*Precambrian Research*, Vol. 8, pp. 303 – 318.

Olarewaju, V.O and Ajayi, T.R. 1993. Microprobe studies of main ferromagnesian minerals in the amphibilites of Ife-Ilesha Schist Belt, South-west Nigeria. *Jour. Min. & Geol*. 29 (2): 50-69.

Olarewaju, V.O and Ajayi, T.R. 1993. Microprobe studies of main ferromagnesian minerals in the amphibilites of Ife-Ilesha Schist Belt, South-west Nigeria. *Jour. Min. & Geol*. 29 (2): 50-69

Olayinka, A.I. 1992.Geophysical siting of boreholes in crystalline basement areas of Africa.*J Afr Earth Sci* 14:197-207.

Olobaniyi, S. B., 2008. Petrochemistry and tectonic setting of metabasic rocks of Isanlu, southwest Nigeria.*Global journal of Geological Sciences* 6, pp. 113-122.

Olobaniyi, S. B., Adekeye, J. I. D. and Annor, A. E., 2001. Chemical character of garnets in semipelitic schist and banded iron-formation, in relation to the metamorphic history of the Isanlu area, southwestern Nigeria. *Journal of Mining and Geology* 37:1-6.

Olobaniyi, S.B. 2006. Mineral chemistry and metamorphic conditions of Isanlu amphibolites southwest Nigeria.*European journal of sciences and research* 13, pp 119-131.

Olobaniyi, S.B. and Mucke, A. 2011.Chemical composition of chromite and intergrown chlorite in metamorphosed ultramafic rocks (serpentinite and talc schist) of the Egbe-Isanlu schist-belt, southwestern Nigeria: genetic implicatins. *Journal of Mining and Geology,* 47: (2), pp 115-134.

Ouzegane, K., Bendaoud, A., Kienast, J-R. and Touret J.L.R. 2001.Pressure-temperature fluid evolution in Eburnean metabasites and metapelites from Tamanrasset, Hoggar, Algeria.*Journal of Geology*. 109:247-263.

Oyawoye, M.O. 1972. *The basement complex of Nigeria.*Edited by T.F.J. Dessauvagie, and A.J. Whiteman (eds) African Geology. Ibadan University Press, pp. 67 – 99.

Ozkan, A. 2003. "Coagulation and flocculation characteristics of talc by using different flocculants in presence of cations", *Minerals Engineering*, Vol. 16, pp. 59-61.

Park, H.I, Lee, I.S., Hur, S.D. and Shin, D.B. 1997. Talc mineralization in the middle Ogchean metamorphic belt (II): peongien talc deposit. *Econ. Environ. Geol*. 30, 543-551 *(in Korean).*

Parkinson, C. D., Miyazaki, K., Wakita, K., Barber, A. J. and Carswell, D. A.1998. An overview and tectonic synthesis of the pre-Tertiary very-high-pressure metamorphic and associated rocks of Java, Sulawesi (Indonesia): constraints on the Cenozoic geodynamic history of the Sunderland active margin. *Tectonophysics* 272, 69-92.

Parkinson, I.J. and Pearce, J.A. (1998): Peridotites from the Izu-Bonin-Mariana forearc (ODP Leg 125): Evidence for mantle melting and melt-mantle interaction in a supra-subdution zone setting. *Journal of Petrology*, **39(9)**, 1577-1618.

Pearce, J. A. 1980. *Geochemical evidence for the genesis and eruptive setting of lavas from Tethyan ophiolites*, in: Panayiotou, A. (Ed.). Ophiolites. Geological Survey Department, Cyprus, 261-272.

Pearce Julian, Baker, P., Edwards, S. Parkinson, Ian, Leat, Philip (2000).Geochemistry and tectonic significance of peridotites from the South Sandwich Arc–Basin system, South Atlantic.*Contributions to Mineralogy and Petrology*36, 53, 139.

Pearce, J. A. (2008). Geochemical fingerprinting of oceanic basalts with applications to ophiolite classification and the search for Archean oceanic crust. *Lithos*, 100, 14-48.

Pearce, J. A., Harris, N. B. W. & Tindle, A. G. (1984). Trace element discrimination diagrams for the tectonic interpretation of granitic rocks. *Journal of Petrology*25, 956–983.

Pearce, J. A.and Norry, M. J. 1979. Petrogenetic implication of Ti, Zr, Y and Nb varieties in volcanic rocks.*Contribution to Mineralogy and Petrology*, 69, 33 – 92.

Pearce, T. H., Gorman, B. E., and Birkett, T. C. 1975. The $TiO_2 – K_2O – P_2O_5$ diagram – a method of discriminating between oceanic and non-oceanic basalts. *Earth Planetary Science Letter*, 24, 419 – 426.

Percival, J. B. Ames, D.E. (1993) Clay mineralogy of active hydrothermal chimneys and an associated mound.Middle Valley, northern Juan de Fuca Ridge.*Can Mineral* 31:957-971.

Petrasova, K., Faryad, S. W., Jerabek, P., Zackova, E. (2007) Origin and metamorphic evolution of a magnesite-talc and adjacent rocks near GemerskPoloma, Slovak Republic. *Journal of Geosciences,* 52, 125-132.

Petrasova, K., Faryad, S. W., Jerabek, P., Zackova, E. (2007) Origin and metamorphic evolution of a magnesite-talc and adjacent rocks near GemerskPoloma, Slovak Republic. *Journal of Geosciences,* 52, 125-132.

Pettijohn, F.I. 1975. *Sedimentary rocks*, Haper and Row, New York, 628p.

Piercey, S. J., Murphy, D. C., Mortensen, J. K. and Paradis, S. (2001) Boninite magmatism in a continental margin setting. Yukon-Tanana terrane, southeastern Yukon, Canada.*Geology* 29, 731-734.

Piga, L. and Marruzz, G., 1992, "Preconcentration of an Italian talc by magnetic separation and attrition", *International Journal of Mineral Processing*, Vol. 35, pp. 291–297.

Piolatto, G. (1996) Valori di riferimento e valorilimite per l'amisnto, In C. Aprea, G. Sciarn, M.L. Fiorcntino, and C. Minois, Eds., I valori di riferimento e i vslorilimitenellsprevenzionesmbientale e occupazionale, p. 153—161. Morgan EdizioniTecniche, Milnno (in Italian).

Poidevin, J. L. (1994) Boninite-like rocks from the Paleoproterozoic greenstone belt of Bogoin, Central African Republic: geochemistry and petrogenesis. *Precamb.Res*. 68, 97-113.

Polat, A., & Kerrich, R. (2001). Magnesian andesites, Nb-enriched basalts-andesites and adakites from late Archean 2.7 Ga Wawa greenstone belts, superior Province, Canada: implications for Late Archean subduction zone petrogenetic processes. *Contributions to Mineralogy and Petrology,* 141, 36-52.

Polat, A., & Kerrich, R. (2002). Nd-isotope systematics of ~2.7 Ga adakites, magnesian andesites, and arc basalts, Superior Province: evidence for shallow crustal recycling at Archean subduction zones.*Earth and Planetary Science Letters,* 202, 345-360.

Polat, A., & Munker, C. (2004). Hf-Nd isotope evidence for contemporaneous subduction processes in the source of late Archean arc lavas from the Superior Province, Canada. *Chemical Geology,* 213, 403-429.

Polat, A., Appel, P. W. U., & Fryer, B. J. (2011). An overview of the geochemistry of Eoarchean to Mesoarchean ultramafic to mafic volcanic rocks, SW Greenland: implications for mantle depletion and petrogenetic processes at subduction zones in the early Earth. *Gondwana Research,* 20, 255-283.

Potra, A. and Macferlane, A.W. 2014. Lead Isotope studies of Gruerrero sComposite Terrane, west-central Mexico: Implications for Ore genesis. *Minerallum Deposita,* vol 49, 1:101-117.

Prinz, M. (1967).*Geochemistry of basaltic rocks: trace elements.* In: Hess HH Poldervaart A. (Eds.) Basalts 2 Interscience New York, 271 – 325.

Prochaska, W. 1989.*Geochemistry and Genesis of Austrian Talc deposits,* Applied Geochemistry 4, 511-525.

Qasim Jan. M., 1990. Petrology and Geochemistry of the Southern Amphibolites of the Kohistan Arc, N Pakistan. In: Sharma K. K. Geology and Geodynamic Evolution of the Himalayan Collision Zone (Part 1*), Physics and Chemistry of the Earth*. *Vol. 17, II, 71-92.*

Rahaman M.A. 1988. *Recent advances in the study of the basement complex of Nigeria.* In: Geological Survey of Nigeria (ed) Precambrain Geol Nigeria, pp 11-43.

Rahaman M.A. and Ocan, O. 1978.On relationships in the Precambrian Migmatite-gneisses of Nigeria.*Nigeria Journal of Mining and Geology*. 15: 23-32.

Rahaman, M.A. 1976. Review of the basement geology of southwestern Nigeria. In: Kogbe, C.A. (eds): *Geology of Nigeria.* Elizabethan Publishing Co., Lagos. pp. 41 – 58. Nh ,

Rajamani, V., Shivkumar, K., Hanson, G. N. and Shirey, S. B. (1985) Geochemistry and petrogenesis of amphibolites, Kolar schist belt. South India: evidence for komatiitic magma derived by low percentage of melting of the mantle. *J. Petrol.* 26, 92-123.

Rankin, A.H., Ramsey, M.H., Coles, B., Van Langevelde, F. and Thomas, C.R.1992.The composition of hypersaline, iron-rich granitic fluids based on laser-ICP and synchrotron-XRF microprobe analysis of individual fluid inclusions in topaz, Mole granite, eastern Australia.*Geochim.Cosmochim*. *Acta* 56, 67–79.

Read, H.H. 1934a.Metamorphic geology of Unsust in the Shetland Island. *Quat. Jour. Geol. Soc.* 360, pp 637-688.

Read, H.H. 1943a. On Zoned associations of antigorite, talc, actinolite, chlorite and biotite in Unst, Shetland Island, *Mineralogical Mag*. 23, pp 519-540.

Richards, J.P. and Kerrich, R. 1993. Observations of zoning and fluid inclusions in pyrite using a transmitted infrared light micro-scope _lF1.9 mm.*Econ. Geol*. 88, 716–723.

Roedder, E. 1967a. Fluid inclusions as samples of ore fluids. In: Barnes, H.L. _Ed.., *Geochemistry of Hydrothermal Ore Deposits*. 1st edn. Holt, Rinehart and Winston, New York, pp. 515–574.

Roedder, E. 1971. Fluid Inclusion studies on the porphyry-type ore deposits at Bingham, Utah, Butte, Montana, and Climax, Colorado. *Econ. Geol*. 66, 98-120.

Roedder, E. 1984.Fluid inclusions.Mineralogical Society of America.*Reviews in Mineralogy,* Vol. 12, 644p.

Roedder, E. and Skinner, B.J. 1968. Experimental evidence that fluid inclusions do not leak.*Econ. Geol*. 63, 715–730.

Roedder, E. Bodnar, R.J. 1997. Fluid inclusion studies of hydrothermal ore deposits. In: Barnes, H.L. Ed.., *Geochemistry of Hydrothermal Ore Deposits*. Wiley, New York, pp. 657–697.

Roedder, E.1958. Technique for the extraction and partial chemical analysis of fluid-filled inclusions from minerals.*Econ. Geol*. 53, 235–269.

Roeder, P.L. Chromite: From the fiery rain of chondrules to the Kilauea Iki lava lake. *Canadian Mineral.* 1994, 32, 729–746.

Rohinson, P., Spear, F. S., Schumacher, J. C. Laird, J., Klein, C., Evans, B. W. and Doolan, B. L., (1982) *Phase relations of metamorphic amphiboles: natural occurrence and theory.* In D. R. Veblen and P. H. Ribbe, Eds., Amphiboles; Petrology and experimental phase relations, 9B, p. 1-228.Reviews in Mineralogy,Mineralogical Society of America, Washington. D.C.

Rohl, A. N. and Langer, A.M. (1974 Identification and quantification of Abestos in Talc.*Environmental Health Perspectives*, 9, 95-109.

Rudnick, R.L. (1992) Xenoliths -- samples of the lower continental crust. In (Fountain, D., Arculus, R. and Kay, R.W., eds.) Continental LowerCrust, *Elsevier,* Amsterdam p. 269-316.

Rudnick, R.L. (1992) Xenoliths – samples of the lower continental crust. In (Fountain, D., Arculus, R. And Kay, R.W., eds). Continental Lower Crust, *Elsevier,* Amsterdam p. 269-316.

Sandrone, R. 1993. *Talc deposits in the Italian Western Alps*, in Fencoll, P, Torres, J., and Gervilla, F., eds., Granada, Current Research in Geology Applied to Ore Deposits: p. 697-700.

Saunders, A. and Tarney, J. 1991. Back-arc basins. In: Floyd, P. A. (eds) Oceanic Basalts. *Springer,* Boston, MA. 9-10.

Savin, S.M. 1967.Oxygen and hydrogen isotope ratios in sedimentary rocks and minerals.*PhD.Thesis*, Califonia Institute of Technology, Pasedena, USA.

Sawyer E.W. (1986) :The influence of source rock type, chemical weathering and sorting on the geochemistry of clastic sediments from the Queticometasedimentary belt, Superior Province, Canada, *Chemical Geology*, Elsevier, 55, 1-2, 77-95.

Schmidt, M.W. 1992. Amphibole composition in tonalite as a function of pressre: An experimentalcalibration of the Al-in-horblende barometer. *Contributions to Mineralogy and Petrology*, 110, 304-310.

Schober, W. 1997. Quality compounds require premium talc grades and sophisticated formulations, *Eurofillers97-filler. Doc, Manchester* (UK), pp. 1-12, September 8-11.

Seyler, M., Mattson P.H., (1989). *Journal of Geophysical Research*: Solid Wiley Online Library.

Shau, Y. H., Peacor, D.R. (1992) Phyllosilicates in hydrothermally altered basalts from DSDP Hole 504B, Leg 83-a TEM and AEM study. *Contrib Mineral* 112:119-133.

Shepherd, T.J. and Chenery, S.R. 1995.Laser ablation ICP-MS elemental analysis of individual fluid inclusions; an evaluation study.*Geochim.Cosmochim.* Acta 59, 3997–4007.

Sheppard, S. M. F. 1986.Characterization and isotope variations in natural waters. Stable Isotope (Valley, J. W., Taylor, H. P., Jr. and O' Neil, J.R., eds.) *Reviews in Mineralogy* 16, 165-183.

Shibayan, Y. and Woakes, M. 1987. Petrochemistry of somechlorite schists and amphibolites in the Anka schist belt, NWNigeria,In: Matheis and Schandelmeier (Eds). *Current Researchin African earth sciences,* Balkema Rotterdam, pp. 69-71.

Shin, D., and Lee, I. 2006. Fluid Inclusions and their stable Isotope Geochemistry of the carbonate hosted talc deposits near the cretaceous Mamsa Granite, South Korea. *Geochemical Journal*, Vol. 40, pp 69 to 85.

Shin, D.B. and Lee, I.S. 2002. Carbonate Hosted Talc deposits in the contact aureole of igneous Intrusion (Hwanggangri Mineralized Zone), South Korea_: Geochemistry, phase relationships, and stable isotope studies. *Ore Geol.* Rev. 22, 17-39.

Shin, D.B. and Lee, L.S. 2000. Geochemical study on the host rocks of the Poogioen talc deposits, Korea: Implication for the source rock *J. Geol Soc*. Korea. 36, 235-248 (in Korean).

Simandle, G.J. and Paradis, S.P. 1999. "*Carbonate-hosted talc",* Industrial Minerals, Ministry of Energy and Mines (Canada), Vol. 3, pp. 1-6.

Simon, K. 1997.H-isotope composition of different 'water' reservoirs in hydrothermal quartz.*Terra Abstr*.9 (Suppl. 1), 554.

Smithies, R. H. (2002) Archaean boninite-like rocks in an intracratonic setting.*Earth Planet*.*Sci. Lett*. 197, 19-34.

Spear, F.S. 1993. Metamorphic and phase equilibrium and pressure-temperature time paths Washington, D.C, *Mineralogical society of America*, 799p.

Spooner, E.T.C. 1981. *Fluid inclusion studies of hydrothermal ore deposits*. In: Hollister, L.S., Crawford, M.L. _Eds.., Fluid Inclusions: Applications to Petrology. Min. Assoc. Canada, Short Course Handbook, vol. 6, pp. 209–240.

Stanton, M.F., Layard, M., Tegeris, A., Miller, E., May, M., Morgan, E., and Smith, A. (1981) Relation of particle dimension to carcinogenicity in amphibole asbestoses and other fibrous minerals. *Journal of the National Cancer Institute*, 67, 965-975.

Stow, S. H., Neilson M. J., Neathery T. L., 1984. Petrography, Geochemistry, and Tectonic significance of the amphibolites of Alabama Piedmont. *.American Journal of Science, Vol 284, P. 416-436.*

Stuart, F.M., Burnard, P.G., Taylor, R.P. and Turner, G. 1995. Resolving mantle and crustal contributions to ancient hydrothermal fluids; He–Ar isotopes in fluid inclusions from Dae Hwa W–Mo mineralisation, South Korea.*Geochim.Cosmochim*. Acta 59, 4663–4673.

Sushchevskaya, T. M., Ignat'ev, A. V. and Velivetskaya, T. A. 2008. New data on oxygen isotopic zoning in the lultin Sn-W deposit. *Geochemistry International.* 46(5):525-530.

Sylvester, P. J. and Attoh, K. 1992. Lithostratigraphy and composition of 2.1Ga Greenstone belts of the West African Craton and their bearing on crustal evolution and the Archean-Proterozoic boundary. *J. Geol*. 100(4):377-393.

Tarney, J. 1977. Petrology, mineralogy and geochemistry of the Falland Plateau basement rocks.Site 30, deep sea drilling project, initial Report, 36, pp893-920.

Tarney, J., Weaver, B.L., 1987. *Mineralogy, petrology and geochemistry of the Scourie dykes:petrogenesis and crystallization processes in dykes intruded at depth.* In: Park, R.G., Tarney, J. (Eds.), Evolution of the Lewisian and

comparable high grade terrains. Spec. Publ. Geol. Soc London 27, 217–233.

Taylor, S. R. and McLennan, S. M. (1981) The composition and evolution of the continental crust: rare earth element evidence from sedimentary rocks. *Phil. Trans. Royal Soc. London* A300, 381-399.

Tesfaye, G. 1992. Ore-microscopic and geochemical characteristics of gold-tellurides-sulphide mineralization in the Macassa Gold mine, Abitibi belt, Canada, *Mineralium Deposita.* 27:66-71.

Thirlwall, M. F., Smith, T. E., Graham, A. M., Theodorou, N., Hollings, P., Davidson, J. P., & Arculus, R. J. (1994). High field strength element anomalies in arc lavas: source or process? *Journal of Petrology*, 35, 819-838.

Thirlwall, M.F. 1982.A triple filament method for rapid and precise analysis of Rare Elements by isotope dilution.*Chem. Geol*. 35, 155-166.

Thirlwall, M.F. 1986.Lead isotope evidence for the nature of the mantle beneath Caledonian Scotland.*Earth and plnate . Sci. Lett. 80, 55-70.*

Thompson, R. N., & Fowler, M. B. (1986). Subduction-related shoshonitic and ultrapotassic magmatism: a study of Siluro-Ordovician syenites from the Scottish Caledonides. *Contributions to Mineralogy and Petrology*, 94, 507-522.

Trompette, R. 2000. Gondwana evolution; its assembly at around 600ma. Competes Rendude I'Academi des sciences series 11A – *Earth and Planetary Science* 330 (5), 305-315.

Truswell, J.F. and Cope, R. N., 1963.*The geology of parts of Nigeria and Zaria provinces, northern Nigeria.*Bulletin of the Geological Survey, Nigeria, p.29.

Turci, F., Gazzano, E., Tomatis, M., Riganti, C., Ghigo, D., and Fubini, B. 2007. La tremolite nellealpioccidentali:un'analisichimico-fisicaconprospectivetossicologiche. Workshop "Anfibolifibrosi: nuoveproblemasiche relative alrischioambientale esanitario." Roma, 27—28 Abstracts, 68—72 (in Italian).

Turner, D.C. 1983. Upper Proterozoic Schist belts in the Nigerian sector of the Pan-African province of West Africa. *Precam.Res*. 21, pp. 55-79.

Turner, R.J.W, Ames, D.E, Franklin, J.M. Goodfellow, W.D, Leitch, C.H.B. Hoy, T (1993) Character of active hydrothermal mounds and nearby altered hemipelagic sediments in the hydrothermal areas of Middle Valley, northern Juan de Fuca Ridge; data on shallow cores. *Can Mineral* 31:973-995.

U.S. National Research Council. (1985) *Abestiformfibres:* Non-occupational health dab, 352 p. National Academy Press, Washington.

Unrug (1998). Rodinia to Gondwana: The geodynamic map of Gondwana supercontinent assembly. *Journal of African Earth Sciences.* 26. IX-IX.

Urey, H. 1947. The thermodynamic properties of Isotope substances, *J. Chem, society* (London), 1947:562-581.

Uysal, I.; Tarkian, M.; Sadiklar, M.B.; Zaccarini, F.; Meisel, T.; Garuti, G.; Heidrich, S. Petrology of Al- and Cr-rich ophiolitic chromitites from the Mug˘la, SW Turkey: Implications from composition of chromite, solid inclusions of platinum-group mineral, silicate, and base-metal mineral, and Os-isotope geochemistry. Contrib. *Mineral. Petrol.* 2009, 158, 659–674.

Van den Kerkhof, F. and Hein, U. 2001.Fluid inclusion petrography.*Lithos* 55, 27–47.

Vidal, O., Baldyrou, A., Beaufort, D., Fritz, B., Geoffroy, N. and Lanson, B. (2012) Experimental study of the stability and phase relations of clays at high temperature in a thermal gradient, *Clays and Clay Minerals, Vol. 60, No. 2, 200-225.*

Vidal, O., de Andrade, V., Lewin, E., Munoz, M., Parra, T., Pascarelli, S. (2006): P-T-deformamion-Fe^{3+}/Fe^{2+} mapping at the thin section scale and comparison with XANES mapping: application to a garnet-hearing metapelite from the Sambagawa metamorphic belt (Japan). *J. Metamorphic Geol*, 24, 669-683.

Vidal, O., Parra, T., Trotet, F. (2001): A thermodynamic model for Fe-Mg aluminous chlorite using data from phase equilibrium experiments and natural pelitic assemblages in the 100 degrees to 600 °C, 1 to 25 kb range. *Am. J. Sci., 301*, 557-592.

Vidal, O., Parra. T., Vieillard, P. (2005): Thermodynamic properties of the Tschcermak solid solution in Fe-chlorite: Application to natural examples and possible role of oxidation. *Am. Mineral*. 90, 347-358.

Vikre, P.G. 1985. Precious metal vein systems in the National District, Humbolt County, Nevada.*Econ. Geol*. 80, 360–393.

Vivallo, W. & Claesson, L. A. 1987: *Intra-rifting and massive sulphide mineralization in an Early Proterozoic volcanic arc, Skellefte district, northern Sweden.* In Pharaoh, T.e., Beckinsale, A.D. & Rikard, D. (eds.) Geoehemistry and mineralization of Proterozoic volcanic suites. Geol. Soc. Spec. Publ. 33, 69-79.

Walshe, J.L. (1986): A six-component chlorite solid solution model and the conditions of chlorite formation in hydrothermal and geothermal systems. *Econ. Geol.,* 81, 681-703.

Wells, P. R. A. 1977. Pyroxene thermometry in simple and complex system: Contrib. *Mineral. Petrol.,* 62, 129-139.

Wiewiora, A. & Weiss, Z. (1990): Crystallochemical classifications of phyllosilicates based on the unified system of projection of chemical composition: II The chlorite group. *Clay Miner*., 25, 83-92.

Wilkinson, J.J. and Johnston, J.D. 1996. Fluid pressure fluctuations, phase separation and gold precipitation during seismic fracture propagation. *Geology* 24, 395–398.

Wilkinson, J.J., Boyce, A.J., Earls, G. and Fallick, A.E. 1999. Gold remobilization by low temperature brines: evidence from the Curraghinalt gold deposit, Northern Ireland. *Econ. Geol*. 94, 289–296.

Wilkinson, J.J.,Rankin, A.H., Mulshaw, S.C., Nolan, J. and Ramsey, M.H. 1994. Laser ablation-ICP-AES for the determination of metals in fluid inclusions: an application to the study of magmatic ore fluids. *Geochim.Cosmochim*. Acta 8, 1133-1146.

Wills, B.A., 1992, "*Mineral processing technology",* Pergamon Press., Great Britain, 5th ed., pp. 491–644.

Woakes, M., Rahaman, M.A., Ajibade, A.C. 1987. Some metallogenetic features of the Nigerian basement*. Journal of African Earth Science*. 6:54-64

Wood, D. A. (1979) A variably veined sub-oceanic upper mantle: genetic significance for mid-ocean ridge basalts from geochemical evidence. *Geology* 7.499-503.

Wood, D.A. 1980: The application of the Th-Hf-Ta diagram to problems of tectonomagmatic classification and to establishing the nature of crustal contamination of basaltic lavas of the British tertiary volcanic province. *Earth Planet. Sci.* Left. 50, 11-30.

Workman, R. K., & Hart, S. R. (2005). Major and trace element composition of the depleted MORB mantle (DMM). *Earth and Planetary Science Letters,* 231, 53-72.

Wright, J. B. and Ogezi, E. A. (1977): Serpentinite in the basement of northwestern. *Nigeria. journal of Mining and Geology* 14 (1), 34, 37.

Yehia, A. and Al-Wakeel, M.I. 2000. "Talc separation from talc-carbonate ore to ore suitable for different industrial applications". *Minerals Engineering*, Vol. 13, No. 1, pp. 111-116.

Yousif, A.A., 2003*, "The national project for upgrading the Egyptian ores required by the local industry*", Final Report submitted to the Egyptian Academy for Scientific Research and Technology, pp. 49–100.

Zaccarini, F.; Garuti, G.; Proenza, J.A.; Campos, L.; Thalhammer, O.A.R.; Aiglsperger, T.; Lewis, J. Chromite and platinum-group-elements mineralization in the Santa Elena ophiolitic ultramafic nappe (Costa Rica): Geodynamic implications*. Geol.* Acta 2011, 9, 407–423.

Zaw, K., Gemmell, J.B., Large, R.R., Mernagh, T.P. and Ryan, C.G. 1996. Evolution and source of ore fluids in the stringer system, Hellyer VHMS deposit, Tasmania, Australia; evidence from fluid inclusion microthermometry and geochemistry. In: Vielreicher, R.M., Groves, D.I., Heinrich, C.A., Walshe, J.L. - Eds.., The Conjunction of Processes Resulting in the Formation of Orebodies. *Ore Geology Reviews*, Vol. 10, pp. 251–278.

Zierenberg, R.A, Schiffiman P, Jonasson, I.R, Tosdal, R.M, Pickthorn, W.J. McClain, J.S (1995) Alteration of basalt hyaloclastite at the oil-axis Sea Cliff hydrothermal field, Gorda Ridge. *Chem. Geol*. 126:77-99.

Zierenberg, R.A. Shanks, W.C III (1983) Mineralogy and geochemistry of epigenetic features in metalliferous sediment, Atlantis II Deep, Red Sea.*Econ. Geol*. 78:57-72.

APPENDIX I

Table A1: Analysis of relict garnet in the fine-grained amphibolite

Analysis							
Oxide	Analysis wt %	Mole Cations	mole oxygen	norm. cations	norm. oxygen	atom units	norm oxygen
SiO2	50.78	0.845	1.690	4.044	8.089	4.044	8.089
TiO2	0.17	0.002	0.004	0.010	0.020	0.010	0.020
Al2O3	21.44	0.421	0.631	2.012	3.019	2.012	3.019
Cr2O3	0.04	0.001	0.001	0.003	0.004	0.003	0.004
Fe2O3	0.00	0.000	0.000	0.000	0.000	0.000	0.000
FeO	23.89	0.333	0.333	1.591	1.591	1.591	1.591
MnO	0.01	0.000	0.000	0.001	0.001	0.001	0.001
MgO	0.02	0.000	0.000	0.002	0.002	0.002	0.002
CaO	3.94	0.070	0.070	0.336	0.336	0.336	0.336
total	**100.29**	**1.672**	**2.730**	**8.000**	**13.062**	**8.000**	**13.062**
ideal						8.000	12.000

calculated charge	5.459	-5.459	26.124	-26.124	26.124	-26.124

Results of normalization are given in the box, below. If some Fe was calculated to be Fe3+, the total for the analysis will inrease.

Normalized Analysis			
oxide	wt %	Cations	atoms
SiO2	50.78	Si	4.044
TiO2	0.17	Ti	0.010
Al2O3	21.44	Al	2.012
Cr2O3	0.04	Cr	0.003
Fe2O3	0.00	Fe3	0.000
FeO	23.89	Fe2	1.591
MnO	0.01	Mn	0.001
MgO	0.02	Mg	0.002
CaO	3.94	Ca	0.336
		tot. cat.	8.000
total	100.29	tot. oxy.	13.062

FeT/FeT+Mg	1.00
Fe2/Fe2+Mg	1.00

Site Occupancies & End Members			
	Cubic	Octahedral	Tetrahedral
	8-fold	6-fold	4-fold
Si			4.044
Ti		0.010	
Al		2.012	
Cr		0.003	
Fe3		0.000	
Fe2	1.591		
Mn	0.001		
Mg	0.002		
Ca	0.336		
total	1.930	2.025	4.044
ideal	3.000	2.000	3.000

end member	**mol % with Fe3+, etc.**	**mol % cation ratio total Fe**	**mol % cation ratio Fe2+**
almandine	82.43	82.43	82.43
pyrope	0.12	0.12	0.12
grossular	17.31	17.42	17.42
spessartine	0.03	0.03	0.03
uvarovite	0.02		
andradite	0.00		
Ca-Ti Gt	0.09		
total	100.00	100.00	100.00

APPENDIX II

Table 14(d): Mineral chemistry of amphibole in coarse grained amphibolites

	CA12/5	**CA12/12**	**CA12/16**	**CA12/43**	**CA12/49**	**CA12/54**	**CA12/56**	**CA12/61**	**CA12/62**	**CA12/65**
SiO_2	50.71	46.21	50.43	47.25	47.92	45.27	48.74	45.95	41.44	48.45
TiO_2	0.30	0.46	0.16	0.42	0.41	0.49	0.43	0.37	0.41	0.43
Al_2O_3	7.57	12.54	8.16	11.01	10.46	12.96	10.16	9.27	10.49	10.14
Cr_2O_3	0.01	0.00	0.00	0.01	0.00	0.00	0.00	0.00	0.01	0.02
Fe_2O_3	6.02	5.65	5.88	4.98	5.32	5.57	4.34	6.47	3.16	5.28
FeO	3.41	5.59	3.78	5.60	5.18	5.72	5.85	4.35	7.45	5.12
MnO	0.14	0.12	0.12	0.13	0.14	0.14	0.14	0.15	0.01	0.14
MgO	16.92	13.96	16.43	14.61	14.96	13.67	15.16	14.51	12.05	15.29
NiO	0.02	0.00	0.03	0.01	0.01	0.02	0.00	0.01	0.01	0.01
CaO	11.83	11.81	11.73	11.90	11.79	11.76	11.98	11.23	11.03	12.00
Na_2O	0.88	1.30	0.90	1.19	1.17	1.49	1.16	1.06	1.09	1.08
K_2O	0.06	0.23	0.07	0.11	0.13	0.19	0.09	0.10	0.13	0.09

H_2O*	2.14	2.10	2.13	2.10	2.11	2.09	2.12	2.02	1.86	2.12
Total	100.00	99.97	99.82	99.32	99.59	99.36	100.16	95.48	89.14	100.17
Structural formulae based on 23 oxygens										
Si	7.119	6.589	7.097	6.759	6.822	6.510	6.894	6.833	6.675	6.853
Al^{iv}	0.881	1.411	0.903	1.241	1.178	1.490	1.106	1.167	1.325	1.147
Al^{vi}	0.372	0.696	0.451	0.615	0.577	0.707	0.588	0.457	0.667	0.543
Ti	0.032	0.049	0.017	0.045	0.044	0.053	0.046	0.041	0.050	0.046
Cr	0.001	0.000	0.000	0.001	0.000	0.000	0.000	0.000	0.001	0.002
Fe^{3+}	0.636	0.606	0.622	0.536	0.570	0.603	0.462	0.724	0.383	0.562
Fe^{2+}	0.400	0.666	0.445	0.670	0.616	0.687	0.692	0.540	1.003	0.606
Mn	0.017	0.014	0.014	0.016	0.017	0.017	0.017	0.019	0.001	0.017
Mg	3.541	2.967	3.447	3.116	3.175	2.931	3.197	3.217	2.894	3.224
Ni	0.002	0.000	0.003	0.001	0.001	0.002	0.000	0.001	0.001	0.001
Ca	1.779	1.804	1.769	1.824	1.798	1.812	1.815	1.789	1.904	1.818
Na	0.240	0.359	0.246	0.330	0.323	0.415	0.318	0.306	0.340	0.296
K	0.011	0.042	0.013	0.020	0.024	0.035	0.016	0.019	0.027	0.016
OH*	2.000	2.000	2.000	2.000	2.000	2.000	2.000	2.000	2.000	2.000
Total	17.030	17.205	17.027	17.174	17.145	17.262	17.150	17.114	17.271	17.131
Group	Ca	Ca	Ca	Ca	Ca	Ca	Ca	Ca	Ca	Ca
(Ca+Na) (B)	2.000	2.000	2.000	2.000	2.000	2.000	2.000	2.000	2.000	2.000
Na (B)	0.221	0.196	0.231	0.176	0.202	0.188	0.185	0.211	0.096	0.182
(Na+K) (A)	0.030	0.205	0.027	0.174	0.145	0.262	0.150	0.114	0.271	0.131
$Mg/(Mg+Fe^{2+})$	0.899	0.817	0.886	0.823	0.837	0.810	0.822	0.856	0.743	0.842
$Fe^{3+}/(Fe^{3+}Al^{vi})$	0.631	0.465	0.580	0.466	0.497	0.460	0.440	0.613	0.365	0.509
Sum of S2	13.000	13.000	13.000	13.000	13.000	13.000	13.000	13.000	13.000	13.000
Calculated pressure of formation of the amphiboles in the coarse-grained amphibolites										
Hammarstrom& Zen (1986)	2.4	6.7	2.9	5.4	4.9	7.1	4.6	4.3	6.1	4.6
Hollister et al. (1987)	2.3	7.1	2.9	5.7	5.1	7.6	4.8	4.4	6.5	4.8
Johnson & Rutherford (1989)	1.8	5.5	2.3	4.4	4.0	5.8	3.7	3.4	5.0	3.7
Schmidt (1992)	3.0	7.0	3.4	5.8	5.3	7.4	5.1	4.7	6.5	5.0

Table 14(e): Mineral chemistry of amphibole in coarse grainedamphibolites

	CA12/69	**AM9/5**	**CA12/52**	**CA12/55**	**CA12/72**	**CA12/42**	**CA12/6**	**CA12/8**	**CA12/71**	**CA12/64**
SiO_2	48.29	47.28	47.78	48.58	49.10	46.91	50.19	50.85	48.05	49.37
TiO_2	0.42	1.56	0.34	0.32	0.33	0.40	0.33	0.26	0.26	0.41
Al_2O_3	10.88	9.10	9.89	8.76	9.14	10.35	8.05	7.51	9.27	13.79
Cr_2O_3	0.05	0.01	0.00	0.00	0.01	0.00	0.01	0.00	0.00	0.01
Fe_2O_3	7.08	0.00	10.03	10.86	10.76	9.31	8.69	8.38	12.27	0.00
FeO	3.61	14.38	1.27	0.00	0.55	1.37	1.80	1.72	0.00	10.72
MnO	0.13	0.01	0.15	0.12	0.17	0.14	0.16	0.16	0.18	0.13
MgO	15.51	10.99	15.63	16.92	16.16	16.30	16.43	17.13	17.90	9.92
NiO	0.02	0.03	0.02	0.03	0.03	0.01	0.03	0.02	0.00	0.01
CaO	11.70	11.55	11.00	10.66	10.88	11.74	11.15	11.49	8.05	10.74
Na_2O	1.32	1.32	1.15	0.89	1.03	1.34	0.84	0.85	0.77	0.95
K_2O	0.11	1.00	0.06	0.07	0.08	0.11	0.06	0.05	0.05	0.19

H_2O*	2.15	2.03	2.12	2.13	2.14	2.12	2.14	2.15	2.12	2.09
Total	101.27	99.26	99.44	99.33	100.38	100.10	99.88	100.57	98.92	98.33
Structural formulae based on 23 oxygens										
Si	6.746	6.982	6.770	6.852	6.868	6.629	7.044	7.083	6.781	7.089
Al^{iv}	1.254	1.018	1.230	1.148	1.132	1.371	0.956	0.917	1.219	0.911
Al^{vi}	0.537	0.566	0.422	0.309	0.374	0.353	0.375	0.316	0.323	1.423
Ti	0.044	0.173	0.036	0.034	0.035	0.043	0.035	0.027	0.028	0.044
Cr	0.006	0.001	0.000	0.000	0.001	0.000	0.001	0.000	0.000	0.001
Fe^{3+}	0.744	0.000	1.069	1.152	1.133	0.990	0.918	0.879	1.303	0.000
Fe^{2+}	0.422	1.776	0.151	0.000	0.064	0.162	0.211	0.200	0.000	1.287
Mn	0.015	0.001	0.018	0.014	0.020	0.017	0.019	0.019	0.022	0.016
Mg	3.230	2.420	3.301	3.558	3.370	3.434	3.437	3.557	3.766	2.124
Ni	0.002	0.004	0.002	0.003	0.003	0.001	0.003	0.002	0.000	0.001
Ca	1.751	1.828	1.670	1.611	1.630	1.778	1.677	1.715	1.217	1.652
Na	0.358	0.378	0.316	0.243	0.279	0.367	0.229	0.230	0.211	0.265
K	0.020	0.188	0.011	0.013	0.014	0.020	0.011	0.009	0.009	0.035
OH*	2.000	2.000	2.000	2.000	2.000	2.000	2.000	2.000	2.000	2.000
Total	17.128	17.335	16.997	16.937	16.924	17.165	16.916	16.953	16.878	16.848
Amphibole group	Ca	Ca	Ca	Ca	Ca	Ca	Ca	Ca	Ca	Ca
(Ca+Na) (B)	2.000	2.000	1.986	1.854	1.910	2.000	1.905	1.944	1.428	1.917
Na (B)	0.249	0.172	0.316	0.243	0.279	0.222	0.229	0.230	0.211	0.265
(Na+K) (A)	0.128	0.394	0.011	0.013	0.014	0.165	0.011	0.009	0.009	0.035
$Mg/(Mg+Fe^{2+})$	0.885	0.577	0.956	1.000	0.981	0.955	0.942	0.947	1.000	0.623
$Fe^{3+}/(Fe^{3+}Al^{vi})$	0.581	0.000	0.717	0.789	0.752	0.737	0.710	0.736	0.801	0.000
Sum of S2	13.000	12.941	13.000	13.070	13.000	13.000	13.000	13.000	13.441	12.897
Calculated pressure of formation of the amphiboles in the coarse-grained amphibolites										
Hammarstrom& Zen (1986)	5.1	4.0	4.4	3.4	3.7	4.8	2.8	2.3	3.8	7.8
Hollister et al. (1987)	5.3	4.2	4.6	3.5	3.7	5.0	2.7	2.2	3.9	8.4
Johnson & Rutherford (1989)	4.1	3.2	3.5	2.7	2.9	3.8	2.2	1.8	3.1	6.4
Schmidt (1992)	5.5	4.5	4.9	3.9	4.2	5.2	3.3	2.9	4.3	8.1

Table 14(f): Mineral chemistry of amphibole in coarse grained amphibolites

	CA12/31	CA12/51	CA12/60	CA12/46	CA12/66	CA12/67
SiO_2	41.81	41.67	44.06	45.13	44.56	45.23
TiO_2	0.32	0.41	0.39	0.36	0.36	0.35
Al_2O_3	11.57	13.25	12.92	11.98	14.06	13.66
Cr_2O_3	0.00	0.00	0.00	0.01	0.00	0.00
Fe_2O_3	10.36	12.25	12.50	11.61	5.87	5.94
FeO	0.00	0.38	0.00	0.00	5.74	5.75
MnO	0.10	0.12	0.12	0.12	0.11	0.12
MgO	16.19	13.94	14.73	15.88	13.29	13.31
NiO	0.02	0.02	0.01	0.01	0.01	0.02
CaO	9.05	11.17	10.94	10.05	11.75	11.65
Na_2O	0.75	1.28	1.39	1.02	1.62	1.52
K_2O	0.09	0.17	0.17	0.09	0.25	0.21

H_2O*	1.97	2.03	2.10	2.09	2.09	2.09
Total	92.23	96.69	99.33	98.36	99.72	99.85
Structural formulae based on 23 oxygens						
Si	6.370	6.154	6.298	6.459	6.398	6.474
Al^{iv}	1.630	1.846	1.702	1.541	1.602	1.526
Al^{vi}	0.447	0.460	0.475	0.480	0.777	0.778
Ti	0.037	0.046	0.042	0.039	0.039	0.038
Cr	0.000	0.000	0.000	0.001	0.000	0.000
Fe^{3+}	1.187	1.362	1.345	1.251	0.635	0.640
Fe^{2+}	0.000	0.046	0.000	0.000	0.690	0.688
Mn	0.013	0.015	0.015	0.015	0.013	0.015
Mg	3.677	3.069	3.139	3.388	2.845	2.840
Ni	0.002	0.002	0.001	0.001	0.001	0.002
Ca	1.477	1.767	1.675	1.541	1.808	1.787
Na	0.222	0.367	0.385	0.283	0.451	0.422
K	0.017	0.032	0.031	0.016	0.046	0.038
OH*	2.000	2.000	2.000	2.000	2.000	2.000
Total	17.080	17.166	17.108	17.015	17.304	17.247
Amphibole group	Ca	Ca	Ca	Ca	Ca	Ca
(Ca+Na) (B)	1.636	2.000	1.984	1.824	2.000	2.000
Na (B)	0.159	0.233	0.309	0.283	0.192	0.213
(Na+K) (A)	0.080	0.166	0.108	0.016	0.304	0.247
$Mg/(Mg+Fe^{2+})$	1.000	0.985	1.000	1.000	0.805	0.805
$Fe^{3+}/(Fe^{3+}Al^{vi})$	0.726	0.747	0.739	0.723	0.449	0.451
Sum of S2	13.364	13.000	13.016	13.175	13.000	13.000
Calculated pressure of formation of the amphiboles in the coarse-grained amphibolites						
Hammarstrom& Zen (1986)	6.5	7.7	7.0	6.2	8.0	7.7
Hollister et al. (1987)	7.0	8.2	7.5	6.6	8.7	8.2
Johnson & Rutherford (1989)	5.3	6.3	5.7	5.1	6.6	6.3
Schmidt (1992)	6.9	8.0	7.4	6.6	8.3	8.0

APPENDIX III

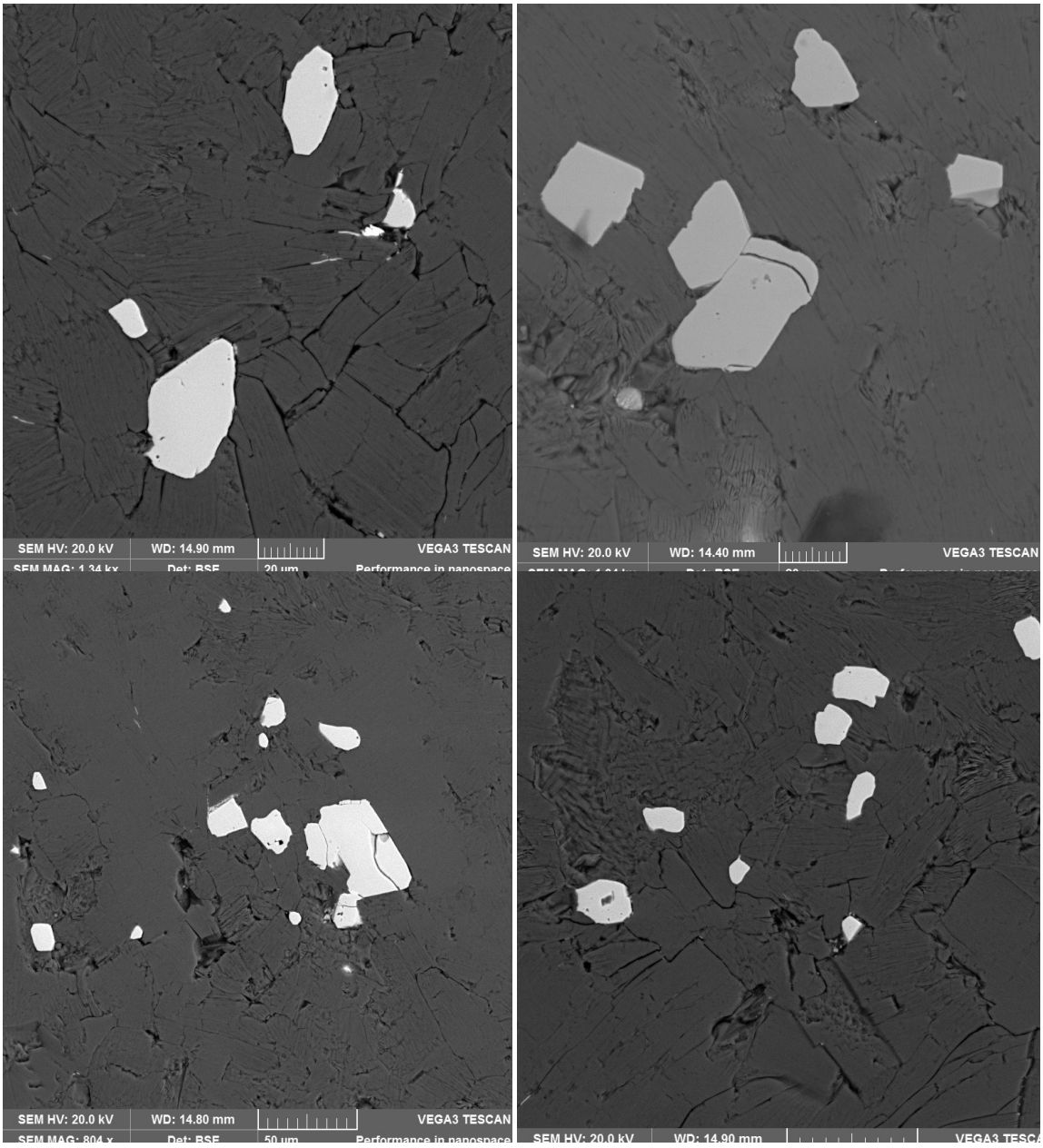

Fig. 4.44: Back-scattered electron images of Cr-spinels (ferritchromite) in talc-chlorite schist of Wonu, Ibadan-Apomu area.

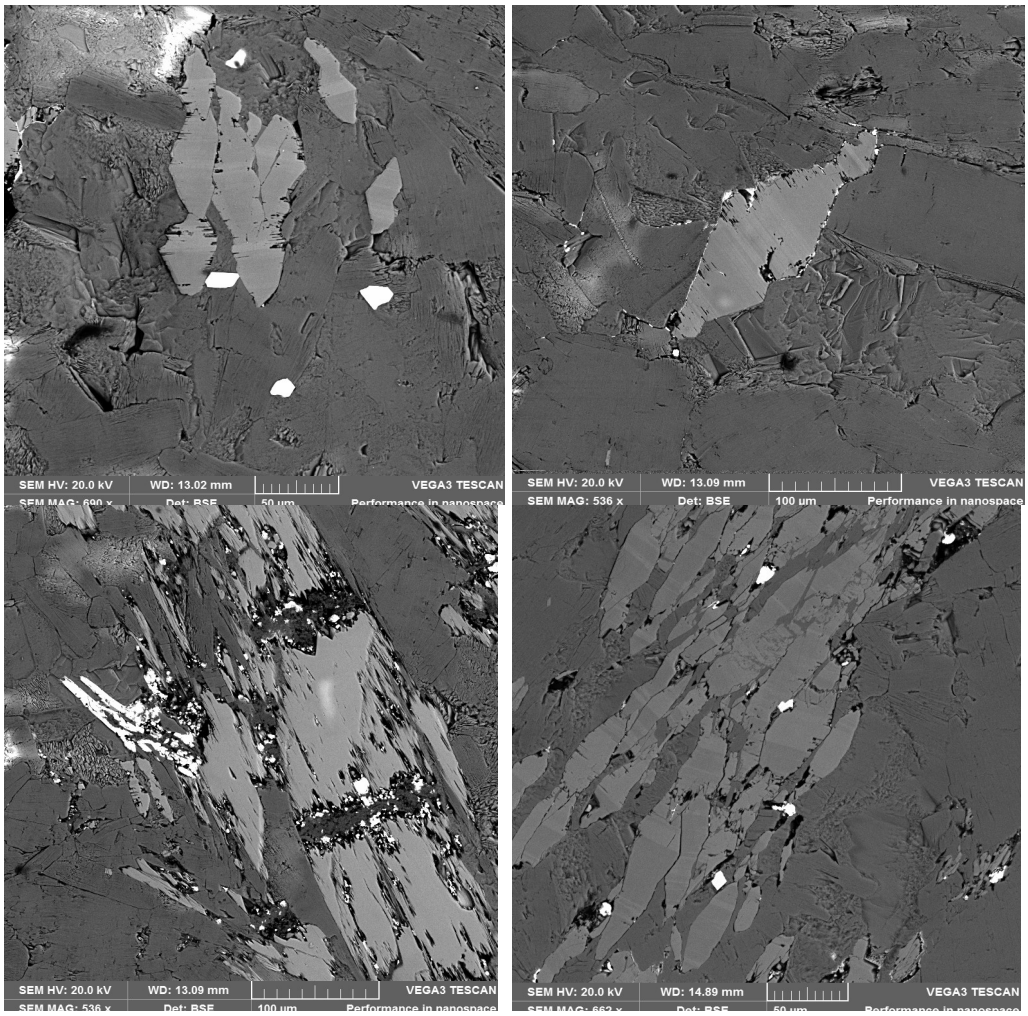

Fig. 4.45: Talc schists of Wonu, Ibadan-Apomu area showing (a and b) tremolite, actinolite and ferritchromite (c) altered olivine and barite(white) (d) sheared clusters of actinolite and graphite(black) in talc and chlorite matrix.

APPENDIX IV

APPENDIX V

Table 4.27(c): Mineral chemistry of amesite in coarse grained amphibolites (lherzolite)

	CA12/1	CA12/2	CA12/3	CA12/11	CA12/13	CA12/14	CA12/15	CA12/71	CA12/72	CA12/73
SiO_2	28.69	28.62	28.60	27.94	27.78	28.15	28.52	28.68	28.59	29.02
TiO_2	0.08	0.04	0.10	0.09	0.09	0.08	0.07	0.09	0.09	0.09
Al_2O_3	22.16	23.66	21.81	20.62	22.10	21.81	21.54	22.40	21.71	21.89
Cr_2O_3	0.02	0.01	0.00	0.01	0.01	0.00	0.00	0.00	0.01	0.01
FeO	10.45	10.63	10.19	9.97	10.42	10.41	10.42	10.50	10.36	10.38
MnO	0.04	0.12	0.03	0.04	0.04	0.03	0.05	0.05	0.04	0.08
MgO	25.38	25.06	25.51	26.92	26.22	25.59	26.10	24.87	25.67	25.33
CaO	0.04	0.13	0.04	0.05	0.05	0.04	0.02	0.03	0.02	0.03
Na_2O	0.01	0.02	0.01	0.01	0.00	0.01	0.01	0.01	0.00	0.01
K_2O	0.01	0.01	0.01	0.01	0.01	0.01	0.00	0.00	0.00	0.01
Total	86.88	88.30	86.30	85.66	86.72	86.13	86.73	86.63	86.49	86.85
	Formula units based on 14 Oxygens									
Si	2.802	2.751	2.809	2.773	2.726	2.777	2.794	2.807	2.805	2.832
Al iv	1.198	1.249	1.191	1.227	1.274	1.223	1.206	1.193	1.195	1.168
Al vi	1.353	1.432	1.334	1.186	1.283	1.314	1.281	1.392	1.316	1.351
Ti	0.006	0.003	0.007	0.007	0.007	0.006	0.005	0.007	0.007	0.007
Cr	0.002	0.001	0.000	0.001	0.001	0.000	0.000	0.000	0.001	0.001
Fe	0.853	0.854	0.837	0.828	0.855	0.859	0.854	0.859	0.850	0.847
Mn	0.003	0.010	0.002	0.003	0.003	0.003	0.004	0.004	0.003	0.007
Mg	3.694	3.590	3.734	3.982	3.834	3.762	3.810	3.628	3.753	3.684
Ca	0.004	0.013	0.004	0.005	0.005	0.004	0.002	0.003	0.002	0.003
Na	0.002	0.004	0.002	0.002	0.000	0.002	0.002	0.002	0.000	0.002
K	0.001	0.001	0.001	0.001	0.001	0.001	0.000	0.000	0.000	0.001
Total	9.918	9.908	9.923	10.015	9.989	9.950	9.958	9.895	9.932	9.903
Fe/Fe+Mg	0.19	0.19	0.18	0.17	0.18	0.19	0.18	0.19	0.18	0.19

Table 4.27(d): Mineral chemistry of amesite in coarse grained amphibolites (lherzolite)

	CA12/74	CA12/75	CA12/76	CA12/77	CA12/78	CA12/79	CA12/80	CA12/82	CA12/83	CA12/86
SiO_2	28.05	27.56	27.50	31.99	26.97	28.64	28.33	28.76	28.78	27.57
TiO_2	0.08	0.09	0.09	0.14	0.08	0.09	0.09	0.09	0.10	0.09
Al_2O_3	21.97	22.29	22.60	18.79	20.60	22.36	22.75	22.07	22.03	22.39
Cr_2O_3	0.00	0.02	0.01	0.01	0.01	0.02	0.01	0.00	0.00	0.01
FeO	10.52	10.65	10.53	10.43	9.44	10.21	10.63	10.31	10.49	10.93
MnO	0.04	0.04	0.09	0.05	0.05	0.04	0.04	0.04	0.05	0.04
MgO	25.85	25.92	24.87	22.92	21.60	24.20	24.66	25.29	25.20	24.67
CaO	0.07	0.03	0.03	2.46	0.09	0.06	0.03	0.02	0.02	0.03
Na_2O	0.01	0.01	0.01	0.20	0.01	0.01	0.01	0.00	0.01	0.00
K_2O	0.01	0.00	0.01	0.02	0.01	0.01	0.00	0.00	0.01	0.01
Total	86.60	86.61	85.74	87.01	78.86	85.64	86.55	86.58	86.69	85.74
	Formula units based on 14 Oxygens									
Si	2.755	2.711	2.728	3.128	2.888	2.830	2.778	2.815	2.816	2.740
Al iv	1.245	1.289	1.272	0.872	1.112	1.170	1.222	1.185	1.184	1.260
Al vi	1.299	1.296	1.371	1.294	1.489	1.434	1.408	1.361	1.357	1.363
Ti	0.006	0.007	0.007	0.010	0.006	0.007	0.007	0.007	0.007	0.007
Cr	0.000	0.002	0.001	0.001	0.001	0.002	0.001	0.000	0.000	0.001
Fe	0.864	0.876	0.874	0.853	0.845	0.844	0.872	0.844	0.858	0.909
Mn	0.003	0.003	0.008	0.004	0.005	0.003	0.003	0.003	0.004	0.003
Mg	3.784	3.800	3.677	3.340	3.447	3.563	3.604	3.689	3.675	3.654
Ca	0.007	0.003	0.003	0.258	0.010	0.006	0.003	0.002	0.002	0.003
Na	0.002	0.002	0.002	0.038	0.002	0.002	0.002	0.000	0.002	0.000
K	0.001	0.000	0.001	0.002	0.001	0.001	0.000	0.000	0.001	0.001
Total	9.968	9.990	9.944	9.799	9.807	9.862	9.900	9.906	9.907	9.942
Fe/Fe+Mg	0.19	0.19	0.19	0.20	0.20	0.19	0.19	0.19	0.19	0.20

Table 4.27(e): Mineral chemistry of amesite in coarse grained amphibolites (lherzolite)

	CA12 /87	CA12 /91	CA12 /95	CA12 /100	CA12 /104	CA12 /115	CA12 /116	CA12 /122	CA12 /127	CA12 /128
SiO_2	27.88	28.25	28.34	29.23	29.17	30.12	28.61	26.74	28.16	26.23
TiO_2	0.09	0.08	0.11	0.11	0.08	0.10	0.09	0.07	0.08	0.10
Al_2O_3	22.18	21.98	22.12	18.39	18.49	23.92	22.54	22.62	22.30	20.57
Cr_2O_3	0.00	0.00	0.00	0.00	0.00	0.00	0.01	0.01	0.00	0.00
FeO	10.78	10.40	10.78	10.03	9.13	10.54	10.43	10.87	10.64	10.47
MnO	0.04	0.04	0.03	0.05	0.04	0.03	0.03	0.04	0.03	0.03
MgO	25.26	25.58	25.11	27.10	26.66	24.16	25.65	25.81	25.57	24.47
CaO	0.02	0.01	0.03	2.65	0.84	0.04	0.02	0.03	0.04	0.05
Na_2O	0.01	0.00	0.00	0.13	0.10	0.01	0.00	0.01	0.00	0.00
K_2O	0.01	0.00	0.01	0.03	0.02	0.01	0.00	0.00	0.01	0.01
Total	86.27	86.34	86.53	87.72	84.53	88.93	87.38	86.20	86.83	81.93
Formula units based on 14 Oxygens										
Si	2.752	2.778	2.785	2.863	2.926	2.857	2.777	2.651	2.758	2.734
Al iv	1.248	1.222	1.215	1.137	1.074	1.143	1.223	1.349	1.242	1.266
Al vi	1.333	1.326	1.348	0.986	1.113	1.532	1.356	1.295	1.333	1.262
Ti	0.007	0.006	0.008	0.008	0.006	0.007	0.007	0.005	0.006	0.008
Cr	0.000	0.000	0.000	0.000	0.000	0.000	0.001	0.001	0.000	0.000
Fe	0.890	0.855	0.886	0.822	0.766	0.836	0.847	0.901	0.871	0.913
Mn	0.003	0.003	0.002	0.004	0.003	0.002	0.002	0.003	0.002	0.003
Mg	3.715	3.749	3.677	3.955	3.985	3.415	3.711	3.813	3.732	3.802
Ca	0.002	0.001	0.003	0.278	0.090	0.004	0.002	0.003	0.004	0.006
Na	0.002	0.000	0.000	0.025	0.019	0.002	0.000	0.002	0.000	0.000
K	0.001	0.000	0.001	0.004	0.003	0.001	0.000	0.000	0.001	0.001
Total	9.953	9.942	9.926	10.082	9.986	9.800	9.926	10.023	9.950	9.994
Fe/Fe+Mg	0.19	0.19	0.19	0.17	0.16	0.20	0.19	0.19	0.19	0.19

APPENDIX VI

Table 4.16: Mineral chemistry of talc sample TC3 of Wonu, Ibadan-Apomu area

	TC3/11	TC3/12	TC3/13	TC3/14	TC3/15	TC3/16	TC3/17	TC3/18	TC3/19	TC3/20
SiO_2	62.58	61.77	60.18	62.08	61.02	61.76	61.57	62.12	62.46	52.75
TiO_2	0.01	0.03	0.02	0.02	0.02	0.00	0.01	0.01	0.02	0.00
Al_2O_3	0.28	0.24	0.33	0.15	0.36	0.48	0.31	0.18	0.27	0.20
FeO	3.13	3.15	3.10	3.21	3.16	3.18	3.22	3.20	3.21	3.14
MnO	0.03	0.03	0.02	0.03	0.03	0.02	0.02	0.03	0.01	0.01
MgO	28.09	27.63	27.94	28.41	27.05	27.31	28.03	28.04	28.23	31.75
CaO	0.01	0.02	0.04	0.01	0.05	0.03	0.01	0.04	0.01	0.01
Na_2O	0.03	0.03	0.04	0.02	0.05	0.04	0.05	0.01	0.03	0.02
K_2O	0.00	0.02	0.04	0.02	0.03	0.02	0.05	0.03	0.01	0.00
Cr_2O_3	0.08	0.06	0.1	0.02	0.09	0.08	0.07	0.06	0.1	0.04
NiO	0.19	0.22	0.22	0.21	0.22	0.22	0.23	0.22	0.22	0.23
H_2O	4.65	4.58	4.51	4.63	4.53	4.58	4.59	4.62	4.65	4.25
Total	99.08	97.78	96.54	98.81	96.61	97.72	98.16	98.56	99.22	92.40
				Formula units based on 22 $(O, OH)_2$)						
Si	8.076	8.081	7.993	8.046	8.082	8.082	8.036	8.068	8.057	7.435
Al iv	0.000	0.000	0.007	0.000	0.000	0.000	0.000	0.000	0.000	0.033
Al vi	0.043	0.037	0.045	0.023	0.056	0.074	0.048	0.028	0.041	0.000
Ti	0.001	0.003	0.002	0.002	0.002	0.000	0.001	0.001	0.002	0.000
Cr	0.008	0.006	0.011	0.002	0.009	0.008	0.007	0.006	0.010	0.004
Fe	0.338	0.345	0.344	0.348	0.350	0.348	0.351	0.348	0.346	0.370
Mn	0.003	0.003	0.002	0.003	0.003	0.002	0.002	0.003	0.001	0.001
Mg	5.404	5.388	5.532	5.489	5.341	5.328	5.454	5.429	5.429	6.671
Ni	0.020	0.023	0.024	0.022	0.023	0.023	0.024	0.023	0.023	0.026
Ca	0.001	0.003	0.006	0.001	0.007	0.004	0.001	0.006	0.001	0.002
Na	0.008	0.008	0.010	0.005	0.013	0.010	0.013	0.003	0.008	0.005
K	0.000	0.003	0.007	0.003	0.005	0.003	0.008	0.005	0.002	0.000
OH*	4.000	4.000	4.000	4.000	4.000	4.000	4.000	4.000	4.000	4.000
TOTAL	17.901	17.900	17.982	17.944	17.892	17.883	17.946	17.918	17.920	18.549
Y total	5.816	5.806	5.959	5.889	5.785	5.783	5.887	5.837	5.852	7.073
X total	0.009	0.014	0.023	0.010	0.025	0.018	0.022	0.013	0.011	0.007
Al total	0.043	0.037	0.052	0.023	0.056	0.074	0.048	0.028	0.041	0.033
Fe/Fe+Mg	0.059	0.060	0.059	0.060	0.062	0.061	0.061	0.060	0.060	0.053
Luhr et al. 1984	812.9	817.5	815.3	815.1	815.2	810.7	812.9	812.9	815.1	810.7

Table 4.16: Mineral chemistry of talc sample TC3 of Wonu, Ibadan-Apomu area

	TC3/21	TC3/22	TC3/23	TC3/24	TC3/25	TC3/26	TC3/27	TC3/28	TC3/29	TC3/30
SiO_2	61.28	62.45	61.60	61.54	59.97	61.52	60.50	63.39	65.21	55.25
TiO_2	0.01	0.00	0.00	0.01	0.00	0.00	0.00	0.01	0.01	0.01
Al_2O_3	0.27	0.07	0.43	0.32	0.55	0.35	0.34	0.21	0.39	12.35
FeO	3.12	3.15	3.23	3.17	3.32	3.18	3.17	3.06	3.25	3.26
MnO	0.03	0.02	0.01	0.02	0.01	0.03	0.02	0.03	0.01	0.02
MgO	28.39	28.41	26.85	27.89	27.36	28.15	28.27	28.03	25.10	17.68
CaO	0.03	0.01	0.05	0.01	0.07	0.02	0.04	0.00	0.01	0.06
Na_2O	0.02	0.01	0.07	0.04	0.05	0.04	0.04	0.03	0.03	0.06
K_2O	0.03	0.01	0.05	0.03	0.03	0.02	0.02	0.01	0.01	0.16
Cr_2O_3	0.08	0.02	0.08	0.07	0.09	0.07	0.1	0.03	0.11	0.04
NiO	0.20	0.23	0.22	0.23	0.21	0.21	0.22	0.22	0.21	0.16
H_2O	4.59	4.64	4.56	4.59	4.49	4.60	4.55	4.68	4.68	4.41
Total	98.05	99.02	97.15	97.92	96.15	98.19	97.27	99.70	99.02	93.46
				Formula units based on 22 $(O, OH)_2$)						
Si	8.009	8.069	8.109	8.047	8.001	8.026	7.980	8.118	8.360	7.510
Al iv	0.000	0.000	0.000	0.000	0.000	0.000	0.020	0.000	0.000	0.490
Al vi	0.042	0.011	0.067	0.049	0.086	0.054	0.032	0.032	0.059	1.489
Ti	0.001	0.000	0.000	0.001	0.000	0.000	0.000	0.001	0.001	0.001
Cr	0.008	0.002	0.008	0.007	0.009	0.007	0.010	0.003	0.011	0.004
Fe	0.341	0.340	0.356	0.347	0.370	0.347	0.350	0.328	0.348	0.371
Mn	0.003	0.002	0.001	0.002	0.001	0.003	0.002	0.003	0.001	0.002
Mg	5.531	5.472	5.269	5.437	5.441	5.475	5.558	5.351	4.797	3.582
Ni	0.021	0.024	0.023	0.024	0.023	0.022	0.023	0.023	0.022	0.017
Ca	0.004	0.001	0.007	0.001	0.010	0.003	0.006	0.000	0.001	0.009
Na	0.005	0.003	0.018	0.010	0.013	0.010	0.010	0.007	0.007	0.016
K	0.005	0.002	0.008	0.005	0.005	0.003	0.003	0.002	0.002	0.028
OH*	4.000	4.000	4.000	4.000	4.000	4.000	4.000	4.000	4.000	4.000
TOTAL	17.970	17.926	17.866	17.931	17.960	17.950	17.996	17.868	17.609	17.519
Y total	5.947	5.851	5.724	5.867	5.931	5.908	5.976	5.741	5.239	5.467
X total	0.014	0.006	0.033	0.017	0.028	0.016	0.019	0.009	0.010	0.052
Al total	0.042	0.011	0.067	0.049	0.086	0.054	0.053	0.032	0.059	1.979
Fe/Fe+Mg	0.058	0.059	0.063	0.060	0.064	0.060	0.059	0.058	0.068	0.094
Luhr et al. 1984	812.9	810.7	810.7	812.9	810.7	810.7	810.7	813.0	812.9	812.8

Table 4.16: Mineral chemistry of talc sample TC3 of Wonu, Ibadan-Apomu area

	TC3/31	TC3/32	TC3/33	TC3/34	TC3/35	TC3/36	TC3/37	TC3/38	TC3/39	TC3/40
SiO_2	61.23	60.27	61.47	61.13	61.67	61.59	62.06	61.30	61.18	61.80
TiO_2	0.00	0.01	0.01	0.00	0.00	0.02	0.00	0.01	0.01	0.10
Al_2O_3	0.13	1.84	0.32	0.35	0.10	0.17	0.18	0.24	0.37	0.85
FeO	3.02	3.27	3.12	3.10	3.22	3.10	2.93	3.02	4.69	2.91
MnO	0.02	0.02	0.02	0.03	0.03	0.02	0.02	0.02	0.02	0.55
MgO	28.11	26.51	27.04	27.85	28.29	26.76	28.60	28.31	29.37	26.49
CaO	0.04	0.04	0.03	0.02	0.03	0.03	0.00	0.02	0.00	0.23
Na_2O	0.03	0.05	0.05	0.03	0.01	0.03	0.02	0.02	0.02	0.06
K_2O	0.08	0.03	0.07	0.04	0.02	0.03	0.01	0.01	0.00	0.01
Cr_2O_3	0.03	0.07	0.08	0.1	0.03	0.04	0.04	0.08	0.04	0.06
NiO	0.21	0.22	0.21	0.21	0.21	0.22	0.21	0.22	0.19	0.15
H_2O	4.56	4.54	4.55	4.56	4.60	4.53	4.63	4.58	4.66	4.58
Total	97.46	96.87	96.97	97.42	98.21	96.54	98.70	97.83	100.55	97.79
				Formula units based on 22 $(O, OH)_2$)						
Si	8.044	7.966	8.105	8.035	8.044	8.147	8.042	8.022	7.872	8.086
Al iv	0.000	0.034	0.000	0.000	0.000	0.000	0.000	0.000	0.056	0.000
Al vi	0.020	0.253	0.050	0.054	0.015	0.027	0.027	0.037	0.000	0.131
Ti	0.000	0.001	0.001	0.000	0.000	0.002	0.000	0.001	0.001	0.010
Cr	0.003	0.007	0.008	0.010	0.003	0.004	0.004	0.008	0.004	0.006
Fe	0.332	0.361	0.344	0.341	0.351	0.343	0.318	0.331	0.505	0.318
Mn	0.002	0.002	0.002	0.003	0.003	0.002	0.002	0.002	0.002	0.061
Mg	5.505	5.223	5.315	5.457	5.501	5.277	5.524	5.523	5.634	5.167
Ni	0.022	0.023	0.022	0.022	0.022	0.023	0.022	0.023	0.020	0.016
Ca	0.006	0.006	0.004	0.003	0.004	0.004	0.000	0.003	0.000	0.032
Na	0.008	0.013	0.013	0.008	0.003	0.008	0.005	0.005	0.005	0.015
K	0.013	0.005	0.012	0.007	0.003	0.005	0.002	0.002	0.000	0.002
OH*	4.000	4.000	4.000	4.000	4.000	4.000	4.000	4.000	4.000	4.000
TOTAL	17.955	17.895	17.877	17.940	17.950	17.842	17.946	17.957	18.099	17.844
Y total	5.884	5.871	5.743	5.888	5.896	5.678	5.898	5.925	6.165	5.709
X total	0.027	0.024	0.029	0.017	0.010	0.017	0.007	0.010	0.005	0.049
Al total	0.020	0.287	0.050	0.054	0.015	0.027	0.027	0.037	0.056	0.131
Fe/Fe+Mg	0.057	0.065	0.061	0.059	0.060	0.061	0.054	0.056	0.082	0.058
Luhr et al. 1984	810.7	812.8	812.9	810.7	810.7	815.3	810.7	813.0	812.2	835.7

Table 4.16: Mineral chemistry of talc sample TC4 of Wonu, Ibadan-Apomu area

	TC4/11	TC4/12	TC4/13	TC4/14	TC4/15	TC4/16	TC4/17	TC4/18	TC4/19	TC4/20
SiO_2	60.87	61.29	61.36	59.51	63.50	62.95	61.99	63.50	62.93	63.93
TiO_2	0.00	0.02	0.00	0.01	0.02	0.00	0.01	0.01	0.00	0.00
Al_2O_3	1.62	0.36	0.34	0.33	0.35	0.24	0.39	0.36	0.08	0.31
FeO	3.26	3.19	3.30	3.31	3.37	3.25	3.23	3.25	3.13	3.27
MnO	0.02	0.02	0.03	0.02	0.02	0.02	0.03	0.02	0.01	0.02
MgO	26.58	28.23	28.36	30.95	25.37	28.60	28.10	27.88	29.16	26.77
CaO	0.00	0.02	0.01	0.00	0.01	0.00	0.03	0.01	0.00	0.01
Na_2O	0.03	0.04	0.04	0.04	0.04	0.02	0.03	0.03	0.01	0.03
K_2O	0.01	0.01	0.00	0.01	0.01	0.00	0.01	0.00	0.00	0.01
Cr_2O_3	0.06	0.1	0.06	0.08	0.08	0.05	0.11	0.06	0.01	0.08
NiO	0.26	0.25	0.28	0.26	0.27	0.26	0.28	0.25	0.27	0.28
H_2O	4.56	4.59	4.60	4.60	4.60	4.69	4.63	4.70	4.70	4.67
Total	97.27	98.12	98.38	99.12	97.64	100.08	98.84	100.07	100.30	99.38
				Formula units based on 22 $(O, OH)_2$)						
Si	8.005	8.007	8.001	7.752	8.282	8.053	8.035	8.110	8.034	8.204
Al iv	0.000	0.000	0.000	0.051	0.000	0.000	0.000	0.000	0.000	0.000
Al vi	0.251	0.055	0.052	0.000	0.054	0.036	0.060	0.054	0.012	0.047
Ti	0.000	0.002	0.000	0.001	0.002	0.000	0.001	0.001	0.000	0.000
Cr	0.006	0.010	0.006	0.008	0.008	0.005	0.011	0.006	0.001	0.008
Fe	0.359	0.349	0.360	0.361	0.368	0.348	0.350	0.347	0.334	0.351
Mn	0.002	0.002	0.003	0.002	0.002	0.002	0.003	0.002	0.001	0.002
Mg	5.211	5.498	5.512	6.010	4.933	5.454	5.430	5.308	5.549	5.121
Ni	0.028	0.026	0.029	0.027	0.028	0.027	0.029	0.026	0.028	0.029
Ca	0.000	0.003	0.001	0.000	0.001	0.000	0.004	0.001	0.000	0.001
Na	0.008	0.010	0.010	0.010	0.010	0.005	0.008	0.007	0.002	0.007
K	0.002	0.002	0.000	0.002	0.002	0.000	0.002	0.000	0.000	0.002
OH*	4.000	4.000	4.000	4.000	4.000	4.000	4.000	4.000	4.000	4.000
TOTAL	17.871	17.964	17.975	18.224	17.691	17.929	17.933	17.863	17.961	17.773
Y total	5.856	5.942	5.963	6.409	5.395	5.872	5.884	5.744	5.925	5.558
X total	0.009	0.015	0.012	0.012	0.013	0.005	0.013	0.009	0.002	0.010
Al total	0.251	0.055	0.052	0.051	0.054	0.036	0.060	0.054	0.012	0.047
Fe/Fe+Mg	0.064	0.060	0.061	0.057	0.069	0.060	0.061	0.061	0.057	0.064
Luhr et al. 1984	810.7	815.1	810.7	812.8	814.9	810.7	812.9	812.9	810.7	810.7

Table 4.16: Mineral chemistry of talc sample TC4 of Wonu, Ibadan-Apomu area

	TC4/21	TC4/22	TC4/23	TC4/24	TC4/25	TC4/26	TC4/41	TC4/42	TC4/43	TC4/44
SiO_2	61.36	61.05	61.52	61.07	62.55	62.36	61.22	62.26	62.26	63.04
TiO_2	0.01	0.01	0.02	0.01	0.01	0.00	0.00	0.00	0.02	0.00
Al_2O_3	0.31	0.33	0.32	0.32	0.35	0.32	1.68	0.16	0.31	0.29
FeO	3.22	3.30	3.31	3.30	3.45	3.33	3.55	2.86	3.31	3.26
MnO	0.01	0.01	0.01	0.02	0.02	0.02	0.02	0.02	0.02	0.06
MgO	27.68	28.45	27.45	28.55	27.97	29.05	26.44	28.62	27.95	28.05
CaO	0.04	0.01	0.01	0.02	0.01	0.01	0.03	0.03	0.01	0.00
Na_2O	0.04	0.03	0.03	0.03	0.05	0.04	0.03	0.01	0.03	0.04
K_2O	0.02	0.02	0.02	0.02	0.01	0.01	0.03	0.02	0.00	0.00
Cr_2O_3	0.07	0.05	0.05	0.05	0.06	0.07	0.06	0.05	0.06	0.07
NiO	0.25	0.27	0.28	0.25	0.28	0.25	0.26	0.27	0.27	0.28
H_2O	4.57	4.58	4.57	4.59	4.65	4.68	4.58	4.64	4.63	4.68
Total	97.58	98.11	97.59	98.23	99.41	100.14	97.90	98.94	98.87	99.77
	Formula units based on 22 $(O, OH)_2$)									
Si	8.053	7.985	8.072	7.979	8.062	7.989	8.009	8.047	8.063	8.085
Al iv	0.000	0.015	0.000	0.021	0.000	0.011	0.000	0.000	0.000	0.000
Al vi	0.048	0.036	0.049	0.028	0.053	0.037	0.259	0.024	0.047	0.044
Ti	0.001	0.001	0.002	0.001	0.001	0.000	0.000	0.000	0.002	0.000
Cr	0.007	0.005	0.005	0.005	0.006	0.007	0.006	0.005	0.006	0.007
Fe	0.353	0.361	0.363	0.361	0.372	0.357	0.388	0.309	0.359	0.350
Mn	0.001	0.001	0.001	0.002	0.002	0.002	0.002	0.002	0.002	0.007
Mg	5.415	5.547	5.369	5.561	5.374	5.548	5.156	5.514	5.396	5.363
Ni	0.026	0.028	0.030	0.026	0.029	0.026	0.027	0.028	0.028	0.029
Ca	0.006	0.001	0.001	0.003	0.001	0.001	0.004	0.004	0.001	0.000
Na	0.010	0.008	0.008	0.008	0.012	0.010	0.008	0.003	0.008	0.010
K	0.003	0.003	0.003	0.003	0.002	0.002	0.005	0.003	0.000	0.000
OH*	4.000	4.000	4.000	4.000	4.000	4.000	4.000	4.000	4.000	4.000
TOTAL	17.925	17.992	17.904	17.998	17.915	17.989	17.865	17.941	17.912	17.894
Y total	5.853	5.979	5.820	5.984	5.837	5.976	5.839	5.883	5.840	5.799
X total	0.019	0.012	0.012	0.014	0.016	0.013	0.017	0.010	0.009	0.010
Al total	0.048	0.051	0.049	0.049	0.053	0.048	0.259	0.024	0.047	0.044
Fe/Fe+Mg	0.061	0.061	0.063	0.061	0.065	0.060	0.070	0.053	0.062	0.061
Luhr et al. 1984	812.9	812.8	815.0	812.8	812.7	810.7	810.7	810.7	815.0	810.7

Table 4.16: Mineral chemistry of talc sample TC4 of Wonu, Ibadan-Apomu area

	TC4/31	TC4/32	TC4/34	TC4/35	TC4/36	TC4/37	TC4/38	TC4/39	TC4/40	TC4/28
SiO_2	62.44	61.73	61.60	62.10	62.32	62.67	62.31	61.75	60.96	58.68
TiO_2	0.02	0.00	0.02	0.01	0.00	0.01	0.00	0.00	0.01	0.00
Al_2O_3	0.34	1.10	0.42	0.33	0.31	0.30	0.32	0.19	0.04	0.26
FeO	3.38	3.49	3.36	3.28	3.30	3.32	3.21	3.21	3.27	11.51
MnO	0.02	0.02	0.02	0.02	0.01	0.02	0.02	0.03	0.00	0.75
MgO	27.96	27.62	25.77	28.67	28.28	28.03	27.87	28.03	28.60	24.29
CaO	0.02	0.02	0.02	0.00	0.01	0.02	0.02	0.03	0.02	0.37
Na_2O	0.05	0.07	0.04	0.04	0.05	0.03	0.05	0.03	0.05	0.02
K_2O	0.02	0.00	0.01	0.01	0.02	0.03	0.02	0.02	0.01	0.00
Cr_2O_3	0.08	0.08	0.08	0.06	0.25	0.24	0.14	0.02	0.07	0.06
NiO	0.24	0.26	0.28	0.24	0.28	0.26	0.26	0.28	0.26	0.16
H_2O	4.64	4.63	4.51	4.65	4.65	4.66	4.63	4.60	4.57	4.49
Total	99.21	99.02	96.13	99.41	99.48	99.59	98.85	98.19	97.86	100.59
				Formula units based on 22 $(O, OH)_2$						
Si	8.061	7.993	8.183	8.008	8.032	8.062	8.069	8.055	7.995	7.828
Al iv	0.000	0.007	0.000	0.000	0.000	0.000	0.000	0.000	0.005	0.041
Al vi	0.052	0.161	0.066	0.050	0.047	0.045	0.049	0.029	0.001	0.000
Ti	0.002	0.000	0.002	0.001	0.000	0.001	0.000	0.000	0.001	0.000
Cr	0.008	0.008	0.008	0.006	0.025	0.024	0.014	0.002	0.007	0.006
Fe	0.365	0.378	0.373	0.354	0.356	0.357	0.348	0.350	0.359	1.284
Mn	0.002	0.002	0.002	0.002	0.001	0.002	0.002	0.003	0.000	0.085
Mg	5.381	5.331	5.103	5.511	5.433	5.375	5.380	5.451	5.592	4.831
Ni	0.025	0.027	0.030	0.025	0.029	0.027	0.027	0.029	0.027	0.017
Ca	0.003	0.003	0.003	0.000	0.001	0.003	0.003	0.004	0.003	0.053
Na	0.013	0.018	0.010	0.010	0.012	0.007	0.013	0.008	0.013	0.005
K	0.003	0.000	0.002	0.002	0.003	0.005	0.003	0.003	0.002	0.000
OH*	4.000	4.000	4.000	4.000	4.000	4.000	4.000	4.000	4.000	4.000
TOTAL	17.915	17.928	17.783	17.969	17.940	17.909	17.908	17.935	18.004	18.151
Y total	5.835	5.907	5.585	5.949	5.891	5.832	5.820	5.865	5.987	6.223
X total	0.019	0.020	0.015	0.012	0.017	0.015	0.019	0.015	0.017	0.058
Al total	0.052	0.168	0.066	0.050	0.047	0.045	0.049	0.029	0.006	0.041
Fe/Fe+Mg	0.064	0.066	0.068	0.060	0.061	0.062	0.061	0.060	0.060	0.210
Luhr et al. 84	814.9	810.7	814.9	812.8	810.7	812.8	810.7	810.7	812.8	810.7